INNOVATIVE APPROACHES AND TECHNIQUES IN THYROID SURGERY

EDITED BY: Hoon Yub Kim, Ralph P. Tufano and Gianlorenzo Dionigi
PUBLISHED IN: Frontiers in Endocrinology

frontiers Research Topics

ISSN 1664-8714
ISBN 978-2-83250-559-5
DOI 10.3389/978-2-83250-559-5

About Frontiers

Frontiers is more than just an open-access publisher of scholarly articles: it is a pioneering approach to the world of academia, radically improving the way scholarly research is managed. The grand vision of Frontiers is a world where all people have an equal opportunity to seek, share and generate knowledge. Frontiers provides immediate and permanent online open access to all its publications, but this alone is not enough to realize our grand goals.

Frontiers Journal Series

The Frontiers Journal Series is a multi-tier and interdisciplinary set of open-access, online journals, promising a paradigm shift from the current review, selection and dissemination processes in academic publishing. All Frontiers journals are driven by researchers for researchers; therefore, they constitute a service to the scholarly community. At the same time, the Frontiers Journal Series operates on a revolutionary invention, the tiered publishing system, initially addressing specific communities of scholars, and gradually climbing up to broader public understanding, thus serving the interests of the lay society, too.

Dedication to Quality

Each Frontiers article is a landmark of the highest quality, thanks to genuinely collaborative interactions between authors and review editors, who include some of the world's best academicians. Research must be certified by peers before entering a stream of knowledge that may eventually reach the public - and shape society; therefore, Frontiers only applies the most rigorous and unbiased reviews.
Frontiers revolutionizes research publishing by freely delivering the most outstanding research, evaluated with no bias from both the academic and social point of view. By applying the most advanced information technologies, Frontiers is catapulting scholarly publishing into a new generation.

What are Frontiers Research Topics?

Frontiers Research Topics are very popular trademarks of the Frontiers Journals Series: they are collections of at least ten articles, all centered on a particular subject. With their unique mix of varied contributions from Original Research to Review Articles, Frontiers Research Topics unify the most influential researchers, the latest key findings and historical advances in a hot research area! Find out more on how to host your own Frontiers Research Topic or contribute to one as an author by contacting the Frontiers Editorial Office: frontiersin.org/about/contact

INNOVATIVE APPROACHES AND TECHNIQUES IN THYROID SURGERY

Topic Editors:
Hoon Yub Kim, Korea University Anam Hospital, South Korea
Ralph P. Tufano, The Johns Hopkins Hospital, Johns Hopkins Medicine, United States
Gianlorenzo Dionigi, University of Milan, Italy

Citation: Kim, H. Y., Tufano, R. P., Dionigi, G., eds. (2022). Innovative Approaches and Techniques in Thyroid Surgery. Lausanne: Frontiers Media SA.
doi: 10.3389/978-2-83250-559-5

Table of Contents

frontiers in Endocrinology

ORIGINAL RESEARCH
published: 20 December 2021
doi: 10.3389/fendo.2021.795627

Ambulatory Endoscopic Thyroidectomy *via* a Chest-Breast Approach Has an Acceptable Safety Profile for Thyroid Nodule

Zeyu Zhang, Fada Xia and Xinying Li**

Department of Thyroid Surgery, Xiangya Hospital, Central South University, Changsha, China

OPEN ACCESS

Edited by:
Hoon Yub Kim,
Korea University Anam Hospital,
South Korea

Reviewed by:
Eliana Piantanida,
University of Insubria, Italy
Erivelto Martinho Volpi,
Centro de referencia no ensino do diagnóstico por imagem (CETRUS), Brazil

****Correspondence:***
Xinying Li
lixinyingcn@protonmail.com
Fada Xia
xiafadaCSU@protonmail.com

Specialty section:
This article was submitted to Thyroid Endocrinology, a section of the journal Frontiers in Endocrinology

Received: *15 October 2021*
Accepted: *01 December 2021*
Published: *20 December 2021*

Citation:
Zhang Z, Xia F and Li X (2021) Ambulatory Endoscopic Thyroidectomy via a Chest-Breast Approach Has an Acceptable Safety Profile for Thyroid Nodule. Front. Endocrinol. 12:795627. doi: 10.3389/fendo.2021.795627

Introduction: With the growing esthetic requirements, endoscopic thyroidectomy develops rapidly and is widely accepted by practitioners and patients to avoid the neck scar caused by open thyroidectomy. Although ambulatory open thyroidectomy is adopted by multiple medical centers, the safety and potential of ambulatory endoscopic thyroidectomy via a chest-breast approach (ETCBA) is poorly investigated.

Material and Methods: Patients with thyroid nodules who received conventional or ambulatory ETCBA at Xiangya hospital, Central South University from January 2017 to June 2020 were retrospectively included. The incidence of postoperative complications, 30-days readmission rate, financial cost, duration of hospitalization, mental health were mainly investigated.

Results: A total of 260 patients were included with 206 (79.2%) suffering from thyroid carcinoma, while 159 of 260 received ambulatory ETCBA. There was no statistically significant difference in the incidence of postoperative complications (P=0.249) or 30-days readmission rate (P=1.000). In addition, The mean economic cost of the ambulatory group had a 29.5% reduction compared with the conventional group (P<0.001). Meanwhile, the duration of hospitalization of the ambulatory group was also significantly shorter than the conventional group (P<0.001). Patients received ambulatory ETCBA showed a higher level of anxiety (P=0.041) and stress (P=0.016). Subgroup analyses showed consistent results among patients with thyroid cancer with a 12.9% higher complication incidence than the conventional ETCBA (P=0.068).

Conclusion: Ambulatory ETCBA is as safe as conventional ETCBA for selective patients with thyroid nodules or thyroid cancer, however with significant economic benefits and shorter duration of hospitalization. Extra attention should be paid to manage the anxiety and stress of patients who received ambulatory ETCBA.

Keywords: ambulatory surgery, endoscopic thyroidectomy, thyroid nodule, postoperative complication, mental health

INTRODUCTION

Thyroid nodule is a very common disease and often discovered by accident mainly because of the asymptomatic feature (1).Although there is an increasing incidence of thyroid malignancy, most of thyroid nodules are benign without the need for invasive therapies (2). For patients who reach the indication of surgery, a traditional open thyroidectomy is the primary choice. However, with the growing esthetic requirements, endoscopic thyroidectomy develops rapidly and is widely accepted by practitioners and patients to avoid the neck scar caused by open thyroidectomy (3). Increasing evidences have shown that endoscopic thyroidectomy has the same efficacy and safety profiles as the open thyroidectomy (4–6).

Ambulatory surgery has become more and more common in recent years, offering various advantages (7). At present, ambulatory open thyroidectomy is adopted by multiple medical centers, showing no difference in readmissions and complications compared with conventional thyroidectomy (8). Moreover, with the development of instruments and techniques, many surgical procedures with a higher complexity are subsequently allowed to be performed with an ambulatory management (9).

Endoscopic thyroidectomy is usually carried out with multiple-day hospitalization, while few medical centers perform ambulatory endoscopic thyroidectomy. In addition, as far as we know, there is no study focusing on the potential of ambulatory endoscopic thyroidectomy. In our medical center, both conventional and ambulatory endoscopic thyroidectomy via a chest-breast approach (ETCBA) is routinely performed. Thus, in this study, we retrospectively evaluated the efficacy and safety of ambulatory ETCBA.

MATERIAL AND METHODS

Study Cohort

Patients with thyroid nodules who received conventional or ambulatory ETCBA at Xiangya hospital, Central South University from January 2017 to June 2020 were retrospectively included. The exclusion criteria were as follows: (1) signs of extrathyroidal tissue invasion; (2) previously received neck surgery or radiation; (3) suffering from infectious diseases or parathyroid disease; (4) lack of essential clinical data, including results of ultrasound, parathyroid hormone, complication data, and assessment of mental health. Patients were divided into conventional group and ambulatory group according to the surgery they received. This study was approved by the Institutional Ethics Committee of Xiangya Hospital, Central South University (No.202011960) and met the guidelines of governmental ethics agency in accordance with the precepts established by the Helsinki Declaration.

Surgical Procedures and Postoperative Management

The preoperative examination, surgeons, and procedures of ETCBA were identical between the two groups. The operative position and the location of operating and observing ports were as same as in the previous report (10). Patients with benign nodules would receive a thyroidectomy, while a central lymph node dissection was additionally performed among patients with malignant nodules. For patients with an undetermined result of fine-needle aspiration (FNA) biopsy, intraoperative frozen section histological examination was performed to determine the further procedures. Generally, ETCBA was not administrated for patients with lateral lymph node metastasis detected by preoperative examinations. However, lateral lymph node dissection was still performed endoscopically when suspicious lateral lymph node metastasis was intraoperatively detected. Patient status and vital signs were carefully monitored after surgery, and discharge assessment included vital signs, consciousness, airway status and sound, incision condition, and serum calcium. Calcium and analgesics were given as appropriate. The removal of the drainage tube and dressing change were performed the next morning. Patients in the conventional group were usually discharged on the third day after ETCBA, while the ambulatory group within 24 hours after ETCBA.

Outcomes and Follow-Up

Medical records and pathological reports were investigated for clinical data and patient characteristics. Every patient was followed up with examinations including ultrasound, thyroid function, and parathyroid hormone (PTH) every 3-6 months after discharge. The outcomes of this study were mainly incidence of postoperative complications, 30-days readmission rate, financial cost, duration of hospitalization. Hypoparathyroidism was recognized as PTH level <15 pg/ml, and hypoparathyroidism and the voice change recovered in six months was considered as transient. An independent surgeon was assigned to record these data.

Furthermore, the mental health of patients was also investigated within one month, using the Depression Anxiety Stress Scales-21 (DASS-21), a screening tool to measure three comorbid depression, anxiety and stress disorders (**Supplement Table 1**) (7).

Statistical Analysis

SPSS 23.0 was used for statistical analyses. The continuous variables were expressed as mean ± standard deviation and analyzed using the independent-sample t-test or Mann-Whitney U test according to its distribution pattern. Categorical variables were expressed as frequency (percentage) and analyzed using Chi-square or Fisher exact test as appropriate. An independent analyst was assigned to assess the statistics, and statistical significance was recognized with $P < 0.05$.

RESULTS

Patient and Tumor Characteristics

Among a total of 260 included patients, 159 received ambulatory ETCBA, while 101 received conventional one (**Table 1**). The mean age of the two groups was 35.74 ± 8.26 and 34.93 ± 9.13 years, and the patients who received ETCBA were mostly female (92.7%). There was no difference in ASA classification between the two groups (P=0.094). 125 (78.6%) and 81 (80.2%) patients

TABLE 1 | Patients and nodules characteristics.

Characteristic	Ambulatory group (n=159)	Conventional group (n=101)	*P*
Age (years)	35.74 ± 8.26	34.93 ± 9.13	0.459
Gender			0.090
Female	151 (95.0)	90 (89.1)	
Male	8 (5.0)	11 (10.9)	
Ethnicity			
Asian	159 (100.0)	101 (100.0)	1.000
ASA classification			0.094
I	61 (38.4)	50 (49.5)	
II	98 (61.6)	51 (50.5)	
Malignant nodules	125 (78.6)	81 (80.2)	0.876
Number of lesion			0.878
Single	124 (78.0)	80 (79.2)	
Multiple	35 (22.0)	21 (20.8)	
Largest tumor size (cm)	1.22 ± 1.19	1.25 ± 1.31	0.840
Surgical procedure			0.246
Unilateral thyroidectomy	27 (17.0)	13 (12.9)	
Unilateral thyroidectomy with CLND	62 (39.0)	49 (48.5)	
Bilateral thyroidectomy	5 (3.1)	7 (6.9)	
Bilateral thyroidectomy with CLND	62 (39.0)	31 (30.7)	
Thyroidectomy with LLND	3 (1.9)	1 (1.0)	

Data are expressed as mean ± standard deviation or n (%). ASA, American Society of Anaesthesiology; CLND, central lymph node dissection; LLND, lateral lymph node dissection.

were diagnosed as malignancy in the ambulatory group and conventional group, respectively. 56 (21.5%) patients suffered from multiple lesions. The largest tumor size was 1.22 ± 1.19 cm and 1.25 ± 1.31 cm in ambulatory group and conventional group, respectively. Moreover, no difference was shown in surgical procedures between the two groups (P=0.246), indicating an identical degree of difficulty of surgery. Overall, there was no difference in the patient and tumor characteristics between two groups.

Surgical Outcomes and Prognosis

As shown in **Table 2**, surgical outcomes and patient prognosis were compared between ambulatory and conventional ETCBA. No difference was shown in the duration of surgery and blood loss. The ambulatory group showed a higher incidence of complications (30.8%) than the conventional group (23.8%), however with no statistically significant difference. Notably, all four patients who suffered from permanent hypoparathyroidism were in the ambulatory group. Two patients failed in the ambulatory management due to seroma or hematoma, and were transferred to the conventional ward for surveillance without re-operation. Furthermore, only one patient in the ambulatory group was readmitted due to hypocalcemia. Till the last follow-up, one patient with a malignant nodule suffered from a recurrence in the ambulatory group and conventional group, respectively. There was no patient suffering from re-operation or death in this study.

Economic Cost and Duration of Hospitalization

Economic cost and duration of hospitalization were also investigated (**Table 3**). The mean economic cost of the ambulatory group had a 29.5% reduction compared with the conventional group. Meanwhile, the duration of hospitalization

TABLE 2 | Surgical outcomes and prognosis.

Characteristic	Ambulatory group (n=159)	Conventional group (n=101)	*P*
Duration of surgery (min)	186.19 ± 31.77	183.78 ± 30.12	0.544
Blood loss (ml)	18.79 ± 10.79	18.84 ± 8.78	0.964
Postoperative complications	49 (30.8)	24 (23.8)	0.258
Transient hypoparathyroidism	39 (24.5)	20 (19.8)	
Permanent hypoparathyroidism	4 (2.5)	0 (0.0)	
Hypoglycemia	0 (0.0)	1 (1.0)	
Transient voice change	5 (3.1)	2 (2.0)	
Seroma	1 (0.6)	0 (0.0)	
Pulmonary infection	0 (0.0)	1 (1.0)	
Hematoma	1 (0.6)	0 (0.0)	
Transfer to the conventional ward	2 (1.3)	–	–
30-days readmission	1 (0.6)	0 (0.0)	1.000
Recurrence of malignancy	1 (0.6)	1 (1.0)	0.627

Data are expressed as mean ± standard deviation or n (%).

TABLE 3 | Economic cost and duration of hospitalization.

Characteristic	Ambulatory group (n=159)	Conventional group (n=101)	*P*
Economic cost (yuan)	14278.57 ± 2194.22	20261.26 ± 4399.18	<0.001
Duration of hospitalization (day)	1.03 ± 0.29	5.51 ± 1.43	<0.001

Data are expressed as mean ± standard deviation.

of the ambulatory group was also significantly shorter than the conventional group.

Mental Health

Table 4 showed the results of DASS-21. While there was no significant difference in the level of depression (P=0.731), higher levels of anxiety (P=0.041) and stress (P=0.016) were shown in the ambulatory group than the conventional group.

Subgroup Analyses for Patients With Thyroid Cancer

To further investigate the role of ambulatory ETCBA in patients with thyroid cancer, subgroup analyses were performed excluding patients with benign nodules (**Table 5**). The difference between two groups remained insignificant in duration of surgery, blood loss, 30-day readmission, and tumor recurrence. Meanwhile, significant reductions in economic cost and the duration of hospitalization were shown in the ambulatory group than the conventional group, which was consistent with the main results. The results of DASS-21 were also consistent with the main results. Notably, though with no significance, the complication incidence of the ambulatory group was 12.9% higher than the conventional group among patients with thyroid cancer.

DISCUSSION

For the very first time, this study summarized the data of patients undergoing ambulatory or conventional ETCBA in our medical center, and evaluated the safety, economic benefits, and mental health of patients, which showed that ambulatory ETCBA was as safe as the conventional ETCBA, but with great economic benefits and shorter duration of hospitalization regardless of patients with thyroid nodules or thyroid cancer. The results also highlighted that extra attention should be paid to manage the anxiety and stress of patients who received ambulatory ETCBA.

Many studies have proven the safety of ambulatory open thyroidectomy. A meta-analysis by Lee et al. consisting of 10 observational studies with 3427 patients suggested identical safety of outpatient thyroidectomy compared with inpatient thyroidectomy (11). More recently, a propensity score-matched study indicated outpatient thyroidectomy was not associated with a higher rate of readmission or complications (8). Furthermore, the safety of endoscopic thyroidectomy, including ETCBA, was well studied compared with open thyroidectomy. Jiang et al. included 20 publications with 5664 patients to perform a meta-analysis, and the results showed endoscopic thyroidectomy was similar to open thyroidectomy in terms of safety (12). This study stepped further to firstly investigate the safety of ambulatory ETCBA, which may provide the evidence for the adoption and development of ambulatory ETCBA. Meantime, the present study also showed significant economic benefits and a shorter duration of hospitalization in ambulatory ETCBA, which was solid but not surprising because the ambulatory management was administrated to achieve these purposes. Additionally, multiple studies on ambulatory surgery reported similar patient benefits (7, 13–16).

We noticed that included patients were mainly female, which might be caused by the low-level of aesthetic demands of male patients and could be noticed in papers focusing on endoscopic thyroid surgery as well (10, 17). Rare complications, such as seroma and hematoma, all occurred in-hospital within 24 hours after ETCBA, and did not need an invasive treatment or re-operation. However, though with no significance, the present study did show a higher complication rate of ambulatory ETCBA than conventional ETCBA (28.3% vs. 21.8%). Among patients with thyroid cancer, the complication incidence of the ambulatory group was even 12.9% higher than the conventional group. Thus, a prospective study with a larger cohort is needed to validate the safety of ambulatory ETCBA, especially among patients with thyroid cancer, and to investigate the reasons of it.

Nevertheless, this study also had some limitations. Firstly, we failed to investigate the role of ambulatory ETCBA due to the ambulatory ETCBA was currently not allowed in most medical centers. However we considered this study could serve as an important foundation from the conventional ETCBA to outpatient ETCBA. Secondly, patients with permanent hypoparathyroidism still had a chance to recover even after

TABLE 4 | Results of DASS-21.

Characteristic	Ambulatory group (n=159)	Conventional group (n=101)	*P*
Depression	3.77 ± 2.06	3.86 ± 1.91	0.731
Anxiety	7.79 ± 2.55	7.12 ± 2.64	0.041
Stress	6.91 ± 2.61	6.07 ± 2.89	0.016

Data are expressed as mean ± standard deviation.

TABLE 5 | Subgroup analyses among patients with thyroid cancer.

Characteristic	Ambulatory group (n=125)	Conventional group (n=81)	*P*
Duration of surgery (min)	193.21 ± 30.44	187.04 ± 28.92	0.149
Blood loss (ml)	19.27 ± 11.07	18.25 ± 8.15	0.446
Postoperative complications	47 (37.6)	20 (24.7)	0.068
Transient hypoparathyroidism	39 (24.5)	17 (21.0)	
Permanent hypoparathyroidism	4 (2.5)	0 (0.0)	
Hypoglycemia	0 (0.0)	0 (0.0)	
Transient voice change	3 (2.4)	2 (2.0)	
Seroma	1 (0.6)	0 (0.0)	
Pulmonary infection	0 (0.0)	1 (1.0)	
Hematoma	1 (0.6)	0 (0.0)	
Transfer to the conventional ward	2 (1.6)	–	–
30-days readmission	1 (0.8)	0 (0.0)	1.000
Recurrence of malignancy	1 (0.8)	1 (1.2)	0.633
Economic cost (yuan)	14778.09 ± 2092.45	20568.27 ± 4476.33	<0.001
Duration of hospitalization (day)	1.04 ± 0.32	5.54 ± 1.50	<0.001
Depression	3.82 ± 2.03	4.00 ± 1.83	0.528
Anxiety	7.92 ± 2.52	7.07 ± 2.65	0.022
Stress	6.95 ± 2.68	6.04 ± 2.91	0.022

Data are expressed as mean ± standard deviation or n (%).

six months, which might cause inaccurate complication data. Thirdly, the follow-up time was too short to fully investigate the long-term outcomes, which would be focused on in the future report with continuous follow-up. Lastly, this study preliminarily showed the mental health assessment of patients undergone ETCBA. However, although no patient was reported to have a history of psychotropic drugs, the correlation may exist between the mental health and the diagnosis of disease. We failed to investigate it because the mental changes may happen before the diagnosis of thyroid nodules, and it is hard to access patients for such assessments before the diagnosis. Future studies will be performed to deal these questions for a more comprehensive assessment of patient mental health.

CONCLUSION

Ambulatory ETCBA is as safe as conventional ETCBA for selective patients with thyroid nodules or thyroid cancer, however with significant economic benefits and shorter duration of hospitalization. Extra attention should be paid to manage the anxiety and stress of patients who received ambulatory ETCBA.

DATA AVAILABILITY STATEMENT

The raw data supporting the conclusions of this article will be made available by the authors, without undue reservation.

ETHICS STATEMENT

The studies involving human participants were reviewed and approved by Institutional Ethics Committee of Xiangya Hospital, Central South University. Written informed consent for participation was not required for this study in accordance with the national legislation and the institutional requirements.

AUTHOR CONTRIBUTIONS

All authors made substantive intellectual contributions to this study to qualify as authors. XL conceived of the design of the study. FX modified the design of the study. ZZ and FX performed the study, collected the data, and contributed to the design of the study. ZZ analyzed the data. ZZ drafted Result, Discussion, and Conclusion sections. FX drafted Methods sections. FX and XL edited the manuscript. All authors read and approved the final manuscript. All authors have agreed to be accountable for all aspects of the work in ensuring that questions related to the accuracy or integrity of any part of the work are appropriately investigated and resolved.

FUNDING

This work was supported by the National Natural Science Foundation of China (grant No. 82073262) and the Hunan Province Natural Science Foundation (grant number 2019JJ40475).

SUPPLEMENTARY MATERIAL

The Supplementary Material for this article can be found online at: https://www.frontiersin.org/articles/10.3389/fendo.2021.795627/full#supplementary-material

REFERENCES

1. Singh Ospina N, Maraka S, Espinosa De Ycaza AE, Ahn HS, Castro MR, Morris JC, et al. Physical Exam in Asymptomatic People Drivers the Detection of Thyroid Nodules Undergoing Ultrasound Guided Fine Needle Aspiration Biopsy. *Endocrine* (2016) 54(2):433–9. doi: 10.1007/s12020-016-1054-y
2. Valderrabano P, Khazai L, Thompson ZJ, Leon ME, Otto KJ, Hallanger-Johnson JE, et al. Cancer Risk Stratification of Indeterminate Thyroid Nodules: A Cytological Approach. *Thyroid: Off J Am Thyroid Assoc* (2017) 27(10):1277–84. doi: 10.1089/thy.2017.0221
3. Wang C, Feng Z, Li J, Yang W, Zhai H, Choi N, et al. Endoscopic Thyroidectomy *via* Areola Approach: Summary of 1,250 Cases in a Single Institution. *Surg Endoscopy* (2015) 29(1):192–201. doi: 10.1007/s00464-014-3658-8
4. Park KN, Jung C, Mok JO, Kwak JJ, Lee SW. Prospective Comparative Study of Endoscopic *via* Unilateral Axillobreast Approach Versus Open Conventional Total Thyroidectomy in Patients With Papillary Thyroid Carcinoma. *Surg Endoscopy* (2016) 30(9):3797–801. doi: 10.1007/s00464-015-4676-x
5. Wu G, Fu J, Lin F, Luo Y, Lin E, Yan W. Endoscopic Central Lymph Node Dissection *via* Breast Combined With Oral Approach for Papillary Thyroid Carcinoma: A Preliminary Study. *World J Surg* (2017) 41(9):2280–2. doi: 10.1007/s00268-017-4015-6
6. Chai YJ, Chung JK, Anuwong A, Dionigi G, Kim HY, Hwang KT, et al. Transoral Endoscopic Thyroidectomy for Papillary Thyroid Microcarcinoma: Initial Experience of a Single Surgeon. *Ann Surg Treat Res* (2017) 93(2):70–5. doi: 10.4174/astr.2017.93.2.70
7. Zhang Z, Xia F, Wang W, Jiang B, Yao L, Huang Y, et al. Ambulatory Thyroidectomy is Safe and Beneficial in Papillary Thyroid Carcinoma: Randomized Controlled Trial. *Head Neck* (2020) 43(4):1116–21. doi: 10.1002/hed.26557
8. Hu QL, Livhits MJ, Ko CY, Yeh MW. Same-Day Discharge Is Not Associated With Increased Readmissions or Complications After Thyroid Operations. *Surgery* (2020) 167(1):117–23. doi: 10.1016/j.surg.2019.06.054
9. Prabhakar A, Helander E, Chopra N, Kaye AJ, Urman RD, Kaye AD. Preoperative Assessment for Ambulatory Surgery. *Curr Pain Headache R* (2017) 21(10):43. doi: 10.1007/s11916-017-0643-7
10. Qu R, Li J, Yang J, Sun P, Gong J, Wang C. Treatment of Differentiated Thyroid Cancer: Can Endoscopic Thyroidectomy *via* a Chest-Breast Approach Achieve Similar Therapeutic Effects as Open Surgery? *Surg Endoscopy* (2018) 32(12):4749–56. doi: 10.1007/s00464-018-6221-1
11. Lee DJ, Chin CJ, Hong CJ, Perera S, Witterick IJ. Outpatient Versus Inpatient Thyroidectomy: A Systematic Review and Meta-Analysis. *Head Neck* (2018) 40(1):192–202. doi: 10.1002/hed.24934
12. Jiang W, Yan PJ, Zhao CL, Si MB, Tian W, Zhang YJ, et al. Comparison of Total Endoscopic Thyroidectomy With Conventional Open Thyroidectomy for Treatment of Papillary Thyroid Cancer: A Systematic Review and Meta-Analysis. *Surg Endoscopy* (2020) 34(5):1891–903. doi: 10.1007/s00464-019-07283-y
13. Nordin AB, Shah SR, Kenney BD. Ambulatory Pediatric Surgery. *Semin Pediatr Surg* (2018) 27(2):75–8. doi: 10.1053/j.sempedsurg.2018.02.003
14. Thompson NB, Calandruccio JH. Hand Surgery in the Ambulatory Surgery Center. *Orthopedic Clinics North America* (2018) 49(1):69–72. doi: 10.1016/j.ocl.2017.08.009
15. Rider CM, Hong VY, Westbrooks TJ, Wang J, Sheffer BW, Kelly DM, et al. Surgical Treatment of Supracondylar Humeral Fractures in a Freestanding Ambulatory Surgery Center is as Safe as and Faster and More Cost-Effective Than in a Children's Hospital. *J Pediatr Orthopedics* (2018) 38(6):e343–8. doi: 10.1097/BPO.0000000000001171
16. Ford MC, Walters JD, Mulligan RP, Dabov GD, Mihalko WM, Mascioli AM, et al. Safety and Cost-Effectiveness of Outpatient Unicompartmental Knee Arthroplasty in the Ambulatory Surgery Center: A Matched Cohort Study. *Orthopedic Clinics North Am* (2020) 51(1):1–5. doi: 10.1016/j.ocl.2019.08.001
17. Guo Y, Qu R, Huo J, Wang C, Hu X, Chen C, et al. Technique for Endoscopic Thyroidectomy With Selective Lateral Neck Dissection *via* a Chest-Breast Approach. *Surg Endoscopy* (2019) 33(4):1334–41. doi: 10.1007/s00464-018-06608-7

Conflict of Interest: The authors declare that the research was conducted in the absence of any commercial or financial relationships that could be construed as a potential conflict of interest.

frontiers in Endocrinology

REVIEW
published: 22 December 2021
doi: 10.3389/fendo.2021.796984

Endoscopic Lateral Neck Dissection: A New Frontier in Endoscopic Thyroid Surgery

Zeyu Zhang, Botao Sun, Hui Ouyang, Rong Cong, Fada Xia and Xinying Li*

Department of Thyroid Surgery, Xiangya Hospital, Central South University, Changsha, China

Background: Endoscopic thyroidectomy and robotic thyroidectomy are effective and safe surgical options for thyroid surgery, with excellent cosmetic outcomes. However, in regard to lateral neck dissection (LND), much effort is required to alleviate cervical disfigurement derived from a long incision. Technologic innovations have allowed for endoscopic LND, without the need for extended cervical incisions and providing access to remote sites, including axillary, chest–breast, face-lift, transoral, and hybrid approaches.

Methods: A comprehensive review of published literature was performed using the search terms "lateral neck dissection", "thyroid", and "endoscopy OR endoscopic OR endoscope OR robotic" in PubMed.

Results: This review provides an overview of the current knowledge regarding endoscopic LND, and it specifically addresses the following points: 1) the surgical procedure, 2) the indications and contraindications, 3) the complications and surgical outcomes, and 4) the technical advantages and limitations. Robotic LND, totally endoscopic LND, and endoscope-assisted LND are separately discussed.

Conclusions: Endoscopic LND is a feasible and safe technique in terms of complete resection of the selected neck levels, complications, and cosmetic outcomes. However, it is recommended to strictly select criteria when expanding the population of eligible patients. A formal indication for endoscopic LND has not yet been established. Thus, a well-designed, multicenter study with a large cohort is necessary to confirm the feasibility, long-term outcomes, oncological safety, and influence of endoscopic LND on patient quality of life (QoL).

Keywords: endoscopic thyroidectomy, robotic thyroidectomy, lateral neck dissection, quality of life, cosmetic outcome

OPEN ACCESS

Edited by:
Hoon Yub Kim,
Korea University Anam Hospital, South Korea

Reviewed by:
Stefano Spiezia,
Local Health Authority Naples 1 Center, Italy
Kyung Tae,
Hanyang University, South Korea

****Correspondence:***
Fada Xia
xiafadaCSU@protonmail.com

Specialty section:
This article was submitted to Thyroid Endocrinology, a section of the journal Frontiers in Endocrinology

Received: *18 October 2021*
Accepted: *01 December 2021*
Published: *22 December 2021*

Citation:
Zhang Z, Sun B, Ouyang H, Cong R, Xia F and Li X (2021) Endoscopic Lateral Neck Dissection: A New Frontier in Endoscopic Thyroid Surgery. Front. Endocrinol. 12:796984. doi: 10.3389/fendo.2021.796984

1 BACKGROUND

In the past 10 years, the incidence of thyroid cancer (TC) has risen significantly among many districts and countries (1). Among the various subtypes, differentiated TC (DTC) accounts for approximately 95% of all TCs, and surgery is widely accepted as the most effective treatment for most DTC patients (2, 3). To date, conventional open thyroidectomy through a collar incision is the standard approach to thyroidectomy (4). While the majority of patients accept a thyroidectomy

scar, a certain percentage of patients are not satisfied with a visible scar on the neck. Some of them with cosmetic needs may even seek out further plastic surgery to improve the appearance of the scar (5, 6). With the growing appreciation of cosmetic needs, as well as the progression of endoscopic technologies, many thyroidectomy approaches have undergone significant development and modification to minimize potential scars, including minimally invasive cervical approaches and remote-access approaches (7).

Neck appearance has an important influence on the quality of life (QoL) of TC patients. Endoscopic thyroidectomy and robotic thyroidectomy have been shown to be effective and safe surgical options for thyroid surgery while providing excellent cosmetic results (8, 9). For patients who need lateral neck dissection (LND) due to metastatic lateral neck lymph nodes (LNs), a conspicuous scar (L-shaped, U-shaped, or extended collar) is often created, causing unsatisfactory experiences after the surgery. In fact, much effort has been made to alleviate cervical disfigurement derived from long incisions (10). Endoscopic LND has limited acceptance for TCs with local metastasis, and only strictly selected patients are eligible for the technique. Technologic innovations have enabled LND without extending the cervical incision and allowing access to remote sites, including axillary, chest–breast, face-lift, transoral, and hybrid approaches. These techniques can also be divided into robotic approaches and endoscopic approaches, depending on the types of instruments used. The endoscopic approaches can be subdivided into total endoscopic and endoscope-assisted approaches by the way the devices are used.

In this review, we discussed the current knowledge regarding endoscopic LND. We specifically addressed the following points: 1) the surgical procedure, 2) the indications and contraindications, 3) the complications and surgical outcomes, and 4) the technical advantages and limitations. LND achieved through a robotic surgery system is recognized as robotic LND. Although there is an ambiguous border between total endoscopic LND and endoscope-assisted LND, we attempted to distinguish them in this review. Total endoscopic LND is performed with trocars in an enclosed area with or without CO_2 insufflation, while endoscope-assisted LND is performed in a semiopen area without a trocar or CO_2 insufflation.

2 ROBOTIC LATERAL NECK DISSECTION

2.1 Surgical Procedures

2.1.1 Gasless, Transaxillary Approach

The robotic transaxillary approach is the most commonly reported robotic LND technique in the literature. A transaxillary approach was attempted *via* a 7- to 8-cm vertical incision located in the anterior axillary fold, and then a flap was created above the anterior surface of the pectoralis major muscle from the axilla to the clavicle (**Figure 1A**). The dissection should be continuously made until the submandibular gland and the posterior belly of the digastric muscle are reached. The skin flap is extended at the subplatysmal level in the neck superiorly to the mandible, posteriorly to the anterior border of the trapezius muscle, and anteriorly to the midline of the neck. The omohyoid muscle is interrupted at the thyroid cartilage, with the identification and dissociation of the internal jugular vein (IJV). A long and wide retractor blade is placed through the tunnel, and the flap and sternocleidomastoid muscle (SCM) are lifted to create a space for the operation. All four robotic arms are inserted through the same tunnel, and thyroidectomy and central neck dissection (CND) are performed as in conventional procedures. After the IJV is skeletonized and level III, IV, and VB dissections are performed, re-docking may be necessary for additional level II dissections. In addition, LNs located in levels IIB and VA, which are not routinely included in lymphadenectomy, can also be exposed and dissected (11–21).

2.1.2 Bilateral Axillary Breast Approach

This approach requires four incisions, including a circumareolar incision in each breast and a vertical incision in each axilla. Compared with a simple thyroidectomy, a larger flap, up to the inferior border of the submandibular gland, superiorly to the angle of the mandible and posteriorly to the anterior edge of the trapezius, is needed for LND (**Figure 1B**). Two suture lines are used to pull the SCM laterally to expose the lateral cervical compartment, which can also be achieved by separating the SCM and the strap muscles. Similar to TA, the camera may need to be moved for better level II dissection. It is very important to preserve the brachial plexus and spinal accessory nerve (SAN) while dissecting level V LNs. Clipped level V LNs are moved to level IV through the bottom of the SCM. Additionally, to preserve the SAN, the posterior belly of the digastric muscle should be exposed while dissecting (22–25).

2.1.3 Unilateral Retroauricular Approach

The retroauricular approach (RA) needs an L-shaped incision behind the auricle, and a flap is created above the SCM, proceeding anteriorly to the midline of the neck and extending superiorly to the submandibular gland and inferiorly to the level of the clavicle and sternal notch (**Figure 1C**). The flap is subsequently retracted and maintained by self-retaining retractors, and three arms of the da Vinci Surgical System are usually used in this approach. Specifically, the dissections are usually performed with the assistance of the robotic arms, while the exposure and dissection of the accessory nerve and LNs of levels II and III can be achieved under direct vision with regular surgical instruments (26, 27).

Kim and Byeon et al. reported a modified transaxillary and retroauricular (TARA) robot-assisted neck dissection. SAN can be identified through the RA incision. LNs of level II, VA, and upper level III can be recognized and dissected under direct vision, while the LNs of levels III, VB, and IV can be recognized and dissected with the assistance of robotic arms through the transaxillary approach. Thyroidectomy and CND can also be accomplished *via* TA (28, 29).

2.1.4 Transoral Approach

Few studies have applied TO during robotic dissection. Tae et al. reported one case of dissecting LNs of levels III and IV.

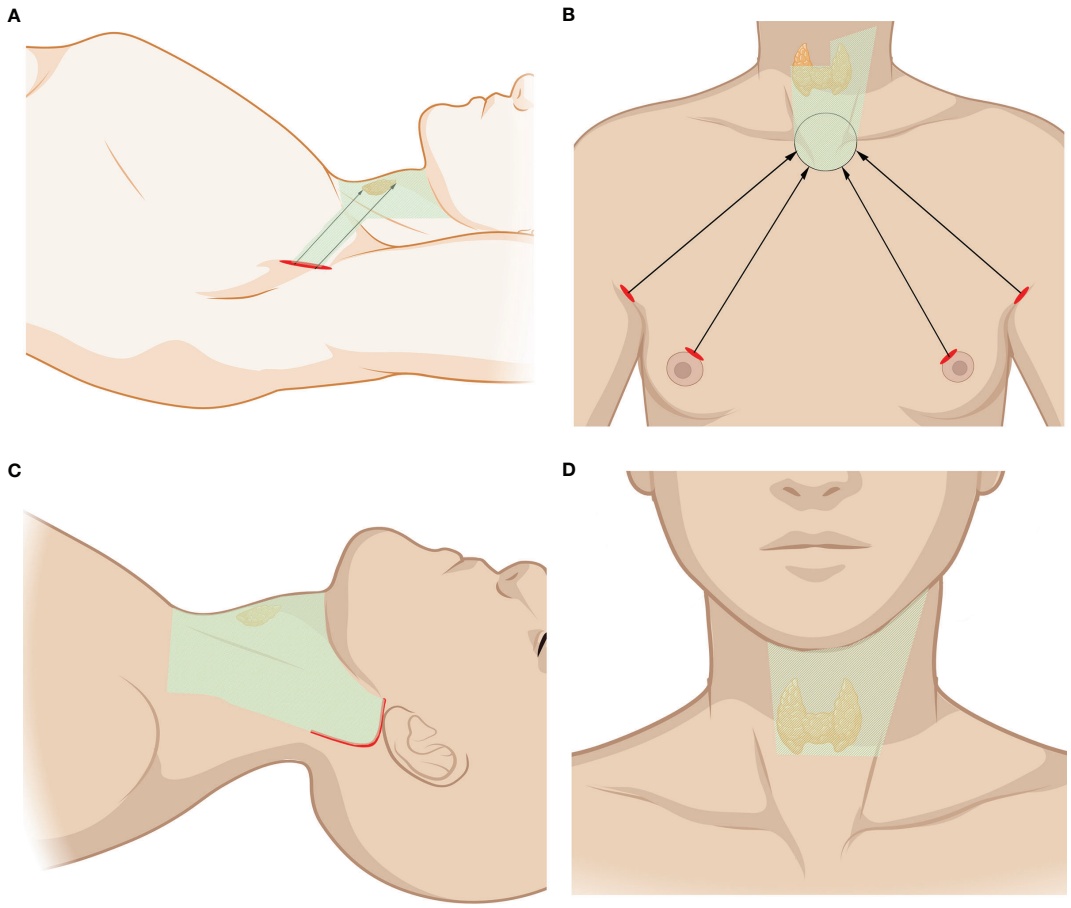

FIGURE 1 | Robotic lateral neck dissection (LND) approaches. **(A)** Transaxillary approach. **(B)** Bilateral axillary breast approach (BABA). **(C)** Unilateral retroauricular approach (RA). **(D)** Transoral approach (TO); incision sites were the same in totally endoscopic TO approach. The area of raised skin flap was marked with green wireframes.

One central incision and two lateral incisions were made on the base of the lower lip frenulum and the oral commissure. A flap is required inferiorly to the sternal and clavicle notch and laterally to the SCM. Another incision is required in the right axillary region for a third robotic instrument (**Figure 1D**). Total thyroidectomy and bilateral CND are similar to those of the endoscopic transoral approach. The SCM can be retracted to obtain a better view of the operation. With good exposure and protection of the IJV, the LNs of levels III and IV can be subsequently dissected (30).

2.2 Indications and Contraindications

2.2.1 Gasless, Transaxillary Approach

Based on the experience of centers that have performed this procedure thus far, the inclusion criteria are as follows: 1) unilateral DTC with cervical LN metastasis and 2) without previous surgical treatments of TC. The exclusion criteria are usually as follows: 1) unrelated pathologic conditions of the neck or shoulder; 2) extensive extrathyroidal spread; 3) metastatic LNs are fused or fixed; 4) metastatic LNs on the substernal or the infraclavicular area; 5) recurrent disease; and 6) distant metastasis.

2.2.2 Bilateral Axillary Breast Approach

The inclusion criteria are as follows: 1) primary tumor size <3 cm without local invasion; 2) LN metastasis derived from DTC; 3) largest LN diameter <2 cm; and 4) an advanced cosmetic need. The exclusion criteria are usually as follows: 1) previous neck or chest surgery; 2) body mass index (BMI) >30 or short neck; 3) extensive extrathyroidal spread; 4) metastatic LNs in the level V regions or below the sternoclavicular joint; 5) metastatic LNs fused or fixed; and 6) distant metastasis.

2.2.3 Unilateral Retroauricular Approach

The inclusion criteria for RA are as follows: 1) unilateral tumor and 2) with no previous history of treatment for thyroid carcinoma. The exclusion criteria are as follows: 1) recurrent disease; 2) unrelated pathologic conditions of the retroauricular area; 3) extensive extrathyroidal spread; 4) metastatic LNs fused or fixed; and 5) distant metastasis.

2.2.4 Transoral Approach

The inclusion criteria for the transoral approach are as follows: 1) primary tumor size <2 cm in the unilateral lobe; 2) without

capsular invasion; 3) suspected level III/IV LN metastases; 4) an advanced cosmetic need; and 5) no evidence of thyroiditis. The exclusion criteria are as follows: 1) previous neck or chest surgery; 2) BMI > 30 or short neck; 3) extensive extrathyroidal spread; 4) metastatic LNs in the level I, II, or V regions; 5) level III or IV metastatic LNs fused or fixed; and 6) distant metastasis.

2.3 Complications and Outcomes

He et al. reported a cohort of 260 patients treated *via* the bilateral axillary breast approach (BABA). After surgery, 19.6% of patients developed transient hypocalcemia, and 1.15% developed transient hoarseness without permanent hypocalcemia or hoarseness. A total of 1.15% of patients developed a seroma, while less than 1% of patients have less chylar leakage or tracheal fistula (24). In Kim's cohort, they reported 42 patients undergoing robotic modified radical neck dissection through TA with a 5-year follow-up time, and a 1:3 matching analysis with the conventional open procedure was conducted. Their results showed no significant difference in the complication rate between groups (58.5% in the robotic group and 62.7% in the conventional group), with transient hypocalcemia as the most common complication in both groups. Lymphatic fistula in one case and transient hypocalcemia in three (6.2%) cases were reported in Lira's cohort with an RA. No other surgical complications were described (26). In other comparative studies, the reported complication rates were not different between robotic and open surgeries (12, 14, 20, 23, 26). Minor chyle leakages, temporary recurrent laryngeal nerve (RLN) palsy, arm movement disorders, and Horner syndrome have been noticed after robotic surgeries (12, 20). Kim et al. reported as many as 500 cases of robotic LND. Permanent hypocalcemia, permanent RLN injury, Horner's syndrome, vagus nerve injury, and wound infection were noticed with extremely low rates (21). The general characteristics, technical safety (complications), and oncological outcomes of robotic surgeries are listed in **Table 1**.

In He's cohort of BABA procedures, all 260 patients experienced varying degrees of paraesthesia in the neck and chest; however, they mainly recovered within 4–12 months. All of the patients were extremely satisfied or satisfied with the cosmetic results. Only one case was identified with a tumor recurrence in the short-term follow-up period (1–48 months) (24). Lee's comparative study concerning TA and conventional thyroidectomy investigated pain scores, paraesthesia, and cosmetic satisfaction. While no significant difference was detected in pain scores, paraesthesia of the neck was found more frequently after conventional thyroidectomy; however, paraesthesia of the chest was more frequent in the robotic group. Moreover, the robotic group had better cosmetic satisfaction than the conventional group, and the neck and shoulder function scores were not different between the two groups (14). The cosmetic effects and other QoL results are listed in **Table 2**.

Meanwhile, robotic surgeries are as effective in harvesting LNs as conventional surgery (20). Serum triglyceride (TG) levels (thyroid-stimulating hormone (TSH) suppressed), neck ultrasound, ultrasound-guided fine-needle aspiration (FNA), CT, and PET-CT were used to evaluate disease recurrence. Multiple studies have revealed that the recurrence and mortality rates are not different between robotic and open surgeries (13, 16, 20, 23, 24). In Kim's two cohorts investigating cancer recurrence, recurrence rates over 5 years (the longest follow-up period as reported) did not differ between the robotic and open groups (2.4 vs. 2.9%), showing a consistent oncological effect (12, 21).

2.4 Technical Advantages and Limitations

Robotic instruments have shown additional superiorities, over other endoscopic instruments, including tremor-free, stabilized, and 7-degree freedom movement of instruments; 3-dimensional endoscopic view; self-controlled traction; and optimized ergonomics. Delicate anatomical operation with versatile instruments can assist with complex intraoperative situations and lead to easier preservation of the parathyroid gland and the identification of nerves, vessels, and lymphangion. With good exposure, dissection of all levels of the neck compartments can be theoretically achievable. In Kim's experience, setting contraindications of robotic LND according to the TNM staging system is unnecessary. They believe that experienced surgeons can determine whether they can complete robotic LND even though a patient may have metastatic nodes in level VII or primary cancer can be a T4 lesion (21). This suggests that the indication for robotic LND can be easily further expanded with growing experience. Several technical difficulties and limitations in the application of robot-assisted LND are as follows: 1) a longer operative time; 2) a wider flap dissection is needed, which means greater trauma and more severe paraesthesia of the flap area; 3) higher costs; 4) a prominent clavicle may make it hard to completely remove LNs of level IV using the TA and BABA approaches; 5) the upper neck (level II) is difficult to remove (except in the RA approach); and 6) splitting the SCM may exaggerate neck pain and stiffness, especially with bilateral procedures.

3 TOTALLY ENDOSCOPIC LATERAL NECK DISSECTION

3.1 Surgical Procedures

3.1.1 Chest–Breast Approach

The chest–breast approach is characterized by CO_2 gas usage and the presence of all of the incisions and working space confined to the anterior chest wall, including the breast. Various total endoscopic approaches have been described, such as approaches *via* the parasternum and bilateral mammary areolas (chest–breast, **Figure 2A**) (37) and total mammary areolas (breast, **Figure 2B**) (38, 39). Epinephrine solution or liquid–gas mix tumescent is used to control bleeding while creating the flap. One 10-mm incision at the margin of the breast (parasternum) or at the right areola for the laparoscope and two 5-mm incisions at the bilateral areola for operating the instruments are made for the trocar location. The working space is filled with CO_2, maintaining a pressure of approximately 7 mmHg. Devices have been introduced in this kind of approach, such as U-shaped retractors, suspension sutures, ultrasonic coagulators, and minilap (31, 37–43).

After thyroidectomy and CND, the working space should be expanded superiorly to the lower edge of the submandibular gland and laterally to the lateral edge of the SCM. The steps of LND are

TABLE 1 | General characteristics, technical safety, and oncological outcomes of robotic studies.

Surgeons	Instruments/ approaches	No. of cases	Study type	Dissected neck levels	Complications (n)	Difference in retrieved nodes*	Follow-up time (months) and recurrence (n)	Ref
Kim et al.	Robotic transaxillary[#]	42	Retrospective/ comparative	IIA, IIB, III, IV, and Vb	Seroma, 4 Chyle leakage, 4 Temporary vocal cord paresis, 3 Transient hypocalcemia, 18 Arm movement disorder, 1	No difference	5 years 1	(12)
Lira et al.	Robotic retroauricular	12	Retrospective/ case series	II–V	Reoperation, 1 Transient hypocalcemia, 2 Vocal cord paresis, 3 Surgical site infection, 1	NA	17.4 (mean) 0	(26)
Tae et al.	Robotic transoral	1	Case report	III, IV	None	NA	NA NA	(30)
Yu et al.	Robotic BABA	15	Retrospective/ case series	II–V	Transient hypocalcemia, 7 Temporary vocal cord paresis, 1 Horner's syndrome, 1	NA	18.7 (mean) 0	(22)
Byeon et al.	Robotic retroauricular	4	Retrospective/ case series	II–V	Seroma, 1 Transient hypocalcemia, 2 Chyle leakage, 1	NA	NA NA	(27)
Kim et al.	Robotic BABA	13	Retrospective/ comparative	II, III, IV, and Vb	Chyle leakage, 1	No difference	15.9 (mean) 0	(23)
He et al.	Robotic BABA	260	Retrospective/ case series	II, III, IV, and Vb**	Transient hypocalcemia, 51 Temporary vocal cord paresis, 3 Seroma, 3 Surgical site infection, 1 Tracheal fistula, 1	Presenting as number of retrieved nodes	28.6 (mean) 0	(24)
Byeon et al.	Robotic TARA	1	Case report	III, IV	None	Presenting as number of retrieved nodes	NA NA	(29)
Kim et al.	Robotic TARA	22	Retrospective/ comparative	II–V	Seroma/hematoma, 3 Transient hypocalcemia, 6 Chyle leakage, 1 Earlobe numbness, 6 Temporary vocal cord paresis, 2	No difference	15.9 (mean) 0	(28)
Song et al.	Robotic BABA	4	Retrospective/ case series	Bilateral MRND***	Pleural effusion (not chylous)	Presenting as number of retrieved nodes	17-36 (range) 0	(25)
Kang et al.	Robotic transaxillary	56	Retrospective/ comparative	IIA, III, IV, and Vb	Seroma/hematoma, 5 Transient hypocalcemia, 27 Chyle leakage, 5 Temporary vocal cord paresis, 2 Reoperation, 1	No difference	One year (fixed time point) 0	(20)
Lee et al.	Robotic transaxillary	62	Retrospective/ comparative	IIA, III, IV, and Vb	Seroma/hematoma, 2 Transient hypocalcemia, 24	No difference	8.4 (mean) 0	(14)

(Continued)

TABLE 1 | Continued

Surgeons	Instruments/ approaches	No. of cases	Study type	Dissected neck levels	Complications (n)	Difference in retrieved nodes*	Follow-up time (months) and recurrence (n)	Ref
					Chyle leakage, 1 Temporary vocal cord paresis, 2			
Kim et al.	Robotic transaxillary	500	Retrospective/ case series	II–V	Transient hypocalcemia, 151 Permanent hypocalcemia, 20 Temporary vocal cord paresis, 20 Permanent vocal cord paresis, 5 Seroma/hematoma, 19 Chyle leakage, 26 Horner's syndrome, 2 Vagus nerve injury, 1 Wound infection, 1	Presenting as number of retrieved nodes	NA 5	(21)

NA, not available; MRND, modified radical neck dissection; LND, lateral neck dissection.
#Only studies regarding robotic transaxillary approaches with case number >40 have been included.
**Compared with those retrieved in conventional open surgery.*
***Unilateral LND was performed in 239 cases and bilateral LND in 21 cases.*
****Dissected levels were not described.*

basically identical to those of conventional thyroidectomy after the SCM is split longitudinally to expose the lateral cervical compartment. Particularly, the posterior border of the IJV and the SAN should be carefully anatomized when removing the LNs of levels 2A and 2B. The transverse cervical artery, phrenic nerve, vagus nerve, brachial plexus, and cervical plexus are exposed and protected (31, 37–43).

3.1.2 Transoral Approach

Tan et al. reported selective LND *via* a transoral endoscopic approach in 20 PTC cases. Ngo et al. also reported a case of LND *via* a transoral endoscopic approach. Three vestibular incisions were made in the mouth vestibular (**Figure 1D**). The working space is described as between the sternohyoid muscles and the platysma muscle. Upon completing the thyroid lobectomy and

TABLE 2 | Cosmetic results and other quality of life (QoL) results in retrieved references.

Surgeons	Cosmetic evaluation methods	Cosmetic results	Other QoL evaluation	Other results	Ref
He et al.	Five-point scale	4.68 ± 0.35 (score)*	None	None	(24)
Kim et al.	Five-point scale	3.9 ± 1.0, better than open group	None	None	(28)
Lee et al.	Five-point scale	Better than open group**	Pain score, voice handicap index, etc.#	No difference	(14)
Song et al.	Five-point scale	1.64 ± 0.61 (one month), better than open group	Pain and paresthesia scores of the neck and anterior chest area	No difference or higher in robotic group***	(13)
Guo et al.	NA	8.3 ± 0.7, better than open group	Pain scores	No difference	(31)
Lin et al.	Visual analog scale (VAS)	9 (mean, range 5–10)*	Pain score, voice handicap index, etc.#	Presenting as scores	(32)
Zhang et al.	Verbal response scale and numeric rating scale	2.8 ± 0.5 and 7.0 ± 0.9, better than open group	Pain score (VAS)	Better in endoscopic assisted group	(33)
Zhang et al.	Verbal response scale and numeric rating scale	7.0 ± 1.2 and 2.7 ± 0.6, Better than open group	None	None	(34)
Lin et al.	Verbal response scale	9 (mean, range 9–10), better than open group	Pain score, voice handicap index, etc.#	No difference	(35)
Zhang et al.	Five-point scale	1.4 ± 0.6 (3 months), better than open group	Pain and paresthesia scores of the neck	Better in endoscopic assisted group	(36)

NA, not available.
**Case series studies.*
***Presenting as numbers of satisfied or dissatisfied patients.*
****Pain and paresthesia scores of the neck were similar as those in open surgery, while pain and paresthesia scores of the anterior chest area were higher.*
#Other QoL evaluation included swallowing impairment score (SIS-6), neck dissection impairment index (NDII), and arm abduction test (AAT) in these studies.

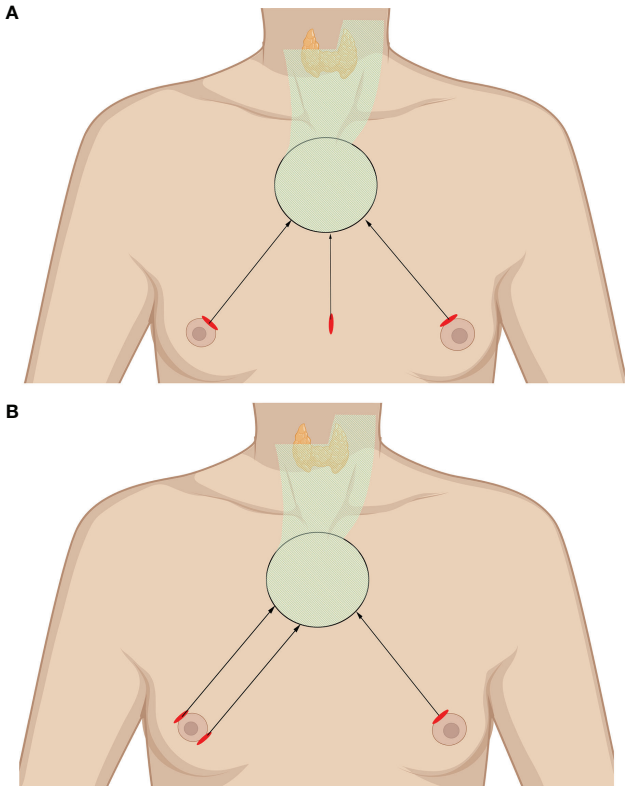

FIGURE 2 | Totally endoscopic lateral neck dissection (LND) approaches. **(A)** Chest–breast approach. **(B)** Total mammary areolas approach. The area of raised skin flap was marked with green wireframes.

CND, selective LND is performed through the two heads of the SCM. After removal of the omohyoid muscle to create a larger space, the IJV should be anatomized and well protected. The LNs of levels III and IV can be subsequently resected starting from the level of the carotid bifurcation to the clavicle (44, 45).

3.2 Indications and Contraindications

3.2.1 Chest–Breast Approach

Based on the experience of centers that have performed this procedure thus far, the inclusion criteria for chest–breast approach are as follows: 1) primary tumor size <3 cm without local invasion; 2) LN metastasis derived from DTC; 3) largest LN diameter <2 cm; and 4) an advanced cosmetic need. The exclusion criteria are usually as follows: 1) previous neck or chest surgery; 2) BMI >30 or short neck; 3) extensive extrathyroidal spread; 4) metastatic LNs in the level V regions or below the sternoclavicular joint; 5) metastatic LNs fused or fixed; and 6) distant metastasis (39, 40, 42).

3.2.2 Transoral Approach

The inclusion criteria for the transoral approach are as follows: 1) primary tumor size <2 cm in the unilateral lobe; 2) without capsular invasion; 3) suspected level III/IV LN metastases; 4) an advanced cosmetic need; and 5) no evidence of thyroiditis. The exclusion criteria are as follows: 1) previous neck or chest surgery; 2) BMI > 30 or short neck; 3) extensive extrathyroidal spread; 4) metastatic LNs in the level I, II, or V regions; 5) level III or IV metastatic LNs fused or fixed; and 6) distant metastasis (44).

3.3 Complications and Outcomes

Several centers have reported the perioperative complications of totally endoscopic LND. Common complications of thyroidectomy and lymphadenectomy may also occur during endoscopic surgery. Yan et al. performed and reported their rich experience with endoscopic thyroidectomy *via* a breast approach with levels II, III, and IV LND. They retrospectively compared the endoscopic LND group with 155 patients and the conventional open LND group with 102 patients. Operation-related complications, such as transit hoarseness, hematoma, IJV rupture, and limb lift restriction occurred in both the endoscopic LND group and the open group. No significant difference was found for the complication incidences between the groups. However, the mean operating duration was longer in the endoscopic LND group than in the open group (40). Guo et al. also confirmed the prolonged LND time of endoscopic thyroidectomy. Consistently, no significant difference was found in transient voice change, transient hypoparathyroidism, postoperative lymphatic leakage, or intraoperative large blood vessel injury, while no severe complications, such as hematoma, permanent hypoparathyroidism, and permanent nerve injury were found to occur (31). Wang et al. reported one case of conversion to open surgery due to right RLN invasion. Injury to the SAN was found in 2 patients, who subsequently developed light SCM dystrophy (41). Cervical plexus and hypoglossal nerve injury have been reported in Chen's study (46). The general characteristics, technical safety (complications), and oncological outcomes of totally endoscopic surgeries are listed in **Table 3**.

In contrasting analyses, no difference was found in the number of dissected lateral LNs between the endoscopic LND group and the conventional open LND group (31). Yan et al. calculated the number of dissected LNs in levels II, III, and IV. The numbers at each level were statistically identical in the endoscopic group and open group (40). Cosmetic satisfaction scores were mentioned in only one study, and the endoscopic group had a higher score than the open group (**Table 2**) (31). The median follow-up period in Wang's cohort was 24 months, ranging from 4 to 59 months. Postoperative thyroglobulin (Tg) levels were used to evaluate tumor recurrence, and Tg < 1 ng/ml was achieved in 80% of individuals 1 year after surgery, with only one recurrence at the LNs of level VII. All 37 patients were satisfied with the cosmetic results (41). The study by Yan et al. reported local recurrence in four patients (2 in the endoscopic group and 2 in the open group) during follow-up, while no patients developed distant metastases or tumor-related death (40).

3.4 Technical Advantages and Limitations

Although the endoscopic device is not as versatile as the robotic device, it is easy and economical to apply in most hospitals. The effectiveness and safety of endoscopic surgery have been widely proven to be the same as those of robotic surgery in the treatment

TABLE 3 | General characteristics, technical safety, and oncological outcomes of totally endoscopic and endoscope-assisted studies.

Surgeons	Instruments/ approaches	No. of cases	Study type	Dissected neck levels	Complications (n)	Difference in retrieved nodes*	Follow-up time (months) and Recurrence (n)	Ref
Guo et al.	Totally endoscopic/ chest–breast[#]	24	Retrospective/ case series and comparative	II, III, IV	Blood vessels injury, 2 Transient hypocalcemia, 4 Chyle leakage, 2 Temporary vocal cord paresis, 1	No difference	NA 0	(31, 47)**
Huo et al.	Totally endoscopic/ chest–breast	20	Retrospective/ case series	II, III, IV	Blood vessels injury, 2 Chyle leakage, 1 Temporary vocal cord paresis, 1 Transient hypocalcemia, 4	NA	NA NA	(43)
Wang et al.	Totally endoscopic/ chest–breast	37	Retrospective/ case series	II– V	Temporary vocal cord paresis, 3 Transient hypocalcemia, 12 Permanent hypocalcemia, 1 Spinal accessory nerve injury, 2 Chyle leakage, 1 Chest wall ecchymosis, 1	Presenting as number of retrieved nodes	24 (mean) 1	(41)
Wang et al.	Totally endoscopic/ chest–breast	155	Retrospective/ comparative	II, III, IV	Temporary vocal cord paresis, 8 Seroma, 3 Chyle leakage, 4 Infection, 2 Internal jugular vein rupture, 19 Limb lift restriction, 6	No difference	10 years (max) 2	(37, 40, 42)**
Chen et al	Totally endoscopic/ chest–breast	35	Retrospective/ case series	IIA, III, IV	Chyle leakage, 1 cervical plexus injury, 7 hypoglossal nerve injury, 1 accessory nerve injury, 3 internal jugular vein injuries, 2	Presenting as number of retrieved nodes	18.1 (mean) None	(46)
Huo et al.	Totally endoscopic/ chest–breast	12	Retrospective/ comparative	II, III, IV, VB	Chyle leakage, 1 Temporary vocal cord paresis, 2	No difference	NA None	(48)
Kitagawa et al.	Endoscope assisted/ anterior chest	3	Retrospective/ case series	Lateral zone***	None	NA	NA NA	(49)
Wu et al.	Endoscope assisted	26	Retrospective/ case series	IIA, III, IV	Temporary vocal cord paresis, 2 Transient hypocalcemia, 4	Presenting as number of retrieved nodes	19 (mean) None	(10)
Zhang et al.	Endoscope assisted	26	Retrospective/ case series	II– V	Spinal accessory nerve injury, 1	Presenting as number of retrieved nodes	NA NA	(50, 51)**
Zhang et al	Endoscope assisted	130	Retrospective/ case series	II– IV or II–V	Transient hypocalcemia, 19 Temporary vocal cord paresis, 7 Permanent vocal cord paresis, 3 Spinal accessory nerve injury, 2 Chyle leakage, 4 Seroma, 1	Presenting as number of retrieved nodes	19 (mean) None	(34, 52)**
Lin et al.	Endoscope assisted	18	Retrospective/ case series	II– IV	Transient hypocalcemia, 1	NA	54.5 (mean) None	(32)
Zhang et al.	Endoscope assisted	32	Prospective/ comparative	II– IV, VB	Temporary vocal cord paresis, 1 transient hypocalcemia, 4 Seroma, 1 Horner's syndrome, 1 Chyle leakage, 1	No difference	NA None	(33)

(Continued)

TABLE 3 | Continued

Surgeons	Instruments/ approaches	No. of cases	Study type	Dissected neck levels	Complications (n)	Difference in retrieved nodes*	Follow-up time (months) and Recurrence (n)	Ref
Lin et al.	Endoscope assisted/ anterior chest	31	Retrospective/ comparative	II– IV	Transient hypocalcemia, 2	No difference	NA None	(35)
Zhang et al	Endoscope assisted	18	Prospective/ comparative	II– V	Temporary vocal cord paresis, 6 Transient hypocalcemia, 3	No difference	NA NA	(36)

NA, not available.
#Only studies regarding total totally endoscopic/chest–breast and endoscope assisted (collar incision) with case number >10 have been included.
**Compared with those retrieved in conventional open surgery.*
***These studies may include repeatedly reported cases.*
****Dissected levels were not described.*

of TC. However, it is slightly inferior to robotic surgery in terms of the diversity of surgical approaches and the range of indications. Several technical difficulties and limitations in the application of endoscopic thyroidectomy and LND are as follows: 1) unexpected complications in endoscopic instrument usage, such as CO_2 embolism, tumor or metastatic LN rupture, and chest wall ecchymosis. 2) Poor surgical techniques, working space building, and lateral compartment exposure lead to a longer surgical time, which means a longer anesthesia time, increased cost, and a higher incidence of possible complications. 3) At present, the cosmetic evaluations are only descriptive. A quantitative, reproducible scoring system is needed. 4) In the breast approaches, level IV and VI lymph dissections are restricted by claviculation, while level V lymph dissections are restricted by the lateral border of the SCM. Due to endoscopic magnification and less space restriction, it will be easier to perform level IIB LND with endoscopic techniques than with open surgery. 5) Difficulty in level II and V lymph dissection with oral approaches: it will be difficult to expose level II LNs during surgical manipulation from the superior to inferior direction. Level V LNs are also restricted by the lateral border of the SCM. 6) SCM stiffness: in all of the studies, the SCM was split longitudinally to expose the lateral cervical compartment. However, the consequences of SCM splitting, such as stiffness, numbness, pain, and constriction, have not been evaluated.

4 ENDOSCOPE-ASSISTED LATERAL NECK DISSECTION

4.1 Surgical Procedure

Endoscope-assisted LND is characterized by the endoscopic removal of lateral LNs through an incision of approximately 2–4 cm without a trocar. Unlike total endoscopic LND, the working space of endoscope-assisted LND is not fully enclosed and is often remedied by a gasless traction system. Special instruments are introduced to lift the anterior neck skin without CO_2 gas as originally described by Miccoli and Lombardi (53, 54). Zhang et al. invented a working space creator and reported a cohort with the largest number of cases by using this instrument (34, 52). The working space is created from the posterior belly of the digastric muscle to the posterior border of the SCM (**Figure 3A**). The SCM and IJV are dissected and retracted reversely to expose the lateral lymph. The vagus nerve is carefully anatomized, followed by the removal of the LNs and surrounding fibroadipose tissue. Level II, III, and IV LNs can be dissected in the caudad to cephalad direction, while level III and IV LNs can also be dissected in the cephalad to caudad direction due to freedom from restriction. The SAN, cervical plexus, phrenic nerve, brachial plexus, and transverse cervical should be carefully protected (10, 32–34, 50–53).

Kitagawa and Lin et al. reported a totally gasless anterior chest approach. A 3.5-cm incision and another 0.5-cm incision were made on the tumor side of the chest wall and the lateral neck with a widely created working space (**Figure 3B**). The incision on the lateral neck should be widened to 2 cm when LND is required. The working space is subsequently widened to the

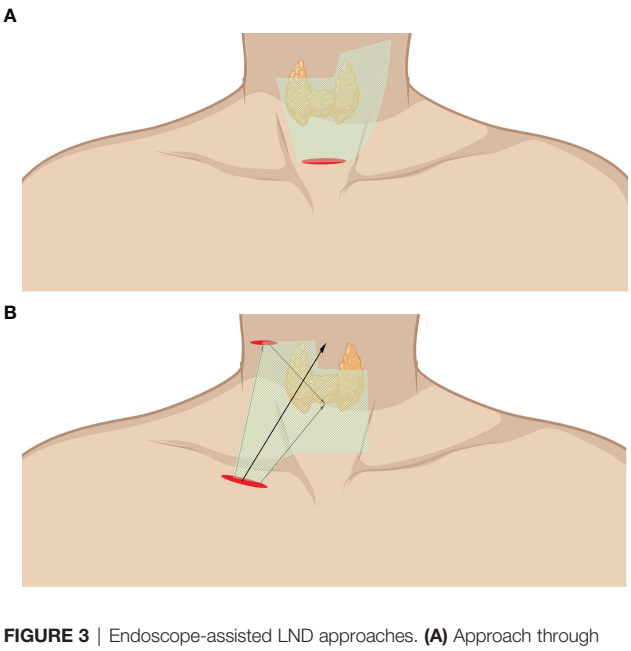

FIGURE 3 | Endoscope-assisted LND approaches. **(A)** Approach through the collar incision. **(B)** Approach through chest wall incision (infraclavicular incision). The area of raised skin flap was marked with green wireframes.

level of the lobulus auriculae, the posterior belly of the digastric muscle, the posterior border of the SCM, and the space beneath the SCM (35, 49).

4.2 Indications and Contraindication

The eligibility criteria were usually as follows: 1) unilateral tumor and 2) largest diameter <4 cm. The exclusion criteria were usually as follows: 1) extrathyroidal extension; 2) distant metastases; 3) LN metastases in level I or VA; and 4) history of previous neck surgery or radiation therapy (33, 34, 49).

4.3 Complications and Outcomes

Thyroidectomy and CND are performed as conventional open procedures. Transient RLN palsy and hypoparathyroidism rates are similar to those of the conventional open procedure. Wu et al. reported no conversion to open surgery, no significant blood loss, and only mild postoperative pain in their 26 cases (10). Zhang et al. reported an injury of the trapezius branch of the accessory nerve, causing weakness that recovered within 2 years (50). Kitagawa reported lateral LN clearance in three patients through a totally gasless anterior neck skin lifting method without any severe complications (49). Zhang et al. designed a prospective randomized study to compare video-assisted and open LND. One transient sympathetic nerve injury and one minor chyle leak were observed in the video-assisted group (33).

Cosmetic outcomes were generally better in endoscope-assisted surgery than in open surgery (32, 34, 36, 52). In Zhang's cohort, postoperative pain was significantly less severe in the endoscope-assisted group at 24 and 48 h after surgery (33). The incidence of voice change, swallowing, neck impairment, and arm abduction was not significantly different in Lin's cohort (the details can be found in **Table 2**) (35). In Wu's cohort, the postoperative Tg level was dramatically decreased to zero in most patients. Eleven patients received ^{131}I diagnostic whole-body scans at the 6- to 12-month follow-up, and no recurrence or metastasis was found (10). In Zhang's prospective cohorts, no patients showed any uptake of ^{131}I outside the thyroid bed as assessed by whole-body scans performed after the administration of 100 mCi of ^{131}I. Neck ultrasound showed no tumor recurrence or residual disease in either group during follow-up (33).

4.4 Technical Advantages and Limitations

Unlike other remote extracervical approaches, endoscope-assisted LND is characterized by less trauma, a shorter learning curve, and less demand for specific instruments. When uncontrolled bleeding or unexpected aggressiveness of the disease occurs, it is also not hard to convert to conventional thyroidectomy. As it is similar to the conventional open procedure, the indications for endoscope-assisted LND can be easily extended with growing experience. The extension of lateral neck clearance has been reported to include levels IIA, IIB, III, IV, and partly V (33). Zhang et al. have made some efforts to extend the indications, showing the feasibility of endoscopic upper mediastinal LN dissection in the treatment of papillary thyroid carcinoma with promising results (55).

Several technical difficulties and limitations in the application of endoscope-assisted LND still exist: 1) it leaves an obvious scar on the neck, although it is better than the scar from conventional thyroidectomy. 2) LNs of level I and VA are hard to reach and remove. 3) It has a longer operative time (which will decline rapidly with greater experience).

CONCLUSIONS AND FUTURE PERSPECTIVES

Endoscopic LND allows comprehensive en bloc removal of all lateral neck levels through a remote extracervical incision or an unextended collar incision. They are feasible and safe techniques in terms of the complete resection of selected neck levels, complications, and cosmetic outcomes. As the most commonly reported approach, robotic LND has more selective remote sites for robotic system docking. Device intelligence makes the theoretical indications less limited, but the obvious disadvantage is the high cost. In general, endoscopic LND is easy to carry out. The completeness of the surgical resection in selected compartments is satisfactory; however, some neck levels are difficult to achieve. Endoscope-assisted LND (cervical approach) is characterized by less trauma, close to open vision, and not limited by local tumor progression, and it can even be feasible for mediastinal LN dissection. Nevertheless, an obvious scar is still left on the neck. There is still controversy concerning the technical challenges, the introduction of new complications, and the operative trauma of endoscopic LND. Technical difficulties and limitations affect the different approaches. It is also challenging for all of the techniques to dissect all of the metastatic LNs in hard-to-reach areas or invaded areas. Moreover, unlike other procedures, additional trauma following the creation of the working space is inevitable due to the lack of free space in the neck. Theoretically, endoscopic approaches can provide meticulous dissection in the lateral neck. Complete surgical resection, a reduction in the time required, and less trauma will be achieved with the growing experience of surgeons. Regardless, it is recommended to strictly apply selection criteria when expanding the population of eligible patients in centers with a high volume of thyroid surgery. A formal indication for endoscopic LND has not yet been established. Thus, a well-designed, multicenter study with a large cohort is necessary to confirm the feasibility, long-term outcomes, oncological safety, and influence of endoscopic LND on patient QoL.

AUTHOR CONTRIBUTIONS

All authors contributed to drafting or revising the article, gave final approval of the version to be published, agreed to the submitted journal, and agree to be accountable for all aspects of the work.

FUNDING

This work was supported by the National Natural Science Foundation of China (grant no. 82073262) and the Hunan Province Natural Science Foundation (grant no. 2019JJ40475).

REFERENCES

1. Kitahara CM, Sosa JA. The Changing Incidence of Thyroid Cancer. *Nat Rev Endocrinol* (2016) 12:646–53. doi: 10.1038/nrendo.2016.110
2. Cabanillas ME, McFadden DG, Durante C. Thyroid Cancer. *Lancet* (2016) 388:2783–95. doi: 10.1016/S0140-6736(16)30172-6
3. Van Den Heede K, Tolley NS, Di Marco AN, Palazzo FF. Differentiated Thyroid Cancer: A Health Economic Review. *Cancers (Basel)* (2021) 13:2253. doi: 10.3390/cancers13092253
4. Duek I, Duek OS, Fliss DM. Minimally Invasive Approaches for Thyroid Surgery-Pitfalls and Promises. *Curr Oncol Rep* (2020) 22:77. doi: 10.1007/s11912-020-00939-2
5. Best AR, Shipchandler TZ, Cordes SR. Midcervical Scar Satisfaction in Thyroidectomy Patients. *Laryngoscope* (2017) 127:1247–52. doi: 10.1002/lary.26177
6. Russell JO, Sahli ZT, Shaear M, Razavi C, Ali K, Tufano RP. Transoral Thyroid and Parathyroid Surgery via the Vestibular Approach-A 2020 Update. *Gland Surg* (2020) 9:409–16. doi: 10.21037/gs.2020.03.05
7. Rossi L, Materazzi G, Bakkar S, Miccoli P. Recent Trends in Surgical Approach to Thyroid Cancer. *Front Endocrinol (Lausanne)* (2021) 12:699805. doi: 10.3389/fendo.2021.699805
8. Song CM, Bang HS, Kim HG, Park HJ, Tae K. Health-Related Quality of Life After Transoral Robotic Thyroidectomy in Papillary Thyroid Carcinoma. *Surgery* (2021) 170(1):99–105. doi: 10.1016/j.surg.2021.02.042
9. Nguyen HX, Nguyen LT, Nguyen HV, Nguyen HX, Trinh HL, Nguyen TX, et al. Comparison of Transoral Thyroidectomy Vestibular Approach and Unilateral Axillobreast Approach for Endoscopic Thyroidectomy: A Prospective Cohort Study. *J Laparoendosc Adv Surg Tech A* (2021) 31:11–7. doi: 10.1089/lap.2020.0272
10. Wu B, Ding Z, Fan Y, Deng X, Guo B, Kang J, et al. Video-Assisted Selective Lateral Neck Dissection for Papillary Thyroid Carcinoma. *Langenbecks Arch Surg* (2013) 398:395–401. doi: 10.1007/s00423-012-1045-2
11. Kang SW, Kim MJ, Chung WY. Gasless, Transaxillary Robotic Neck Dissection: The Technique and Evidence. *Gland Surg* (2018) 7:466–72. doi: 10.21037/gs.2017.09.09
12. Kim MJ, Lee J, Lee SG, Choi JB, Kim TH, Ban EJ, et al. Transaxillary Robotic Modified Radical Neck Dissection: A 5-Year Assessment of Operative and Oncologic Outcomes. *Surg Endosc* (2017) 31:1599–606. doi: 10.1007/s00464-016-5146-9
13. Song CM, Ji YB, Sung ES, Kim DS, Koo HR, Tae K. Comparison of Robotic Versus Conventional Selective Neck Dissection and Total Thyroidectomy for Papillary Thyroid Carcinoma. *Otolaryngol Head Neck Surg* (2016) 154:1005–13. doi: 10.1177/0194599816638084
14. Lee J, Kwon IS, Bae EH, Chung WY. Comparative Analysis of Oncological Outcomes and Quality of Life After Robotic Versus Conventional Open Thyroidectomy With Modified Radical Neck Dissection in Patients With Papillary Thyroid Carcinoma and Lateral Neck Node Metastases. *J Clin Endocrinol Metab* (2013) 98:2701–8. doi: 10.1210/jc.2013-1583
15. Tae K, Ji YB, Song CM, Min HJ, Lee SH, Kim DS. Robotic Lateral Neck Dissection by a Gasless Unilateral Axillobreast Approach for Differentiated Thyroid Carcinoma: Our Early Experience. *Surg Laparosc Endosc Percutan Tech* (2014) 24:e128–132. doi: 10.1097/SLE.0b013e3182a4bfa1
16. Kang SW, Park JH, Jeong JS, Lee CR, Park S, Lee SH, et al. Prospects of Robotic Thyroidectomy Using a Gasless, Transaxillary Approach for the Management of Thyroid Carcinoma. *Surg Laparosc Endosc Percutan Tech* (2011) 21:223–9. doi: 10.1097/SLE.0b013e3182266f31
17. Kang SW, Lee SH, Ryu HR, Lee KY, Jeong JJ, Nam KH, et al. Initial Experience With Robot-Assisted Modified Radical Neck Dissection for the Management of Thyroid Carcinoma With Lateral Neck Node Metastasis. *Surgery* (2010) 148:1214–21. doi: 10.1016/j.surg.2010.09.016
18. Kiriakopoulos A, Linos D. Gasless Transaxillary Robotic Versus Endoscopic Thyroidectomy: Exploring the Frontiers of Scarless Thyroidectomy Through a Preliminary Comparison Study. *Surg Endosc* (2012) 26:2797–801. doi: 10.1007/s00464-012-2281-9
19. Song CM, Park JS, Park W, Ji YB, Cho SH, Tae K. Feasibility of Charcoal Tattooing for Localization of Metastatic Lymph Nodes in Robotic Selective Neck Dissection for Papillary Thyroid Carcinoma. *Ann Surg Oncol* (2015) 22 Suppl 3:S669–675. doi: 10.1245/s10434-015-4860-1
20. Kang SW, Lee SH, Park JH, Jeong JS, Park S, Lee CR, et al. A Comparative Study of the Surgical Outcomes of Robotic and Conventional Open Modified Radical Neck Dissection for Papillary Thyroid Carcinoma With Lateral Neck Node Metastasis. *Surg Endosc* (2012) 26:3251–7. doi: 10.1007/s00464-012-2333-1
21. Kim JK, Lee CR, Kang SW, Jeong JJ, Nam KH, Chung WY. Robotic Transaxillary Lateral Neck Dissection for Thyroid Cancer: Learning Experience From 500 Cases. *Surg Endosc* (2021). doi: 10.1007/s00464-021-08526-7
22. Yu HW, Chai YJ, Kim SJ, Choi JY, Lee KE. Robotic-Assisted Modified Radical Neck Dissection Using a Bilateral Axillo-Breast Approach (Robotic BABA MRND) for Papillary Thyroid Carcinoma With Lateral Lymph Node Metastasis. *Surg Endosc* (2018) 32:2322–7. doi: 10.1007/s00464-017-5927-9
23. Seup Kim B, Kang KH, Park SJ. Robotic Modified Radical Neck Dissection by Bilateral Axillary Breast Approach for Papillary Thyroid Carcinoma With Lateral Neck Metastasis. *Head Neck* (2015) 37:37–45. doi: 10.1002/hed.23545
24. He Q, Zhu J, Zhuang D, Fan Z, Zheng L, Zhou P, et al. Robotic Lateral Cervical Lymph Node Dissection *via* Bilateral Axillo-Breast Approach for Papillary Thyroid Carcinoma: A Single-Center Experience of 260 Cases. *J Robot Surg* (2020) 14:317–23. doi: 10.1007/s11701-019-00986-3
25. Song RY, Sohn HJ, Paek SH, Kang KH. The First Report of Robotic Bilateral Modified Radical Neck Dissection Through the Bilateral Axillo-Breast Approach for Papillary Thyroid Carcinoma With Bilateral Lateral Neck Metastasis. *Surg Laparosc Endosc Percutan Tech* (2020) 30:e18–22. doi: 10.1097/SLE.0000000000000590
26. Lira RB, Chulam TC, Kowalski LP. Variations and Results of Retroauricular Robotic Thyroid Surgery Associated or Not With Neck Dissection. *Gland Surg* (2018) 7:S42–s52. doi: 10.21037/gs.2018.03.04
27. Byeon HK, Holsinger FC, Tufano RP, Chung HJ, Kim WS, Koh YW, et al. Robotic Total Thyroidectomy With Modified Radical Neck Dissection *via* Unilateral Retroauricular Approach. *Ann Surg Oncol* (2014) 21:3872–5. doi: 10.1245/s10434-014-3896-y
28. Kim WS, Koh YW, Byeon HK, Park YM, Chung HJ, Kim ES, et al. Robot-Assisted Neck Dissection *via* a Transaxillary and Retroauricular Approach Versus a Conventional Transcervical Approach in Papillary Thyroid Cancer With Cervical Lymph Node Metastases. *J Laparoendosc Adv Surg Tech A* (2014) 24:367–72. doi: 10.1089/lap.2013.0296
29. Byeon HK, Ban MJ, Lee JM, Ha JG, Kim ES, Koh YW, et al. Robot-Assisted Sistrunk's Operation, Total Thyroidectomy, and Neck Dissection *via* a Transaxillary and Retroauricular (TARA) Approach in Papillary Carcinoma Arising in Thyroglossal Duct Cyst and Thyroid Gland. *Ann Surg Oncol* (2012) 19:4259–61. doi: 10.1245/s10434-012-2674-y
30. Tae K, Kim KH. Transoral Robotic Selective Neck Dissection for Papillary Thyroid Carcinoma: Dissection of Levels III and IV. *Head Neck* (2020) 42 (10):3084–8. doi: 10.1002/hed.26379
31. Guo Y, Qu R, Huo J, Wang C, Hu X, Chen C, et al. Technique for Endoscopic Thyroidectomy With Selective Lateral Neck Dissection *via* a Chest-Breast Approach. *Surg Endosc* (2019) 33:1334–41. doi: 10.1007/s00464-018-06608-7
32. Lin PL, Liang FY, Han P, Chen RH, Yu ST, Cai Q, et al. Gasless Endoscopic Selective Lateral Neck Dissection *via* an Anterior Chest Approach for Papillary Thyroid Carcinomas. *Zhonghua Er Bi Yan Hou Tou Jing Wai Ke Za Zhi* (2017) 52:915–20. doi: 10.3760/cma.j.issn.1673-0860.2017.12.008
33. Zhang D, Gao L, Xie L, He G, Chen J, Fang L, et al. Comparison Between Video-Assisted and Open Lateral Neck Dissection for Papillary Thyroid Carcinoma With Lateral Neck Lymph Node Metastasis: A Prospective Randomized Study. *J Laparoendosc Adv Surg Tech A* (2017) 27:1151–7. doi: 10.1089/lap.2016.0650
34. Zhang D, Xie L, He G, Fang L, Miao Y, Wang Z, et al. A Comparative Study of the Surgical Outcomes Between Video-Assisted and Open Lateral Neck Dissection for Papillary Thyroid Carcinoma With Lateral Neck Lymph Node Metastases. *Am J Otolaryngol* (2017) 38:115–20. doi: 10.1016/j.amjoto.2016.07.005
35. Lin P, Liang F, Cai Q, Han P, Chen R, Xiao Z, et al. Comparative Study of Gasless Endoscopic Selective Lateral Neck Dissection via the Anterior Chest Approach Versus Conventional Open Surgery for Papillary Thyroid Carcinoma. *Surg Endosc* (2020) 35(2):693–701. doi: 10.1007/s00464-020-07434-6

36. Zhang Z, Zhao X. A Comparative Study of Endoscopic Assisted Lateral Neck Dissection and Open Lateral Neck Dissection in the Treatment of Cervical Lymph Node Metastasis of Papillary Thyroid Carcinoma. *Lin Chung Er Bi Yan Hou Tou Jing Wai Ke Za Zhi* (2020) 34:836–9; 843. doi: 10.13201/j.issn.2096-7993.2020.09.015
37. Li Z, Wang P, Wang Y, Xu S, Cao L, Que R, et al. Endoscopic Lateral Neck Dissection *via* Breast Approach for Papillary Thyroid Carcinoma: A Preliminary Report. *Surg Endosc* (2011) 25:890–6. doi: 10.1007/s00464-010-1292-7
38. Zhao W, Wang B, Yan S, Zhang L. Minilaparoscopy-Assisted Modified Neck Dissection Through Bilateral Breast Approach. *VideoEndocrinology* (2016) 3: ve.2015.0038. doi: 10.1089/ve.2015.0038
39. Xiang D, Xie L, Li Z, Wang P, Ye M, Zhu M. Endoscopic Thyroidectomy Along With Bilateral Central Neck Dissection (ETBC) Increases the Risk of Transient Hypoparathyroidism for Patients With Thyroid Carcinoma. *Endocrine* (2016) 53:747–53. doi: 10.1007/s12020-016-0884-y
40. Yan HC, Xiang C, Wang Y, Wang P. Scarless Endoscopic Thyroidectomy (SET) Lateral Neck Dissection for Papillary Thyroid Carcinoma Through Breast Approach: 10 Years of Experience. *Surg Endosc* (2020) 35(7):3540–6. doi: 10.1007/s00464-020-07814-y
41. Wang B, Weng YJ, Wang SS, Zhao WX, Yan SY, Zhang LY, et al. Feasibility and Safety of Needle-Assisted Endoscopic Thyroidectomy With Lateral Neck Dissection for Papillary Thyroid Carcinoma: A Preliminary Experience. *Head Neck* (2019) 41:2367–75. doi: 10.1002/hed.25705
42. Yan H, Wang Y, Wang P, Xie Q, Zhao Q. "Scarless" (in the Neck) Endoscopic Thyroidectomy (SET) With Ipsilateral Levels II, III, and IV Dissection *via* Breast Approach for Papillary Thyroid Carcinoma: A Preliminary Report. *Surg Endosc* (2015) 29:2158–63. doi: 10.1007/s00464-014-3911-1
43. Huo JL, Qu R, Guo YM, Chen C. Endoscopic Selective Lateral Neck Dissection *via* a Chest-Breast Approach for Papillary Thyroid Carcinoma: Preliminary Experience in 20 Cases. *Lin Chung Er Bi Yan Hou Tou Jing Wai Ke Za Zhi* (2019) 33:346–50. doi: 10.13201/j.issn.1001-1781.2019.04.014
44. Tan Y, Guo B, Deng X, Ding Z, Wu B, Niu Y, et al. Transoral Endoscopic Selective Lateral Neck Dissection for Papillary Thyroid Carcinoma: A Pilot Study. *Surg Endosc* (2019) 34(12):5274–82. doi: 10.1007/s00464-019-07314-8
45. Ngo DQ, Tran TD, Le DT, Ngo QX, Van Le Q. Transoral Endoscopic Modified Radical Neck Dissection for Papillary Thyroid Carcinoma. *Ann Surg Oncol* (2021) 28(5):2766. doi: 10.1245/s10434-020-09466-7
46. Chen ZX, Song YM, Chen JB, Zhang XB, Lin ZH, Cai BY, et al. Qin's Seven Steps for Endoscopic Selective Lateral Neck Dissection via the Chest Approach in Patients With Papillary Thyroid Cancer: Experience of 35 Cases. *Surg Endosc* (2021). doi: 10.1007/s00464-021-08540-9
47. Qu R, Hu X, Guo Y, Zhou X, Huo J, Chen Y, et al. Endoscopic Lateral Neck Dissection (IIA, IIB, III, and IV) Using a Breast Approach: Outcomes From a Series of the First 24 Cases. *Surg Laparosc Endosc Percutan Tech* (2020) 31:66–70. doi: 10.1097/SLE.0000000000000849
48. Huo J, Guo Y, Hu X, Chen X, Liu W, Luo L, et al. Endoscopic Thyroidectomy With Level Vb Dissection *Via* a Chest-breast Approach: Technical Updates for Selective Lateral Neck Dissection. *Surg Laparosc Endosc Percutan Tech* (2021) 31:342–5. doi: 10.1097/SLE.0000000000000887
49. Kitagawa W, Shimizu K, Akasu H, Tanaka S. Endoscopic Neck Surgery With Lymph Node Dissection for Papillary Carcinoma of the Thyroid Using a Totally Gasless Anterior Neck Skin Lifting Method. *J Am Coll Surg* (2003) 196:990–4. doi: 10.1016/S1072-7515(03)00130-3
50. Zhang Z, Xu Z, Li Z, An C, Liu J, Zhu Y, et al. Minimally-Invasive Endoscopically-Assisted Neck Dissection for Lateral Cervical Metastases of Thyroid Papillary Carcinoma. *Br J Oral Maxillofac Surg* (2014) 52:793–7. doi: 10.1016/j.bjoms.2014.05.009
51. Zhang ZM, Xu ZG, Li ZJ, An CM, Liu J, Zhu YM, et al. Minimally Invasive Endoscopy-Assisted Neck Dissection to Treat Lateral Cervical Metastasis of Thyroid Papillary Carcinoma. *Zhonghua Er Bi Yan Hou Tou Jing Wai Ke Za Zhi* (2013) 48:712–5.
52. Zhang DG, Gao L, Xie L, He GF, Fang L, Chen J, et al. Modified Minimally Invasive Video-Assisted Lateral Neck Dissection for Papillary Thyroid Carcinoma: A Series of 130 Cases. *Zhonghua Wai Ke Za Zhi* (2016) 54:864–9. doi: 10.3760/cma.j.issn.0529-5815.2016.11.015
53. Lombardi CP, Raffaelli M, Princi P, De Crea C, Bellantone R. Minimally Invasive Video-Assisted Functional Lateral Neck Dissection for Metastatic Papillary Thyroid Carcinoma. *Am J Surg* (2007) 193:114–8. doi: 10.1016/j.amjsurg.2006.02.024
54. Miccoli P, Materazzi G, Berti P. Minimally Invasive Video-Assisted Lateral Lymphadenectomy: A Proposal. *Surg Endosc* (2008) 22:1131–4. doi: 10.1007/s00464-007-9564-6
55. Zhang D, Chen J, He G, Gao L, Fang L, Chen Z. Application of Endoscopic Upper Mediastinal Lymph Node Dissection in Treatment of Papillary Thyroid Carcinoma. *Chin J Gen Surg* (2018) 27:1583–8.

Conflict of Interest: The authors declare that the research was conducted in the absence of any commercial or financial relationships that could be construed as a potential conflict of interest.

frontiers in Endocrinology

ORIGINAL RESEARCH
published: 12 January 2022
doi: 10.3389/fendo.2021.770824

Papillary Thyroid Microcarcinoma: A Nomogram Based on Clinical and Ultrasound Features to Improve the Prediction of Lymph Node Metastases in the Central Compartment

*Jing Ye[1], Jia-Wei Feng[1], Wan-Xiao Wu[1], Jun Hu[1], Li-Zhao Hong[1], An-Cheng Qin[2], Wei-Hai Shi[3] and Yong Jiang[1]**

[1] Department of Thyroid Surgery, The Third Affiliated Hospital of Soochow University, Changzhou First People's Hospital, Changzhou, China, [2] The Affiliated Suzhou Hospital of Nanjing Medical University, Suzhou Municipal Hospital, Suzhou, China, [3] The Affiliated Hospital of Nanjing Medical University, Changzhou Second People's Hospital, Changzhou, China

OPEN ACCESS

Edited by:
Gianlorenzo Dionigi,
University of Milan, Italy

Reviewed by:
Masha Livhits,
UCLA David Geffen School of Medicine, United States
Marina Caputo,
Università degli Studi del Piemonte Orientale, Italy

***Correspondence:**
Yong Jiang
yjiang8888@hotmail.com

Specialty section:
This article was submitted to Thyroid Endocrinology, a section of the journal Frontiers in Endocrinology

Received: 05 September 2021
Accepted: 21 December 2021
Published: 12 January 2022

Citation:
Ye J, Feng J-W, Wu W-X, Hu J, Hong L-Z, Qin A-C, Shi W-H and Jiang Y (2022) Papillary Thyroid Microcarcinoma: A Nomogram Based on Clinical and Ultrasound Features to Improve the Prediction of Lymph Node Metastases in the Central Compartment. Front. Endocrinol. 12:770824. doi: 10.3389/fendo.2021.770824

Background: Accurate preoperative identification of central lymph node metastasis (CLNM) is essential for surgical protocol establishment for patients with papillary thyroid microcarcinoma (PTMC). We aimed to develop a clinical and ultrasound characteristics-based nomogram for predicting CLNM.

Methods: Our study included 399 patients who were pathologically diagnosed with PTMC between January 2011 and June 2018. Clinical and ultrasound features were collected for univariate and multivariate analyses to determine risk factors of CLNM. A nomogram comprising the prognostic model to predict the CLNM was established, and internal validation in the cohort was performed. The Cox regression model was used to determine the risk factors for recurrence-free survival (RFS) and cumulative hazard was calculated to predict prognosis.

Results: Three variables of clinical and US features as potential predictors including sex (odd ratio [OR] = 1.888, 95% confidence interval [CI], 1.160-3.075; P =0.011), tumor size (OR = 1.933, 95% CI, 1.250-2.990; P =0.003) and ETE (OR = 6.829, 95% CI, 3.250-14.350; P <0.001) were taken into account. The predictive nomogram was established by involving all the factors above used for preoperative prediction of CLNM in patients with PTMC. The nomogram showed excellent calibration in predicting CLNM, with area under curves (AUC) of 0.684 (95% CI, 0.635 to 0.774). Furthermore, tumor size, multifocality, presence of ETE, vascular invasion, and CLNM were the significant factors related to the RFS.

Conclusion: Through this easy-to-use nomogram by combining clinical and US risk factor, the possibility of CLNM can be objectively quantified preoperatively. This prediction

model may serve as a useful clinical tool to help clinicians determine an individual's risk of CLNM in PTMC, thus make individualized treatment plans accordingly.

Keywords: thyroid cancer, microcarcinoma, nomogram, central lymph node metastases, recurrence-free survival

INTRODUCTION

Papillary thyroid carcinoma (PTC) has become one of the most common malignancies of the endocrine system, with an average annual incidence growth rate of 6% worldwide (1). If the maximum size of PTC is ≤ 1.0 cm, it is defined as papillary thyroid microcarcinoma (PTMC) by the World Health Organization (2). Although most thyroid cancer usually grows slowly and has a good prognosis, some PTMC tend to metastasize to regional lymph nodes (3). As previous reported (4–6), the incidence of central lymph node metastasis (CLNM) was the highest among the neck compartment, ranging from 19% to 76%. Once diagnosed with CLNM, especially with large macroscopic lymph node metastases, patients were at high risk for poor prognosis and regional recurrence (7).

With the application of routine ultrasonography (US) and the necessary fine-needle aspiration biopsy (FNAB), the diagnostic rate of PTMC has been greatly improved (8). However, the preoperative detection rate of CLNM still remains quite low due to the limitations of current imaging technology (9). A recent meta-analysis showed that the sensitivity of preoperative US to diagnose CLNM of PTC was only 0.33 (10). Considering the high prevalence of CLNM, prophylactic central lymph node dissection (CLND) is usually performed in Asian countries such as Japan and China. As a result, this may cause more complications after thyroid surgery, such as recurrent laryngeal nerve injury, hypoparathyroidism, and chyle leakage (11–14). Hence, an effective and noninvasive tool that could evaluate the invasion of tumors and determine the extent of operation before surgery may help to develop the best treatment plan for PTMC patients.

Unlike other researchers who simply identified the risk factors for CLNM (3), we developed a clinical and US characteristics-based nomogram to evaluate the probability of CLNM in patients with PTMC. With our accurate and convenient evaluation system, clinicians would be able to quantify the possibility of CLNM preoperatively and make better clinical decisions. Moreover, risk factors of recurrence-free survival (RFS) and cumulative hazards were calculated for individualized treatment plan formulation and patient outcomes would be improved eventually.

MATERIALS AND METHODS

Patient Recruitment

This research was performed according to the Declaration of Helsinki. The multi-center retrospective cohort research was approved by the Ethical Committee of the Third Affiliated Hospital of Soochow University and Suzhou Municipal Hospital. All patients provided written informed consent and agreed to use their clinical data for this study. From January 2011 to June 2018, all pathologically proven PTMC cases who were treated at this two hospitals were reviewed retrospectively. In our research, the inclusion criteria were: (1) All patients received surgery for the first time; (2) The primary lesion was located in the thyroid gland; (3) No family history of thyroid cancer; (4) No other malignant tumors; (5) No head and neck radiation exposure history; (6) No distant metastasis; (7) Postoperative pathology confirmed PTC; (8) Complete clinical data. The exclusion criteria were: (1) patients who also had other types of TC; (2) patients who did not undergo radical surgery or CLND; (3) reoperation; (4) diagnosed tumors of other organs previously; (5) history of neck radiation exposure or hereditary malignancy; (6) clinically and/or pathologically detected distant metastasis; (7) patients who were lost to follow-up midway or with incomplete clinical information. In the end, we included and assessed a total of 399 patients in the research.

Preoperative Examination and Surgical Procedures

A thorough examination would be conducted once a thyroid nodule was discovered. In addition to routine testing of serum thyroid hormones, neck US was usually carried out to assess the characteristics of thyroid nodules and lymph nodes in the central compartment. Moreover, FNAB was performed preoperatively to diagnose benign or malignant nodules and pathological types. The BRAF V600E mutation was only conducted since 2017. In our research, the preoperative US variables of thyroid nodules mainly included: tumor size (the largest dimension of primary tumor), multifocality (two or more PTC lesions), and extrathyroidal extension (ETE).

Considering FNAB and imaging findings, if PTMC patients were in any of the following conditions (isthmus lesion, bilateral lesions, or presence of gross ETE), a total thyroidectomy (TT) with bilateral CLND would be performed. Otherwise, only lobectomy with CLND on the affected side would be performed (2). The central compartment (CC) means level VI of neck lymph node partition. The histological analysis of all surgical specimens was routinely conducted in the department of pathology.

Histopathological Examination

Pathological sections and further immunohistochemistry of the specimens were performed by at least two experienced pathologists. Vascular invasion was confirmed by pathologists through the microscope. Disease recurrence was categorized as local (regional cervical lymph nodes or thyroid bed) or distant (other organs) and confirmed by cyto-histopathology or imaging. RFS was identified as the length of time between the

date of completion of the thyroid surgery and dates of recurrence. RFS and cumulative hazards were used to evaluate the outcomes.

Postoperative Strategies and Follow-up

The postoperative patients were treated with levothyroxine suppression therapy. Serum thyroglobulin (Tg) and Tg antibodies, US scan of the neck area and physical examinations were conducted every 3 to 6 months for high-risk patients and every 6 to 12 months for middle- and low-risk patients according to the 2015 ATA guidelines. When detected serum Tg and/or Tg antibody levels were significantly elevated, imaging examinations like CT or MRI or further histological confirmation would be performed. Follow-up information was acquired through telephone contact or outpatient consultations.

Statistical Analysis

Clinical data analysis in our study was conducted by utilizing software SPSS for Windows (version 25.0) and the R software (version 3.6.0). Categorical data were presented as numbers and percentages, while continuous data were presented as means ± standard deviations. Pearson's chi-square test or Fisher's exact test was applied for categorical data depending on the situation. Univariate analysis of CLNM-related risk factors in PTMC patients was also performed by using Pearson's chi-square test or Fisher's exact test. The statistically significant variables in the univariate analysis were further included in the multivariate logistic regression analysis to identify independent risk factors of CLNM. Next, the rms/pROC package in the R software was used to construct a predictive nomogram of risk factors based on the results of multivariate logistic regression, which could convert each variable coefficient into a score from 0 to 100. The receiver operating characteristic (ROC) curve was employed to quantify and compare the ability of predicted cases and observed cases to predict CLNM in PTMC. The R software was also used to evaluate the accuracy of the best cut-off value. In order to assess the performance of the nomogram, a calibration chart containing 1,000 bootstrap samples was further performed to compare the predicted probabilities with the actual probabilities of CLNM. Univariate Cox regression analysis was used to identify the risk factors of RFS. The Kaplan-Meier method and the Log rank test were performed to calculate cumulative hazard to assess the differences between groups.

RESULTS

Base Clinical and US Features of PTMC Patients

The clinical data of 399 patients with PTMC were collected in our study. 103 (25.8%) men and 296 (74.2%) women at a mean age of 46.0 ± 11.3 years (range 21-77 years) were included in our study. According to our US findings, the average maximum tumor diameter was 0.60 ± 0.25 cm; 212 (53.1%) were larger than 0.5 cm and 187 (46.9%) were 0.5 cm or smaller. One hundred and four (26.1%) patients had multifocal lesions. ETE were detected in 49 (12.3%) patients. Among 39 patients undergoing BRAF mutation analysis, 34 (87.2%) were positive for the gene mutation. Vascular invasion was evident in 12 (3.0%) cases.

In our study, all 399 PTMC patients underwent CLND, of which 156 (39.1%) patients were detected with CLNM after surgery. Pathology after surgery confirmed that the mean number of central lymph nodes resected was 5.8 ± 4.6 (range 2-26), while the mean number of metastases was 2.3 ± 1.2 (range 0-13). According to postoperative pathology, the average size of positive central lymph node was 0.6 ± 0.3 cm. The post-operative median follow-up was 25 months (range 3-89 months). During the follow-up, 18 patients (4.5%) developed recurrent disease, including 12 patients (3.0%) who had cervical lymph node recurrence, 3 patients (0.7%) who had contralateral lobe recurrence, 2 patients (0.5%) who had both lymph node and contralateral lobe recurrence and 1 patient (0.3%) who had lung recurrence.

Correlation Between Clinical and US Features and CLNM in PTMC Patients

In 399 PTMC cases, clinical variables that significantly related to CLNM were age, sex, tumor size, ETE and vascular invasion. In our univariate analysis, compared with non-CLNM, the incidence of CLNM in patients with age <55 years, male, tumor size >0.5 cm, ETE, and vascular invasion was substantially higher (P=0.027, P=0.001, P=0.001, P<0.001, and P=0.010, respectively). Further, the multivariate analysis indicated that male (OR: 1.888, 95% CI: 1.160-3.075, P=0.011), tumor size >0.5 cm (OR: 1.933, 95% CI: 1.250-2.990, P=0.003) and ETE (OR: 6.829, 95% CI: 3.250-14.350, P<0.001) were independent predictive factors associated with CLNM in PTMC (**Table 1**).

Development and Performance of the Nomogram

As mentioned above, a nomogram was created from previous independent risk factors (sex, tumor size, and ETE) to assess the CLNM incidence of PTMC preoperatively (**Figure 1**). According to the analysis, ETE contributes the most to the prediction model, followed by tumor size. These variables were finally rated on a scale of 0-100, and the risk rate of CLNM would be calculated by summing up all total scores. The usage of nomogram (**Figure 2**) is as follows: locate the patient's sex on the sex axis. Draw a line straight upward to the point axis to establish how many points toward the probability of CLNM the patient may get. Repeat the process for each of the other variables. Calculate total points for each of the predictors. Pinpoint the final score on the total point axis. Draw a line straight down to determine the patient's predicted probability of CLNM. For example, the nomogram predicted a PTC male (33 points) patient with the tumor more than 0.5cm (34 points). The tumor had the ETE (100 points). The total point was 167 for this patient. This patient had more than 80.0% chance of CLNM.

The ROC curve was also constructed, and an area under curves (AUC) of 68.4% (95% CI: 0.635-0.774) with specificity and sensitivity as 0.885 and 0.391 respectively showed good

TABLE 1 | Univariate and multivariate analyses of factors associated with CLNM and score in patients with PTMC.

Characteristics	CLNM, No. (%)			Multivariate analysis	*P* value	Score
	Presence (n = 156)	Absence (n = 243)	*P* value	Adjusted OR (95% CI)		
Age (Y)						
≥55	69 (44.2%)	135 (55.6%)		1		
<55	87 (55.8%)	108 (44.4%)	0.027	1.408 (0.911-2.177)	0.123	
Sex						
Female	102 (65.4%)	194 (79.8%)		1		0
Male	54 (34.6%)	49 (20.2%)	0.001	1.888 (1.160-3.075)	0.011	33
Tumor size (cm)						
≤0.5	57 (36.5%)	130 (53.5%)		1		0
>0.5	99 (63.5%)	113 (46.5%)	0.001	1.933 (1.250-2.990)	0.003	34
Multifocality						
Absence	107 (68.6%)	188 (77.4%)				
Presence	49 (31.4%)	55 (22.6%)	0.051			
ETE						
Absence	117 (75.0%)	233 (95.9%)		1		0
Presence	39 (25.0%)	10 (4.1%)	<0.001	6.829 (3.250-14.350)	<0.001	100
Vascular invasion						
Absence	147 (94.2%)	240 (98.8%)		1		
Presence	9 (5.8%)	3 (1.2%)	0.010	1.092 (0.201-5.923)	0.919	
BRAF V600E mutation*						
Negative	2 (10.5%)	3 (15.0%)				
Positive	17 (89.5%)	17 (85.0%)	0.676			

Y, year; SD, standard deviation; ETE, extrathyroidal extension; CLNM, central lymph node metastasis.
**BRAF mutation analysis was started in 2017 and it was performed in 39 patients with PTMC.*

calibration (**Figure 3**). Additionally, the optimal cut-off value of the nomogram was 1.437, which was considered good in the differential diagnosis of CLNM. The calibration chart graphically showed an excellent agreement between the actual probability of CLNM and the metastasis probability predicted by the nomogram, with a mean absolute error of 0.028 (**Figure 4**).

Risk Factors for RFS

We performed univariate analysis related to RFS to identify variables that affect the risk of recurrence (**Table 2**). Risk factors such as tumor size, multifocality, ETE, vascular invasion, and CLNM showed statistically significance associated with RFS (P=0.003, P=0.024, P=0.015, P=0.003, P=0.005, respectively). However, RFS was not significantly related to other factors studied. The risk of recurrence was 3.700, 8.831, 2.934, and 4.340 times higher in patients with tumor size > 0.5 cm, multifocality, ETE and vascular invasion, respectively. It was also found that patients with CLNM had a 3.730 times higher risk of recurrence than that of whom without CLNM. Furthermore, with the extension of follow-up time, the cumulative risk of CLNM patients was substantially higher than that of whom without CLNM (*P*<0.001) (**Figure 5**).

DISCUSSION

The prevalence of PTMC has increased rapidly in the past few years thanks to the development and application of US and necessary FNAB (15). According to Chinese Guidelines for Diagnosis and Treatment of Differentiated Thyroid Cancer (2012), lobectomy and prophylactic CLND was recommended for patients with tumors <1 cm in size. However, previous studies had shown that preventive CLND does not significantly benefit patients with low-risk PTC (16, 17). It was suggested that active surveillance rather than surgery could be taken for low-risk PTMC by the guidelines of the American Thyroid Association (2015) (2). However, some previously considered low-risk PTMCs still progressed during surveillance (18, 19). Therefore, surgical treatment options are more often taken by patients diagnosed with PTMC in China (20–22). Nevertheless, considering the uncertain efficacy and high risk of complications, it was still controversial whether to perform preventive CLND while no obvious evidence of CLNM was found before surgery (23). Thus, careful assessment of cervical lymph node status and determination of risk factors related to CLNM before surgery could guide PTMC patients to adopt appropriate surgical methods and avoid unnecessary complications (24).

According to our study, a logistic regression model based on US and clinical variables was set up to predict the probability of CLNM in patients with PTMC. Factors associated with CLNM of PTMC patients were studied in depth through univariate and multivariate analyses. As previously reported, the occurrence rate of CLNM confirmed by pathologists was between 29.3% and 60.9% in cN0 PTC patients (25–28). In present study, the occurrence rate of CLNM was 39.1%, which was in accordance with the results of previous studies. The incidence of CLNM was higher in patients of male, age <55 years, tumor size >0.5 cm, ETE, and vascular invasion respectively according to our research. Further, multivariate analysis revealed that male, tumor size and ETE were independent risk factors for CLNM. These were similar to the results of some previous studies (29, 30). In addition, tumor size, multifocality, ETE, vascular invasion, and CLNM were found to be significantly correlated

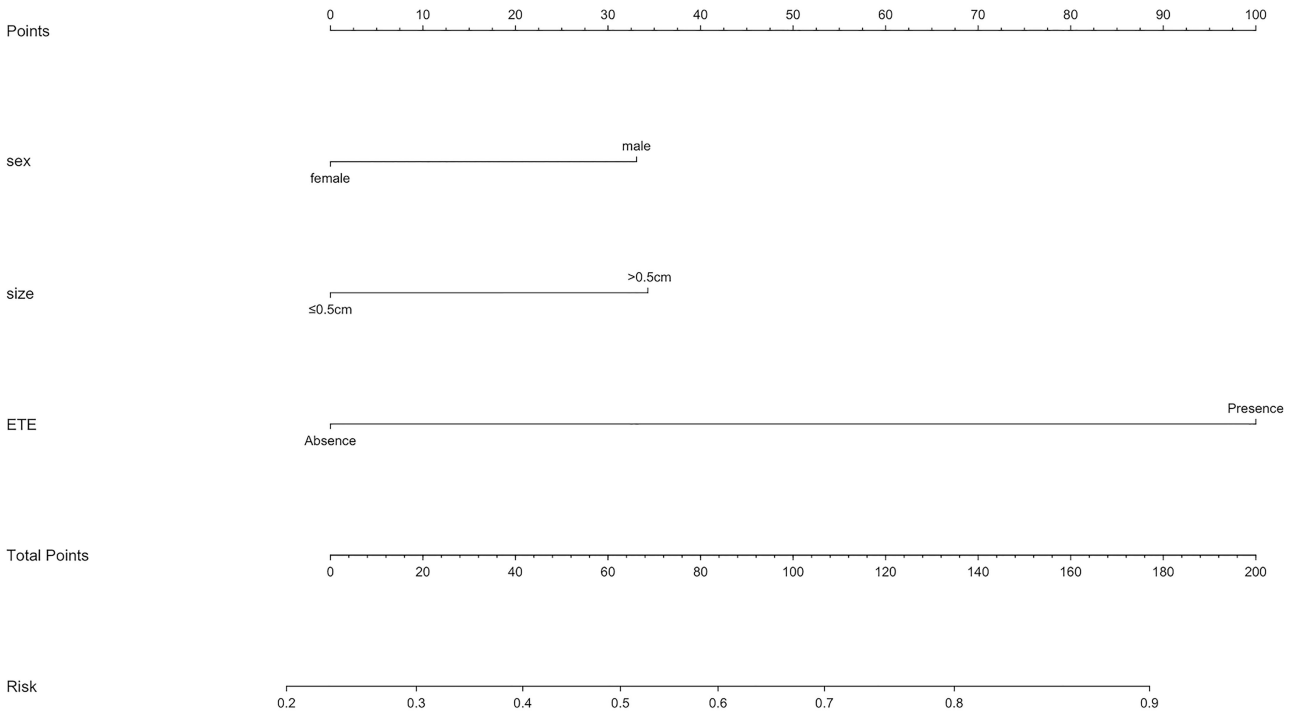

FIGURE 1 | Nomogram for predicting CLNM in patients with PTMC.

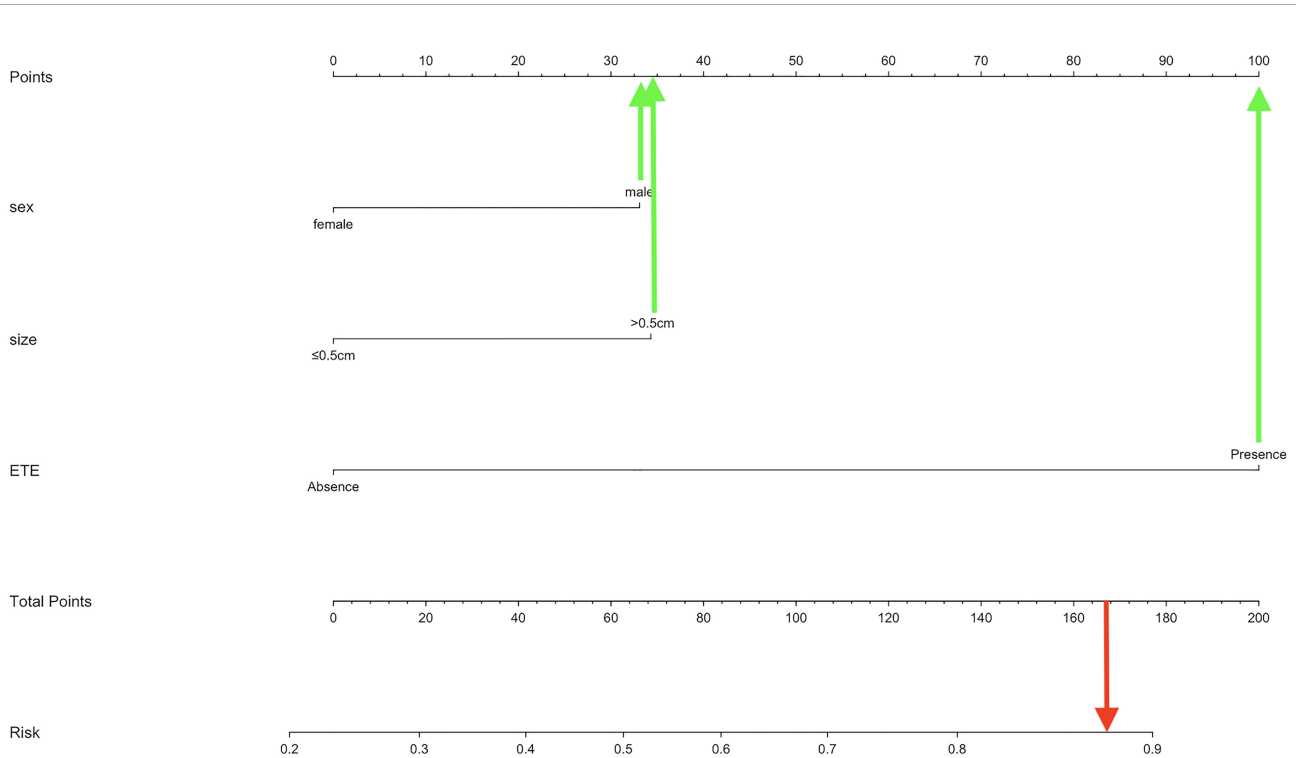

FIGURE 2 | Demonstration of the usage of our nomogram.

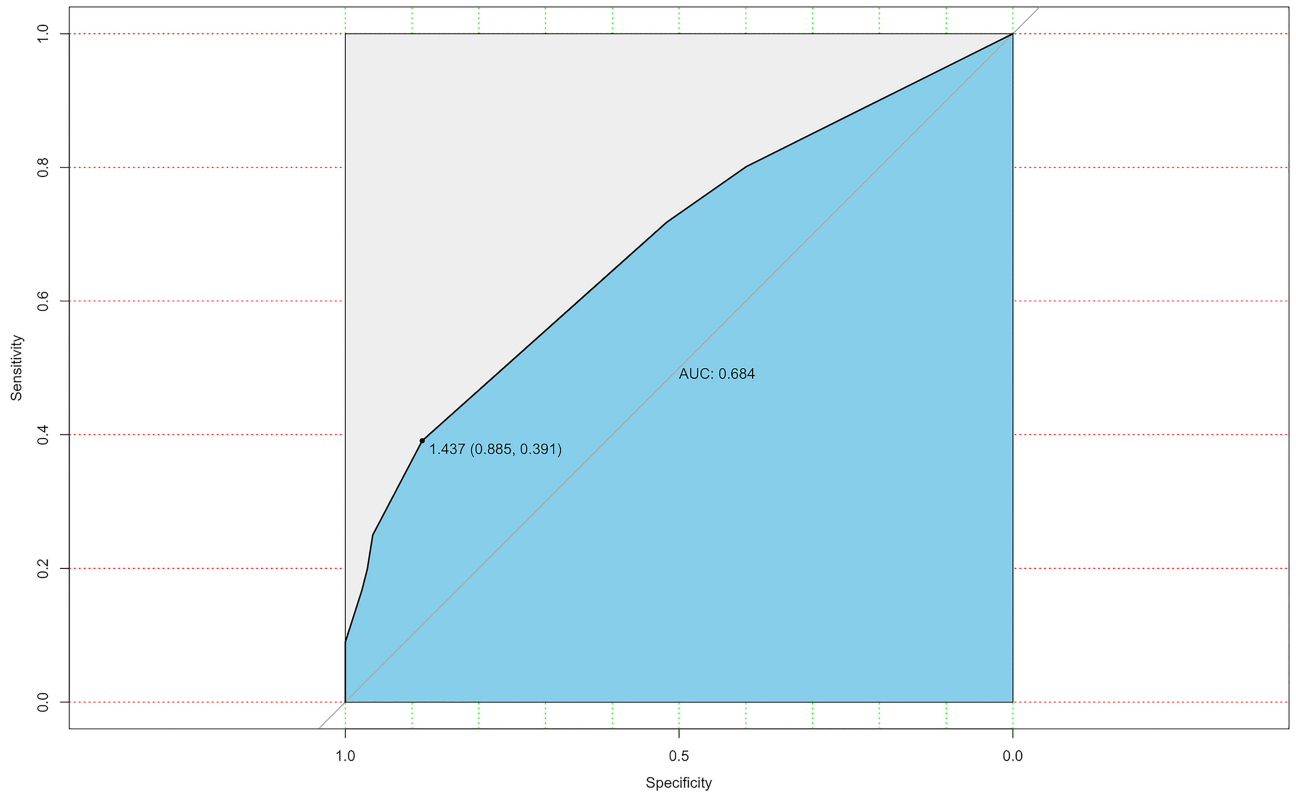

FIGURE 3 | ROC curve for predicting model.

TABLE 2 | Cox proportional hazards model demonstrating factors associated with recurrence-free survival in PTMC patients.

Characteristics	HR	95% CI	*P* value	Cumulative risk
Age (Y)				
≥55	1			
<55	1.601	0.654-3.924	0.303	
Sex				
Female	1			
Male	1.474	0.549-3.959	0.442	
Tumor size (cm)				
≤0.5	1			
>0.5	3.700	1.543-8.875	0.003	
Multifocality				
Absence	1			
Presence	3.111	1.165-8.306	0.024	
ETE				
Absence	1			
Presence	2.934	1.238-6.955	0.015	
Vascular invasion				
Absence	1			
Presence	4.340	1.648-11.432	0.003	
CLNM				
Absence	1			
Presence	3.730	1.482-9.388	0.005	<0.001

Y, year; SD, standard deviation; ETE, extrathyroidal extension; CLNM, central lymph node metastasis.

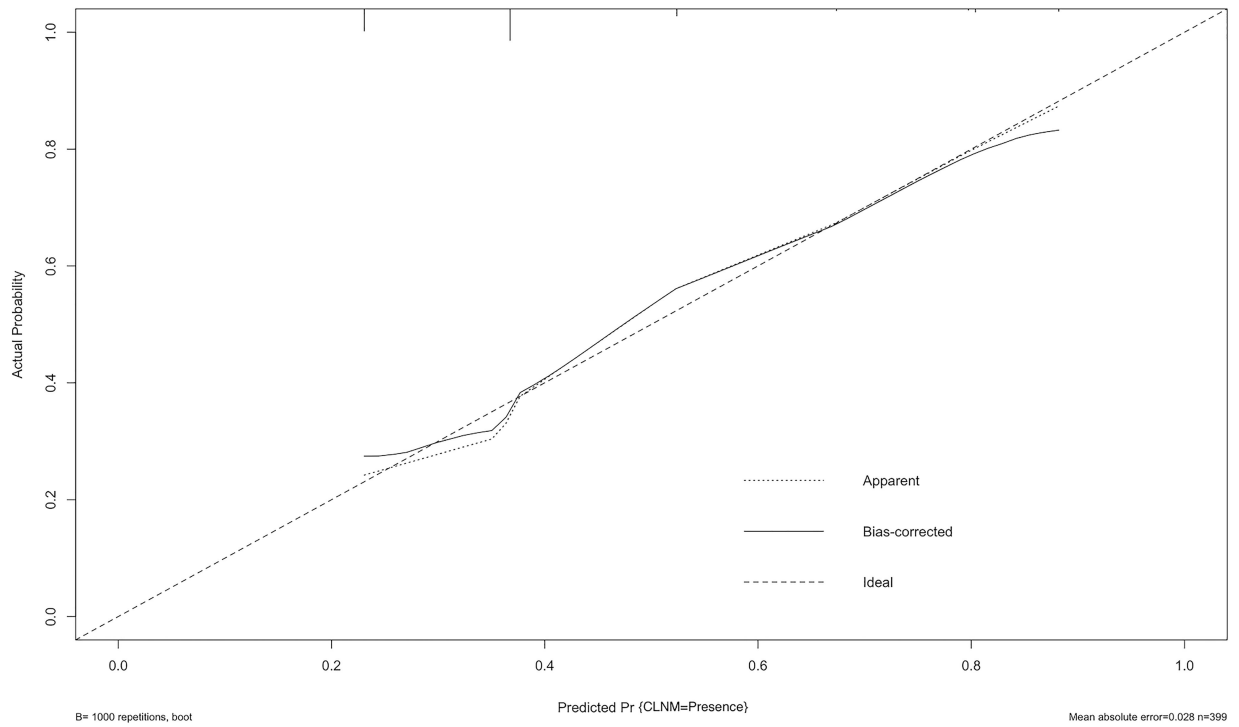

FIGURE 4 | Calibration curve of the model. The diagonal dashed line represents the ideal prediction by the perfect nomogram; the solid line represents the calibration estimate from internally validated model; the dotted line indicates the apparent predictive accuracy. The closer the solid line is to the dotted line, the stronger the predictive ability of the model.

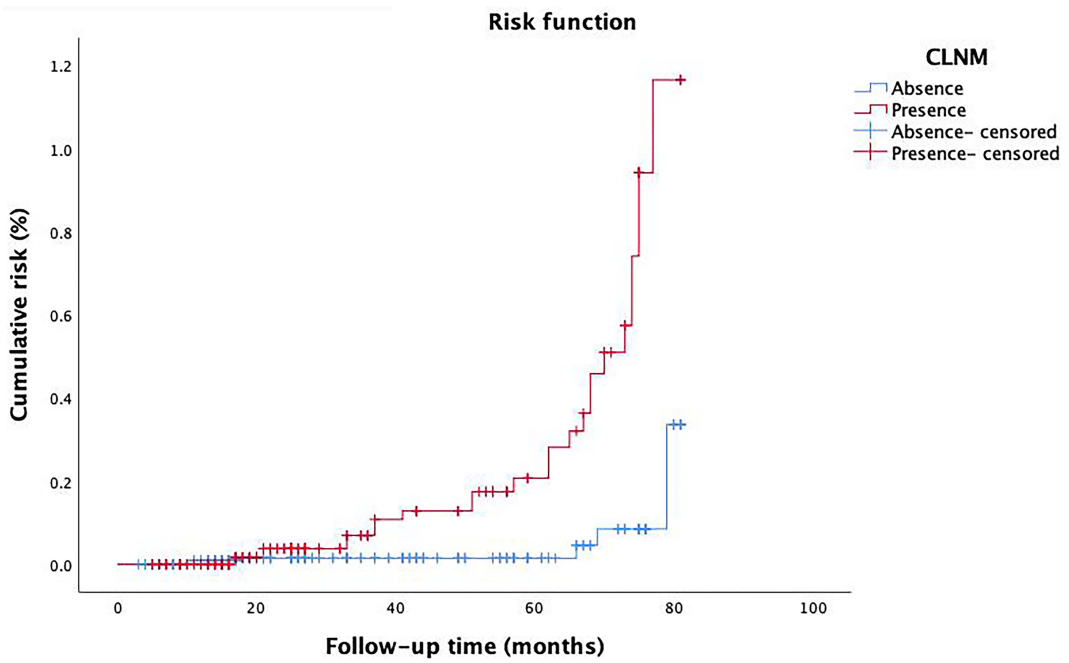

FIGURE 5 | The cumulative risk in patients with CLNM and patients without CLNM.

with RFS in patients with PTMC, and the cumulative hazard of CLNM patients was closely related to the postoperative follow-up time. Therefore, we urgently need a prediction system for individual CLNM probability to determine the extent of surgery and ultimately improve the prognosis.

To further predict the probability of CLNM, our study utilized the previous variables based on the multivariate analysis to construct a nomogram system (**Figure 2**). According to the point scale, we assigned a score to each variable. Next, the CLNM risk for each subject was determined by adding up all the total scores and identifying them on the total point scale. The nomogram incorporates all related clinical and US features to provide an individual risk assessment of CLNM preoperatively, which may avoid unnecessary expansion of extent of surgery. The AUC of the nomogram in our study was 0.684 (95%CI, 0.635-0.774), suggesting good discrimination. Surgeons could make individualized treatment plans accordingly, which is in conformity with the present tendency of personalized precision healthcare (31–34).

Our research still has some potential limitations which we hope to address in the following research. First, this was a retrospective observational research. Biases and errors in retrospective studies are often higher than in prospective studies (35). Hence, the prediction performance may be affected by the retrospective design of the study. Second, although we gathered cases from two hospitals, the sample size and the number of variables studied was not sufficiently large. Therefore, future studies involving more sample sizes and variables are needed, and further multicenter external validation are also needed to develop high-level evidence. More latent variables that are significant for CLNM prediction may be discovered, which can make the nomogram more complete. Third, the performance of the nomogram may be partially affected by different US instruments and operators with different experience. Because of the limitations of US, occult metastasis may not be detected during follow-up and cumulative risk calculation may also be affected (10, 36). Furthermore, we did not discuss whether prophylactic CLND in high-risk patients would reduce the risk of recurrence and improve patient outcomes. We plan to conduct prospective studies in the future, including setting up a comparison group of patients who will not receive prophylactic CLND to explore the impact of prophylactic CLND on postoperative complications and recurrence.

In summary, sex, tumor size, and ETE were significantly related to CLNM of PTMC in our research. By using above variables, we were able to construct a nomogram to evaluate CLNM risk of PTMC and provide a reference for clinicians to make individualized treatment decisions. For patients with high-risk factors for RFS, active surgical strategies are especially important.

DATA AVAILABILITY STATEMENT

The raw data supporting the conclusions of this article will be made available by the authors, without undue reservation.

ETHICS STATEMENT

Written informed consent was obtained from the individual(s) for the publication of any potentially identifiable images or data included in this article.

AUTHOR CONTRIBUTIONS

JY and J-WF: Writing - Original Draft, Software, Data Curation. W-XW and L-ZH: Validation, Formal analysis, Data Curation. JH: Conceptualization. W-HS and A-CQ: Validation, Investigation. YJ: Writing - Review & Editing, Visualization, Supervision. All authors contributed to the article and approved the submitted version.

ACKNOWLEDGMENTS

Lei Qin, the English language editor, was responsible for correcting language and grammar issues.

REFERENCES

1. Siegel RL, Miller KD, Fuchs HE, Jemal A. Cancer Statistics, 2021. *CA Cancer J Clin* (2021) 71(1):7–33. doi: 10.3322/caac.21654
2. Haugen BR, Alexander EK, Bible KC, Doherty G, Mandel SJ, Nikiforov YE, et al. 2015 American Thyroid Association Management Guidelines for Adult Patients With Thyroid Nodules and Differentiated Thyroid Cancer: The American Thyroid Association Guidelines Task Force on Thyroid Nodules and Differentiated Thyroid Cancer. *Thyroid* (2016) 26(1):1–133. doi: 10.1089/thy.2015.0020
3. Liu C, Xiao C, Chen J, Li X, Feng Z, Gao Q, et al. Risk Factor Analysis for Predicting Cervical Lymph Node Metastasis in Papillary Thyroid Carcinoma: A Study of 966 Patients. *BMC Cancer* (2019) 19(1):622. doi: 10.1186/s12885-019-5835-6
4. Yu XM, Wan Y, Sippel RS, Chen H. Should All Papillary Thyroid Microcarcinomas be Aggressively Treated? An Analysis of 18,445 Cases. *Ann Surg* (2011) 254(4):653–60. doi: 10.1097/SLA.0b013e318230036d
5. Chow SM, Law S, Chan J, Au SK, Yau S, Lau WH. Papillary Microcarcinoma of the Thyroid-Prognostic Significance of Lymph Node Metastasis and Multifocality. *Cancer* (2003) 98(1):31–40. doi: 10.1002/cncr.11442
6. Zheng X, Peng C, Gao M, Zhi J, Hou X, Zhao J, et al. Risk Factors for Cervical Lymph Node Metastasis in Papillary Thyroid Microcarcinoma: A Study of 1,587 Patients. *Cancer Biol Med* (2019) 16(1):121–30. doi: 10.20892/j.issn.2095-3941.2018.0125
7. Jiang LH, Yin KX, Wen QL, Chen C, Ge MH, Tan Z. Predictive Risk-Scoring Model For Central Lymph Node Metastasis and Predictors of Recurrence in Papillary Thyroid Carcinoma. *Sci Rep* (2020) 10(1):710. doi: 10.1038/s41598-019-55991-1
8. Burgess JR, Tucker P. Incidence Trends for Papillary Thyroid Carcinoma and Their Correlation With Thyroid Surgery and Thyroid Fine-Needle Aspirate Cytology. *Thyroid* (2006) 16(1):47–53. doi: 10.1089/thy.2006.16.47
9. Kim E, Park JS, Son KR, Kim JH, Jeon SJ, Na DG. Preoperative Diagnosis of Cervical Metastatic Lymph Nodes in Papillary Thyroid Carcinoma: Comparison of Ultrasound, Computed Tomography, and Combined

Ultrasound With Computed Tomography. *Thyroid* (2008) 18(4):411–8. doi: 10.1089/thy.2007.0269
10. Zhao H, Li H. Meta-Analysis of Ultrasound for Cervical Lymph Nodes in Papillary Thyroid Cancer: Diagnosis of Central and Lateral Compartment Nodal Metastases. *Eur J Radiol* (2019) 112:14–21. doi: 10.1016/j.ejrad.2019.01.006
11. Sancho JJ, Lennard T, Paunovic I, Triponez F, Sitges-Serra A. Prophylactic Central Neck Disection in Papillary Thyroid Cancer: A Consensus Report of the European Society of Endocrine Surgeons (ESES). *Langenbecks Arch Surg* (2013) 399(2):155–63. doi: 10.1007/s00423-013-1152-8
12. Park I, Her N, Choe JH, Kim JS, Kim JH. Management of Chyle Leakage After Thyroidectomy, Cervical Lymph Node Dissection, in Patients With Thyroid Cancer. *Head Neck* (2018) 40(1):7–15. doi: 10.1002/hed.24852
13. Polistena A, Monacelli M, Lucchini R, Triola R, Conti C, Avenia S, et al. Surgical Morbidity of Cervical Lymphadenectomy for Thyroid Cancer: A Retrospective Cohort Study Over 25 Years. *Int J Surg (London England)* (2015) 21:128–34. doi: 10.1016/j.ijsu.2015.07.698
14. Orloff LA, Wiseman SM, Bernet VJ, Fahey TJ3rd, Shaha AR, Shindo ML, et al. American Thyroid Association Statement on Postoperative Hypoparathyroidism: Diagnosis, Prevention, and Management in Adults. *Thyroid* (2018) 28(7):830–41. doi: 10.1089/thy.2017.0309
15. Yoon JH, Lee HS, Kim EK, Youk JH, Kim HG, Moon HJ, et al. Short-Term Follow-Up US Leads to Higher False-Positive Results Without Detection of Structural Recurrences in PTMC. *Medicine* (2016) 95(1):e2435. doi: 10.1097/MD.0000000000002435
16. Alsubaie KM, Alsubaie HM, Alzahrani FR, Alessa MA, Abdulmonem SK, Merdad MA, et al. Prophylactic Central Neck Dissection for Clinically Node-Negative Papillary Thyroid Carcinoma. *Laryngoscope* (2021). doi: 10.1002/lary.29912
17. Yuan J, Li J, Chen X, Lin X, Du J, Zhao G, et al. Identification of Risk Factors of Central Lymph Node Metastasis and Evaluation of the Effect of Prophylactic Central Neck Dissection on Migration of Staging and Risk Stratification in Patients With Clinically Node-Negative Papillary Thyroid Microcarcinoma. *Bull Cancer* (2017) 104(6):516–23. doi: 10.1016/j.bulcan.2017.03.005
18. Oh HS, Ha J, Kim HI, Kim TH, Kim WG, Lim DJ, et al. Active Surveillance of Low-Risk Papillary Thyroid Microcarcinoma: A Multi-Center Cohort Study in Korea. *Thyroid* (2018) 28(12):1587–94. doi: 10.1089/thy.2018.0263
19. Jeong SY, Baek JH, Choi YJ, Lee JH. Ethanol and Thermal Ablation for Malignant Thyroid Tumours. *Int J Hyperthermia* (2017) 33(8):938–45. doi: 10.1080/02656736.2017.1361048
20. Zhang H, Zheng X, Liu J, Gao M, Qian B. Active Surveillance as a Management Strategy for Papillary Thyroid Microcarcinoma. *Cancer Biol Med* (2020) 17(3):543–54. doi: 10.20892/j.issn.2095-3941.2019.0470
21. Ze Y, Zhang X, Shao F, Zhu L, Shen S, Zhu D, et al. Active Surveillance of Low-Risk Papillary Thyroid Carcinoma: A Promising Strategy Requiring Additional Evidence. *J Cancer Res Clin Oncol* (2019) 145(11):2751–9. doi: 10.1007/s00432-019-03021-y
22. Du L, Wang Y, Sun X, Li H, Geng X, Ge M, et al. Thyroid Cancer: Trends in Incidence, Mortality and Clinical-Pathological Patterns in Zhejiang Province, Southeast China. *BMC Cancer* (2018) 18(1):291. doi: 10.1186/s12885-018-4081-7
23. Raffaelli M, Tempera SE, Sessa L, Lombardi CP, De Crea C, Bellantone R. Total Thyroidectomy Versus Thyroid Lobectomy in the Treatment of Papillary Carcinoma. *Gland Surg* (2020) 9(Suppl 1):S18–27. doi: 10.21037/gs.2019.11.09
24. Xue S, Zhang L, Pang R, Wang P, Jin M, Guo L, et al. Predictive Factors of Central-Compartment Lymph Node Metastasis for Clinical N0 Papillary Thyroid Carcinoma With Strap Muscle Invasion. *Front Endocrinol* (2020) 11:511. doi: 10.3389/fendo.2020.00511
25. Wada N, Duh QY, Sugino K, Iwasaki H, Takanashi Y. Lymph Node Metastasis From 259 Papillary Thyroid Microcarcinomas: Frequency, Pattern of Occurrence and Recurrence, and Optimal Strategy for Neck Dissection. *Ann Surg* (2003) 237(3):399–407. doi: 10.1097/01.SLA.0000055273.58908.19
26. Lim YC, Choi EC, Yoon YH, Kim EH, Koo BS. Central Lymph Node Metastases in Unilateral Papillary Thyroid Microcarcinoma. *Br J Surg* (2010) 96(3):253–7. doi: 10.1002/bjs.6484
27. Jin K, Li L, Liu Y, Wang X. The Characteristics and Risk Factors of Central Compartment Lymph Node Metastasis in Cn0 Papillary Thyroid Carcinoma Coexistent With Hashimoto's Thyroiditis. *Gland Surg* (2020) 9(6):2026–34. doi: 10.21037/gs-20-699
28. Li M, Zhu XY, Lv J, Lu K, Shen MP, Xu ZL, et al. Risk Factors for Predicting Central Lymph Node Metastasis in Papillary Thyroid Microcarcinoma (CN0): A Study of 273 Resections. *Eur Rev Med Pharmacol Sci* (2017) 21(17):3801–7.
29. Qu N, Zhang L, Ji QH, Chen JY, Zhu YX, Cao YM, et al. Risk Factors for Central Compartment Lymph Node Metastasis in Papillary Thyroid Microcarcinoma: A Meta-Analysis. *World J Surg* (2015) 39(10):2459–70. doi: 10.1007/s00268-015-3108-3
30. Kim SK, Park I, Woo JW, Lee JH, Choe JH, Kim JH, et al. Predictive Factors for Lymph Node Metastasis in Papillary Thyroid Microcarcinoma. *Ann Surg Oncol* (2016) 23(9):2866–73. doi: 10.1245/s10434-016-5225-0
31. Balachandran VP, Gonen M, Smith JJ, Dematteo RP. Nomograms in Oncology: More Than Meets the Eye. *Lancet Oncol* (2015) 16(4):e173–80. doi: 10.1016/S1470-2045(14)71116-7
32. Huang GQ, Lin YT, Wu YM, Cheng QQ, Cheng HR, Wang Z. Individualized Prediction Of Stroke-Associated Pneumonia For Patients With Acute Ischemic Stroke. *Clin Interv Aging* (2019) 14:1951–62. doi: 10.2147/CIA.S225039
33. Chen S, Liu Y, Yang J, Liu Q, You H, Dong Y, et al. Development and Validation of a Nomogram for Predicting Survival in Male Patients With Breast Cancer. *Front Oncol* (2019) 9:361. doi: 10.3389/fonc.2019.00361
34. Choudhury P, Gupta M. Personalized & Precision Medicine in Cancer: A Theranostic Approach. *Curr Radiopharm* (2017) 10(3):166–70. doi: 10.2174/1874471010666170728094008
35. Sessler DI, Imrey PB. Clinical Research Methodology 2: Observational Clinical Research. *Anesth Analg* (2015) 121(4):1043–51. doi: 10.1213/ANE.0000000000000861
36. Ha SM, Baek JH, Kim JK. Detection of Malignancy Among Suspicious Thyroid Nodules Less Than 1 Cm on Ultrasound With Various Thyroid Image Reporting and Data Systems. *Thyroid* (2017) 27(10):1307–15. doi: 10.1089/thy.2017.0034

Conflict of Interest: The authors declare that the research was conducted in the absence of any commercial or financial relationships that could be construed as a potential conflict of interest.

Publisher's Note: All claims expressed in this article are solely those of the authors and do not necessarily represent those of their affiliated organizations, or those of the publisher, the editors and the reviewers. Any product that may be evaluated in this article, or claim that may be made by its manufacturer, is not guaranteed or endorsed by the publisher.

frontiers in Endocrinology

ORIGINAL RESEARCH
published: 21 January 2022
doi: 10.3389/fendo.2021.819503

Evaluation of Autofluorescence in Identifying Parathyroid Glands by Measuring Parathyroid Hormone in Fine-Needle Biopsy Washings

*Zhen Liu[1], Run-sheng Ma[1], Jun-li Jia[2], Tao Wang[1], Dao-hong Zuo[1] and De-tao Yin[1]**

[1] Department of Thyroid Surgery, The First Affiliated Hospital of Zhengzhou University, He'nan, China, [2] Department of Respiratory, The First Affiliated Hospital of Zhengzhou University, He'nan, China

Background: Near-infrared autofluorescence imaging has potentially great value for assisting endocrine surgeons in identifying parathyroid glands and may dramatically change the surgical strategy of endocrine surgeons in thyroid surgery. This study is designed to objectively evaluate the role of near-infrared autofluorescence imaging in identifying parathyroid glands during thyroid surgery by measuring intraoperative parathyroid hormone in fine-needle aspiration biopsy washings.

Methods: This study was conducted at a tertiary referral teaching hospital in China from February 2020 to June 2020. Patients undergoing total thyroidectomy with or without neck lymph node dissection were consecutively included. The surgeon used near-infrared autofluorescence imaging to identify parathyroid glands during thyroid surgery and confirmed suspicious parathyroid tissues by measuring their intraoperative parathyroid hormone. Nanocarbon was injected into the thyroid gland if the thyroid autofluorescence intensity was too strong. The sensitivity and accuracy of near-infrared autofluorescence imaging and vision for identifying parathyroid glands, and the difference in autofluorescence intensity in various tissues were the main outcomes.

Results: Overall, 238 patients completed the trial. Based on the pathological and aIOPTH results, the sensitivity of near-infrared autofluorescence imaging for detecting parathyroid glands (568 of 596 parathyroid glands; 95.30%)was significantly higher than that of vision (517 of 596 parathyroid glands; 86.74%, $P<.001$). The accuracy of near-infrared autofluorescence imaging (764 of 841 tissues; 90.84%) was significantly higher than that of vision (567 of 841 tissues; 67.42%, $P<.001$) when the evaluations of certain tissues were inconsistent. There was a significant difference between the autofluorescence intensity of the parathyroid glands and that of the lymph nodes (74.19 ± 17.82 *vs* 33.97 ± 10.64, $P<.001$).

Conclusion: The use of near-infrared autofluorescence imaging, along with intraoperative parathyroid hormone and nanocarbon for the identification of parathyroid glands in thyroid surgery may increase the number of confirmed parathyroid glands. Using near-infrared

OPEN ACCESS

Edited by:
Gianlorenzo Dionigi, University of Milan, Italy

Reviewed by:
Gianluca Donatini, Centre Hospitalier Universitaire (CHU) de Poitiers, France
Fang Dong, Huazhong University of Science and Technology, China

****Correspondence:***
De-tao Yin
detaoyin@zzu.edu.cn

Specialty section:
This article was submitted to Thyroid Endocrinology, a section of the journal Frontiers in Endocrinology

Received: *21 November 2021*
Accepted: *27 December 2021*
Published: *21 January 2022*

Citation:
Liu Z, Ma R-s, Jia J-l, Wang T, Zuo D-h and Yin D-t (2022) Evaluation of Autofluorescence in Identifying Parathyroid Glands by Measuring Parathyroid Hormone in Fine-Needle Biopsy Washings. Front. Endocrinol. 12:819503. doi: 10.3389/fendo.2021.819503

autofluorescence imaging can effectively distinguish lymph nodes and parathyroid glands during lymph node dissection.

Keywords: autofluorescence, parathyroid, thyroid surgery, nanocarbon, lymph node

INTRODUCTION

Hypocalcemia after thyroid surgery is a problem that has long plagued endocrine surgeons. In a statistical analysis of 14,540 patients undergoing thyroidectomies in the United States from 2013 to 2015, 450 cases of severe postoperative hypocalcemia occurred (3.3% overall, 0.6% after partial, and 4.7% after subtotal or total thyroidectomy) (1). Severe postoperative hypocalcemia can be life-threatening and seriously impair quality of life. Accurate identification of parathyroid glands (PGs) is the first step to reduce postoperative hypocalcemia. At present, the recognition of PGs mainly depends on visual identification by the surgeon. However, due to their small size and unstable location, as well as the difficulty in distinguishing them in color and shape from lymph nodes and adipose tissue, highly subjective visual identification is often unreliable. Therefore, any technologies that might assist the visual identification of PGs can be of great clinical application value.

There have been a few reported studies relating to parathyroidectomy or thyroidectomy combined with autofluorescence, fluorescent methylene blue, 5-aminolevulinic acid, indocyanine green, optical coherence tomography, laser speckle contrast imaging, dynamic optical contrast imaging and Raman spectroscopy (2). These optical technologies could become complementary to the surgeon's eyes and thus may reduce the hypocalcemia rate after thyroid surgery. Among them, near infrared-induced autofluorescence (NIRAF) technology based on the spontaneous auto fluorescent signal of the PG is most widely reported (3). Studies have shown that NIRAF can reduce the risk of postoperative hypocalcemia (4–6). However, reduction in hypocalcemia is only an indirect proof since it is also highly related to the further protection of recognized PGs.

The exact number of PGs identified by NIRAF is crucial to its clinical evaluation. In previous studies, NIRAF showed good sensitivity and specificity in the identification of PGs (7–9). However, all identified PGs during thyroid surgery need to be retained. Therefore, the pathological examination based on the study's purpose is against ethical requirements since it would cause permanent damage. Visual identification by the surgeon has been used in most trials as a confirmation method for PGs (10). The subjective visual identification itself lacks accuracy and is less persuasive to be used as the criterion. Although some of the trials used pathological examination to confirm PGs, the included patients mostly had parathyroid tumors or hyperparathyroidism (7). Many studies have shown that the NIRAF of diseased PGs is completely different from that of normal PGs, so it is better to exclude these patients in the study to explain the value of NIRAF in thyroid surgery (11, 12).

The intraoperative parathyroid aspiration for parathyroid hormone assay (aIOPTH) technology is considered to have high sensitivity (80%-100%) for the confirmation of PGs and has a high specificity close to 100% (13). Meanwhile, aIOPTH, as a minimally invasive examination method, causes minimal damage to PGs; consequently, evaluating suspected parathyroid tissues with aIOPTH completely meets the ethical requirements. Thus, aIOPTH is very suitable as an alternative to parathyroid pathology to evaluate the value of NIRAF.

This study was a large sample case series study including patients undergoing thyroidectomies. The purpose was to use aIOPTH to evaluate the value of NIRAF in thyroid surgery. We introduced several new methods to improve the effect of NIRAF during the study and tried to find a new strategy using NIRAF and aIOPTH to improve the identification of PGs.

METHODS

The study was approved by the institutional review board of the First Affiliated Hospital of Zhengzhou University (2019-KY-283) and registered on Chictr.org.cn (ChiCTR2000030025)and all patients gave written informed consent. Patients undergoing thyroidectomy with or without neck lymph node dissection between February 2020 to June 2020 were consecutively included in a prospective cohort. Previous thyroid or parathyroid surgery, parathyroid tumor and parathyroid dysfunction, including primary and secondary hyperparathyroidism, were exclusion criteria.

The equipment used in this study was a commercially available, handheld NIR camera (PDE-Neo II; Hamamatsu Photonics). The camera emits infrared light at a wavelength of 760 nm and captures NIR wavelengths of 790–830 nm. Since the light from an LED lamp has little influence on the imaging process, we were able to keep the routine lighting of the operating room and simply move the surgical light away from the surgical field, which reduced the impact of frequent light switching (**Supplementary Figure 1**).

Surgical Process

After routine dissection of the band muscles and exposure of the thyroid gland, the first fluorescence imaging was performed. If the thyroid autofluorescence intensity was too strong, then nanocarbon (Chongqing Laimei Pharmaceutical Co) was slowly injected into the thyroid gland until the gland was black-stained. While the surgeon used NIRAF to identify PGs, he also identified PGs through routine visual observation (**Supplementary Video 1**). The fluorescent images using NIRAF to identify the PGs were saved, and the assistant took pictures with a high-resolution camera of the same operative field for subsequent image comparison. The tissues co-identified by vision and NIRAF as PGs were considered as confirmed PGs. If NIRAF revealed PGs in areas that had been visually neglected, it was considered that NIRAF first discovered

them. If the judgment of tissue was inconsistent, the measurement of aIOPTH was used for confirmation (**Supplementary Video 2**). The specific method was to puncture the suspicious tissue with a 1 ml syringe containing 0.1 ml saline and then to drip the 0.1 ml saline through the needle onto the reaction area of the test strip and culture for 10 minutes according to the instructions of the parathyroid hormone (PTH) detection kit (Bioda Diagnosis Co) (**Supplementary Figure 2**). If the saline contained PTH, it would combine with PTH antibodies in the reaction zone to form a complex. The strip included the distal control band and the proximal test band. When the liquid containing the complex flowed from the reaction zone to the test band, the complex bound to the anti-PTH antibody in the test band, making it appear red. Furthermore, the detector was used to calculate the PTH level according to the color depth of the band, which ranged from 10 pg/mL to 1,000 pg/mL. A PTH dose greater than 130 pg/mL was regarded as the standard to justify the node as a parathyroid gland (**Figure 1**).

Finally, all tissues not identified as PGs during the procedure were examined pathologically. Among them, nonparathyroid tissues confirmed by aIOPTH were classified into two groups (the visually suspected parathyroid group and the NIRAF suspected parathyroid group) and submitted for pathology separately. The pathologist composed a report for each punctured tissue and carefully searched for the presence of PGs in all tissues.

Lymph Node Fluorescence Imaging

To observe the fluorescence intensity of the lymph nodes, we separated the specimens of lateral neck lymph node dissection into a high fluorescence intensity group and a low fluorescence

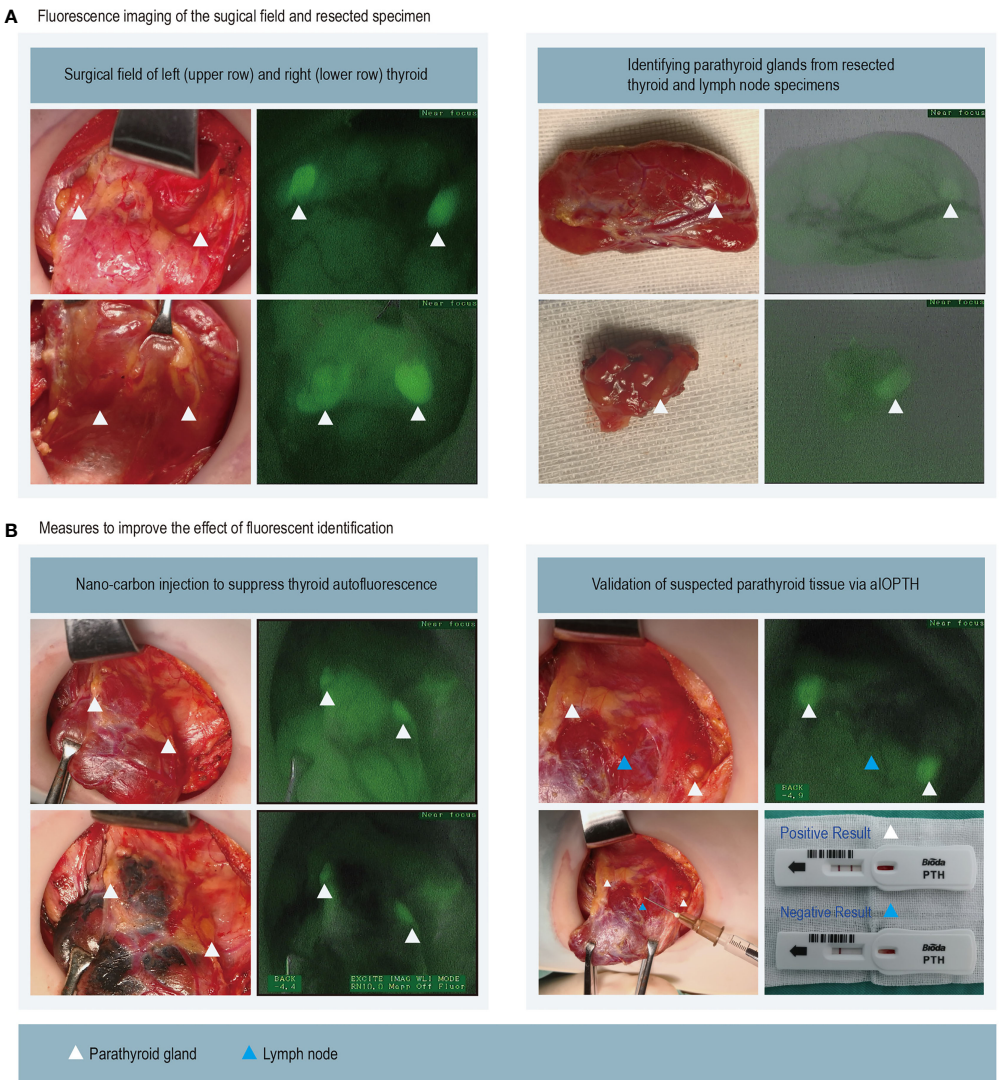

FIGURE 1 | We used fluorescence imaging of the surgical field and resected thyroid and lymph nodes specimens to locate the parathyroid gland. Parathyroid tissues can be highlighted as green in the images **(A)**. Nano-carbon can suppress the fluorescence of the thyroid gland and thus make it easier to recognize parathyroid glands. The lymph node (blue triangle) was visually recognized as the parathyroid gland, but it had weak fluorescence and was finally excluded via aIOPTH **(B)**.

intensity group under the fluorescence image and sent them separately for pathological examination. The number of lymph nodes in both groups was collected.

Data Collection

The following variables were collected during the trial: sex, age, body mass index (BMI; calculated as weight in kilograms divided by height in meters squared), preoperative calcium level, preoperative PTH level, type of surgery, number of patients who used nanocarbon during surgery, number of PGs first identified by NIRAF, number of identified PGs during total thyroidectomy and thyroid lobectomy separately, number of autotransplanted PGs, number of inadvertently resected PGs, PTH in fine-needle aspiration washout fluids from the PG, final diagnosis, postoperative hypocalcemia at postoperative day 1 or 2, nadir of postoperative calcium (considered in the normal range when it was >8.0 mg/dL; to convert to mmol/L, multiply by 0.25), PTH level at postoperative day 1 (considered in the normal range when it was ≥15 pg/mL; to convert to ng/L, multiply by 1.0), number of lymph nodes in lateral neck lymph nodes dissection and hypocalcemia at postoperative month 1.

Because the fluorescence intensity in the image could not be quantified in the imaging system, we used ImageJ software (National Institutes of Health, Bethesda, MD) to measure the fluorescence intensity of different tissues after surgery. First, we confirmed the type of certain tissue in the image and then used the ROI tool in ImageJ software to circle the boundaries of different tissues in the image and measure the average fluorescence intensity of the tissue within the boundary. When multiple identical tissues existed in one image, these tissues were continuously circled, and then the overall average fluorescence intensity was measured.

Quality Control of the Surgical Process and Data Collection

All operations were performed by the same high-volume surgeon and his assistant, who completed over 800 thyroidectomies a year together. Opinions for visual identification of the PGs were obtained from the surgeon. Before the end of the operation, the assistant checked to ensure that the necessary images and photos were correctly retained and that all specimens sent for pathological examination were correctly labeled.

The image analysis process was completed by the surgeon and his assistant after obtaining the postoperative pathological report. The first step was to compare the image with the operation record and pathological report and then to mark the corresponding tissue type in the fluorescent image. The confirmation of the thyroid and lymph nodes was based on the pathological report, confirmation of the PGs was obtained from aIOPTH results and the pathology report, and adipose tissue confirmation came from the pathological report and the judgment of the surgeon. The process of circle tissue boundary in ImageJ was completed by the surgeon and assistant. To reduce the error in the circle selection process, the arithmetic mean of the measurement results from both of them was used as the final result.

Statistical Analysis

Non-Gaussian distribution continuous variables (BMI, Preoperative calcium, Parathyroid hormone) are reported using medians and interquartile ranges (IQRs); autofluorescence intensity of tissues was tested to be normally distributed and thus reported as Mean±SD; categorical variables are reported using counts, percentages, and 95% CIs. Pearson's chi-square analysis was performed to compare the sensitivity and accuracy of NIRAF with vision in identifying parathyroid glands. The sensitivity was calculated by dividing the detected PGs by the final confirmed PGs. The accuracy was calculated by dividing the number of correctly judged tissues by the number of all suspicious tissues in this study. A paired-sample t-test was performed to compare the fluorescence intensity of PGs and other tissues separately. All analyses were 2-tailed, with $p \leq 0.05$ set as the criterion for statistical significance. All data were analyzed using SPSS statistical software, version 24.0 (SPSS, Inc.).

RESULTS

Overall, 250 patients were enrolled in this study, 122 patients used nanocarbon tracers due to strong thyroid autofluorescence during initial imaging, of whom 12 patients had contaminated the surgical field after injecting nanocarbon into the thyroid gland, which made subsequent NIRAF difficult to perform and thus were excluded from the study. The remaining 238 patients completed the trial; 145 patients underwent thyroid lobectomy, and 93 patients underwent total thyroidectomy. Most of them (198 of 238 patients; 83.2%) were diagnosed with malignant tumors. A total of 186 patients (186 of 238 patients; 78.2%) underwent lymph node dissection. Fifty-seven of 93 patients (61.3%) who underwent total thyroidectomy had 4 PGs confirmed, while 118 of 145 patients (81.4%) who underwent thyroid lobectomy had 2 PGs confirmed. Forty-nine patients (20.6%) developed hypocalcemia on the first or second postoperative day. A total of 234 patients were followed up for postoperative calcium, 2 of whom still had hypocalcemia one month after surgery, but these two patients had recovered in the second follow-up at 3 months (**Table 1**).

Overall, 841 suspicious parathyroid tissues were identified; 490 tissues were co-confirmed by vision and NIRAF as PGs, of which 88 PGs were first identified by NIRAF. A total of 351 tissues showed inconsistency between vision and NIRAF, and fine-needle aspiration was performed. Of the 128 tissues recognized as PGs only by NIRAF, 78 were eventually confirmed. Correspondingly, of 223 tissues only visually recognized, only 27 were confirmed as PGs. The mean PTH in fine-needle aspiration washout fluids of the parathyroid was 264 pg/mL.

Pathological examinations were performed on all the resected specimens during the surgery, including 246 labeled tissues with aIOPTH lower than 130 pg/ml. Of the 246 tissues, no parathyroid tissue was found, which was consistent with the aIOPTH results. There were 167 lymph nodes, 28 adipose tissues and 1 thyroid tissue among the tissues misidentified as PGs visually. Forty-nine tissues misidentified by NIRAF were adipose

TABLE 1 | Clinical Characteristic of Participants.

Characteristic	Patients No. (%) (N=238)	
Preoperative Variables		
Sex, No. (%)		
Male	54 (22.7)	
Female	184 (77.3)	
Age, median (IQR), y	45.0 (36.0-54.0)	
BMI, median (IQR)	25.4 (22.3-27.4)	
Preoperative calcium, median (IQR), pg/mL	9.20 (8.91-9.56)	
Preoperative parathyroid hormone, median (IQR), pg/mL	33.9 (27.6-43.6)	
Operative Variables		
Type of surgery.		
Total thyroidectomy with lymph nodes dissection	89 (37.4)	
Total thyroidectomy without lymph nodes dissection	4 (1.69)	
Thyroid lobectomy with lymph nodes dissection	97 (40.8)	
Thyroid lobectomy without lymph nodes dissection	48 (20.2)	
Patients who used nano-carbon during surgery	110 (46.2)	
Identified parathyroid glands during total thyroidectomy, No.		
1	1 (1.1)	n=93
2	1 (1.1)	
3	34 (36.6)	
4	57 (61.3)	
Identified parathyroid glands during thyroid lobectomy, No.		
0	1 (0.7)	n=145
1	26 (17.9)	
2	118 (81.4)	
Autotransplanted parathyroid glands, No.		
0	215 (90.3)	
1	21 (8.8)	
2	2 (0.8)	
Inadvertently resected parathyroid glands	1 (0.4)	
Parathyroid hormone[a] in fine-needle aspiration washout fluids of parathyroid, median (IQR), mg/dL	264 (198-367)	
Postoperative Variables		
Final diagnosis		
Benign condition	47 (19.7)	
Malignant condition	198 (83.2)	
Postoperative hypocalcemia at postoperative day 1 or 2	49 (20.6)	
Nadir of postoperative calcium, median (IQR), mg/dL	8.54 (8.21-9.07)	
Parathyroid hormone at postoperative day 1, median (IQR), pg/ml	24.6 (17.8-34.5)	
Hypocalcemia at postoperative 1 month	2[b]	

BMI, body mass index (calculated as weight in kilograms divided by height in meters squared); IQR, interquartile range. SI conversion factor: To convert calcium to mmol/L, multiply by 0.25; to convert parathyroid hormone to ng/L, multiply by 1. [a]Parathyroid hormone was tested by the rapid parathyroid hormone detection based on immune colloidal gold technique. [b]There were 4 losses in the follow-up period.

in pathology, and 1 tissue was thyroid (**Figure 2**). An inadvertently resected PG was found in the regular specimens sent for the final pathological examination.

Based on the pathological and aIOPTH results, the sensitivity of NIRAF to detect PGs (568 of 596 PGs; 95.30%) was significantly higher than that of vision (517 of 596 PGs; 86.74%, *P*<.001). Out of 841 suspected parathyroid tissues, there were 595 PGs, 167 lymph nodes, 77 adipose tissues and 2 thyroid tissues (**Figure 2**). The accuracy rate of NIRAF (764 of 841 tissues; 90.84%) was significantly higher than that of vision (567 of 841 tissues; 67.42%, *P*<.001) (**Supplementary Table 1**).

Combined with the final parathyroid identification results, a retrospective analysis was performed on the selected 331 fluorescent images. The mean fluorescence intensity was 74.19 ± 17.82 for parathyroid tissue in 331 images, 63.24 ± 17.53 for thyroid tissue in 331 images, 48.22 ± 15.31 for adipose tissue in 266 images, and 33.97 ± 10.64 for lymph nodes in 167 images (**Figure 3**). The fluorescence intensity of the parathyroid was significantly higher than that of other tissues in paired samples. The mean increase in parathyroid fluorescence intensity was 10.96 (95% CI, 9.18-12.73) with thyroid tissue (*P*<.001), 26.49 (95% CI, 24.63-28.36) with adipose tissue (*P*<.001), and 40.30

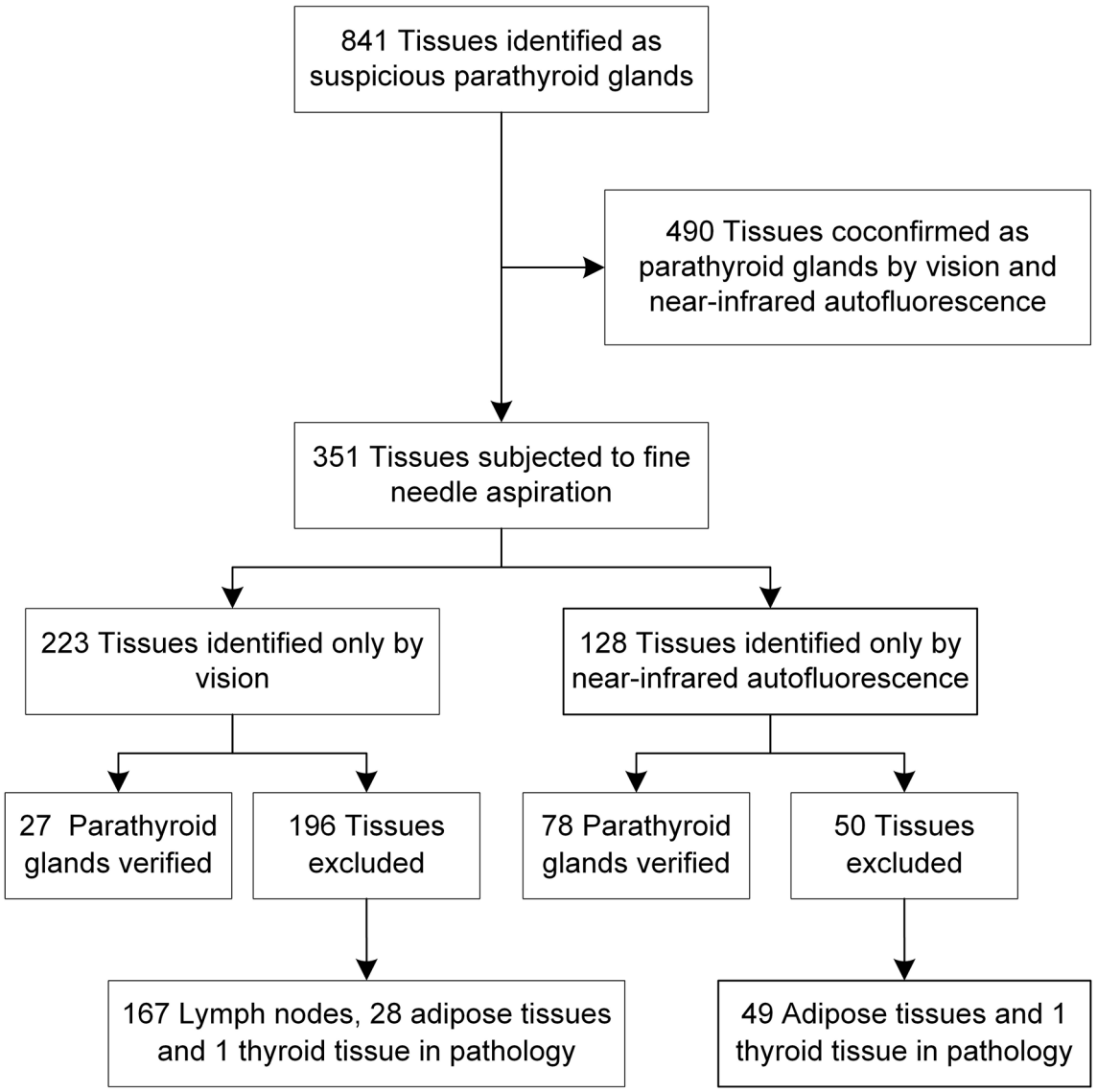

FIGURE 2 | The verification process of 841 suspicious parathyroid tissues.

(95% CI, 38.00-15.02) with lymph node tissue (P<.001) (**Supplementary Table 2**).

The lateral neck dissection specimens of 22 patients were sorted according to the autofluorescence intensity. The final pathological results showed that there were 536 lymph nodes in the tissues with low fluorescence intensity. No lymph nodes were found in the tissues with high fluorescence intensity (**Figure 4**).

DISCUSSION

To date, the highest quality of evidence on the effect of NIRAF comes from a multicenter randomized controlled study published by Benmiloud et al. (4), which showed that the rate of postoperative low calcium was significantly lower than that of the control group (from 26% to 11%). The rate of postoperative hypocalcemia after using NIRAF in our study was 20.6%. Our study included a higher proportion of patients with malignant tumors (83.2% *vs* 25.6%), and lymph node dissection was performed in most patients (186 of 238 patients, 78%), which led to a higher rate of postoperative hypocalcemia. However, the mean number of PGs found on each side of the thyroid in their study was 1.61 (390 PGs of 242 patients), compared to 1.80 (595 PGs of 331 patients) in our study. We found more PGs benefiting from the use of nanocarbon but the incidence of postoperative hypocalcemia increased, which indicated that the scope of the operation and protection of the parathyroid blood supply also had a crucial impact (14, 15). The effect of NIRAF is limited to the identification of PGs. Therefore, in evaluating the effect of

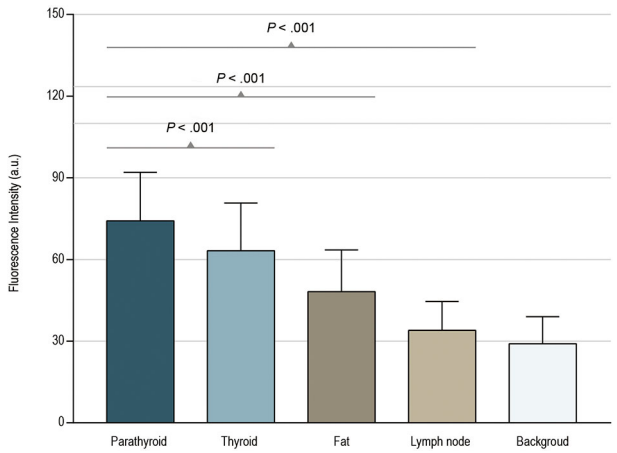

FIGURE 3 | Paired-samples t-test of fluorescence intensity in different tissues.

this technique, the number of identified PGs during surgery is a more direct variable.

The innovation of this study is the introduction of aIOPTH as a confirmatory method for PGs. The application of aIOPTH may provide an alternative to frozen section examination, dodging the injurious effect of the bioptic process and achieving similar or even more accurate results (16–18). However, the application of aIOPTH is not widespread, many endocrine surgeons are not familiar with this technology, and traditional PTH detection methods take much time (19). The rapid PTH detection method used in this study only takes approximately 10 minutes. In actual use, the test strip can turn red in an even shorter time with a positive result. When the cut-off value is 130 pg/mL, this method has proven to be highly consistent with pathological results in identifying PGs (20, 21). It has already been widely used in China and written in the 2018 perioperative parathyroid function protection guidelines for thyroid surgery by the Chinese Thyroid Association. Comparing the pathological results, aIOPTH achieved 100% specificity in our study.

To date, most studies have used visual recognition to confirm PGs due to ethical limitations. The results showed that NIRAF had extremely high sensitivity in identifying PGs (from 76% to 100%) (5, 8, 22). Most studies found that NIRAF could detect PGs before vision in nearly two-thirds of cases (4, 8, 23). Our study concluded that the sensitivity of NIRAF for identifying PGs was 95% by combining aIOPTH results and pathological results, and in the inconsistent cases between vision and NIRAF, the accuracy of NIRAF was 90.84%, while the accuracy of vision was only 67%, indicating that NIRAF was more trustworthy. Among the co-confirmed PGs, 88 PGs were first detected by NIRAF, and 78 PGs were found only by NIRAF. Therefore, of the 596 PGs found in the trial, the surgeon benefited from NIRAF in identifying 166 (28%) PGs.

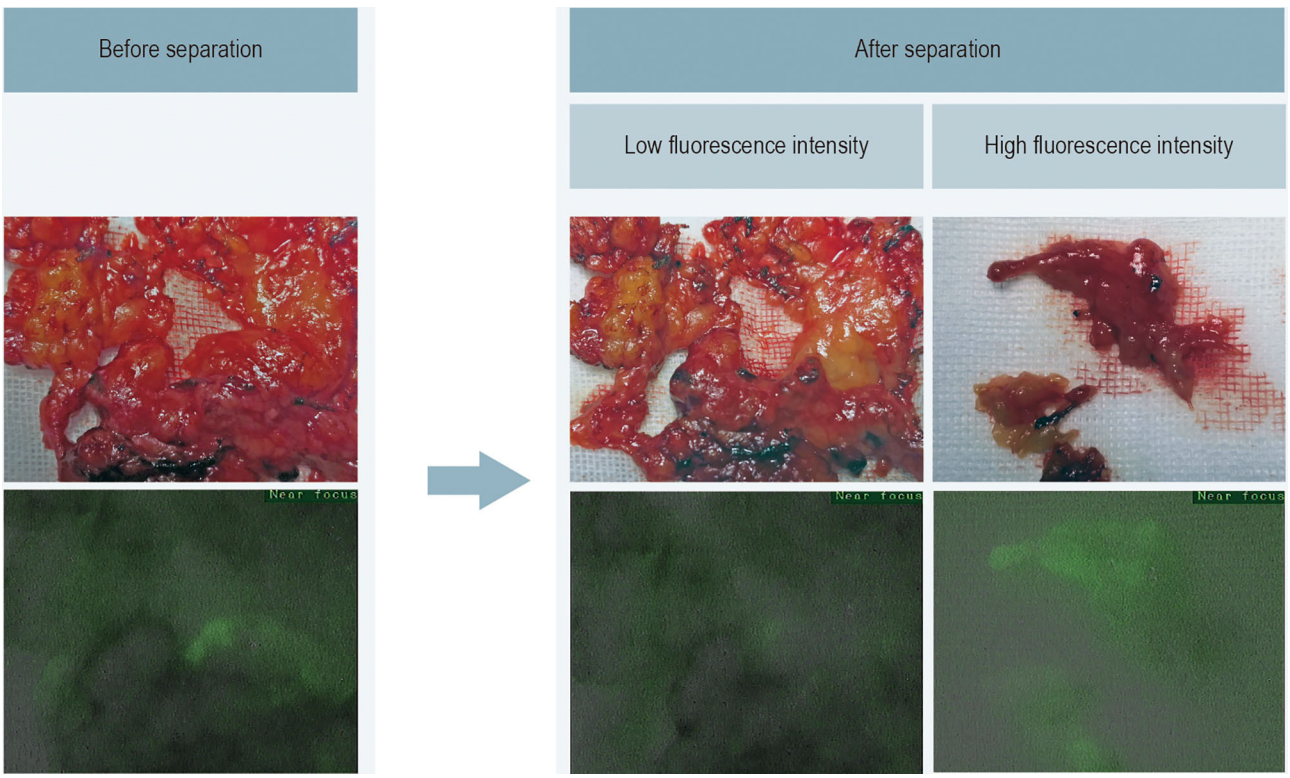

FIGURE 4 | Fluorescence imaging of lateral neck lymph node dissection specimens.

By comparing the fluorescence intensity of different tissues, we found that the autofluorescence intensity of the thyroid gland was closest to that of the PG (74.19 ± 17.82 *vs* 63.24 ± 17.53). This is concordant with a study by Falco et al. (22). The phenomenon that the autofluorescence intensity of the thyroid gland occasionally approaches or even exceeds the PG during surgery often affects the detection of PGs, and we suppressed the autofluorescence of the thyroid by injecting nanocarbon into the thyroid gland, thereby improving the fluorescence contrast of the PGs.

Of note, there was a significant difference in the autofluorescence intensity of the parathyroid and lymph nodes (74.19 ± 17.82 *vs* 33.97 ± 10.64), which is consistent with the result from Shinden et al. (24). Therefore, no lymph nodes were found in the 50 NIRAF false-positive tissues. Furthermore, we used NIRAF to sort out the tissues with no obvious fluorescence in lateral neck lymph node dissection, in which 536 lymph nodes were found pathologically. Meanwhile, no lymph nodes were found in the tissues with strong fluorescence intensity. We conclude from this result that the fluorescence intensity of lymph nodes is pretty weak compared to that of PGs. Lymph nodes are often misidentified as PGs during thyroid surgery. Of the 196 visual false-positive tissues in this study, 167 were lymph nodes. The surgical strategy of retaining all tissues with strong fluorescence intensity will help ensure a thorough dissection of lymph nodes, thereby reducing the tumor residue caused by misidentifying lymph nodes as PGs.

A total of 351 fine-needle aspirations were performed in 238 patients. According to the final result, the tissues with strong fluorescence intensity are mostly parathyroid and adipose tissues, thyroid tissues appear only in rare cases, which can be retained without further testing. During the trial, even if we identified a PG in a certain area, we still tried to find other suspicious parathyroid tissues. It is not necessary to do so in clinical applications, so the frequency of aIOPTH can be largely reduced, thereby shortening the operation time. The use of NIRAF requires only a small amount of time to remove the surgical lamp. Therefore, the use of NIRAF and aIOPTH technology in thyroid surgery will not significantly increase the duration of surgery.

To date, NIRAF has satisfied but not perfect sensitivity and specificity in published studies (10, 25). However, the strong fluorescence of thyroid sometimes may cover the fluorescence of PGs and thus decrease the sensitivity of NIRAF. The use of nanocarbon can solve the problem. Meanwhile, aIOPTH can separate false-positive tissues with high fluorescence from PGs and enhance the specificity. All these measures are time-saving and easy to implement. These methods along with NIRAF form a perfect complement in thyroid surgery, which can effectively find atypical PGs and prevent them from being inadvertently resected.

This case series study, despite its careful experimental design, strict quality control, and a large number of patients, is still not enough to show that this new surgical strategy can improve the number of identified PGs. Therefore, we plan to conduct a further randomized controlled study to illustrate this issue. Another drawback is that we did not puncture the PGs identified by both vision and NIRAF, which is mainly based on the purpose of reducing parathyroid damage. Although fine-needle biopsy poses minimal damage to the tissue, there is still a report that such puncture may cause secondary lesions of the PGs (26).

CONCLUSIONS

In conclusion, we evaluated the effect of NIRAF in identifying PGs in thyroid surgery through a large-sample case series. Using NIRAF in thyroid surgery can effectively assist surgeons in identifying PGs and distinguishing lymph nodes when lymph node dissection is performed. Measuring aIOPTH was an ideal objective method to evaluate the effect of NIRAF. It may work with nanocarbon as complements to NIRAF and thus improves the sensitivity and specificity.

DATA AVAILABILITY STATEMENT

The original contributions presented in the study are included in the article/**Supplementary Material**. Further inquiries can be directed to the corresponding author.

ETHICS STATEMENT

The studies involving human participants were reviewed and approved by The institutional review board of the First Affiliated Hospital of Zhengzhou University. The patients/participants provided their written informed consent to participate in this study.

AUTHOR CONTRIBUTIONS

Conception and design: ZL and D-tY. Administrative support: ZL and D-tY. Provision of study materials or patients: ZL and D-tY. Collection and assembly of data: ZL, R-sM, J-lJ, TW, and D-hZ. Data analysis and interpretation: ZL and J-lJ. All authors contributed to the article and approved the submitted version.

FUNDING

This work was supported by the following funds: Young Talents Promotion Program of Henan Science and Technology Department (2020HYTP055), Major Scientific Research Projects of Traditional Chinese Medicine in Henan Province (No.20-21ZYZD14), and Cultivation of Young and Middle-aged Health Science and Technology Innovation Leading Talents in Henan Province (YXKC2020015).

ACKNOWLEDGMENTS

The authors would like to acknowledge the support of colleagues from the operation department.

SUPPLEMENTARY MATERIAL

The Supplementary Material for this article can be found online at: https://www.frontiersin.org/articles/10.3389/fendo.2021.819503/full#supplementary-material

Supplementary Table 1 | Comparing the sensitivity and accuracy of NIRAF with vision in identifying parathyroid glands. PGs parathyroid glands; [a]The sensitivity of NIRAF was significantly higher than vision in 596 parathyroid glands, *P*<.001. [b]The accuracy of NIRAF was significantly higher than vision in 841 suspected parathyroid tissues. *P*<.001

Supplementary Table 2 | Paired-samples t-test of fluorescence intensity in different tissues.

Supplementary Figure 1 | Fluorescence imaging device and operating environment. The operating room illuminated by LED light sources does not need to turn off the light, only needs to remove the operating lamp, but the operating room illuminated by a halogen lamp needs to turn off the light source. During the NIRAF imaging process, it is necessary to avoid the camera shooting of the surgery field, which will cause the flicker of the fluorescent image. The electrocautery should be used with caution during the operation to reduce the generation of eschar, which has extremely strong autofluorescence under fluorescent imaging.

Supplementary Figure 2 | Test strip and parathyroid hormone detector for measuring intraoperative parathyroid hormone in fine-needle aspiration biopsy washings. **(A)** Control line **(B)** Test line **(C)** Reaction zone. The test line requires a 10-minute incubation time to reach a stable final result, but in most cases, the test line can turn red in a shorter time with a positive result. Parathyroid hormone detector is not needed if exact values are not required

Supplementary Video 1 | Intraoperative near-infrared autofluorescence imaging of parathyroid glands. The NIRAF probe is wrapped with a sterile lens cover, and the surgeon holds the NIRAF probe with one hand to perform fluorescence imaging of the surgical field. The operating room lighting can be kept after removing the surgical lamp from the surgical field.

Supplementary Video 2 | Measuring intraoperative parathyroid hormone in fine-needle aspiration biopsy washings of the suspicious parathyroid gland. The suspicious tissue with strong fluorescence intensity was punctured with a 1 ml syringe containing 0.1 ml saline and then drip the 0.1 ml saline through the needle onto the reaction area of the test strip.

REFERENCES

1. Liu JB, Sosa JA, Grogan RH, Liu Y, Cohen ME, Ko CY, et al. Variation of Thyroidectomy-Specific Outcomes Among Hospitals and Their Association With Risk Adjustment and Hospital Performance. *JAMA Surg* (2018) 153:1–10. doi: 10.1001/jamasurg.2017.4593
2. Abbaci M, De Leeuw F, Breuskin I, Casiraghi O, Lakhdar AB, Ghanem W, et al. Parathyroid Gland Management Using Optical Technologies During Thyroidectomy or Parathyroidectomy: A Systematic Review. *Oral Oncol* (2018) 87:186–96. doi: 10.1016/j.oraloncology.2018.11.011
3. Rudin AV, Berber E. Impact of Fluorescence and Autofluorescence on Surgical Strategy in Benign and Malignant Neck Endocrine Diseases. *Best Pract Res Clin Endocrinol Metab* (2019) 33:101311. doi: 10.1016/j.beem.2019.101311
4. Benmiloud F, Godiris-Petit G, Gras R, Gillot JC, Turrin N, Penaranda G, et al. Association of Autofluorescence-Based Detection of the Parathyroid Glands During Total Thyroidectomy With Postoperative Hypocalcemia Risk: Results of the PARAFLUO Multicenter Randomized Clinical Trial. *JAMA Surg* (2019) 155:106–12. doi: 10.1001/jamasurg.2019.4613
5. Benmiloud F, Rebaudet S, Varoquaux A, Penaranda G, Bannier M, Denizot A. Impact of Autofluorescence-Based Identification of Parathyroids During Total Thyroidectomy on Postoperative Hypocalcemia: A Before and After Controlled Study. *Surg (United States)* (2018) 163:23–30. doi: 10.1016/j.surg.2017.06.022
6. Dip F, Falco J, Verna S, Prunello M, Loccisano M, Quadri P, et al. Randomized Controlled Trial Comparing White Light With Near-Infrared Autofluorescence for Parathyroid Gland Identification During Total Thyroidectomy. *J Am Coll Surg* (2019) 228:744–51. doi: 10.1016/j.jamcollsurg.2018.12.044
7. Kose E, Rudin AV, Kahramangil B, Moore E, Aydin H, Donmez M, et al. Autofluorescence Imaging of Parathyroid Glands: An Assessment of Potential Indications. *Surg (United States)* (2019) 228:744–51. doi: 10.1016/j.surg.2019.04.072
8. Kahramangil B, Dip F, Benmiloud F, Falco J, de la Fuente M, Verna S, et al. Detection of Parathyroid Autofluorescence Using Near-Infrared Imaging: A Multicenter Analysis of Concordance Between Different Surgeons. *Ann Surg Oncol* (2018) 25:957–62. doi: 10.1245/s10434-018-6364-2
9. McWade MA, Sanders ME, Broome JT, Solórzano CC, Mahadevan-Jansen A. Establishing the Clinical Utility of Autofluorescence Spectroscopy for Parathyroid Detection. *Surg (United States)* (2016) 159:193–203. doi: 10.1016/j.surg.2015.06.047
10. Wang B, Zhu C-R, Liu H, Yao X-M, Wu J. The Accuracy of Near Infrared Autofluorescence in Identifying Parathyroid Gland During Thyroid and Parathyroid Surgery: A Meta-Analysis. *Front Endocrinol (Lausanne)* (2021) 12:701253. doi: 10.3389/fendo.2021.701253
11. Squires MH, Shirley LA, Shen C, Jarvis R, Phay JE. Intraoperative Autofluorescence Parathyroid Identification in Patients With Multiple Endocrine Neoplasia Type 1. *JAMA Otolaryngol - Head Neck Surg* (2019) 145:897–902. doi: 10.1001/jamaoto.2019.1987
12. Kose E, Kahramangil B, Aydin H, Donmez M, Berber E. Heterogeneous and Low-Intensity Parathyroid Autofluorescence: Patterns Suggesting Hyperfunction at Parathyroid Exploration. *Surg (United States)* (2019) 165:431–7. doi: 10.1016/j.surg.2018.08.006
13. Trimboli P, D'Aurizio F, Tozzoli R, Giovanella L. Measurement of Thyroglobulin, Calcitonin, and PTH in FNA Washout Fluids. *Clin Chem Lab Med* (2017) 55:914–25. doi: 10.1515/cclm-2016-0543
14. Giordano D, Valcavi R, Thompson GB, Pedroni C, Renna L, Gradoni P, et al. Complications of Central Neck Dissection in Patients With Papillary Thyroid Carcinoma: Results of a Study on 1087 Patients and Review of the Literature. *Thyroid* (2012) 22:911–7. doi: 10.1089/thy.2012.0011
15. Wang X, Xing T, Wei T, Zhu J. Completion Thyroidectomy and Total Thyroidectomy for Differentiated Thyroid Cancer: Comparison and Prediction of Postoperative Hypoparathyroidism. *J Surg Oncol* (2016) 113:522–5. doi: 10.1002/jso.24159
16. Shawky MS. Quick Parathyroid Hormone Assays: A Comprehensive Review of Their Utility in Clinical Practice. *Hormones* (2016) 15:355–67. doi: 10.14310/horm.2002.1689
17. Ketha H, Lasho MA, Algeciras-Schimnich A. Analytical and Clinical Validation of Parathyroid Hormone (PTH) Measurement in Fine-Needle Aspiration Biopsy (FNAB) Washings. *Clin Biochem* (2016) 49:16–21. doi: 10.1016/j.clinbiochem.2015.09.006
18. Pelizzo MR, Losi A, Boschin IM, Toniato A, Pennelli G, Sorgato N, et al. Rapid Intraoperative Parathyroid Hormone Assay in Fine Needle Aspiration for Differential Diagnosis in Thyroid and Parathyroid Surgery. *Clin Chem Lab Med* (2010) 48:1313–7. doi: 10.1515/CCLM.2010.247
19. Coan KE, Yen TWF, Carr AA, Evans DB, Wang TS. Confirmation of Parathyroid Tissue: Are Surgeons Aware of New and Novel Techniques? *J Surg Res* (2020) 246:139–44. doi: 10.1016/j.jss.2019.08.006
20. James BC, Nagar S, Tracy M, Kaplan EL, Angelos P, Scherberg NH, et al. A Novel, Ultrarapid Parathyroid Hormone Assay to Distinguish Parathyroid From Nonparathyroid Tissue. *Surg (United States)* (2014) 156:1638–43. doi: 10.1016/j.surg.2014.08.081
21. Wei H, Huang M, Fan J, Wang T, Ling R. Intraoperative Rapid Aspiration Cytological Method for Parathyroid Glands Identification and Protection. *Endocr J* (2019) 66:135–41. doi: 10.1507/endocrj.EJ18-0363
22. Falco J, Dip F, Quadri P, de la Fuente M, Prunello M, Rosenthal RJ. Increased Identification of Parathyroid Glands Using Near Infrared Light During

Thyroid and Parathyroid Surgery. *Surg Endosc* (2017) 31:3737–42. doi: 10.1007/s00464-017-5424-1
23. Kim SW, Lee HS, Ahn YC, Park CW, Jeon SW, Kim CH, et al. Near-Infrared Autofluorescence Image-Guided Parathyroid Gland Mapping in Thyroidectomy. *J Am Coll Surg* (2018) 226:165–72. doi: 10.1016/j.jamcollsurg.2017.10.015
24. Shinden Y, Nakajo A, Arima H, Tanoue K, Hirata M, Kijima Y, et al. Intraoperative Identification of the Parathyroid Gland With a Fluorescence Detection System. *World J Surg* (2017) 41:1506–12. doi: 10.1007/s00268-017-3903-0
25. Solórzano CC, Thomas G, Baregamian N, Mahadevan-Jansen A. Detecting the Near Infrared Autofluorescence of the Human Parathyroid: Hype or Opportunity? *Ann Surg* (2020) 272:973–85. doi: 10.1097/SLA.0000000000003700
26. Kim J, Horowitz G, Hong M, Orsini M, Asa SL, Higgins K. The Dangers of Parathyroid Biopsy. *J Otolaryngol - Head Neck Surg* (2017) 46:2–5. doi: 10.1186/s40463-016-0178-7

Conflict of Interest: The authors declare that the research was conducted in the absence of any commercial or financial relationships that could be construed as a potential conflict of interest.

frontiers in Endocrinology

ORIGINAL RESEARCH
published: 08 February 2022
doi: 10.3389/fendo.2021.790730

Clinical Characteristics-Assisted Risk Stratification for Extent of Thyroidectomy in Patients With 1–4 cm Solitary Intrathyroidal Differentiated Thyroid Cancer

Fang Dong[1†], *Lin Zhou*[1†], *Shuntao Wang*[1], *Jinqian Mao*[2], *Chunping Liu*[1*] *and Wei Shi*[1*]

[1] *Department of Breast and Thyroid Surgery, Union Hospital, Tongji Medical College, Huazhong University of Science and Technology, Wuhan, China,* [2] *Department of Vascular Surgery, Union Hospital of Tongji Medical College, Huazhong University of Science and Technology, Wuhan, China*

OPEN ACCESS

Edited by:
Gianlorenzo Dionigi, University of Milan, Italy

Reviewed by:
Zeming Liu, Huazhong University of Science and Technology, China
Liang Guo, Wuhan University, China
Jie Ming, Huazhong University of Science and Technology, China

***Correspondence:**
Chunping Liu
liucpwhxh@hust.edu.cn
Wei Shi
shiweihust@163.com

[†]*These authors have contributed equally to this work*

Specialty section:
This article was submitted to Thyroid Endocrinology, a section of the journal Frontiers in Endocrinology

Received: *07 October 2021*
Accepted: *31 December 2021*
Published: *08 February 2022*

Citation:
Dong F, Zhou L, Wang S, Mao J, Liu C and Shi W (2022) Clinical Characteristics-Assisted Risk Stratification for Extent of Thyroidectomy in Patients With 1–4 cm Solitary Intrathyroidal Differentiated Thyroid Cancer. Front. Endocrinol. 12:790730. doi: 10.3389/fendo.2021.790730

Background: Differentiated thyroid cancer (DTC) is the most common type of thyroid cancer. The 2015 American Thyroid Association (ATA) guidelines recommend that lobectomy is suitable for solitary intrathyroidal DTC (SI-DTC) of 1–4 cm. However, some SI-DTC patients with other high-risk characteristics still have poor prognosis and require more aggressive surgical methods. This study aimed to explore the clinical characteristics that are important for the identification and treatment of high-risk patients with SI-DTC of 1–4 cm.

Methods: The study cohort was obtained from the SEER database, consisting of data between 2004 and 2013. The outcome measures were thyroid carcinoma-specific mortality (CSM) and all-cause mortality (ACM). Patient survival curves were examined using Kaplan–Meier analyses with log-rank tests and Cox proportional hazards regression analyses. Hazard ratios (HRs) were used to show the magnitude of the effect of disease stage on DTC-specific patient mortality.

Results: The study included 55,947 patients with SI-DTC of 1–4 cm and 4,765 patients with DTC >4 cm. Tumor size, surgical approach, age, sex, race, and radiation exposure were independent risk factors for CSM and ACM. SI-DTC patients with female, age ≤45, and 1 cm< tumor size ≤2 cm were at low risk of CSM [HR = 0.014 (0.002–0.115)] and ACM [HR = 0.115 (0.077–0.171)] when stratified by age, sex, and tumor size. Compared to T3 patients, CSM was not significantly different in male patients, age >45, 2 cm< tumor size ≤3 cm [HR = 0.839 (0.414–1.700)] and male patients, age >45, 1 cm< tumor size ≤2 cm [HR = 0.751 (0.410–1.377)]. Furthermore, compared to T3 patients without extrathyroidal extension (ETE) and lymph node metastasis (LNM), more subgroups of SI-DTC of 1–4 cm had a similar prognosis. In addition, patients with SI-DTC of 1–4 cm showed similar rates of CSM and ACM to T3 patients without ETE, LNM, and distant metastasis (DM). Similar results were obtained when we set the age cut-off value as 55 years, according to the 8th edition of AJCC TNM system.

Conclusions: Our study demonstrated that sex, age, and tumor size clearly differentiate SI-DTC of 1–4 cm into low-and high-risk categories. Survival rates were significantly lower in subgroups containing old males with larger tumors compared to younger females with small tumors. Total thyroidectomy may be favored in these high-risk subgroup patients.

Keywords: differentiated thyroid cancer, SEER, surgery approaches, tumor size, thyroidectomy

INTRODUCTION

Thyroid cancer is a frequently encountered endocrine malignancy, and differentiated thyroid cancer (DTC), namely, papillary thyroid cancer (PTC) and follicular thyroid cancer (FTC), are the most common types of thyroid cancer, accounting for about 90% of all thyroid malignancies (1–3). DTC is curable and inert with low mortality, but some patients have an aggressive disease course, such as recurrence (4, 5).

Effective risk stratification based on the evaluation of clinicopathological risk features is important for appropriate treatment of DTC patients to balance treatment, such as surgical benefits and complications (6, 7). This can be referenced in the American Thyroid Association's guidelines (6th, 7th, and 8th versions) on the management of DTC (5, 8, 9). The 8th version (2015 American Thyroid Association (ATA) guideline) recommended that lobectomy is suitable for solitary intrathyroidal DTC (SI-DTC: without extrathyroidal invasion, lymph node metastasis, and distant metastasis) of tumor size between 1 and 4 cm and is accepted by most clinicians for the treatment of thyroid cancer.

However, the worldwide impact of this recommendation on the treatment of thyroid cancer remains controversial (10–12). Because other high-risk characteristics in patients with SI-DTC may also affect survival, this subgroup may not be suitable for union surgical strategy. Therefore, in this study, we tried to investigate the high-risk patients among the ST-DTC of 1–4 cm and attempted to provide clues for precision treatment of SI-DTC of 1–4 cm.

MATERIALS AND METHODS

Patient Population

The DTC study cohort was obtained from the Surveillance, Epidemiology, and End Results (SEER) from 18 regions in the United States, consisting of data between 2004 and 2013. The SEER project is a United States population-based cancer registry that began in 1973 and is supported by the National Cancer Institute and the Centers for Disease Control and Prevention. It covers approximately 30% of the population of the United States and contains data across multiple geographic regions on incidence, prevalence, mortality, population-based variables, primary characteristics of the tumor, and other attributes.

Data Collection

Study participants included patients with a diagnosis of DTC, defined by a combination of International Classification of Diseases for Oncology (ICD-O) site code C73.9 (i.e., thyroid) and diagnostic codes of papillary and/or follicular histology. The diagnostic codes used in the study included "papillary carcinoma", "papillary adenocarcinoma", "follicular adenocarcinoma", and "papillary & follicular adenocarcinoma". Patients without follow-up information were excluded from the study.

Statistical Analyses

Patients were followed up until December 2013. The outcome measures were thyroid carcinoma-specific mortality and all-cause mortality. Patient survival curves were examined using Kaplan–Meier analyses with log-rank tests and Cox proportional hazards regression analyses. Hazard ratios (HRs) were used to show the magnitude of the effect of disease stage on DTC-specific patient mortality, and 95% confidence intervals (CIs) were used to indicate the significance of the risk. All *P*-values were 2-sided, and $P < 0.05$ was considered significant. Analyses were performed using SPSS version 19.0, Stata/SE version 12 (Stata Corp), and GraphPad Prism version 6 (GraphPad Software Inc.).

RESULTS

Characteristics for Patients With SI-DTC of 0–4 cm

This study assessed the prognosis of 55,947 patients with SI-DTC with tumor size 1–4 cm and 4,765 patients with DTC with tumor size >4 cm. The mean age and follow-up duration according to the different histological subtypes are shown in **Table 1**. The clinicopathological features of patients with SI-DTC of 0–4 cm were analyzed according to tumor size (**Table 1**). Age at diagnosis, sex, race, radiation, multifocality, and surgical approaches all showed significant differences among the different tumor size groups.

Risk Factors for Cancer-Specific and All-Cause Mortality

The results of the univariate Cox regression analyses demonstrated that cancer-specific mortality was associated with age, sex, race, tumor size, and treatment approaches (radiation and surgery). Furthermore, all-cause mortality was also found to be associated with age, sex, race, radiation, and surgery. Meanwhile, the multivariate Cox regression model showed that tumor size, surgical approach, age, sex, race, and radiation were independent risk factors for cancer-specific mortality and all-cause mortality (**Table 2**).

TABLE 1 | Charectaristic for patients with EXE (–), N0, M0, tumor size 0–4 cm.

Covariate	Level	0–1 cm	1–2 cm	2–3 cm	3–4 cm	p-value
Age*		51.44 ± 13.75	48.81 ± 14.54	47.74 ± 15.43	47.77 ± 15.99	<0.001
sex	female	24,000 (83.1%)	12,643 (80.9%)	5,893 (77.7%)	2,823 (73.1%)	<0.001
	male	4,879 (16.9%)	2,979 (19.1%)	1,691 (22.3%)	1,039 (26.9%)	
race	white	24,306 (84.2%)	13,106 (83.9%)	6,219 (82.0%)	3,109 (80.5%)	<0.001
	black	2,023 (7.0%)	941 (6.0%)	588 (7.8%)	380 (9.8%)	
	other	2,550 (8.8%)	1,575 (10.1%)	777 (10.2%)	373 (9.7%)	
radiation	none of refused	22,509 (77.9%)	6,948 (44.5%)	2,820 (37.2%)	1,381 (35.8%)	<0.001
	radiation	6,370 (22.1%)	8,674 (55.5%)	4,764 (62.8%)	2,481 (64.2%)	
multifocality	no	19,763 (68.4%)	9,218 (59.0%)	4,774 (62.9%)	2,556 (66.2%)	<0.001
	yes	9,116 (31.6%)	6,404 (41.0%)	2,810 (37.1%)	1,306 (33.8%)	
surgery	lobectomy	7,306 (25.3%)	1,638(10.5%)	991 (13.1%)	579 (15.0%)	<0.001
	subtotal or near total	1,349 (4.7%)	548 (3.5%)	300 (4.0%)	169 (4.4%)	
	total	20,224 (70.0%)	13,436 (86.0%)	6,293 (83.0%)	3,114 (80.6%)	
survival months		48.71 ± 33.22	51.11 ± 33.83	52.40 ± 34.29	52.53 ± 34.29	<0.001

**Age at diagnosis.*

TABLE 2 | Risk factors for survival: Outcome of thyroid cancer specific mortality and all-cause mortality.

Covariate	Level	Thyroid cancer specific mortality				All-cause mortality			
		Univariate cox regression		Multivariate Cox regression		Univariate Cox regression		Multivariate Cox regression	
		Hazard Ratio (95%CI)	p-value	Hazard Ratio (95%CI)	p-value	Hazard Ratio (95%CI)	p-value	Hazard Ratio (95%CI)	p-value
age at diagnosis		1.096 (1.079–1.114)	<0.001	1.099 (1.081–1.116)	<0.001	1.083 (1.079–1.087)	<0.001	1.081 (1.077–1.085)	<0.001
sex	female	ref		ref		ref		ref	
	male	2.770 (1.845–4.159)	<0.001	1.900 (1.261–2.862)	0.002	2.200 (1.994–2.427)	<0.001	1.680 (1.521–1.856)	<0.001
race	white	ref		ref		ref		Ref	
	black	0.447 (0.150–1.509)	0.208	0.570 (0.180–1.810)	0.341	1.304 (1.106–1.538)	0.002	1.467 (1.243–1.731)	<0.001
	other	1.876 (1.096–3.211)	0.022	2.130 (1.242–3.651)	0.006	0.722 (0.598–0.872)	<0.001	0.871 (0.721–1.051)	0.149
tumor size	0–1 cm	ref		ref		ref		ref	
	1–2 cm	1.476 (0.876–2.486)	0.143	1.170 (0.680–2.014)	0.571	0.897 (0.802–1.002)	0.055	1.085 (0.965–1.219)	0.172
	2–3 cm	2.966 (1.761–4.996)	<0.001	2.217 (1.279–3.843)	0.005	0.993 (0.865–1.140)	0.921	1.195 (1.035–1.380)	0.015
	3–4 cm	3.352 (1.809–6.210)	<0.001	2.171 (1.137–4.148)	0.019	1.074 (0.901–1.281)	0.426	1.160 (0.967–1.392)	0.109
multifocality	No	ref		ref		ref		ref	
	yes	1.200 (0.795–1.810)	0.386	0.886 (0.584–1.345)	0.569	0.938 (0.850–1.035)	0.205	0.982 (0.888–1.087)	0.732
radiation	none of refused	ref		ref		ref		ref	
	radiation	2.371 (1.568–3.586)	<0.001	2.185 (1.377–3.466)	<0.001	0.683 (0.620–0.753)	<0.001	0.827 (0.741–0.923)	0.001
surgery	lobectomy	ref		ref		ref		ref	
	subtotal or near total	2.118 (0.710–6.321)	0.179	1.976 (0.657–5.947)	0.226	0.904 (0.727–1.125)	0.366	1.023 (0.821–1.274)	0.838
	total	2.381 (1.197–4.735)	0.013	1.983 (0.969–4.056)	0.061	0.788 (0.705–0.880)	<0.001	0.987 (0.877–1.109)	0.822

Subgroups Analysis With High-Risk Mortality

When three common clinical factors, age, sex, and tumor size, were included to select the high-risk mortality of SI-DTC, we found that compared to patients with male sex, age >45 years, and 3 cm< tumor size ≤4 cm, female patients with 1 cm <tumor size ≤3 cm aged ≤45 years, female patients with 0< tumor size ≤3 cm aged >45 years, and male patients with 0< tumor size ≤2 cm aged >45 years were at a lower risk of cancer-specific mortality (**Table 3**).

Moreover, age ≤45 years was a low-risk factor for all-cause mortality in all patients regardless of sex or tumor size when compared to male patients with age >45 years old and 3 cm< tumor size ≤4 cm. For patients aged >45 years, female sex and 0< tumor size ≤3 cm were low-risk factors for all-cause mortality (**Table 3**).

Comparison Between SI-DTC With T3 Patients

When T3 patients were included for comparison, we found that the cancer-specific mortality showed no significant difference between T3 patients, SI-DTC patients with male sex, age >45 years, and 2 cm< tumor size ≤3 cm (HR: 0.839, 95%CI: 0.414–1.700), and SI-DTC patients with male sex, age >45 years, and 1 cm< tumor size ≤2 cm (HR: 0.751, 95%CI: 0.410–1.377). Similar results were obtained for all-cause mortality (**Table 4** and **Figure 1**).

Furthermore, when we selected T3 patients with tumor size >4 cm and excluded T3 patients without ETE and LNM for reference, we found that more subgroups of SI-DTC with a tumor size of 1–4 cm had a similar prognosis (cancer-specific mortality) with T3 patients having a tumor size >4 cm. Similar results were obtained for all-cause mortality (**Table 5** and **Figure 2**).

TABLE 3 | Age, sex, tumor size factors for survival: outcome of thyroid cancer specific mortality and all-cause mortality.

Covariate	Level	Thyroid cancer specific mortality		All-cause mortality	
		Univariate Cox regression		Univariate Cox regression	
		Hazard Ratio (95%CI)	p-value	Hazard Ratio (95%CI)	p-value
0		ref		ref	
1		0.014 (0.002–0.115)	<0.001	0.115 (0.077–0.171)	<0.001
2		0.084 (0.022–0.318)	<0.001	0.098 (0.059–0.164)	<0.001
3			0.971	0.068 (0.031–0.150)	<0.001
4			0.975	0.159 (0.084–0.299)	<0.001
5			0.976	0.173 (0.092–0.326)	<0.001
6			0.981	0.217 (0.110–0.429)	<0.001
7			0.985	0.289 (0.137–0.611)	0.001
8		0.120 (0.053–0.272)	<0.001	0.593 (0.442–0.796)	0.001
9		0.217 (0.094–0.502)	<0.001	0.559 (0.411–0.760)	<0.001
10		0.342 (0.140–0.838)	0.019	0.640 (0.460–0.890)	0.008
11		0.427 (0.155–1.177)	0.1	0.817 (0.571–1.169)	0.269
12		0.275 (0.111–0.684)	0.005	1.116 (0.821–1.518)	0.484
13		0.363 (0.136–0.967)	0.043	1.137 (0.821–1.574)	0.441
14		0.910 (0.366–2.264)	0.84	1.310 (0.925–1.855)	0.128
15			0.93	0.086 (0.058–0.128)	<0.001

Ref: age >45 years old, Male, 3< tumor size ≤4 cm.
1: age ≤45 years old, Female, 1< tumor size ≤2 cm.
2: age ≤45 years old, Female, 2< tumor size ≤3 cm.
3: age ≤45 years old, Female, 3< tumor size ≤4 cm.
4: age ≤45 years old, Male, 0< tumor size ≤1 cm.
5: age ≤45 years old, Male, 1< tumor size ≤2 cm.
6: age ≤45 years old, Male, 2< tumor size ≤3 cm.
7: age ≤45 years old, Male, 3< tumor size ≤4 cm.
8: age >45 years old, Female, 0< tumor size ≤1 cm.
9: age >45 years old, Female, 1< tumor size ≤2 cm.
10: age >45 years old, Female, 2< tumor size ≤3 cm.
11: age >45 years old, Female, 3< tumor size ≤4 cm.
12: age >45 years old, Male, 0< tumor size ≤1 cm.
13: age >45 years old, Male, 1< tumor size ≤2 cm.
14: age >45 years old, Male, 2< tumor size ≤3 cm.
15: age ≤45 years old, Female, 0< tumor size ≤1 cm.

In addition, when we selected T3 patients without ETE, LNM, and DM as references, we found that more subgroups and patients with SI-DTC with a tumor size of 1–4 cm showed similar rates of cancer-specific mortality and all-cause mortality (**Table 6** and **Figure 3**). Similar results were obtained when we set the age cut-off value as 55 years according to the 8th edition of the American Joint Committee on Cancer (AJCC) Tumor, Node, Metastasis (TNM) system (13) (**Tables S1–S3** and **Figures S1–S3**).

DISCUSSION

The current trend in the management of DTC has become more conservative. Unilateral lobectomy is now suggested as a viable alternative to total thyroidectomy for patients with SI-DTC 1–4 cm in size based on the ATA 2015 guidelines (4). Although overall prognosis seems to be excellent after lobectomy, some patients that appear to be at low risk, in fact, have high intrinsic risk for poor prognosis and should benefit from an aggressive treatment. Even in papillary thyroid microcarcinoma, cases evaluated as having a low risk of recurrence preoperatively showed intermediate to high-risk disease post-surgery, leading to a higher rate of radioiodine therapy (14).

Lobectomy for low-risk SI-DTC can be beneficial for thyroid function preservation and decreased risk of surgical complications, such as postoperative hypoparathyroidism and recurrent laryngeal nerve injury, according to many reports (15, 16). Despite these advantages, total thyroidectomy is generally accepted for SI-DTC because total thyroidectomy can provide convenience for the use of radioactive iodine in surveillance and postoperative treatment (4). It is easier to detect recurrence early *via* follow-up and dynamically monitoring serum thyroglobulin levels. In addition, Benjamin et al. reported that nearly half of low-risk DTC patients were found to have tumors in the contralateral lobe and may be more adequate for total thyroidectomy (17).

This study suggested that there were still some patients with high-risk prognosis among the SI-DTC with 1–4 cm, and selecting low-risk patients based on ETE, LNM, and DM was not precise. Our results provided some estimate for this possible need for completion of a total thyroidectomy after an initial lobectomy for these otherwise low-risk patients and can provide a future guide for the precision treatment for patients with SI-DTC of 1–4 cm.

In addition, some patients who underwent lobectomy may be reclassified as intermediate or high risk after surgery based on the

TABLE 4 | Analysis of si-DTC patients and patients with total T3 (ETE+, N1, M1).

Covariate	Level	Thyroid cancer specific mortality		All-cause mortality	
		Univariate Cox regression		Univariate Cox regression	
		Hazard Ratio (95%CI)	p-value	Hazard Ratio (95%CI)	p-value
0		ref		ref	
1		0.012 (0.002–0.086)	<0.001	0.150 (0.112–0.200)	<0.001
2		0.071 (0.023–0.221)	<0.001	0.128 (0.083–0.197)	<0.001
3		0		0.088 (0.042–0.186)	<0.001
4		0		0.206 (0.117–0.365)	<0.001
5		0		0.226 (0.128–0.399)	<0.001
6		0		0.284 (0.152–0.529)	<0.001
7		0		0.377 (0.188–0.756)	0.006
8		0.099 (0.063–0.157)	<0.001	0.770 (0.692–0.856)	<0.001
9		0.180 (0.110–0.295)	<0.001	0.726 (0.631–0.834)	<0.001
10		0.285 (0.160–0.510)	<0.001	0.832 (0.693–0.999)	0.049
11		0.355 (0.167–0.754)	0.007	1.063 (0.844–1.337)	0.604
12		0.228 (0.124–0.418)	<0.001	1.448 (1.260–1.664)	<0.001
13		0.301 (0.148–0.609)	0.001	1.475 (1.238–1.757)	<0.001
14		0.751 (0.410–1.377)	0.354	1.699 (1.372–2.103)	<0.001
15		0.839 (0.414–1.700)	0.627	1.311 (0.980–1.755)	0.068
16		0		0.112 (0.084–0.149)	<0.001

Ref: total T3 (includes M1, N1, ETE+).
1: age ≤45 years old, Female, 0< tumor size ≤1 cm.
2: age ≤45 years old, Female, 1< tumor size ≤2 cm.
3: age ≤45 years old, Female, 2< tumor size ≤3 cm.
4: age ≤45 years old, Female, 3< tumor size ≤4 cm.
5: age ≤45 years old, Male, 0< tumor size ≤1 cm.
6: age ≤45 years old, Male, 1< tumor size ≤2 cm.
7: age ≤45 years old, Male, 2< tumor size ≤3 cm.
8: age ≤45 years old, Male, 3< tumor size ≤4 cm.
9: age >45 years old, Female, 0< tumor size ≤1 cm.
10: age >45 years old, Female, 1 <tumor size ≤2 cm.
11: age >45 years old, Female, 2< tumor size ≤3 cm.
12: age >45 years old, Female, 3< tumor size ≤4 cm.
13: age >45 years old, Male, 0< tumor size ≤1 cm.
14: age >45 years old, Male, 1< tumor size ≤2 cm.
15: age >45 years old, Male, 2< tumor size ≤3 cm.
16: age >45 years old, Male, 3< tumor size ≤4 cm.

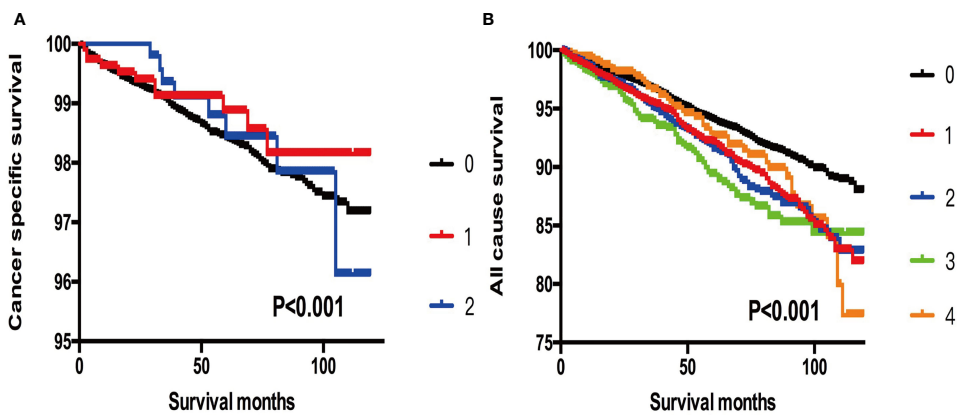

FIGURE 1 | **(A)** Kaplan-Meier curves among patients stratified by tumor size for cancer-specific mortality (Log rank test, p < 0.001). 0 For patients with thyroid cancer > 4 cm in size, gross extrathyroidal extension (clinical T3), or clinically apparent metastatic disease to nodes (clinical N1) or distant sites (clinical M1). 1 Male, > 45 years old, tumor size 2-3 cm. 2 Male, > 45 years old, tumor size 3-4 cm. **(B)** Kaplan-Meier curves among patients stratified by tumor size for all-cause mortality (Log rank test, p < 0.001). 0 For patients with thyroid cancer> 4 cm, gross extrathyroidal extension (clinical T3), or clinically apparent metastatic disease to nodes (clinical N1) or distant sites (clinical M1). 1 Male, > 45 years old, tumor size 0-1 cm. 2 Male, > 45 years old, tumor size 1-2 cm. 3 Male, > 45 years old, tumor size 2-3 cm. 4 Male, > 45 years old, tumor size 3-4 cm.

TABLE 5 | Age, T3 and sex, tumor size factors for survival: outcome of thyroid cancer specific mortality and all-cause mortality.

Covariate	Level	Thyroid cancer specific mortality			All-cause mortality		
		Univariate Cox regression			Univariate Cox regression		
		Hazard Ratio (95%CI)	p-value	Mortality (%)	Hazard Ratio (95%CI)	p-value	Mortality (%)
0		ref			ref		
1		0.019 (0.003–0.136)	<0.001	0.02	0.135 (0.099–0.184)	<0.001	0.85
2		0.110 (0.034–0.354)	<0.001	0.1	0.115 (0.074–0.180)	<0.001	0.72
3			0.967		0.080 (0.038–0.169)	<0.001	0.5
4			0.971		0.187 (0.105–0.333)	<0.001	1.05
5			0.973		0.204 (0.114–0.363)	<0.001	1.27
6			0.978		0.256 (0.136–0.481)	<0.001	1.68
7			0.983		0.340 (0.168–0.687)	0.003	2.17
8		0.154 (0.090–0.262)	<0.001	0.13	0.696 (0.603–0.805)	<0.001	3.82
9		0.279 (0.159–0.491)	<0.001	0.24	0.656 (0.553–0.778)	<0.001	3.73
10		0.442 (0.233–0.842)	0.013	0.4	0.752 (0.611–0.925)	0.007	4.5
11		0.551 (0.247–1.228)	0.145	0.5	0.960 (0.748–1.233)	0.752	5.66
12		0.353 (0.181–0.687)	0.002	0.29	1.310 (1.105–1.553)	0.002	7.07
13		0.466 (0.219–0.994)	0.048	0.39	1.334 (1.091–1.631)	0.005	7.29
14		1.166 (0.599–2.269	0.651	1	1.538 (1.216–1.945)	<0.001	8.57
15		1.301 (0.610–2.776)	0.496	1.19	1.185 (0.872–1.611)	0.279	7.15
16			0.92		0.101 (0.075–0.136)	<0.001	0.59

Ref: T3, with EXE(–), N0.
1: age ≤45 years old, Female, 0< tumor size ≤1 cm.
2: age ≤45 years old, Female, 1< tumor size ≤2 cm.
3: age ≤45 years old, Female, 2< tumor size ≤3 cm.
4: age ≤45 years old, Female, 3< tumor size ≤4 cm.
5: age ≤45 years old, Male, 0< tumor size ≤1 cm.
6: age ≤45 years old, Male, 1< tumor size ≤2 cm.
7: age ≤45 years old, Male, 2< tumor size ≤3 cm.
8: age ≤45 years old, Male, 3< tumor size ≤4 cm.
9: age >45 years old, Female, 0< tumor size ≤1 cm.
10: age >45 years old, Female, 1< tumor size ≤2 cm.
11: age >45 years old, Female, 2< tumor size ≤3 cm.
12: age >45 years old, Female, 3< tumor size ≤4 cm.
13: age >45 years old, Male, 0< tumor size ≤1 cm.
14: age >45 years old, Male, 1< tumor size ≤2 cm.
15: age >45 years old, Male, 2< tumor size ≤3 cm.
16: age >45 years old, Male, 3< tumor size ≤4 cm.

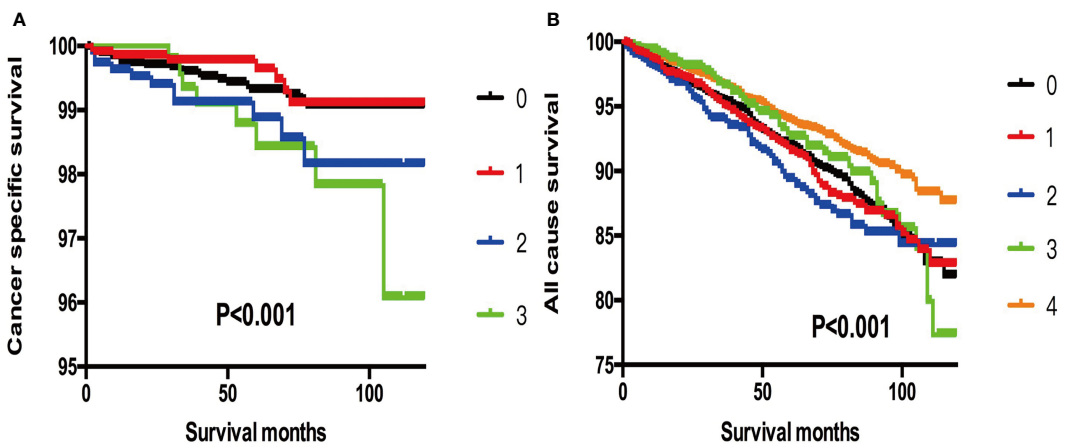

FIGURE 2 | **(A)** Kaplan-Meier curves among patients stratified by tumor size for cancer-specific mortality (Log rank test, $p < 0.001$). 0 For patients with thyroid cancer>4 cm and without gross extrathyroidal extension (clinical T3) and no clinically apparent metastatic disease to nodes (clinical N0) or distant sites (clinical M0). 1 Male, > 45 years old, tumor size 1-2 cm. 2 Male, > 45 years old, tumor size 2-3 cm. 3 Male, > 45 years old, tumor size 3-4 cm. **(B)** Kaplan-Meier curves among patients stratified by tumor size for all-cause mortality (Log rank test, $p < 0.001$). 0 For patients with thyroid cancer>4 cm and without gross extrathyroidal extension (clinical T3) and no clinically apparent metastatic disease to nodes (clinical N0) or distant sites (clinical M0). 1 Male, > 45 years old, tumor size 0-1 cm. 2 Male, > 45 years old, tumor size 1-2 cm. 3 Male, > 45 years old, tumor size 2-3 cm. 4 Male, > 45 years old, tumor size 3-4 cm.

TABLE 6 | Analysis of SI-DTC and T3 (ETE–, N0, M0) subgroup.

Covariate	Level	Thyroid cancer specific mortality		All-cause mortality	
		Univariate Cox regression		Univariate Cox regression	
		Hazard Ratio (95%CI)	p-value	Hazard Ratio (95%CI)	p-value
0		Ref		ref	
1		0.029 (0.004–0.217)	0.001	0.148 (0.108–0.201)	<0.001
2		0.172 (0.052–0.571)	0.004	0.126 (0.081–0.197)	<0.001
3				0.087 (0.041–0.185)	<0.001
4				0.204 (0.114–0.365)	<0.001
5				0.223 (0.125–0.398)	<0.001
6				0.279 (0.148–0.526)	<0.001
7				0.372 (0.184–0.752)	0.006
8		0.243 (0.135–0.437)	<0.001	0.762 (0.655–0.886)	<0.001
9		0.440 (0.238–0.816)	0.009	0.718 (0.602–0.856)	<0.001
10		0.697 (0.350–1.388)	0.305	0.822 (0.665–1.016)	0.07
11		0.868 (0.376-2.008)	0.741	1.050 (0.815–1.353)	0.705
12		0.558 (0.274–1.134)	0.107	1.433 (1.203–1.709)	<0.001
13		0.736 (0.332–1.633)	0.451	1.460 (1.188–1.793)	<0.001
14		1.844 (0.907–3.747)	0.091	1.682 (1.324–2.136)	<0.001
15		2.051 (0.925–4.548)	0.077	1.296 (0.950–1.767)	0.102
16				0.111 (0.082–0.150)	<0.001

Ref: T3, with EXE(–), N0, M0.
1: age ≤45 years old, Female, 0< tumor size ≤1 cm.
2: age ≤45 years old, Female, 1< tumor size ≤2 cm.
3: age ≤45 years old, Female, 2< tumor size ≤3 cm.
4: age ≤45 years old, Female, 3< tumor size ≤4 cm.
5: age ≤45 years old, Male, 0< tumor size ≤1 cm.
6: age ≤45 years old, Male, 1< tumor size ≤2 cm.
7: age ≤45 years old, Male, 2< tumor size ≤3 cm.
8: age ≤45 years old, Male, 3< tumor size ≤4 cm.
9: age >45 years old, Female, 0< tumor size ≤1 cm.
10: age >45 years old, Female, 1< tumor size ≤2 cm.
11: age >45 years old, Female, 2< tumor size ≤3 cm.
12: age >45 years old, Female, 3< tumor size ≤4 cm.
13: age >45 years old, Male, 0< tumor size ≤1 cm.
14: age >45 years old, Male, 1< tumor size ≤2 cm.
15: age >45 years old, Male, 2< tumor size ≤ 3cm.
16: age >45 years old, Male, 3< tumor size ≤ 4cm.

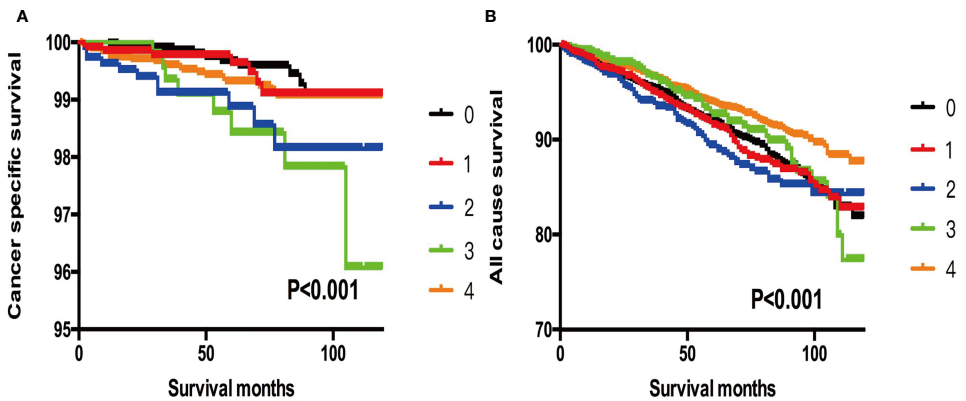

FIGURE 3 | **(A)** Kaplan-Meier curves among patients stratified by tumor size for cancer-specific mortality (Log rank test, p < 0.001). 0 For patients with thyroid cancer>4 cm and without gross extrathyroidal extension (clinical T3) and no clinically apparent metastatic disease to nodes (clinical N0) and no distant sites (clinical M0). 1 Male, > 45 years old, tumor size 0-1 cm. 2 Male, > 45 years old, tumor size 1-2 cm. 3 Male, > 45 years old, tumor size 2-3 cm. 4 Male, > 45 years old, tumor size 3-4 cm. **(B)** Kaplan-Meier curves among patients stratified by tumor size for all-cause mortality (Log rank test, p < 0.001). 0 For patients with thyroid cancer>4 cm and without gross extrathyroidal extension (clinical T3) and no clinically apparent metastatic disease to nodes (clinical N0) and no distant sites (clinical M0). 1 Male, > 45 years old, tumor size 0-1 cm. 2 Male, > 45 years old, tumor size 1-2 cm. 3 Male, > 45 years old, tumor size 2-3 cm. 4 Male, > 45 years old, tumor size 3-4 cm.

histological findings, and Pedro et al. suggested that total thyroidectomy might be a better option for these patients (13). Previous retrospective studies have estimated that 40–60% of patients with low-risk 1–4 cm PTCs, if initially treated with lobectomy, would require a completion thyroidectomy due to high-risk pathological features in postoperative pathology reports (18, 19). These results underscore the importance of preoperative and intraoperative meticulous assessments by the surgeon during lobectomy for SI-PTCs.

Recently, Huang et al. (20) revealed that in tumors larger than 2.0 to 3.0 cm, recurrences of BRAF V600E mutation-positive SI-PTC were comparable with those of counterpart invasive solitary PTC and need more aggressive treatment. However, these adverse features are only apparent on histopathology and cannot be identified preoperatively. If a lobectomy has been performed, a completion thyroidectomy may be required, which may be associated with certain additional risks. It is essential to know the prevalence of these adverse pathological features to enable surgical planning and patient counseling. A recent study stated that for low-risk PTC patients, identification of intraoperative risk factors such as evidence or suspicion of invasion into local structures (namely, muscle, recurrent laryngeal nerve, esophagus, trachea, or other structures) or positive lymph nodes confirmed on intraoperative frozen section analysis can reduce the need for a later completion thyroidectomy in 21% of cases, but not exclude this need completely. Up to 30% of patients would be deemed intermediate or high risk, requiring a second operation (21). Thus, further studies are needed on preoperative risk stratification.

In this study, we included more clinicopathological factors (age, sex, and tumor size) for analysis to evaluate the reclassification of SI-DTC. Considering that age and sex are easily available preoperatively, including these characteristics for analysis may be more reasonable to select high-risk patients with SI-DTC and reconsider the treatment approaches. We found that survival rates were significantly lower in patients with male sex, age >45 years, and larger tumor size when compared to female patients with age ≤45 years and smaller tumor size, indicating that the former group have a poor prognosis and may require a more radical treatment plan. Our findings are consistent with the role of tumor size in the aggressiveness of PTC. Given that cancer-specific mortality occurred frequently in patients with 3–4 cm in size compared to other subgroups, a close preoperative and intraoperative evaluation of tumor size is important in SI-DTC patients.

A common clinical scenario for SI-DTC with 1–4 cm tumor size is that preoperative ultrasonography does not show suspicious LNM and extrathyroidal extension, as preoperative ultrasonography has a limited sensitivity in detecting central LNM; therefore, many patients with SI-DTC may have occult LNM and ETE, which can synergize with other high-risk characteristics, such as male sex and old age, in promoting DTC mortality. If such patients are treated by lobectomy without neck dissection and radioiodine ablation, the mortality risk could be higher. The present study found that the prognosis of SI-DTC was affected by other clinicopathological characteristics such as sex, age, and tumor size; thus, lobectomy for SI-DTC regardless of the specific clinical status seems to be unreasonable.

Some inherent limitations must be considered when interpreting our results. First, all the risk characteristics included clinicopathological features from the SEER database, but other factors such as ultrasonic data, molecular mutations, vascular invasion, and family history were not obtained nor included in our analysis. Second, data regarding recurrence are not captured in the SEER database, and the designation of cancer-specific death is susceptible to overestimation bias, particularly for diseases such as DTC. Furthermore, given the generally favorable prognosis of PTC, the relatively short study period and follow-up period (2010–2013) is a limitation of our analysis.

Conclusion

Our study demonstrated that sex, age, and tumor size clearly differentiate SI-DTC with a tumor size of 1–4 cm into low and high risk categories. Survival rates were significantly lower in subgroups containing males, older patients, and patients with larger tumor size compared to females, younger patients, and patients with smaller tumor size. Therefore, total thyroidectomy may be favored for these high-risk subgroup patients, and more clinicopathological factors should be included for risk stratification in managing patients with SI-DTC with tumors that are 1–4 cm in size.

DATA AVAILABILITY STATEMENT

The raw data supporting the conclusions of this article will be made available by the authors, without undue reservation.

AUTHOR CONTRIBUTIONS

SW, LZ, FD, and CL designed the study. FD, LZ, WS, and JM collected and analyzed the data. FD and LZ wrote the manuscript. All authors contributed to the article and approved the submitted version.

ACKNOWLEDGMENTS

All authors are grateful to all subjects who participated in this study.

SUPPLEMENTARY MATERIAL

The Supplementary Material for this article can be found online at: https://www.frontiersin.org/articles/10.3389/fendo.2021.790730/full#supplementary-material

REFERENCES

1. Chen W, Zheng R, Baade PD, Zhang S, Zeng H, Bray F, et al. Cancer Statistics in China, 2015. *CA Cancer J Clin* (2016) 66(2):115–32. doi: 10.3322/caac.21338
2. Davies L, Hoang JK. Thyroid Cancer in the USA: Current Trends and Outstanding Questions. *Lancet Diabetes Endocrinol* (2021) 9(1):11–2. doi: 10.1016/S2213-8587(20)30372-7
3. Liu C, Chen T, Zeng W, Wang S, Xiong Y, Liu Z, et al. Reevaluating the Prognostic Significance of Male Gender for Papillary Thyroid Carcinoma and Microcarcinoma: A SEER Database Analysis. *Sci Rep* (2017) 7(1):11412. doi: 10.1038/s41598-017-11788-8
4. Liu C, Wang S, Zeng W, Guo Y, Liu Z, Huang T. Total Tumour Diameter is Superior to Unifocal Diameter as a Predictor of Papillary Thyroid Microcarcinoma Prognosis. *Sci Rep* (2017) 7(1):1846. doi: 10.1038/s41598-017-02165-6
5. Haugen BR, Alexander EK, Bible KC, Doherty GM, Mandel SJ, Nikiforov YE, et al. 2015 American Thyroid Association Management Guidelines for Adult Patients With Thyroid Nodules and Differentiated Thyroid Cancer: The American Thyroid Association Guidelines Task Force on Thyroid Nodules and Differentiated Thyroid Cancer. *Thyroid* (2016) 26(1):1–133. doi: 10.1089/thy.2015.0020
6. Zhang F, Zheng B, Yu X, Wang X, Wang S, Teng W. Risk Factors for Contralateral Occult Carcinoma in Patients With Unilateral Papillary Thyroid Carcinoma: A Retrospective Study and Meta-Analysis. *Front Endocrinol (Lausanne)* (2021) 12:675643. doi: 10.3389/fendo.2021.675643
7. Luo H, Yan F, Lan L, Ma B, Zhao H, He Y, et al. Ultrasonographic Features, Nodule Size, Capsular Invasion, and Lymph Node Metastasis of Solitary Papillary Carcinoma of Thyroid Isthmus. *Front Oncol* (2020) 10:558363. doi: 10.3389/fonc.2020.558363
8. Tran CH, Johnston LE, Chang DC, Bouvet M. A Critical Analysis of the American Joint Committee on Cancer (AJCC) Staging System for Differentiated Thyroid Carcinoma in Young Patients on the Basis of the Surveillance, Epidemiology, and End Results (SEER) Registry. *Surgery* (2012) 152(2):145–51. doi: 10.1016/j.surg.2012.02.015
9. Perrier ND, Brierley JD, Tuttle RM. Differentiated and Anaplastic Thyroid Carcinoma: Major Changes in the American Joint Committee on Cancer Eighth Edition Cancer Staging Manual. *CA Cancer J Clin* (2018) 68(1):55–63. doi: 10.3322/caac.21439
10. Liu W, Yan X, Cheng R. Continuing Controversy Regarding Individualized Surgical Decision-Making for Patients With 1-4 Cm Low-Risk Differentiated Thyroid Carcinoma: A Systematic Review. *Eur J Surg Oncol* (2020) 46 (12):2174–84. doi: 10.1016/j.ejso.2020.08.014
11. Xu Y, Huang K, Huang P, Ke N, Zeng J, Wang L, et al. Benefits and Harms of Hemithyroidectomy, Total or Near-Total Thyroidectomy in 1-4 Cm Differentiated Thyroid Cancer. *Clin Endocrinol (Oxf)* (2021) 95(4):668–76. doi: 10.1111/cen.14495
12. Wang X, Zhang C, Srivastava A, Yu W, Liu C, Wei D, et al. Risk Factors That Influence Surgical Decision-Making for Patients With Low-Risk Differentiated Thyroid Cancer With Tumor Diameters of 1-4 Cm. *Cancer Manag Res* (2020) 12:12423–8. doi: 10.2147/CMAR.S268716
13. Schmid KW, Synoracki S, Dralle H, Wittekind C. Proposal for an Extended pTNM Classification of Thyroid Carcinoma: Commentary on Deficits of the 8th Edition of the TNM Classification. *Pathologe* (2019) 40(Suppl 1):18–24. doi: 10.1007/s00292-018-0418-x
14. Gao R, Jia X, Liang Y, Fan K, Wang X, Wang Y, et al. Papillary Thyroid Micro Carcinoma: The Incidence of High-Risk Features and Its Prognostic Implications. *Front Endocrinol (Lausanne)* (2019) 10:74. doi: 10.3389/fendo.2019.00074
15. Liang J, Li Z, Fang F, Yu T, Li S. Is Prophylactic Central Neck Dissection Necessary for Cn0 Differentiated Thyroid Cancer Patients at Initial Treatment? A Meta-Analysis of the Literature. *Acta Otorhinolaryngol Ital* (2017) 37(1):1–8. doi: 10.14639/0392-100X-1195
16. McMullen C, Rocke D, Freeman J. Complications of Bilateral Neck Dissection in Thyroid Cancer From a Single High-Volume Center. *JAMA Otolaryngol Head Neck Surg* (2017) 143(4):376–81. doi: 10.1001/jamaoto.2016.3670
17. Papachristos AJ, Glover A, Sywak MS, Sidhu SB. Pros and Cons of Hemi-Thyroidectomy for Low-Risk Differentiated Thyroid Cancer. *ANZ J Surg* (2021) 91(9):1704–10. doi: 10.1111/ans.16553
18. Murthy SP, Balasubramanian D, Subramaniam N, Nair G, Babu M, Rathod PV, et al. Prevalence of Adverse Pathological Features in 1 to 4 Cm Low-Risk Differentiated Thyroid Carcinoma. *Head Neck* (2018) 40(6):1214–8. doi: 10.1002/hed.25099
19. DiMarco AN, Wong MS, Jayasekara J, Cole-Clark D, Aniss A, Glover AR, et al. Risk of Needing Completion Thyroidectomy for Low-Risk Papillary Thyroid Cancers Treated by Lobectomy. *BJS Open* (2019) 3(3):299–304. doi: 10.1002/bjs5.50137
20. Huang Y, Qu S, Zhu G, Wang F, Liu R, Shen X, et al. BRAF V600E Mutation-Assisted Risk Stratification of Solitary Intrathyroidal Papillary Thyroid Cancer for Precision Treatment. *J Natl Cancer Inst* (2018) 110(4):362–70. doi: 10.1093/jnci/djx227
21. Craig SJ, Bysice AM, Nakoneshny SC, Pasieka JL, Chandarana SP. The Identification of Intraoperative Risk Factors Can Reduce, But Not Exclude, the Need for Completion Thyroidectomy in Low-Risk Papillary Thyroid Cancer Patients. *Thyroid* (2020) 30(2):222–8. doi: 10.1089/thy.2019.0274

Conflict of Interest: The authors declare that the research was conducted in the absence of any commercial or financial relationships that could be construed as a potential conflict of interest.

The reviewer ZL declared a shared affiliation with the authors to the handling editor at time of review. The reviewer JM declared a shared affiliation with the authors to the handling editor at time of review.

frontiers in Endocrinology

ORIGINAL RESEARCH
published: 17 February 2022
doi: 10.3389/fendo.2022.842148

Comparison of Different Mandibular Jawlines Classifications on Transoral Endoscopic Thyroidectomy for Papillary Thyroid Carcinoma: Experiences of 690 Cases

Xing Yu[1], Yuancong Jiang[2], Yujun Li[2], Qionghua He[2], Lei Pan[2], Peifeng Zhu[2], Yong Wang[1] and Ping Wang[1]**

[1] Department of Thyroid Surgery, The Second Affiliated Hospital, Zhejiang University School of Medicine, Hangzhou, China, [2] College of Medicine, Zhejiang University, Hangzhou, China

OPEN ACCESS

Edited by:
Gianlorenzo Dionigi, University of Milan, Italy

Reviewed by:
Erivelto Martinho Volpi, Centro de referencia no ensino do diagnóstico por imagem (CETRUS), Brazil
Yin Detao, First Affiliated Hospital of Zhengzhou University, China

***Correspondence:**
Yong Wang
surgwy@zju.edu.cn
Ping Wang
p.wang@zju.edu.cn

Specialty section:
This article was submitted to Thyroid Endocrinology, a section of the journal Frontiers in Endocrinology

Received: *23 December 2021*
Accepted: *24 January 2022*
Published: *17 February 2022*

Citation:
Yu X, Jiang Y, Li Y, He Q, Pan L, Zhu P, Wang Y and Wang P (2022) Comparison of Different Mandibular Jawlines Classifications on Transoral Endoscopic Thyroidectomy for Papillary Thyroid Carcinoma: Experiences of 690 Cases. Front. Endocrinol. 13:842148. doi: 10.3389/fendo.2022.842148

Background: The influences of patients' different mandibular jawlines on transoral endoscopic thyroidectomy *via* vestibular approach (TOETVA) have not been described before. The objective of this study was to introduce a new classification to assess different mandibular jawlines, and to evaluate the effects on TOETVA in terms of safety, feasibility, and postoperative feelings in the treatment of papillary thyroid carcinoma (PTC).

Methods: The crossing angle of esthetic plane and mandibular plane was defined as Wang Angle, used to assess patients' different mandibular jawlines. Mandibular classifications of A (angle: 80° ~ 110°), B (angle > 110°), and C (angle < 80°) types were compared to evaluate the surgical outcomes of TOETVA by a retrospective study. 690 patients of PTC who received TOETVA were included in this study, which were divided into three groups according to mandibular classifications.

Results: Clinicopathological characteristics of the patients including age, gender, body mass index, tumor size, Hashimoto thyroiditis were similar in the three groups. Patients' length of jay in group C was significantly longer than group A and group B ($P < 0.01$). The ratios of using suspension system in group C were significantly higher than group A and group B ($P < 0.01$). The scores of postoperative visual analogue scale (VAS) and ratios of mandibular swell in group C were significantly higher than group A and group B ($P < 0.01$). There was no significant difference in the three groups regarding surgical outcomes, including postoperative vocal cord paralysis, hypocalcemia, serum white blood cells and C-reactive protein levels.

Conclusions: The Wang angle and mandibular jawline classifications were firstly introduced in TOETVA. All the patients of class A, B, and C mandibular jawline can achieve safe and effective surgical outcomes in the treatment of PTC with TOETVA. Patients of class C need more assistance of suspension system, would experience higher scores of VAS, and higher ratios of mandibular swell compared with class A and B.

Keywords: mandibular jawlines, length of jay, transoral endoscopic thyroidectomy, papillary thyroid carcinoma, surgical outcomes

INTRODUCTION

Transoral endoscopic thyroidectomy is new that does not cause neck scarring and requires a smaller subcutaneous flap elevation than that of remote access thyroid surgery methods (1). Because of these advantages above, there has been a rapid development of transoral endoscopic thyroidectomy *via* vestibular approach (TOETVA) in the past 10 years (2). However, the influences of patients' different mandibular jawlines on TOETVA have not been described before (3). The angle's classifications of malocclusion were initially used to assess the mesio-distal relationships of the dental arches (4), which was modified by us and used to assess the mandibular jawlines. The objective of this study was to introduce a new classification of mandibular jawlines into transoral endoscopic thyroidectomy, and to evaluate the effects on TOETVA in terms of safety, feasibility, surgical outcomes, and postoperative feelings in the treatment of papillary thyroid carcinoma (PTC).

MATERIALS AND METHODS

Patients' Enrollment

Between January 2015 and June 2020, we retrospectively enrolled 690 patients with PTC who underwent total thyroidectomy or ipsilateral thyroidectomy and lymph node dissection of central compartment in the Second Affiliated Hospital, Zhejiang University School of Medicine. All enrolled patients had cosmetic requirements, and they chose the operation of TOETVA. Patients were divided into three groups according to the different types of mandibular jawlines. The clinicopathological characteristics such as age, gender, body mass index (BMI), tumor size, multiple lesions ratio, and Hashimoto's thyroiditis ratio were compared in the three groups. This study was approved by the ethical committee of the Second Affiliated Hospital of Zhejiang University School of Medicine.

Introduction of Wang Angle and Mandibular Jawlines Classifications

The crossing angle of esthetic plane and mandibular plane was defined as Wang Angle (**Figure 1**). Patients' different mandibular jawlines were classified into three types according to the degree of Wang Angle, including A (angle: 80° ~ 110°), B (angle > 110°), and C (angle < 80°) types. This new classification was firstly introduced in TOETVA. As shown in the **Figure 1**, patients' different mandibular jawlines were exhibited with schematic diagrams and realistic photos. The Wang Angle of each patient was defined as the crossing of esthetic plane and mandibular plane (red line), which was used to assess the different mandibular jawline classifications.

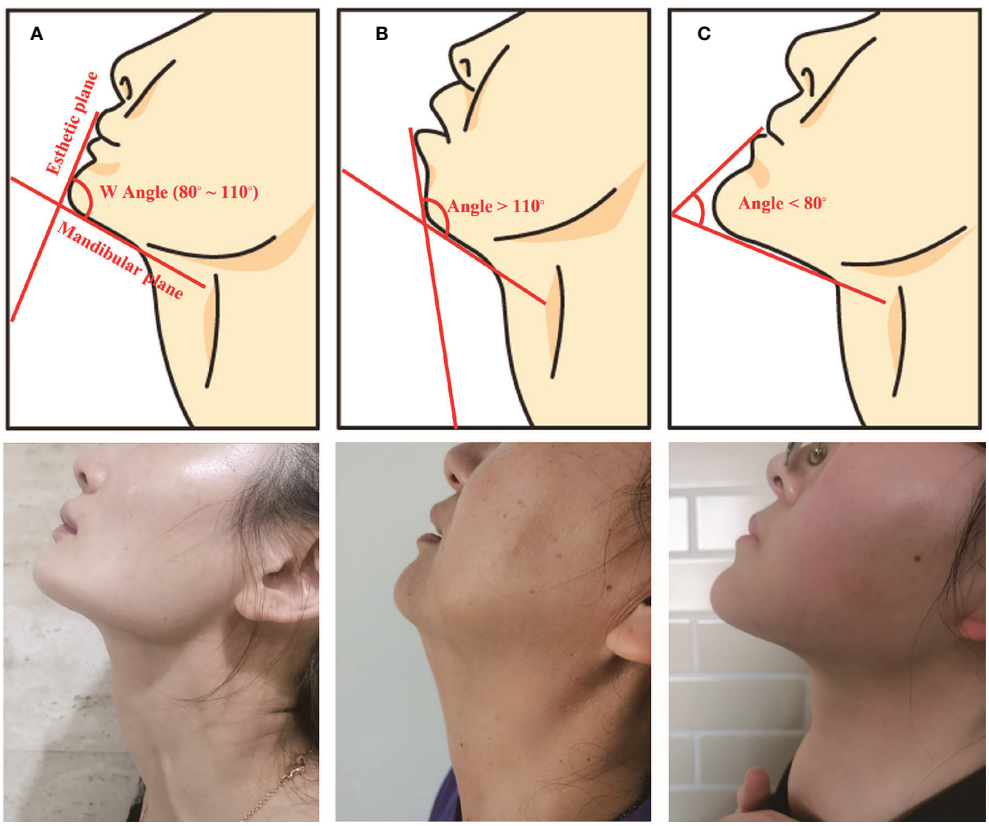

FIGURE 1 | Schematic diagram and realistic photos of the three classifications: **(A)** (angle: 80° ~ 110°), **(B)** (angle > 110°), and **(C)** (angle < 80°) types.

Measure the Length of Jaw

The length of jaw was measured in the A, B, and C types of mandibular jawlines. The length of jaw is a quantitative index, which may be useful to evaluate the level of difficulty to maintain the surgical space in TOETVA. As shown in **Figure 2**, patients were chosen horizontal position, and the length of jaw was defined as the distance from anterior neck plane to the anterior border plane of jaw (red line). The length was measured by a flexible ruler, which was analyzed and compared in the three groups.

Procedures of TOETVA

The procedures of TOETVA were briefly described in the following. A 10-mm incision for the camera port was cautiously made in the middle of the vestibule and frenulum. Another two 5-mm trocars were applied through the mucosa incision at the level of the first premolars for auxiliary use. A 30° angled camera was then advanced through the 10-mm port. Ultrasonic coagulation devices (Harmonic Scalpel, Ethicon Endosurgery, USA) were used to manage thyroid surrounding vessels and the inferior thyroid arteries (5). Thyroid gland was completely resected, and central node dissection (CND) was conducted including the prelaryngeal, pretracheal, and paratracheal areas (6).

Comparison of Surgical Outcomes

Preoperative laryngoscope, thyroid hormones, parathyroid hormone (PTH) and calcium were recorded 3 days before surgery. Postoperative laryngoscope, laboratory tests including PTH, calcium, white blood cell (WBC), and C-reactive protein (CRP) were examined at the day next to the operation. Thyroid hormones, PTH, and calcium were detected at one month postoperatively. Patients receive postoperative review every 3 months after surgery, thyroid function and cervical B ultrasound were included each time.

Statistical Analysis

The results are presented as number (%) and average ± SD appropriate. Data were analyzed by one-way ANOVA, Welch ANOVA, student *t*-test, the $\chi 2$ test, Fisher's exact test, and non-parametric Wilcoxon-Mann-Whitney test appropriately using SPSS 20.0 software (SPSS Inc., Chicago, IL, USA). A *p* value less than 0.05 was considered to be statistically significant.

RESULTS

Clinicopathologic Characteristics

The clinicopathologic characteristics were summarized in **Table 1**. This study enrolled 690 patients, comprising 342 (Type A), 281 (Type B), and 67 (Type C) patients respectively. Patient's age, sex ratio, and BMI were similar in the groups of type A, B, and C. Tumor characteristics were compared in the three groups, and there was no significant difference in the max tumor size, multiple lesions ratio, and Hashimoto's thyroiditis ratio. Total thyroidectomy ratio was similar between the three groups of type A, B, and C respectively. The length of jaw was compared and has significant difference in the three groups ($P < 0.01$). In the pairwise comparison, the length of jaw in group C was significantly more than group A (7.26 ± 0.23 *vs.* 6.85 ± 0.23, $P < 0.01$), and group B (7.26 ± 0.23 *vs.* 6.17 ± 0.42, $P < 0.01$). And the length of jaw in group A was also more than group B significantly (6.85 ± 0.23 *vs.* 6.17 ± 0.42, $P < 0.01$).

Postoperative Feelings

The ratio of mandibular swell and visual analogue scale (VAS) feeling were compared in the three groups. As shown in **Table 2**, the ratio of mandibular swell was compared and has significant difference in the three groups ($P < 0.01$). In the pairwise comparison, the ratio of mandibular swell in group C was significantly more than group A (10.4% *vs.* 1.2%, $P < 0.01$), and group B (10.4% *vs.* 0.7%, $P < 0.01$). While there was no significant difference in the comparison of mandibular swell between group A and group B (1.2% *vs.* 0.7%, $P = 0.560$). The scores of VAS were compared and has significant difference in the three groups ($P < 0.01$). In the pairwise comparison, the scores of VAS in group C was significantly more than group A (2.1 ± 0.6 *vs.* 1.7 ± 0.5, $P < 0.01$), and group B (2.1 ± 0.6 *vs.* 1.7 ± 0.5, $P < 0.01$). While there was no significant difference in the comparison of VAS scores between group A and group B (1.7 ± 0.5 *vs.* 1.7 ± 0.5, $P = 0.980$).

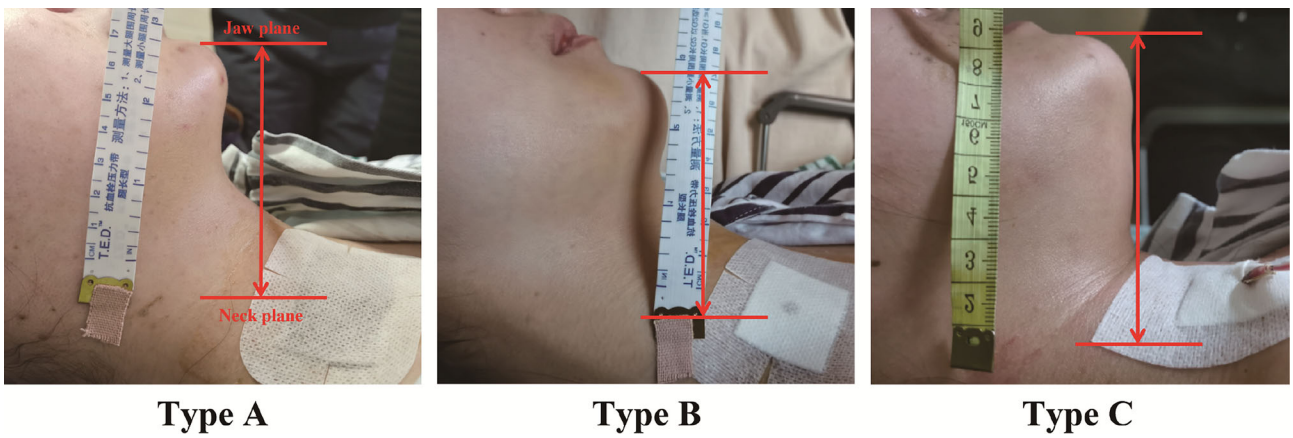

FIGURE 2 | The length of jay was measured from anterior neck plane to the anterior border plane of jaw (red line) in the three groups.

TABLE 1 | Comparation of clinicopathological characteristics in the groups of type A, B, and C.

	Type A (n = 342)	Type B (n = 281)	Type C (n = 67)	*P value*
Age (years)	37.3 ± 9.8	37.6 ± 9.9	35.8 ± 9.2	0.423
Male (%)	90 (26.3%)	74 (26.3%)	25 (37.3%)	0.159
BMI (kg/m^2)	23.7 ± 3.7	23.7 ± 3.7	23.9 ± 3.8	0.825
Max tumor size (cm)	1.23 ± 0.59	1.20 ± 0.61	1.31 ± 0.71	0.175
Multiple lesions (%)	81 (23.7%)	88 (31.3%)	22 (32.8%)	0.065
Hashimoto's thyroiditis (%)	100 (29.2%)	97 (34.5%)	25 (27.3%)	0.238
Total thyroidectomy (%)	111 (32.5%)	98 (34.9%)	25 (37.3%)	0.675
Bilateral CND (%)	108 (31.6%)	96 (34.2%)	19 (28.4%)	0.606
Length of jaw (cm)	6.85 ± 0.23	6.17 ± 0.42	7.26 ± 0.23	<0.01

BMI, body mass index; CND, central node dissection.

TABLE 2 | Effective assessment of surgical results in the groups of type A, B, and C malocclusion.

	Type A (n = 342)	Type B (n = 281)	Type C (n = 67)	*P value*
EMG changes (%)	28 (8.2%)	21 (7.5%)	2 (3.0%)	0.330
Transient vocal cord paralysis (%)	7 (2.0%)	9 (3.2%)	1 (1.5%)	0.563
Postoperative PTH (pg/ml)	34.7 ± 16.5	36.0 ± 18.4	35.7 ± 18.9	0.642
Postoperative calcium	2.09 ± 0.14	2.11 ± 0.13	2.08 ± 0.13	0.360
numbness in limbs (%)	36 (10.5%)	30 (10.7%)	10 (14.9%)	0.559
Total number of CLN	8.83 ± 5.75	9.16 ± 6.14	8.67 ± 4.61	0.715
Number of metastatic CLN	1.70 ± 2.41	1.64 ± 2.37	1.84 ± 2.57	0.827
WBC (×10^9/L)	9.2 ± 2.7	9.5 ± 4.7	9.9 ± 2.9	0.330
Postoperative CRP (mg/L)	8.3 ± 7.0	9.3 ± 8.3	9.4 ± 7.7	0.172
Operative time (min)	116.2 ± 44.3	118.5 ± 46.6	121.7 ± 40.3	0.601
Mandibular swell	4 (1.2%)	2 (0.7%)	7 (10.4%)	<0.01
Visual VAS	1.7 ± 0.5	1.7 ± 0.5	2.1 ± 0.6	<0.01
Hospital stay (days)	3.89 ± 1.09	3.99 ± 1.07	3.88 ± 1.12	0.515
Quality of life	7.89 ± 0.80	7.94 ± 0.71	7.88 ± 0.69	0.609

EMG, electromyography; PTH, parathyroid hormone; CLN, central lymph nodes; WBC, white blood cell; CRP, C-reactive protein; VAS, visual analogue scale.

Surgical Complications

The surgical complications, including postoperative vocal cord paralysis and hypocalcemia were recorded. The electromyography (EMG) changes during the surgery, and the complains of hoarseness and laryngoscope examinations postoperatively were recorded. As shown in **Table 2**, there was no significant difference in the comparison of EMG changes (8.2% *vs.* 7.5% *vs.* 3.0%, $P = 0.330$) and post-operative transient vocal cord paralysis (2.0% *vs.* 3.2% *vs.* 1.5%, $P = 0.563$) in the groups of A, B, and C type. No permanent vocal cord paralysis occurred in all the three groups. The levels of PTH and serum calcium were recorded at the next day postoperatively. It was similar in PTH levels (34.7 ± 16.5 *vs.* 36.0 ± 18.4 *vs.* 35.7 ± 18.9, $P = 0.642$) and serum calcium (2.09 ± 0.14 *vs.* 2.11 ± 0.13 *vs.* 2.08 ± 0.13, $P = 0.360$) in the comparison of type A, B, and C. The incidences of numbness in limbs were also similar in the comparison of type A, B, and C (10.5% *vs.* 10.7% *vs.* 14.9%, $P = 0.559$).

Comparison of Lymph Node Dissection in the Central Compartment

The total number and metastatic central lymph nodes (CLN) were recorded. It was similar in the total number of CLN in the comparison of group A, B, and C (8.83 ± 5.75 *vs.* 9.16 ± 6.14 *vs.* 8.67 ± 4.61, $P = 0.715$). And no difference was found in the number of metastatic CLN in the comparison of group A, B, and C (1.70 ± 2.41 *vs.* 1.64 ± 2.37 *vs.* 1.84 ± 2.57, $P = 0.827$).

Comparison of Postoperative Inflammatory Response

WBC and CRP were recorded to assess the postoperative inflammatory response. There was no difference in the number of WBC in the comparison of group A, B, and C (9.2 ± 2.7 *vs.* 9.5 ± 4.7 *vs.* 9.9 ± 2.9, $P = 0.330$). And it was similar in postoperative CRP level in the comparison of group A, B, and C (8.3 ± 7.0 *vs.* 9.3 ± 8.3 *vs.* 9.4 ± 7.7, $P = 0.172$).

Operative Assessment and Qof Evaluation in the Follow-Up

The operative time and postoperative hospital stay were recorded. And the Quality of life (Qof) was assessed at 3 months postoperatively during the follow-up. The operative time was similar in the three groups of type A, B, and C (116.2 ± 44.3 *vs.* 118.5 ± 46.6 *vs.* 121.7 ± 40.3, $P = 0.601$). And it was similar in the comparation of postoperative hospital stay in the three groups (3.89 ± 1.09 *vs.* 3.99 ± 1.07 *vs.* 3.88 ± 1.12, $P = 0.515$). There was no difference in Qof assessment in the three groups of type A, B, and C (7.89 ± 0.80 *vs.* 7.94 ± 0.71 *vs.* 7.88 ± 0.69, $P = 0.609$).

DISCUSSION

Since a large case series of transoral endoscopic thyroidectomy was reported in 2016, multiple hospital centers worldwide have

introduced this technique and reported their initial experience (7). Up to now, transoral endoscopic thyroidectomy *via* vestibular approach (TOETVA) has become one of the most widely used techniques in scarless endoscopic thyroidectomy (8). Our group has reported a large cohort of TOETVA cases, in which we demonstrated that transoral endoscopic thyroidectomy has the same surgical safety compared with total endoscopic thyroidectomy *via* areola approach, and conventional open thyroidectomy (9). Recently, it has been found by us that the surgical outcomes of transoral endoscopic thyroidectomy are safe in the treatment of PTC with a diameter between > 1cm and ≤ 3.5cm (3).

Hence, we compared the different classified types of mandibular jawlines on TOETVA. It was found safe of TOETVA in the treatment of PTC patients with all the three types of mandibular jawlines. No case was needed to transverse conventional open choice in all the 690 cases. No significant difference was found in the comparison of surgical complications in the types of A, B, and C, including postoperative vocal cord paralysis and hypoparathyroidism. Mental nerve injury is a unique complication of TOETVA (10). And the incidence of mental nerve injury is quite diverse (11). In our institute, only 2 cases of mental nerve injury were detected at the initial period after TOETVA performed. There was no mental nerve injury found in this study of 690 PTC cases. These results might provide evidence mental nerve injury rarely occurs with TOETVA in all the patients of class A, B, and C mandibular jawline.

The effect and feasibility were also verified with the largest case series of TOETVA for PTC in the present study. Total and metastatic number of central lymph nodes were similar in the comparison of all the three types, which represents the effect was similar during the implementation of TOETVA in the patients of type A, B, and C. The postoperative inflammatory response, including WBC and CRP, were recorded similar, which represents the feasibility of TOETVA was comparable in type A, B and C.

According to the results of comparative analyses, the length of jaw in the patients of type C was significantly more than type A and B. Due the longer jawline, it had more difficulty in maintaining the surgical space, and the ratios of using suspension assisted system in the patients of type C were also higher than type A and B significantly. Additionally, patients of type C experienced a higher ratio of mandibular swell, and the mandibular swell would be absorbed at 7 ~ 10 days post TOETVA. Patients of type C had higher scores of VAS at the next day post TOETVA, and the pain feelings would be reduced at 3 ~ 5 days post TOETVA according to our experience. Moreover, there was no difference found in the comparison of Qof in the period of follow-up, which represents the longtime postoperative feelings were similar in the comparison of type A, B, and C. Furthermore, several innovative techniques were implemented in TOETVA, which was useful to maintain the surgical space, especially in the patients of type C.

Injecting Epinephrine Solution

Epinephrine solution of diluted adrenaline solution (1:500 000) was injected from the vestibule to the anterior of the neck at the subcutaneous layer (12). The uneven surface of the mandibular would be topped up by the epinephrine solution. Additionally, diluted adrenaline contributed to microvascular constriction, which would be helpful to reduce bleeding during the process of space creating.

Real-Time Observation

We firstly designed a visual separation device, which was used for the separation of skin flap (13). The visual separation bar has a see-through head, could be used for real-time observation during blunt separation. The correct fascia layer is shown white, while a yellow appearance means over superficial or fat layer, and red appearance been over deep or muscle layer. With this help, the tissue separation layer could be adjusted at any time during the process of flap dissection. Additionally, anterior jugular microvascular could also be observed, which would be helpful to avoid bleeding in the procedure of building working space.

Hybrid Space-Maintaining Method

The hybrid space-maintaining system combining constant low pressure gas insufflation with a flap lifting device. We have reported this method before, which was described briefly in the following (14). During the operation, the CO_2 was insufflated and maintained at a low pressure of 6 mm Hg. Additionally, the flap was lifted to expand the space by wires or silk sutures, which retracted by a suspension system. As the critical device of suspension system, a disinfected L-shaped pole was wrapped by a sterile protective cover and then fixed on the side of the head as the suspension frame.

Add Another Vacuum Tube for Working Space Building

The middle curvilinear incision was expanded to 2 cm, which used for observation port and another vacuum tube. Vacuum tube shore up and air inhalation were alternatively used for flap suspension during working space building. Order to reduce the smoke circumstance, the operation space was kept a negative pressure during the whole process. Additional vacuum tube was placed next to the observation port for flap suspension to keep the operation space under negative pressure **(Figure 3)**. And the vacuum tube could also be used for air inhalation when much smoke generated in the surgical circumstance.

The Advantages and Disadvantages of TOETVA

TOETVA provides a cranial-caudal perspective that can better expose and more completely central nodes dissection, especially for the lower part including levels VI and VII (15). However, it increases difficulty of handling the thyroid superior pole at the beginning, identifying the superior thyroid artery and superior laryngeal nerve (SLN) (16). Due to the limitations, it is important to evaluate whether different mandibular jawline types would increase the surgical complications in TOETVA. In this study, all tumors were completely removed, and no skin flap disruption or permanent SLN injury occurred. And the different mandibular jawline types, especially for type C, can be overcome with the development of operative proficiency and the improvement of surgical instruments. Additionally, patients chosen TOETVA had

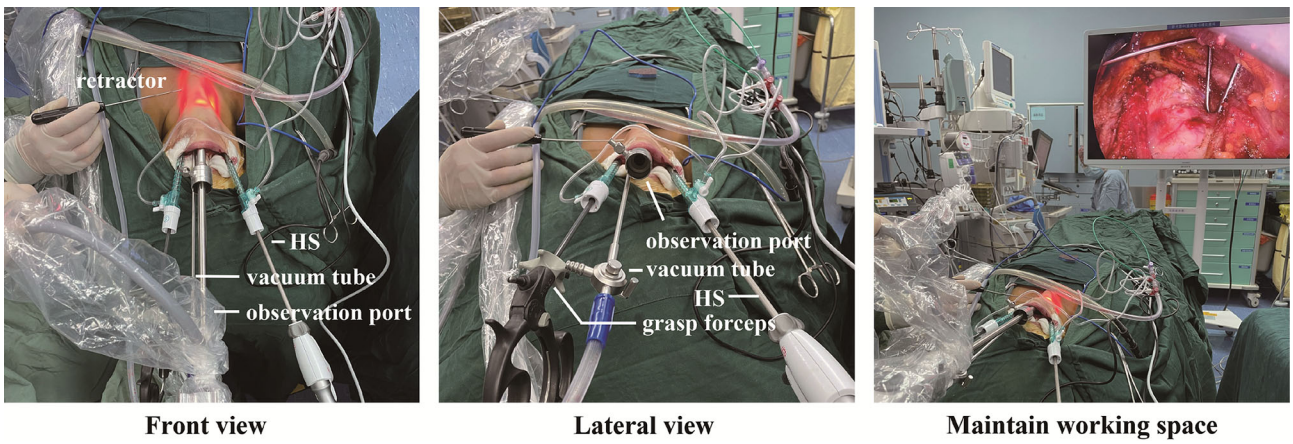

FIGURE 3 | Introduce another vacuum tube for working space building in TOETVA.

FIGURE 4 | Cosmetic results 1 month and 6 months postoperatively of TOETVA.

much more scores of Qof (17), especially in the aspect of cosmetic result (18), which can hide incisions in the mouth without any scars on the body appearance (**Figure 4**).

Our study has some limitations. Firstly, it was a retrospective study, we only enrolled patients who had a pathological diagnosis of PTC from January 2015 to June 2020 at our single center. Secondly, the operation choices of ipsilateral lobectomy or total thyroidectomy, and central node dissections were according to Chinese guidelines. Additionally, all cases were performed within 18 – 36 months period, and the follow-up time was not long enough to observe tumor recurrence.

CONCLUSION

A new classification was introduced in TOETVA, so as to evaluate the influence of different mandibular jawlines. It has been found that the safety, effect and feasibility were similar in the treatment of PTC with TOETVA in all the mandibular jawlines of type A, B, and C. However, patients of type C would experience a higher ratio of mandibular swell, and higher scores of VAS post TOETVA. New techniques, including real-time observation, hybrid space-maintaining, and adding another vacuum tube may be helpful for working space building of TOETVA, especially in the patients of type C.

DATA AVAILABILITY STATEMENT

The original contributions presented in the study are included in the article/supplementary material. Further inquiries can be directed to the corresponding authors.

ETHICS STATEMENT

Written informed consent was obtained from the individual(s) for the publication of any potentially identifiable images or data included in this article.

AUTHOR CONTRIBUTIONS

XY, YJ, and YW substantial contributed to conception and design. YL, QH, YJ, LP, and PZ contributed to acquisition of data. YL analysis and interpretation of data. YW and XY contributed to draft the article. All authors contributed to the article and approved the submitted version.

FUNDING

This study is financially supported by Health Innovation Talents Project of Zhejiang Province (2021RC004) and Basic Public Welfare Research Project of Zhejiang Province (LGF22H070002).

REFERENCES

1. Ahn JH, Yi JW. Transoral Endoscopic Thyroidectomy for Thyroid Carcinoma: Outcomes and Surgical Completeness in 150 Single-Surgeon Cases. *Surg Endosc* (2020) 34(2):861–7. doi: 10.1007/s00464-019-06841-8
2. Wang Y, Zhou S, Liu X, Rui S, Li Z, Zhu J, et al. Transoral Endoscopic Thyroidectomy Vestibular Approach vs Conventional Open Thyroidectomy: Meta-Analysis. *Head Neck* (2021) 43(1):345–53. doi: 10.1002/hed.26486
3. Liu Z, Li Y, Wang Y, Xiang C, Yu X, Zhang M, et al. Comparison of the Transoral Endoscopic Thyroidectomy Vestibular Approach and Open Thyroidectomy: A Propensity Score-Matched Analysis of Surgical Outcomes and Safety in the Treatment of Papillary Thyroid Carcinoma. *Surgery* (2021) 170(6):1680–6. doi: 10.1016/j.surg.2021.06.032
4. Masucci C, Oueiss A, Maniere-Ezvan A, Orthlieb JD, Casazza E. What is a Malocclusion? *Orthod Fr* (2020) 91(1-2):57–67. doi: 10.1684/orthodfr.2020.11
5. Yu X, Liu C, Yan M, Gong W, Wang Y. Hyperthermal Liquid, Spray, and Smog may be Potential Risk Factors for Recurrent Laryngeal Nerve Thermal Injury During Thyroid Surgeries. *Endocrine* (2021) 72(1):198–207. doi: 10.1007/s12020-020-02451-w
6. You JY, Kim HY, Park DW, Yang HW, Kim HK, Dionigi G, et al. Transoral Robotic Thyroidectomy Versus Conventional Open Thyroidectomy: Comparative Analysis of Surgical Outcomes Using Propensity Score Matching. *Surg Endosc* (2021) 35(1):124–9. doi: 10.1007/s00464-020-07369-y
7. Anuwong A. Transoral Endoscopic Thyroidectomy Vestibular Approach: A Series of the First 60 Human Cases. *World J Surg* (2016) 40(3):491–7. doi: 10.1007/s00268-015-3320-1
8. Lira RB, De Cicco R, Rangel LG, Bertelli AA, Duque Silva A, de Medeiros Vanderlei JP, et al. Transoral Endoscopic Thyroidectomy Vestibular Approach: Experience From a Multicenter National Group With 412 Patients. *Head Neck* (2021) 43(11):3468–75. doi: 10.1002/hed.26846
9. Sun H, Zheng H, Wang X, Zeng Q, Wang P, Wang Y. Comparison of Transoral Endoscopic Thyroidectomy Vestibular Approach, Total Endoscopic Thyroidectomy *via* Areola Approach, and Conventional Open Thyroidectomy: A Retrospective Analysis of Safety, Trauma, and Feasibility of Central Neck Dissection in the Treatment of Papillary Thyroid Carcinoma. *Surg Endosc* (2020) 34(1):268–74. doi: 10.1007/s00464-019-06762-6
10. You JY, Kim H, Park DW, Yang HW, Dionigi G, Tufano RP. Prevention of Transoral Thyroidectomy Complications: An Analysis of Surgical Outcomes in 423 Consecutive Series. *Surgery* (2021) 170(4):1155–9. doi: 10.1016/j.surg.2021.05.003
11. Tae K. Complications of Transoral Thyroidectomy: Overview and Update. *Clin Exp Otorhinolaryngol* (2021) 14(2):169–78. doi: 10.21053/ceo.2020.02110
12. Yan HC, Xiang C, Wang Y, Wang P. Scarless Endoscopic Thyroidectomy (SET) Lateral Neck Dissection for Papillary Thyroid Carcinoma Through Breast Approach: 10 Years of Experience. *Surg Endosc* (2021) 35(7):3540–6. doi: 10.1007/s00464-020-07814-y
13. Xie QP, Xiang C, Wang Y, Yan HC, Zhao QZ, Yu X, et al. The Patterns and Treatment of Postoperative Hemorrhage and Hematoma in Total Endoscopic Thyroidectomy *via* Breast Approach: Experience of 1932 Cases. *Endocrine* (2019) 63(3):422–9. doi: 10.1007/s12020-018-01837-1
14. Wang Y, Zhang Z, Zhao Q, Xie Q, Yan H, Yu X, et al. Transoral Endoscopic Thyroid Surgery *via* the Tri-Vestibular Approach With a Hybrid Space-Maintaining Method: A Preliminary Report. *Head Neck* (2018) 40(8):1774–9. doi: 10.1002/hed.25157
15. Wang D, Wang Y, Zhou S, Liu X, Wei T, Zhu J, et al. Transoral Thyroidectomy Vestibular Approach Versus non-Transoral Endoscopic Thyroidectomy: A Comprehensive Systematic Review and Meta-Analysis. *Surg Endosc* (2021). doi: 10.1007/s00464-021-08836-w
16. Ji YB, Jeong JH, Wu CW, Chiang FY, Tae K. Neural Monitoring of the External Branch of the Superior Laryngeal Nerve During Transoral Thyroidectomy. *Laryngoscope* (2021) 131(2):E671–6. doi: 10.1002/lary.28883
17. Wongwattana P, Laoveerakul P, Santeerapharp A. A Comparison of Efficacy and Quality of Life Between Transoral Endoscopic Thyroidectomy Vestibular Approach (TOETVA) and Endoscopic Thyroidectomy Axillo-Breast Approach (ETABA) in Thyroid Surgery: non-Randomized Clinical Trial. *Eur Arch Otorhinolaryngol* (2021) 278(10):4043–9. doi: 10.1007/s00405-021-06639-2

18. Lee DW, Bang HS, Jeong JH, Kwak SG, Choi YY, Tae K. Cosmetic Outcomes After Transoral Robotic Thyroidectomy: Comparison With Transaxillary, Postauricular, and Conventional Approaches. *Oral Oncol* (2021) 114:105139. doi: 10.1016/j.oraloncology.2020.105139

Conflict of Interest: The authors declare that the research was conducted in the absence of any commercial or financial relationships that could be construed as a potential conflict of interest.

Publisher's Note: All claims expressed in this article are solely those of the authors and do not necessarily represent those of their affiliated organizations, or those of the publisher, the editors and the reviewers. Any product that may be evaluated in this article, or claim that may be made by its manufacturer, is not guaranteed or endorsed by the publisher.

frontiers in Endocrinology

METHODS
published: 18 February 2022
doi: 10.3389/fendo.2021.774174

Endoscopic-Assisted Transoral Thyroglossal Cyst Resection

Shanwen Chen, Dong Wang, Jianxin Qiu, Yehai Liu and Yi Zhao *

Department of Otorhinolaryngology-Head and Neck Surgery, The First Affiliated Hospital of Anhui Medical University, Hefei, China

Sistrunk procedure is the standard method for thyroglossal duct cyst resection. While this procedure is successful and safe, it results in postoperative scars on the front of neck. We propose a total transoral technique without external incision that starts with careful separation of the floor of the mouth and genioglossus muscle followed by the exact localization of the cyst using methylene blue. Simultaneously, the hyoid bone connected to the cyst and tract was removed. Finally, routine hemostasis is conducted, and the operative cavity is closed. All patients who received this operation in our department recovered successfully without experiencing severe intraoperative or postoperative complications.

Keywords: endoscopic surgery, thyroglossal cyst, transoral procedures, outcome, cosmetic (plastic) surgery

OPEN ACCESS

Edited by:
Paolo Miccoli,
University of Pisa, Italy

Reviewed by:
Kyung Tae,
Hanyang University, South Korea
Che-Wei Wu,
Kaohsiung Medical University, Taiwan

***Correspondence:**
Yi Zhao
zhaoyi112659@163.com

Specialty section:
This article was submitted to Thyroid Endocrinology, a section of the journal Frontiers in Endocrinology

Received: *11 September 2021*
Accepted: *30 December 2021*
Published: *18 February 2022*

Citation:
Chen S, Wang D, Qiu J, Liu Y and Zhao Y (2022) Endoscopic-Assisted Transoral Thyroglossal Cyst Resection. Front. Endocrinol. 12:774174. doi: 10.3389/fendo.2021.774174

INTRODUCTION

Thyroglossal duct cyst (TGDC) is one of the most commonly observed neck masses in clinical medicine. It is characterized by an active, painless mass in the midline or slightly to one side of the neck, usually located below the hyoid bone (about 75% of patients), and can move along with the tongue. This cyst develops embryologically when the thyroid primordium descends from the base of the tongue to its typical location in front of the trachea. If the tract does not degenerate, clinical cysts may develop (1).

Sistrunk procedure is the widely accepted surgical treatment for TGDC and is similar to open thyroid surgery. This procedure entails the removal of the central part of hyoid bone and thyroid remnants. However, the procedure leaves a roughly 5 cm scar in front of the neck.

Kim et al. (2) were the first to report a successful transoral TGDC resection. No other teams have reported the clinical application of this method. Considering different details, our goal is to share our experience with this approach. Informed consent and ethical review were obtained (IRB number: PJ2021-03-22).

METHODS

We describe this procedure using the example of a 24-year-old woman who required it for cosmetic purposes. Therefore, we decided to perform a scarless procedure. **Figure 1** illustrates relevant anatomical diagrams. The proposed technique was conducted under general anesthesia and oral endotracheal intubation. To maintain oral operating space, a unilateral oral distractor was employed. Subsequently, methylene blue was injected into the cyst from the outside (**Figure 2A**).

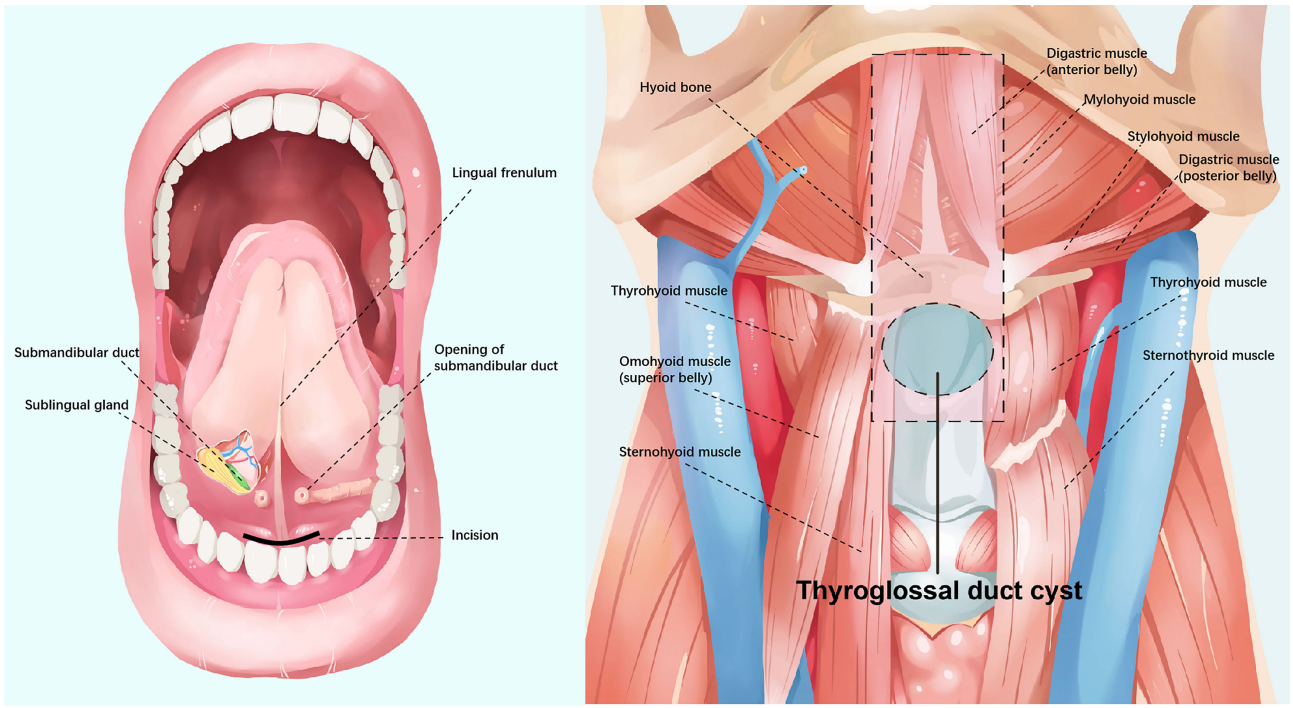

FIGURE 1 | Illustration of anatomy.

At the oral lingual frenulum, a transverse incision of about 2 cm in length was made (**Figure 2B**). The soft tissue of the mouth floor was meticulously dissected, and genioglossus muscles with marked morphological characteristics were identified, separated, and retracted bilaterally (**Figure 2C**). Using a 4 mm rigid nasal endoscope, we longitudinally separated and transected suprahyoid muscles (**Figure 2D**). Then the hyoid bone was located and identified (**Figure 3A**). The hyoid bone's body was then cut using a Kerrison rongeur (**Figure 3B**). Following this step, it was often found that the partially blue-stained cyst remained in the operation cavity. We employed a cryogenic plasma knife to transect the infrahyoid muscles at a distance of 0.5 cm from the hyoid bone. By pulling the hyoid bone upward using forceps, the cyst was completely exposed. Using a plasma knife, the tissue surrounding the cyst was meticulously dissected, and the hyoid bone was pulled out (**Figure 3C**). The hyoid bone and cyst were removed together (**Figure 3D**). After sufficient hemostasis, the operative cavity was flushed with distilled water. A drainage tube was inserted from the mouth floor and fixed under the chin. Finally, the oral mucosa was sutured with a 4-0 suture and bandaged with external neck pressure (**Video 1, Supporting Information**).

The drain was removed when drainage volume was less than 5 mL per 24 h. After operation, no special dietary restrictions were found, and patients were given saline to gargle and maintain their mouth clean. Patients were discharged two days following extubation unless there were special circumstances and were required to comply with regular outpatient follow-up.

RESULTS

Our technique was successful in five patients. The characteristics of patients and operations are listed in **Table 1**. During at least a half-year follow-up, no recurrences or peri/postoperative complications were observed, and all patients achieved excellent cosmetic outcomes with their necks (**Figures 4** and **5**).

DISCUSSION

After diagnosis with a thyroglossal duct cyst, patients tended to seek surgical treatment with an otolaryngologist. A standard Sistrunk procedure is often adopted to resect the lesion. However, growing esthetic concerns motivate patients to seek cosmetic treatment for their unsightly scar in the neck. While the auxiliary use of local drugs and the improvement of surgical hardware can indeed reduce the obvious degree of postoperative scarring, they can also introduce complications such as pruritus and local pain.

Currently, researchers have focused on hidden scars or scarless cosmetic surgery. Cai et al. (3) used endoscope-assisted surgery to successfully resect TGDC *via* a small submental incision, but scarring remains inevitable. One study published by Qu et al. (4) presented a study in which they successfully executed the breast approach on 13 patients, but one had an infection, one developed skin bruising, and another had subcutaneous fluid. Anuwong et al. (5) also completed this

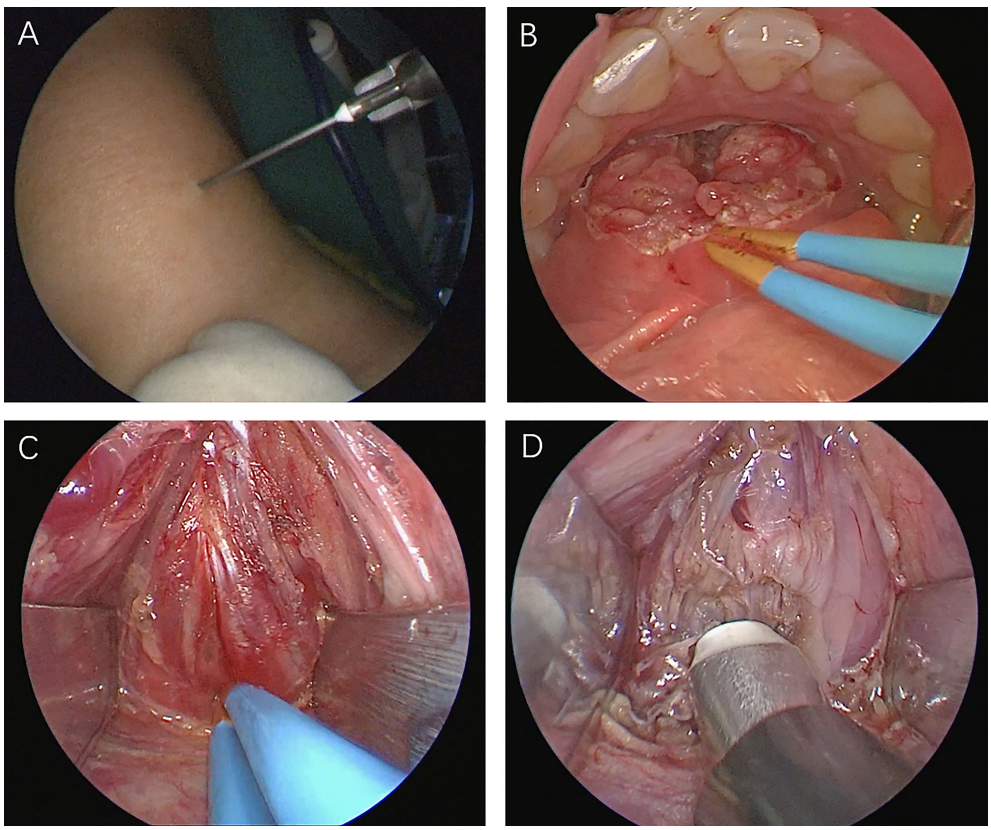

FIGURE 2 | **(A)** Methylene blue injection. **(B)** Transverse frenotomy incision. **(C)** The genioglossus muscles were retracted bilaterally. **(D)** Transection of suprahyoid muscles.

operation with the bilateral areola approach. Considering the author's experience with endoscopic surgery, none of the 11 patients included in their study experienced postoperative complications, and the operation time was shorter. Paek et al. (6) successfully completed TGDC resection for two patients using the bilateral axillo-breast approach. However, this procedure requires more incisions. Kim et al. (7) and Lee et al. (8) selected the retroauricular approach, successfully removed TGDC with robot assistance, and the incision can be hidden, but the costs and hardware constraints obstruct wider accessibility. Han et al. (9) and Banuchi et al. (10) completed the operation by employing the transoral vestibular approach. The former adopts a single incision without insufflation, while the latter adopts the same three incisions with CO_2 insufflation as the vestibular approach for thyroid. Both operations were completed successfully without complications. However, the single incision method of Han et al. (9) does not avoid the problem of narrow operation space. Asians have a relatively flat jaw, which may impede the use of this

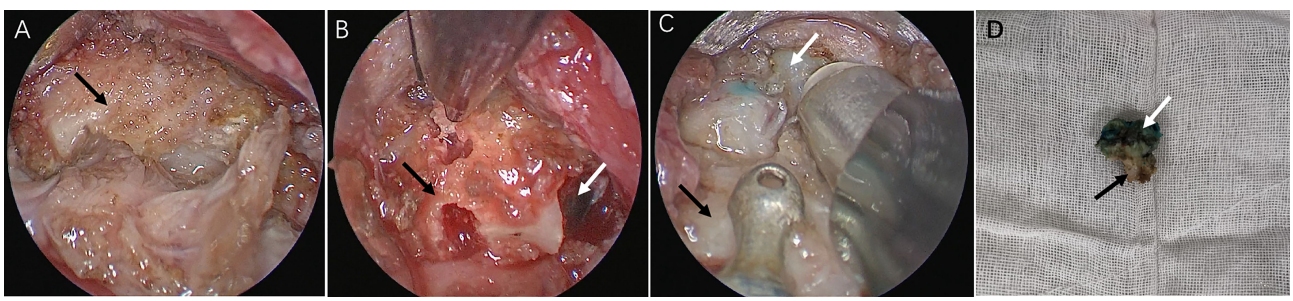

FIGURE 3 | **(A)** Identification of hyoid bone (black arrow). **(B)** Identification of TGDC (white arrow). **(C)** Dissection of the cyst. **(D)** Specimen.

TABLE 1 | Patient demographics and outcomes for undergoing transoral approach for TGDC.

Patient	Age,y	Sex	Lesion size (cm)	Operative time (min)	Bleeding volume (ml)	Drainage volume (ml)	Complication
1	43	Female	1.5×1.2×0.5	180	10	10	None
2	42	Female	2.0×2.0×1.0	190	10	35	None
3	24	Female	1.5×1.0×0.6	210	15	10	None
4	34	Female	2.0×1.0×0.5	165	15	20	None
5	22	Female	2.0×1.4×0.4	130	5	30	None

TGDC, thyroglossal duct cyst.

FIGURE 4 | Tongue movement after operation.

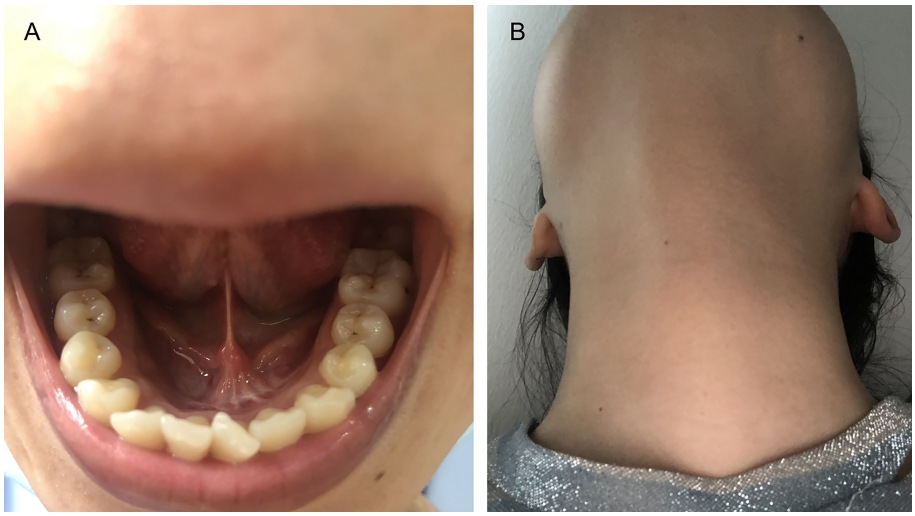

FIGURE 5 | **(A)** Incision at 6-month follow-up. **(B)** Appearance at 6-month follow-up.

technology among other races. Compared with the above approaches, the distance of frenotomy incision is the shortest, and this approach conforms to the law of anatomy. The surgical path is positioned in the midline without important vessels and nerves and does not require extensive tissue dissection and CO_2 insufflation, which avoids possible complications of hypercapnia and numbness in the operation area. However, it should be noted that limitations are still present. The frenotomy incision may bring the risk of incision infection; sublingual edema may cause airway obstruction; narrow operation space significantly increases the difficulty of this procedure, requiring more patience and time. Our operation time was between two and four hours, while the time reported by Woo et al. (11) was about one hour. Similarly, the operation time of Anuwong et al. (5) is also shorter compared with Qu et al. (4) We believe that this technique can be executed more efficiently as experience grows.

The tongue must be retracted upward to expose the mouth floor and the frenum. After recognizing Wharton's duct orifice, we made a frenotomy incision closer to the mandible. Then, blunt separation was used for tissue dissection. In so doing, risk of Wharton's duct injury can be avoided (12). The next issue is the limited operating space, implying why we used 4 mm nasal endoscope. Based on our experience, it is critical to precisely locate the cyst when using the transoral approach. As a result, we used methylene blue for intraoperative localization. The next step requires the surgeon to have extensive experience with endoscopic procedures to avoid cyst rupture because the rupture would lead to blue staining in the operation field, making boundary identification is difficult.

At present, there remain a few reports on endoscopic TGDC surgery, and there are insufficient materials to define indications and contraindications of this operation. In our study, the patients had strong cosmetic intentions and had no history of neck surgery, neck radiotherapy, thyroglossal cyst infection, or thyroglossal fistula. In the above literature, most specimens are 2-3 cm, with the largest specimen of 6 cm in the study of Woo et al. (11) There is no consensus on lesion size limitation. In our method, syringe can be utilized to extract part of the capsule, which may overcome the sample size limitation, but this must be confirmed by follow-up research.

CONCLUSION

TGDC removal using a frenotomy incision is an alternative to conventional procedure with a safe, effective, cosmetic, and well-tolerated outcome. However, because the sample size was relatively small, additional research on indications, complications, and recurrences is still required.

DATA AVAILABILITY STATEMENT

The raw data supporting the conclusions of this article will be made available by the authors, without undue reservation.

ETHICS STATEMENT

The studies involving human participants were reviewed and approved by Ethics Committee of the First Affiliated Hospital of Anhui Medical University. The patients/participants provided their written informed consent to participate in this study.

AUTHOR CONTRIBUTIONS

Concept and design: All authors. Acquisition, analysis, or interpretation of data: All authors. Drafting of the manuscript:

SC. Critical revision of the manuscript for important intellectual content: All authors. Statistical analysis: SC. Administrative, technical, or material support: All authors. Supervision: YZ. All authors contributed to the article and approved the submitted version.

REFERENCES

1. Thompson LD. Thyroglossal Duct Cyst. *Ear Nose Throat J* (2017) 96:54–5. doi: 10.1177/014556131709600204
2. Kim JP, Park JJ, Lee EJ, Woo SH. Intraoral Removal of a Thyroglossal Duct Cyst Using a Frenotomy Incision. *Thyroid* (2011) 21:1381–4. doi: 10.1089/thy.2011.0180
3. Cai Q, Huang X, Liang F, Chen J, Liang M, Pan Y, et al. Endoscope-Assisted Concurrent Resection of Thyroglossal Duct Cysts and Benign Thyroid Nodules *via* a Small Submental Incisions. *Eur Arch Otorhinolaryngol* (2014) 271:1771–5. doi: 10.1007/s00405-013-2688-5
4. Qu R, Wang C, Dong Z, Li J, Liu D. Another Strategy for the Treatment of Thyroglossal Duct Cyst: Totally Endoscopic Surgery by Breast Approach. *Surg Laparosc Endosc Percutan Tech* (2018) 28:118–22. doi: 10.1097/SLE.0000000000000514
5. Anuwong A, Jitpratoom P, Sasanakietkul T. Bilateral Areolar Endoscopic Sistrunk Operation: A Novel Technique for Thyroglossal Duct Cyst Surgery. *Surg Endosc* (2017) 31:1993–8. doi: 10.1007/s00464-016-5137-x
6. Paek SH, Choi JY, Lee K-E, Youn Y-K. Bilateral Axillo-Breast Approach (BABA) Endoscopic Sistrunk Operation in Patients With Thyroglossal Duct Cyst: Technical Report of the Novel Endoscopic Sistrunk Operation. *Surg Laparosc Endosc Percutan Tech* (2014) 24:e95–8. doi: 10.1097/SLE.0b013e31828fa7bf
7. Kim C-H, Byeon HK, Shin YS, Koh YW, Choi EC. Robot-Assisted Sistrunk Operation *via* a Retroauricular Approach for Thyroglossal Duct Cyst. *Head Neck* (2014) 36:456–8. doi: 10.1002/hed.23422
8. Lee DW, Tae K. Robot-Assisted Excision of Thyroglossal Duct Cyst by a Postauricular Facelift Approach. *Wideochir Inne Tech Maloinwazyjne* (2020) 15:245–8. doi: 10.5114/wiitm.2019.88751
9. Han P, Liang F, Cai Q, Chen R, Yu S, Huang X. Endoscope-Assisted Resection of Thyroglossal Duct Cysts *via* a Submaxillary Vestibular Approach. *Head Neck* (2018) 40:377–83. doi: 10.1002/hed.24972
10. Banuchi VE, Long SM, Sachs BY, Kostas JC, Ali KM, Russell JO. Transoral Endoscopic Vestibular Approach Sistrunk Procedure: First Reported Case Series. *Head Neck* (2021) 44:1–5. doi: 10.1002/hed.26889
11. Woo SH, Park JJ, Hong JC, Wang S-G, Park GC, Eun YG, et al. Endoscope-Assisted Transoral Removal of a Thyroglossal Duct Cyst Using a Frenotomy Incision: A Prospective Clinical Trial. *Laryngoscope* (2015) 125:2730–5. doi: 10.1002/lary.25508
12. Wilhelm T, Harlaar JJ, Kerver A, Kleinrensink G-J, Benhidjeb T. Surgical Anatomy of the Floor of the Oral Cavity and the Cervical Spaces as a Rationale for Trans-Oral, Minimal-Invasive Endoscopic Surgical Procedures: Results of Anatomical Studies. *Eur Arch Otorhinolaryngol* (2010) 267:1285–90. doi: 10.1007/s00405-010-1219-x

SUPPLEMENTARY MATERIAL

The Supplementary Material for this article can be found online at: https://www.frontiersin.org/articles/10.3389/fendo.2021.774174/full#supplementary-material

Conflict of Interest: The authors declare that the research was conducted in the absence of any commercial or financial relationships that could be construed as a potential conflict of interest.

frontiers in Endocrinology

ORIGINAL RESEARCH
published: 31 March 2022
doi: 10.3389/fendo.2022.809835

Successful Applications of Food-Assisted and -Simulated Training Model of Thyroid Radiofrequency Ablation

*Yan-Rong Li[1,2], Wei-Yu Chou[1], Wai-Kin Chan[1], Kai-Lun Cheng[3,4], Jui-Hung Sun[1], Feng-Hsuan Liu[1,2], Szu-Tah Chen[1,2] and Miaw-Jene Liou[1,2]**

[1] Division of Endocrinology and Metabolism, Department of Internal Medicine, Linkou Chang Gung Memorial Hospital, Taoyuan, Taiwan, [2] College of Medicine, Chang Gung University, Taoyuan, Taiwan, [3] Department of Medical Imaging, Chung Shan Medical University Hospital, Taichung, Taiwan, [4] School of Medical Imaging and Radiological Sciences, Chung Shan Medical University, Taichung, Taiwan

OPEN ACCESS

Edited by:
Terry Francis Davies, Icahn School of Medicine at Mount Sinai, United States

Reviewed by:
Joachim Feldkamp, Bielefeld University, Germany
Emrah Karatay, Marmara University Istanbul Pendik Education and Research Hospital, Turkey
Che-Wei Wu, Kaohsiung Medical University, Taiwan

***Correspondence:**
Miaw-Jene Liou
lioumj@cgmh.org.tw

Specialty section:
This article was submitted to Thyroid Endocrinology, a section of the journal Frontiers in Endocrinology

Received: 05 November 2021
Accepted: 07 March 2022
Published: 31 March 2022

Citation:
Li Y-R, Chou W-Y, Chan W-K, Cheng K-L, Sun J-H, Liu F-H, Chen S-T and Liou M-J (2022) Successful Applications of Food-Assisted and -Simulated Training Model of Thyroid Radiofrequency Ablation. Front. Endocrinol. 13:809835. doi: 10.3389/fendo.2022.809835

Background: Radiofrequency ablation (RFA) for benign thyroid nodules is one kind of scarless treatment for symptomatic or cosmetic benign thyroid nodules. However, how to train RFA-naive physicians to become qualified operators for thyroid RFA is an important issue. Our study aimed to introduce a successful training model of thyroid RFA.

Materials and Methods: We used a food-assisted and -simulated training model of thyroid RFA. Chicken hearts were simulated into thyroid nodules, three-layer pork meats were simulated into peri-thyroid structure, and gel bottles were simulated into trachea, respectively. Successful training ablations were defined as chicken hearts that were fully cooked. After repeating training ablations of chicken hearts at least 100 times with the nearly 100% success rates for three young trainees, they served as the first assistant for the real procedures of thyroid RFA and then were qualified to perform thyroid RFA on real patients under the supervision of one experienced interventional radiologist.

Results: 23 real patients who received RFA and follow-up at least 6 months after treatment were included in Linkou Chang Gung Memorial Hospital from January 1, 2020 to October 1, 2021. Three young endocrinologists performed thyroid RFA independently. The outcomes were volume reduction rate (VRR), major complications and minor complications. The median VRR at 12 months was 82.00%, two major complications were transient hoarseness, and three minor complications were wound pain. All complications were completely recovered within three days.

Conclusions: For young and RFA-native physicians without any basic skills of echo-guided intervention, this food-assisted and -simulated training model of thyroid RFA was useful for medical training and education.

Keywords: thyroid, nodule, radiofrequency ablation, training model, medical education

INTRODUCTION

With the exams by ultrasonography, thyroid nodules are common in general populations, and the prevalence was ever reported 50-60% (1, 2). Among of them, around 7-15% nodules are malignant; therefore, most thyroid nodules are benign (1, 2). For benign thyroid nodules with symptoms and signs of compression or cosmetic problem, treatment should be considered to alleviate the patients' suffering, such as dyspnea, dysphagia, voice change, or the cosmetic reasons of neck. Radiofrequency ablation (RFA) for benign thyroid nodules is one kind of treatment for symptomatic benign thyroid nodules, especially for cosmetic problem because thyroid RFA is a scarless procedure (3).

Thyroid RFA is a minimally invasive procedure using friction heat productions due to tissue ions agitated by alternating electric current of electrodes and performed with generators and 7-cm electrodes which are 18-gauge, and internally cooled with an active tip measuring 5, 7, or 10 mm (4, 5). The reported volume reduction rate (VRR) by thyroid RFA was from 69% to 78% after 1-year follow-up (6, 7). Some guidelines suggested that thyroid RFA can be used for treating benign thyroid nodules for volume reduction to relieve compression or cosmetic problem (8–10). The core skills are trans-isthmic approach method and moving-shot technique (11). Although knowing these two core techniques, young physicians who have never received step-by-step training by experienced operators and lack in practical experience in real patients may be unable to perform thyroid RFA well and still need a longer learning curve. In addition, young physicians with immature basic and core skills may lead to more complications while learning thyroid RFA in real patients.

As a result, the aim of our study was to investigate the feasibility of the food-assisted and -simulated training model of thyroid RFA in three young endocrinologists who had never performed echo-guided aspiration cytology and thyroid RFA in real patients.

MATERIALS AND METHODS

We used a food-assisted and -simulated training model of thyroid RFA for three young endocrinologists who never performed echo-guided aspiration cytology and RFA. Chicken hearts (size around 2 x 1.5 x 1 cm^3) were simulated into thyroid nodules and three-layer pork meats (size around 25-30 x 15-20 x 7-10 cm^3) were simulated into peri-thyroid structure, and gel bottles were simulated into trachea, respectively (**Figure 1**). The generators of RFA were RF Medical Radiofrequency Generator (Mygen M-2004 and M-3004). The electrodes of RFA were RF Electrodes (RFT Series: RFT0707LN). Sequential echo-guided procedures for training the trans-isthmic approach method and the moving shot technique were performed with the food-assisted and -simulated training model of thyroid RFA (**Figure 2**). The successful ablations were defined as the color of chicken hearts from bright red to off-white, indicating that the meat was fully cooked (**Figure 3**).

After repeating ablations of chicken hearts at least 100 times with the nearly 100% success rates for three young endocrinologists and the trainees can performed echo-guided aspirations for cytology of small nodules/lesions on real patients smoothly, they served as the first assistant for the real procedures of thyroid RFA at least five times and then were qualified to perform thyroid RFA on real patients independently under the supervision of one experienced interventional radiologist for patients' safety. This is a retrospective study of thyroid RFA treatment effectiveness and prognosis after our learning model. Therefore, after training by this model and under the supervision of the leader in our hospital, our hospital permitted that we performed RFA in real patients with patients' consent and collected data retrospectively after getting certificate of IRB for a retrospective study. This study was approved by the Institutional Review Board, Chang Gung Memorial Hospital, Taiwan (IRB No.: 202101301B0).

Patients with nodular goiter (2 cm in at least one diameter), and predominantly solid nodules which contributed to compressive symptoms and/or cosmetic problem were

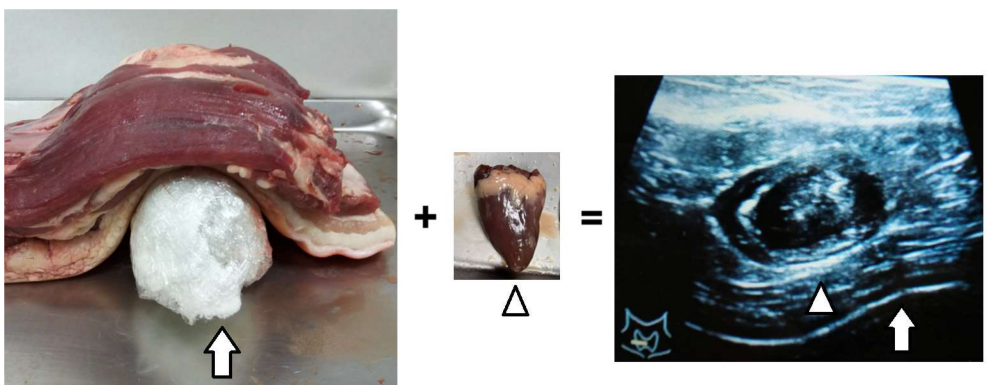

FIGURE 1 | Chicken hearts simulated into thyroid nodules (arrowhead), three-layer pork meats simulated into peri-thyroid skin structure, and gel bottles simulated into trachea (arrow).

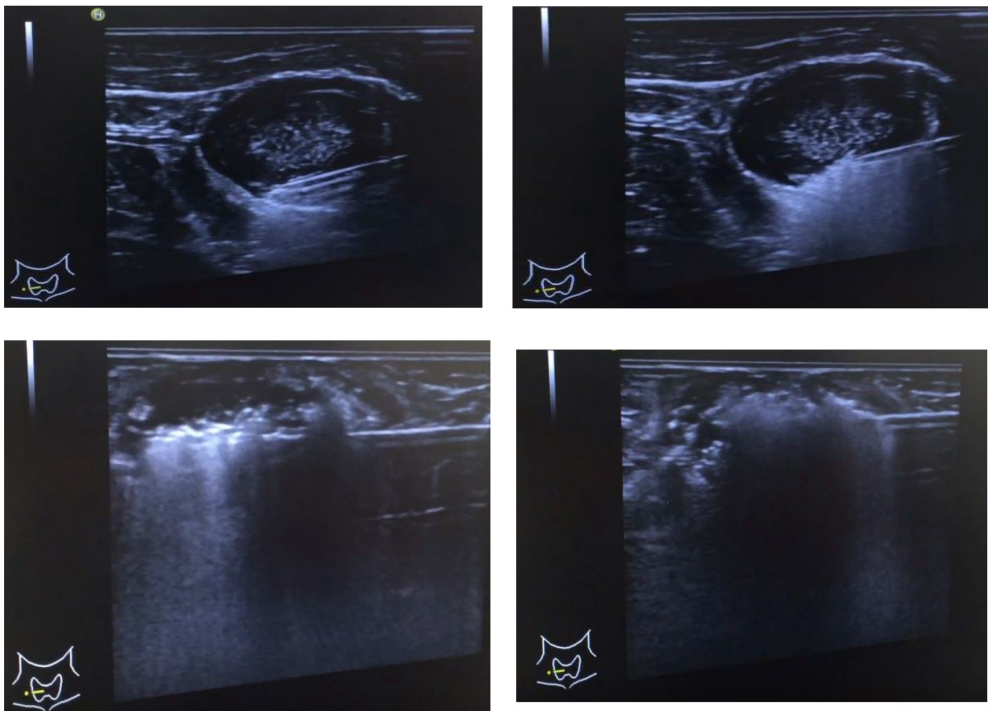

FIGURE 2 | Sequential echo-guided procedures for training the trans-isthmic approach method and the moving shot technique.

arranged to receive echo-guided fine-needle aspiration cytology. If the results of cytology showed benign lesions at least twice and patient refused surgical intervention, there were suggested to receive thyroid RFA for the treatment. If patients had multinodular goiter, the predominant and growing nodule was thought to be responsible for symptoms or cosmetic problems and was selected for the thyroid RFA. Patients with nodules > 5 cm in at least one diameter who may need multiple sessions of thyroid RFA were excluded from this study.

From January 1, 2020 to October 1, 2021, a total of 23 real patients who received thyroid RFA and had follow-up for at least 6 months after treatment in Linkou Chang Gung Memorial Hospital were included in the analysis finally.

OUTCOME MEASUREMENT

The patients were retrospectively reviewed with the medical records to assess the efficacy and the complications of thyroid RFA at the baseline and during the follow-up. The follow-up ultrasonography was performed at 1, 3, 6, and 12 months after thyroid RFA. The volume of nodule and the VRR were calculated

FIGURE 3 | The successful ablations were defined as the color of chicken hearts from bright red to off-white, indicating that the meat was fully cooked.

using the following equations: volume (mL) = length (cm) × width (cm) × depth (cm) × π/6 and VRR = [(initial volume – final volume)/initial volume] × 100%, respectively.

The major outcomes were changes in the volume of nodules, VRR, major complications, and minor complications one year after thyroid RFA. Major complications included voice change, Horner syndrome, brachial plexus injury, and nodule rupture. Minor complications included wound pain, skin burn and hematoma.

STATISTICAL ANALYSIS

Categorical data were determined by frequency and percentage. Kolmogorov-Smirnov test was applied to check the normality of continuous data. Continuous data without normal distributions were expressed as medians with interquartile ranges (IQR). Differences in various continuous parameters during the period of follow-up were examined for statistical significance by using Wilcoxon signed rank test as appropriate because of repeated and non-parametric measurements from a single group. A p value < 0.05 was considered statistically significant. All data analyses were performed using IBM SPSS Statistics for Windows, Version 22.0. (IBM Corp., Armonk, NY, USA).

RESULTS

Baseline Characteristics of Study Patients

23 patients (17 women and 6 men) with 23 benign nodules received thyroid RFA for the treatment. Two trainees performed 8 cases respectively, and the other trainee performed 7 cases. The median age of patients was 51 years (IQR, 43-55 years). The nodules had a median volume of 7.23 mL (IQR, 4.49-13.09 mL) before the thyroid RFA. All nodules were > 50% solidity and 95.65% of nodules were > 90% solidity. All patients had euthyroid status before the treatment of thyroid RFA. The baseline characteristics of study patients are summarized in **Table 1**. No patients had previous surgical intervention, radioactive iodine therapy, thermal/cryo ablation, or radiotherapy which may have an influence on the VRR after thyroid RFA.

TABLE 1 | Baseline characteristics in 23 patients with thyroid radiofrequency ablation.

Clinical characteristics	Value
Main nodule for RFA	23
Age at treatment (year)	51 (43-55)
Female gender	17 (73.91)
Largest diameter (cm)	3.50 (2.80-4.01)
Initial volume	7.23 (4.49-13.09)
Small (< 10 ml)	9 (39.13)
Medium (> 10 to ≤ 20 ml)	5 (21.74)
Large (> 20 to ≤ 30 ml)	6 (26.09)
Very large (> 30 ml)	3 (13.04)
Solidity > 50%	23 (100)
Solidity > 90%	22 (95.65)
Euthyroid status	23 (100)

Data were presented as median (interquartile range) or number (percentage).

Treatment Outcomes and Complications

The sequential changes in the median volume of nodules before and after thyroid RFA were 7.23 mL (IQR, 4.49-13.09 mL) at baseline, 3.49 mL (IQR, 2.36-6.13 mL) at one month, 1.93 mL (IQR, 1.29-4.45 mL) at three months, 1.42 mL (IQR, 0.63-2.30 mL) at six months and 1.30 mL (IQR, 0.22-2.42 mL) at 12 months, respectively (**Table 2** and **Figure 4**). The sequential median VRR after thyroid RFA were 40.89% (IQR, 32.26-56.78%) at one month, 69.62% (IQR, 60.17-79.06%) at three months, 79.89% (61.91-85.44%) at six months and 82.00% (62.17-87.63%) at 12 months, respectively (**Table 2** and **Figure 4**). Each nodule was ablated with single session. One of our real patients was with good response after thyroid RFA and had near 97% VRR at 12 months (**Figures 5A, B**).

Hoarseness could be one kind of major complications after thyroid RFA. There were two patients having transient voice change and both patients recovered totally; one was within five minutes and another was within one day. There were three patients having wound pain and needed non-steroidal anti-inflammatory drugs (NSAIDs) for pain control. Wound pain of these three patients was improved and all patients discontinued NSAIDs within three days. During the follow-up, there was no event of Horner syndrome, brachial plexus injury, nodule rupture, skin burn or hematoma. Due to the small case number of each trainee, the differences of efficacy/complications among these three physicians were not statistically significant.

DISCUSSION

There could be a long learning curve for some physicians to perform thyroid RFA. One recent study showed that there was a measurable learning curve in thyroid RFA until a total of 90 patients for the efficacy of benign thyroid nodules (12). In other words, there could be a minimum number of thyroid RFA for a physician to optimize patients' outcomes. The acceptable VRR after thyroid RFA is at least ≥ 50% at 12 months (13). This concept is like a previous study for evaluation of outcomes in thyroidectomy and the result showed that a surgeon volume threshold (> 25 total thyroidectomies per year) is correlated with improved patients' outcomes (14).

The strength of our study is that it is the first established food-assisted and -simulated training model of thyroid RFA and the result showed successful outcomes (the median VRR at 12 months: 82.00%) for medical training and education. This kind of simulated training model may shorten the learning curve in real patients and could prevent the bad outcomes in the initial 90 patients undergoing thyroid RFA. In other words, by our learning model, trainees can improve their major skills and ability and may be able to prevent excessive trial-and-error learning in the initial 90 real patients.

In Taiwan, thyroid RFA developed later than Korea. In the search of literatures, the first documented case of thyroid RFA in

TABLE 2 | Outcomes of main nodules after thyroid radiofrequency ablation.

	Initial (N = 23)	1 month after RFA (N = 23)	3 month after RFA (N = 23)	6 month after RFA (N = 23)	12 month after RFA (N = 18)
Volume of nodule (mL)	7.23 (4.49-13.09)	3.49 (2.36-6.13)*	1.93 (1.29-4.45)*	1.42 (0.63-2.30)*	1.30 (0.22-2.42)*
VRR (%)	0	40.89 (32.26-56.78)*	69.62 (60.17-79.06)*	79.89 (61.91-85.44)*	82.00 (62.17-87.63)*
Major complications					
Voice change	2	0	0	0	0
Horner syndrome	0	0	0	0	0
Brachial plexus injury	0	0	0	0	0
Nodule rupture	0	0	0	0	0
Minor complications					
Wound pain	3	0	0	0	0
Skin burn	0	0	0	0	0
Hematoma	0	0	0	0	0
Euthyroid status (%)	100	100	100	100	100

RFA, radiofrequency ablation; VRR, volume reduction rate; N, number.
Data were presented as median (interquartile range), number, or percentage.
**p value < 0.05 when compared with the initial nodules.*

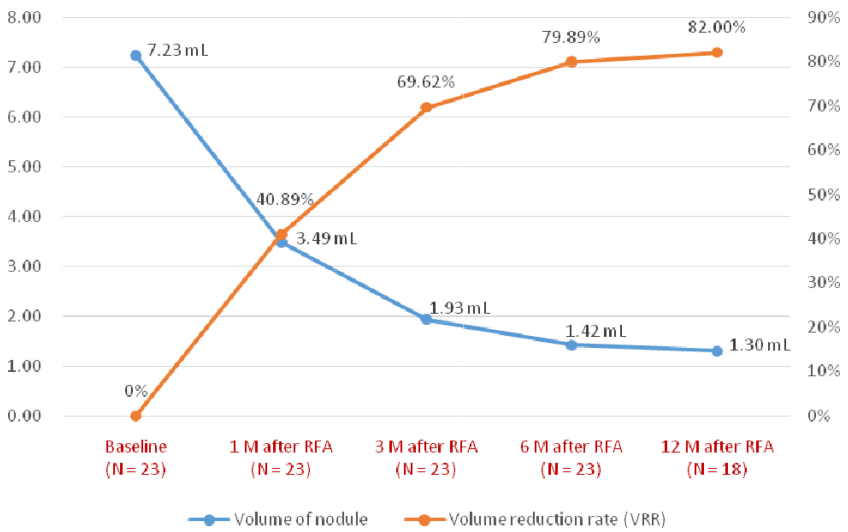

FIGURE 4 | The median changes in the volume of nodules and volume reduction rate during the follow-up.

Taiwan was published in 2016 (15). In Korea, Professor Jung Hwan Baek started thyroid RFA since 2002 (16) and ever published a large population study of thyroid RFA in 2008 (17). Nowadays, many guidelines in different countries have suggested thyroid RFA can be a standard of care to treat benign thyroid nodules for volume reduction to relieve compression or cosmetic problem (3, 8–10). However, in Taiwan, for most clinical physicians who have interests in thyroid RFA, they still have no idea how to learn thyroid RFA efficiently. Traditionally, learning a new invasive procedure requires someone who has a lot of experience to teach the trainee step by step. Two most famous physicians in Taiwan, both Dr. Wei-Che Lin and Dr. Kai-Lun Cheng have performed over one hundred cases of thyroid RFA and mainly contributed to publish a multicenter study of 762 cases after thyroid RFA which established the efficacy and safety of RFA for benign thyroid nodules in Taiwan (18) but they can not teach every trainee by the real patients in Taiwan step by step. Therefore, under the supervision of Dr. Kai-Lun Cheng, one experienced interventional radiologist in Taiwan, we worked together to build this kind of food-assisted and -simulated model for thyroid RFA training. Setting a good training model to learn a new invasive procedure is very important. A good simulated training model consists of hands-on training, deliberate practice, training to proficiency, cognitive teaching, and effective provision of feedback (19). Our training model meets the above points and showed good clinical results after training. The key components of our training model were as the followings: ablations of chicken hearts at least 100 times with the nearly 100% success rates, already performing trans-isthmic approach method with moving-shot technique very well, and understanding the critical structures associated with thyroid RFA, such as danger triangle, middle cervical sympathetic ganglion, and vagal nerve after serving as

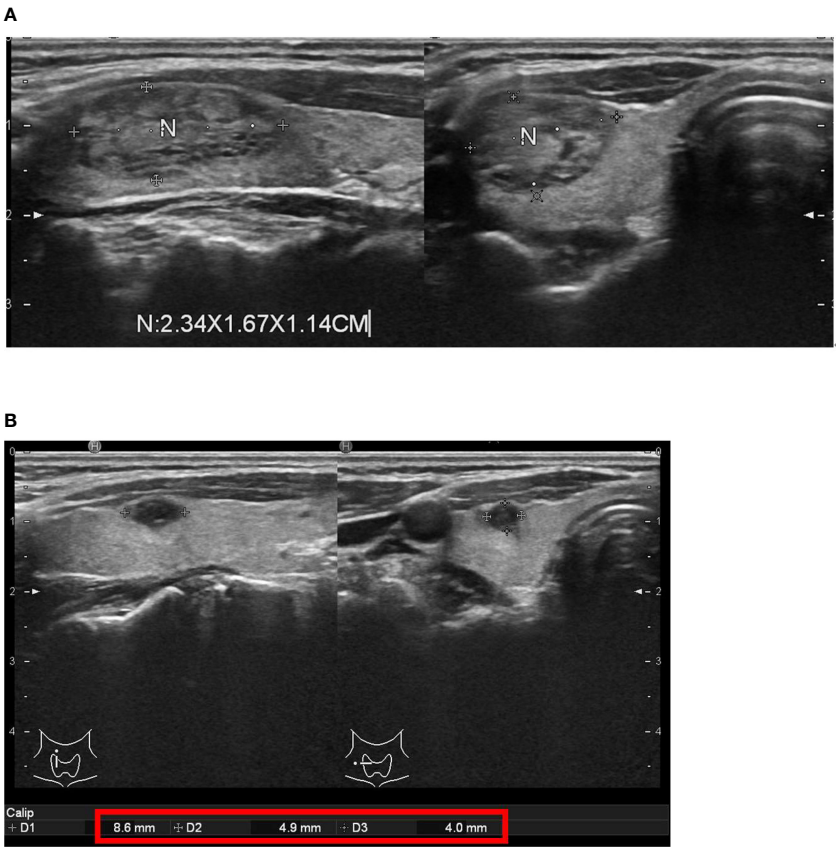

FIGURE 5 | One of our real patients with good response after thyroid radiofrequency ablation (RFA). **(A)** before thyroid RFA **(B)** near 97% volume reduction rate 12 months after thyroid RFA.

the first assistant for the real procedures of thyroid RFA at least five times. Besides, this training model is not expensive, easy to prepare materials and to facilitate the promotion of education. Each round of practice cost around 2500-3500 New Taiwan Dollar and can train multiple trainees at the same time and in the same place. Using this model, we successfully trained and cultivated three physicians simultaneously.

This present study had several major limitations. First, although we tried our best to simulate the peri-thyroid structure but we were unable to simulate the blood vessel, nerves, and esophagus. Therefore, the trainees needed to imagine the locations of the common coratid artery, internal jugular vein, vagal nerve, cervical sympathetic ganglion, danger triangle, and esophagus while practicing the trans-isthmic approach method and moving-shot technique. Second, although the current results of our study showed good applications of our training model with the median VRR 82.00% in real patients, the number of our study subjects is only 23 patients. Third, the longest time of follow-up in our study was 12 months which means we could not confidently evaluate whether the nodular regrowth will occur. Despite these disadvantages, our present study can still provide a valuable training model for those who want to learn how to practice thyroid RFA but do not know where to start.

CONCLUSIONS

For young and RFA-native physicians without any basic skills of echo-guided intervention, this food-assisted and -simulated training model of thyroid RFA was successful for medical training and education.

DATA AVAILABILITY STATEMENT

The raw data supporting the conclusions of this article will be made available by the authors, without undue reservation.

ETHICS STATEMENT

This study was approved by the Institutional Review Board, Chang Gung Memorial Hospital, Taiwan (IRB No.:

202101301B0). The patients/participants provided their written informed consent to participate in this study.

AUTHOR CONTRIBUTIONS

The conceptualization and design of the study was headed by Y-RL, W-KC, K-LC, and M-JL. The manuscript draft was written by Y-RL and M-JL. While the data analysis and interpretation were done by Y-RL, W-YC, W-KC, K-LC, J-HS, F-HL, S-TC, and M-JL. All authors contributed to the article and approved the submitted version.

ACKNOWLEDGEMENTS

We thank GOLEAD BIOPHARM INC for their assistance of providing the food model, generators, and electrodes of thyroid RFA.

REFERENCES

1. Burman KD, Wartofsky L. Clinical Practice. Thyroid Nodules. *N Engl J Med* (2015) 373(24):2347–56. doi: 10.1056/NEJMcp1415786
2. Haugen BR, Alexander EK, Bible KC, Doherty GM, Mandel SJ, Nikiforov YE, et al. American Thyroid Association Management Guidelines for Adult Patients With Thyroid Nodules and Differentiated Thyroid Cancer: The American Thyroid Association Guidelines Task Force on Thyroid Nodules and Differentiated Thyroid Cancer. *Thyroid* (2016) 26(1):1–133. doi: 10.1089/thy.2015.0020
3. Ha EJ, Baek JH, Che Y, Chou YH, Fukunari N, Kim JH, et al. Radiofrequency Ablation of Benign Thyroid Nodules: Recommendations From the Asian Conference on Tumor Ablation Task Force. *Ultrasonography* (2021) 40 (1):75–82. doi: 10.14366/usg.20112
4. Baek JH, Lee JH, Valcavi R, Pacella CM, Rhim H, Na DG. Thermal Ablation for Benign Thyroid Nodules: Radiofrequency and Laser. *Korean J Radiol* (2011) 12(5):525–40. doi: 10.3348/kjr.2011.12.5.525
5. Park HS, Baek JH, Choi YJ, Lee JH. Innovative Techniques for Image-Guided Ablation of Benign Thyroid Nodules: Combined Ethanol and Radiofrequency Ablation. *Korean J Radiol* (2017) 18(3):461–9. doi: 10.3348/kjr.2017.18.3.461
6. Cesareo R, Pasqualini V, Simeoni C, Sacchi M, Saralli E, Campagna G, et al. Prospective Study of Effectiveness of Ultrasound-Guided Radiofrequency Ablation Versus Control Group in Patients Affected by Benign Thyroid Nodules. *J Clin Endocrinol Metab* (2015) 100(2):460–6. doi: 10.1210/jc.2014-2186
7. Deandrea M, Sung JY, Limone P, Mormile A, Garino F, Ragazzoni F, et al. Efficacy and Safety of Radiofrequency Ablation Versus Observation for Nonfunctioning Benign Thyroid Nodules: A Randomized Controlled International Collaborative Trial. *Thyroid* (2015) 25(8):890–6. doi: 10.1089/thy.2015.0133
8. Dobnig H, Zechmann W, Hermann M, Lehner M, Heute D, Mirzaei S, et al. Radiofrequency Ablation of Thyroid Nodules: "Good Clinical Practice Recommendations" for Austria: An Interdisciplinary Statement From the Following Professional Associations: Austrian Thyroid Association (OSDG), Austrian Society for Nuclear Medicine and Molecular Imaging (OGNMB), Austrian Society for Endocrinology and Metabolism (OGES), Surgical Endocrinology Working Group (ACE) of the Austrian Surgical Society (OEGCH). *Wien Med Wochenschr* (2020) 170:6–14. doi: 10.1007/s10354-019-0682-2
9. Papini E, Pacella CM, Solbiati LA, Achille G, Barbaro D, Bernardi S, et al. Minimally-Invasive Treatments for Benign Thyroid Nodules: A Delphi-Based Consensus Statement From the Italian Minimally-Invasive Treatments of the Thyroid (MITT) Group. *Int J Hyperthermia* (2019) 36:376–82. doi: 10.1080/02656736.2019.1575482
10. Kim JH, Baek JH, Lim HK, Ahn HS, Baek SM, Choi YJ, et al. Thyroid Radiofrequency Ablation Guideline: Korean Society of Thyroid Radiology. *Korean J Radiol* (2018) 19:632–55. doi: 10.3348/kjr.2018.19.4.632
11. Na DG, Lee JH, Jung SL, Kim JH, Sung JY, Shin JH, et al. Korean Society of Thyroid Radiology (KSThR); Korean Society of Radiology. Radiofrequency Ablation of Benign Thyroid Nodules and Recurrent Thyroid Cancers: Consensus Statement and Recommendations. *Korean J Radiol* (2012) 13 (2):117–25. doi: 10.3348/kjr.2012.13.2.117
12. Russ G, Ben Hamou A, Poirée S, Ghander C, Ménégaux F, Leenhardt L, et al. Learning Curve for Radiofrequency Ablation of Benign Thyroid Nodules. *Int J Hyperthermia* (2021) 38(1):55–64. doi: 10.1080/02656736.2021.1871974
13. Negro R, Rucco M, Creanza A, Mormile A, Limone PP, Garberoglio R, et al. Machine Learning Prediction of Radiofrequency Thermal Ablation Efficacy: A New Option to Optimize Thyroid Nodule Selection. *Eur Thyroid J* (2020) 9 (4):205–12. doi: 10.1159/000504882
14. Adam MA, Thomas S, Youngwirth L, Hyslop T, Reed SD, Scheri RP, et al. Is There a Minimum Number of Thyroidectomies a Surgeon Should Perform to Optimize Patient Outcomes? *Ann Surg* (2017) 265(2):402–7. doi: 10.1097/SLA.0000000000001688
15. Lee MT, Wang CY. Case Experience of Radiofrequency Ablation for Benign Thyroid Nodules: From an Ex Vivo Animal Study to an Initial Ablation in Taiwan. *J Med Ultrasound* (2016) 24(1):32–8. doi: 10.1016/j.jmu.2016.03.003
16. Sim JS, Baek JH. Unresolved Clinical Issues in Thermal Ablation of Benign Thyroid Nodules: Regrowth at Long-Term Follow-Up. *Korean J Radiol* (2021) 22(8):1436–40. doi: 10.3348/kjr.2021.0093
17. Jeong WK, Baek JH, Rhim H, Kim YS, Kwak MS, Jeong HJ, et al. Radiofrequency Ablation of Benign Thyroid Nodules: Safety and Imaging Follow-Up in 236 Patients. *Eur Radiol* (2008) 18(6):1244–50. doi: 10.1007/s00330-008-0880-6
18. Lin WC, Wang CK, Wang WH, Kuo CY, Chiang PL, Lin AN, et al. Multicenter Study of Benign Thyroid Nodules With Radiofrequency Ablation: Results of 762 Cases Over 4 Years in Taiwan. *J Pers Med* (2022) 12(1):63. doi: 10.3390/jpm12010063
19. Palter VN. Comprehensive Training Curricula for Minimally Invasive Surgery. *J Grad Med Educ* (2011) 3(3):293–8. doi: 10.4300/JGME-D-11-00091.1

Conflict of Interest: The authors declare that the research was conducted in the absence of any commercial or financial relationships that could be construed as a potential conflict of interest.

frontiers | Frontiers in Endocrinology

ORIGINAL RESEARCH
published: 09 June 2022
doi: 10.3389/fendo.2022.884866

Intraoperative Management of the Recurrent Laryngeal Nerve Transected or Invaded by Thyroid Cancer

Hiroo Masuoka * *and Akira Miyauchi*

Department of Surgery, Kuma Hospital Center for Excellence in Thyroid Care, Kobe, Japan

Thyroid cancer often invades the recurrent laryngeal nerve (RLN), causing vocal cord paralysis. In such patients, the invaded portion of the RLN usually needs to be resected through curative surgery. We attempt to preserve the nerve by performing sharp dissection in such cases. During nerve dissection, an intraoperative nerve monitoring system helps identify the course of the RLN in the fibrous tissue around the tumor or even within the tumor, and also helps evaluate the nerve integrity. Because of extensive dissection, the preserved RLN may become much thinner than its original thickness. We refer to this procedure as "partial layer resection" of the RLN. In our cases, although the dissected RLNs became thinner, we found that vocal cord function recovered in most patients. If the RLN is fully involved by thyroid cancer or response of the vocal cord against electric stimulation to the RLN is lost, we resect the portion of the RLN together with the tumor and repair it using one of the reconstruction techniques. When a unilateral RLN is resected, the vocal cord on that side is paralyzed. Symptoms include hoarseness, mis-swallowing, and short phonation. RLN reconstruction using one of the reconstruction techniques leads to the recovery of phonatory and swallowing function, although the normal motion of the vocal cord on the side of the anastomosis is not restored. We used direct anastomosis, free nerve grafting, ansa cervicalis-RLN anastomosis, and vagus-RLN anastomosis to reconstruct the RLN. Thyroid cancer often invades the RLN near the Berry's ligament. In such patients, surgeons might assume that reconstruction of the RLN may not be possible because the peripheral stump of the RLN cannot be observed. However, if we divide the inferior pharyngeal constrictor muscles along the lateral edge of the thyroid cartilage, the peripheral RLN can be identified, and nerve reconstruction can be performed. We refer to this procedure as "laryngeal approach".In summary, of the patients with thyroid cancer who required resection of the RLN, RLN reconstruction led to the recovery of phonatory function. We suggest that all thyroid surgeons familiarize themselves with these reconstruction techniques.

Keywords: Recurrent Laryngeal Nerve, reconstruction, Intraoperative neural monitoring (IONM), laryngeal approach, partial layer resection

OPEN ACCESS

Edited by:
Gianlorenzo Dionigi,
University of Milan, Italy

Reviewed by:
Erivelto Martinho Volpi,
Centro de referencia no ensino do diagnóstico por imagem (CETRUS), Brazil
Hui Ouyang,
Central South University, China

***Correspondence:**
Hiroo Masuoka
masuoka@kuma-h.or.jp

Specialty section:
This article was submitted to Thyroid Endocrinology, a section of the journal Frontiers in Endocrinology

Received: *27 February 2022*
Accepted: *06 May 2022*
Published: *09 June 2022*

Citation:
Masuoka H and Miyauchi A (2022) Intraoperative Management of the Recurrent Laryngeal Nerve Transected or Invaded by Thyroid Cancer. Front. Endocrinol. 13:884866. doi: 10.3389/fendo.2022.884866

INTRODUCTION

Thyroid cancer often invades the recurrent laryngeal nerve (RLN), causing vocal cord paralysis (VCP). In such patients, the invaded portion of the RLN usually needs to be resected through curative surgery. Even in patients with functional vocal cords preoperatively, RLN may be involved when performing thyroid surgery for thyroid cancer. We attempt to preserve the nerve by performing sharp dissection in such cases. Nishida et al. reported that preservation of the RLN invaded by differentiated thyroid cancer with sharp dissection rarely causes local recurrence (1). Our results are in accordance with those of their report.

In recent years, we have routinely used an intraoperative neural monitoring system to evaluate the integrity of the inferior laryngeal nerve (RLN) and external branches of the superior laryngeal nerve during thyroid surgery (2). This system helps assess the electrophysiological response of the RLN prior to dissection. If the response is normal, we try preserving the RLN by shaving off the tumor (3). During nerve dissection, an intraoperative nerve monitoring system helps identify the course of the RLN in the fibrous tissue around the tumor or even within the tumor and also helps evaluate the nerve integrity. If the response is weakened or lost, we resect the portion of the RLN together with the tumor and repair it using one of the reconstruction techniques described below.

In the personal case series of one of the authors (Miyauchi A.), among 721 primary thyroid cancer cases treated between 1998 to 2008, 4.3% of the patients presented with VCP preoperatively, and even in patients with functioning vocal cords preoperatively, 2.2% required resection of the RLN because of cancer invasion. Therefore, in total, 6.4% of the patients required resection of the RLN (**Table 1**). If a unilateral RLN is severed or fully injured, the vocal cord on that side is paralyzed. It remains fixed in a paramedian position, becomes atrophied, and loses its tension during phonation. Symptoms include hoarseness, mis-swallowing, and short phonation due to the waste of exhaled air during phonation. Aspiration can be a dangerous symptom, particularly among elderly patients.

We reported vocal improvement after various methods of RLN reconstruction, although normal vocal cords movements were not restored (4, 5).

Here, we describe how to manage the RLN invaded by thyroid cancer.

PARTIAL LAYER RESECTION OF THE RLN

Because of extensive dissection, the preserved RLN may become much thinner than its original thickness (**Figure 1**). We refer to this procedure as "partial layer resection" of the RLN. In our case, although the dissected RLNs became thinner, we found that vocal cord function recovered in most patients. We reviewed our medical records and found that 18 patients underwent partial layer resection of the RLN to remove thyroid cancer. Postoperatively, two (11%) patients had no VCP, 13 (72%) patients had temporary VCP followed by full recovery of vocal cord function, and only three (17%) patients had permanent VCP (6). These unexpected outcomes prompted us to study the anatomy of the RLN. We studied the histology of the cross-sections of the normal portions of RLNs resected due to thyroid cancer invasion. We found that the true nerve component was surrounded by thick perineural tissue (**Figure 2**). This anatomy may explain the favorable outcomes obtained after partial layer resection of RLNs (6). Even in cases where the preserved RLN becomes thinner than its original thickness following extensive shaving, we concluded that it is worth preserving the nerve if it was functioning well preoperatively.

RECONSTRUCTION OF THE TRANSECTED OR RESECTED RLN

Methods of Reconstruction of the RLN

In 2009, Miyauchi A., one of the co-authors in this paper, reported improvement in phonation following RLN reconstruction performed during thyroid surgery in 88 patients with thyroid cancer invading the nerve in his personal series from 1984 to 2007 at Kuma Hospital or Kagawa Medical University Hospital (7). The patients included 72 women and 16 men aged 18–78 years with a mean age of 55.6 years. Of the patients, 51 (58%) underwent preoperative VCP. Seven patients underwent a second surgery for recurrent disease, while the others were primary cases. We used direct anastomosis (DA), free nerve grafting (FNG), ansa cervicalis-RLN anastomosis (ARA), and vagus-RLN anastomosis (VRA) to reconstruct the RLN (**Figure 3**). ARA was performed in most patients (n=65; 74%). DA was performed in only seven patients, FNG was performed in 14 patients, and VRA was attempted in two patients in whom both the unilateral RLN and its ipsilateral vagus nerve required resection due to cancer invasion. In 3 FNG cases and 31 ARA cases, anastomosis was performed behind the thyroid cartilage. In 8 ARA cases, anastomosis was performed using the contralateral ansa cervicalis. Surgical loupes at 2.5 × magnification were used in 51 patients. The operating microscope was used in 10 patients, and no magnifier was used in 27 patients. The thickness of the thread used for anastomosis ranged from 6-0 to 9-0, with 8-0 being the most common thickness. He generally used three stitches for end-to-end anastomosis of the nerves and used microsurgical instruments to construct the anastomosis. At Kuma Hospital, we use 8-0 monofilament thread and microsurgery instruments and encouraged the use of surgical loupes at 2.5 × magnification.

TABLE 1 | Number (%) of patients who required resection of the recurrent laryngeal nerve in A.M.'s personal series from 1998 to 2008 consisting of primary thyroid cancer cases.

	VCP preoperatively		
	No	Yes	Total
No. of patients	690 (95.7%)	31 (4.3%)	721 (100.0%)
Patients with RLN resection	16 (2.2%)	30 (4.2%)	46 (6.4%)

VCP, vocal cord paralysis.

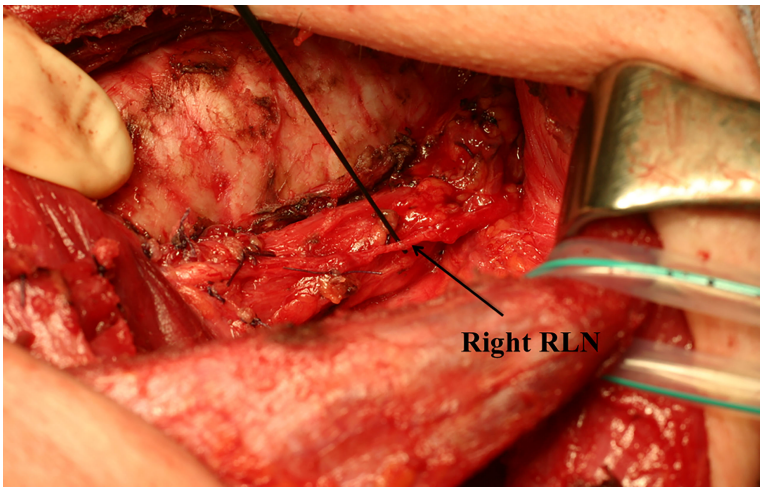

FIGURE 1 | The recurrent laryngeal nerve after partial layer resection. Due to extensive resection, the recurrent laryngeal nerve became much thinner than its original thickness.

In patients with extensive node metastases, the ansa cervicalis on the same side may not be available. In such cases, the contralateral ansa cervicalis can be used for reconstruction. In cases, we inserted a suction tube between the trachea and the esophagus, sucked the contralateral ansa cervicalis into the tube, and then brought it to the side of the defect, where we made a contralateral ansa cervicalis-to-RLN anastomosis (**Figure 4**) (8). This route appears to be the shortest for performing the anastomosis. If the contralateral ansa cervicalis is too short, the FNG technique can be combined for safe anastomosis. However, this would require a longer time for reinnervation of the vocal cords and recovery during phonation. Furthermore, avoiding tension on anastomoses is key to this procedure.

Evaluation of the Reconstructed RLN

Although we examined all patients using a fiberoptic laryngoscope after surgery, a laryngoscopic examination is not suitable for evaluating the recovery of vocal cord function because vocal cords do not return to normal motion after reconstruction of the RLN. Serial measurements of maximum phonation time (MPT) are the easiest and most practical method for evaluating recovery in phonation. We used the MPT one year after surgery to evaluate the outcomes. Thirty-four healthy subjects (26 women and eight men) and 27 patients (18 women and nine men) with unilateral VCP served as controls. Serial measurements of the MPT showed a sudden increase in MPT, usually around 3 months after surgery, when the patient's voice improved. The MPTs were significantly

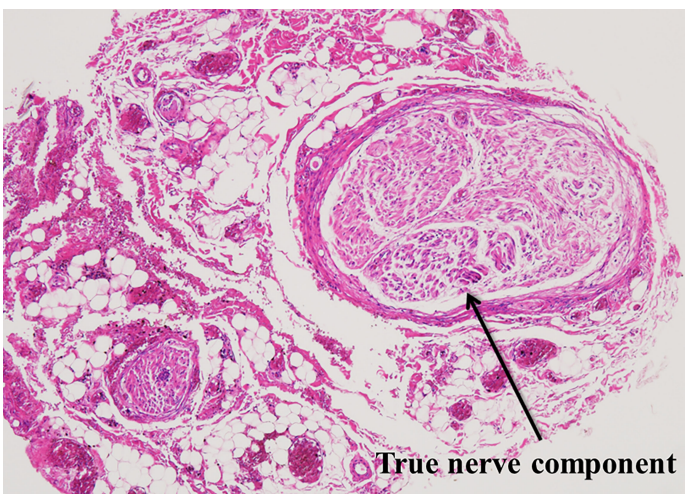

FIGURE 2 | Microscopic cross-section of the normal portion of the recurrent laryngeal nerve resected due to invasion by thyroid cancer. The true nerve component is surrounded by thick peri-neural tissue.

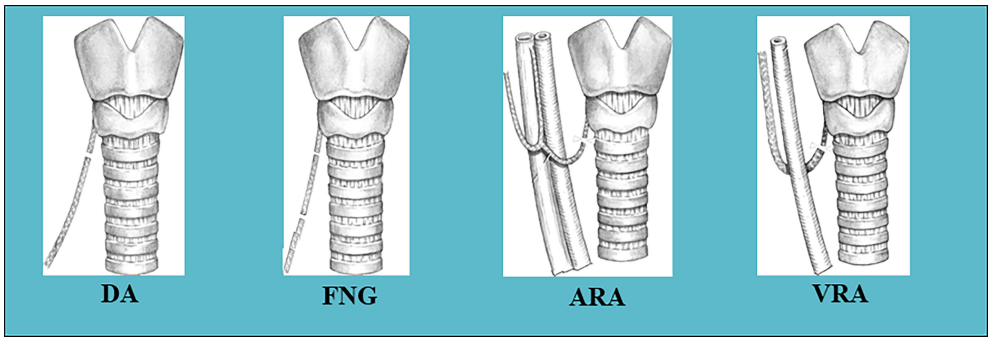

FIGURE 3 | Methods of reconstruction of the RLN used in this series: DA, direct anastomosis; FNG, free nerve grafting; ARA, ansa cervicalis-RLN anastomosis; VRA, vagus-RLN anastomosis.

shorter in patients with VCP than in healthy subjects. Normal MPT values were achieved in patients who underwent RLN reconstruction (**Table 2**) (7).

There were significant sex-specific differences in MPT in healthy subjects and in patients with VCP (**Table 2**). The MPT divided by the VC ratio (sec/L) indicates the vocal cord function of converting a unit volume of exhaled air to a certain length of phonation. This value is called the phonation efficiency index (PEI) (7). When PEIs were calculated, the sex-specific differences in healthy subjects and patients with VCP disappeared completely. It was noted that patients with VCP had significantly smaller PEIs than the healthy subjects. Nearly normal PEI values were achieved in patients who underwent RLN reconstruction (**Table 3**) (7) . Since PEI did not differ based on sex, this value is considered suitable for evaluating vocal cord function regardless of the patient's sex. We analyzed factors that might be related to PEI one year after surgery, such as age at surgery, presence or absence of VCP preoperatively, method of RLN reconstruction, use of magnifier, and thread thickness. None of these factors significantly affected PEI one year after surgery. In general, insignificant data points did not add any value to analysis. However, in this case, they highlighted a very crucial idea. These data indicated that regardless of age or the presence/absence of VCP preoperatively, reconstruction of the transected RLN using any method/technique can help recover the patients' voices to nearly normal levels.

Laryngeal Approach

Thyroid cancer often invades the RLN near the Berry's ligament. In such patients, surgeons might assume that reconstruction of the RLN may not be possible because the peripheral stump of the RLN cannot be observed. However, if we divide the inferior pharyngeal constrictor muscles along the lateral edge of the thyroid cartilage, the peripheral RLN can be identified, and nerve reconstruction can

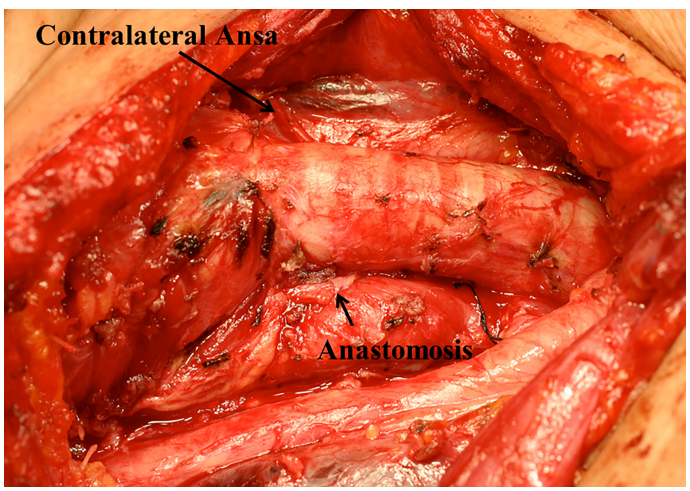

FIGURE 4 | Contralateral ansa cervicalis-to-RLN anastomosis: The contralateral ansa-cervicalis was brought to the side of the defected RLN between the trachea and the esophagus to make contralateral ansa cervicalis-to-RLN anastomosis.

TABLE 2 | Maximum phonation time in healthy subjects, patients with vocal cord paralysis, and patients who underwent reconstruction of the recurrent laryngeal nerve (9).

		Healthy subjects	Patients with VCP	Patients with RLN reconstruction
Male	No. of patients	8	9	16
	MPT	28.6±10.8	10.1±4.3	20.9±11.7
Female	No. of patients	26	18	72
	MPT	16.7±5.1	6.3±2.9	18.8±6.6

MPT, maximum phonation time; values are mean ± SD (seconds). VCP, vocal cord paralysis; RLN, recurrent laryngeal nerve.

TABLE 3 | Phonation efficiency index in healthy subjects, patients with vocal cord paralysis, and patients who underwent reconstruction of the recurrent laryngeal nerve (9).

		Healthy subjects	Patients with VCP	Patients with RLN reconstruction
Male	No. of patients	8	9	16
	PEI	6.79±2.52	3.24±1.49	5.53±2.72
Female	No. of patients	26	18	72
	PEI	6.73±2.04	3.29±1.48	7.59±2.82

PEI: phonation efficiency index; values are mean ± SD (seconds/L). VCP, vocal cord paralysis; RLN, recurrent laryngeal nerve.

be performed (10). The anterior branch should be selected for anastomosis if possible since it usually goes to the adductor muscles. Subsequently, ARA or FNG can be performed behind the thyroid cartilage. However, finding the peripheral portion of the RLN behind the thyroid cartilage after resection of the invaded portion is challenging. We modified the surgical approach to overcome this challenge by identifying the peripheral portion of the RLN by dividing the inferior pharyngeal constrictor muscle before dissecting the nerve. We refer to this procedure as "laryngeal approach (11)". This procedure is illustrated in F**igure 5**. Briefly, we made a small hole in the inferior pharyngeal constrictor muscle using electrocautery at the edge of the thyroid cartilage (**Figure 5A**). Next, we elevated the muscle using the jaws of a mosquito hemostat (**Figure 5B**) and cut the muscle with a pair of bipolar coagulators (**Figure 5C**). Next, we identified the peripheral portion of the RLN behind the thyroid cartilage (**Figure 5D**). This procedure makes dissection of the RLN invaded by thyroid cancer much easier because the RLN can be dissected from the central and peripheral sides. If only a portion of the RLN requires resection, the nerve can be readily reconstructed since the peripheral portion of the nerve is already identified and secured, and ansa cervicalis-to-RLN anastomosis can then be performed (**Figure 5E**) (5). For some special reasons, FNG can be used to fill the defect of the RLN, although this procedure requires two anastomoses. In addition, the divided pharyngeal muscle ends do not need to be fixed.

DISCUSSION

In cases where RLN is transected, surgeons can attempt its repair by direct anastomosis of the cut ends of the nerve. This is a remarkably simple idea for surgeons and was tried more than 100 years ago. The first investigators who performed this procedure reported that the movements of vocal cords were restored after anastomosis. However, other investigators later argued that this was incorrect and that recovery of vocal cord movement did not occur. As a result, anastomosis of the cut ends of the transected RLN was abandoned. However, Ezaki et al. reported that voices of seven patients recovered after direct anastomosis of the transected RLN, although their vocal cords were fixed at the median. They explained the reason behind the recovery of these patients' voices as follows (9).

The RLN includes adductor and abductor nerve fibers without special segregation of these nerve fibers within the RLN. Following anastomosis, even if the anastomosis was performed under an operating microscope, the nerves regenerated in a mixed fashion, which is called misdirected regeneration (**Figure 6**). Therefore, the adductor and abductor muscles contract simultaneously during inspiration and phonation. In the RLN, the number of adductor nerve fibers is three times the number of abductor nerve fibers. The adductor muscles in the larynx are generally much stronger than the abductor muscles. Therefore, the normal motion of the vocal cord on the side of the anastomosis was not restored. While the cord is fixed at the median, it is not paralyzed. This condition is better expressed as synkinesis, simultaneous contraction of the adductor and abductor muscles. Following reinnervation, the vocal cord recovers from atrophy and restores tension during phonation. For good phonation, a narrow gap between the vocal cords, good tension between the vocal cords, and symmetrical volume and weight of the vocal cords are necessary. Following anastomosis, all these conditions seem to be achieved. Consequently, this improves the patient's voice, increases phonation times, and reduced aspiration. However, paradoxical movements of the reinnervated vocal cord may occur in rare cases of extreme misdirection during the regeneration process.

DA is a simple procedure. However, this method can only be performed when the portion of the nerve defect is short or in cases of accidental transection of the RLN. Tension on the anastomosis should be avoided, and the anastomosis should be performed in an end-to-end fashion. If the defect portion is long, it can be repaired using a free nerve graft; however, this method requires two anastomoses. The graft can be harvested from the

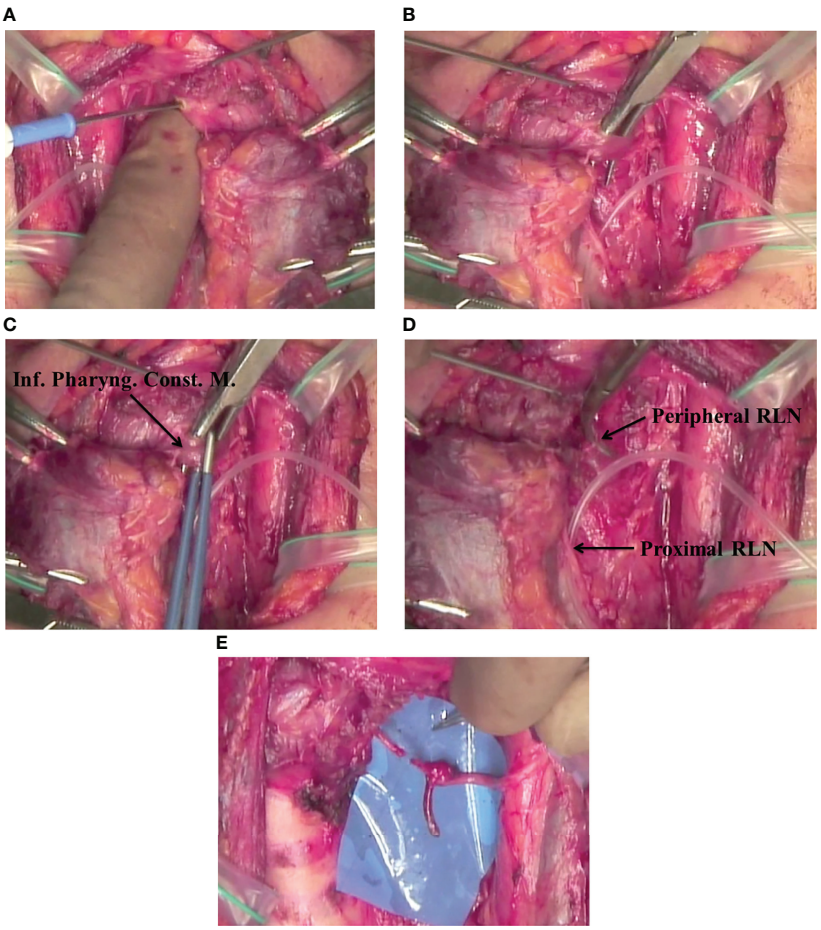

FIGURE 5 | **(A)** Laryngeal approach: Marking a hole in the inferior pharyngeal constrictor muscle at the lateral edge of the thyroid cartilage using electrocautery. **(B)** Laryngeal approach: Dissection of the inferior pharyngeal constrictor muscles along the lateral edge of the thyroid cartilage. **(C)** Laryngeal approach: Cutting the inferior pharyngeal constrictor muscles along the lateral edge of the thyroid cartilage using a pair of bipolar coagulators. **(D)** Laryngeal approach: Locating the peripheral RLN behind the thyroid cartilage. **(E)** Laryngeal approach: Performing ARA with the distal portion of the RLN that was found behind the thyroid cartilage.

supraclavicular cutaneous nerves, transcervical nerves, auricular nerves, and ansa cervicalis, irrespective of the motor or sensory nerves. If the defect extends to the mediastinum, anastomosis at the mediastinal site may be challenging or practically impossible.

In 1990, Miyauchi et al. reported ARA as their own idea (5). However, this method was previously reported by Crumley et al. in 1986 (12). The ansa cervicalis forms a loop in front of the internal jugular vein and branches into the sternothyroid, sternohyoid, and

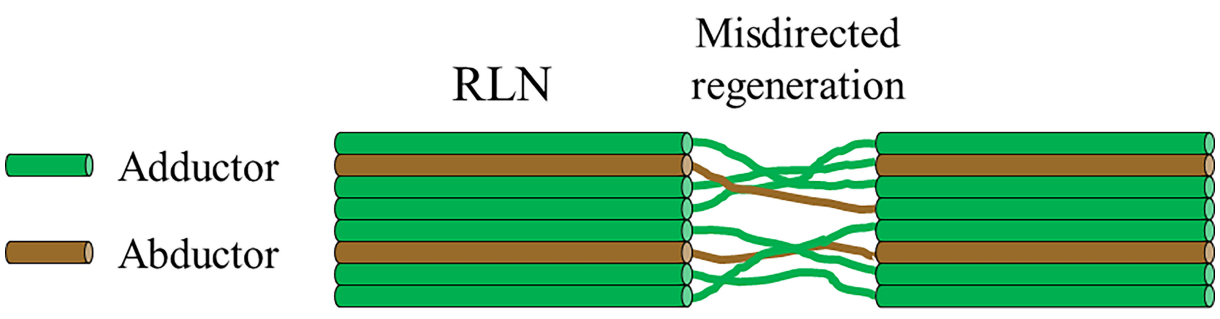

FIGURE 6 | Misdirected regeneration of the recurrent laryngeal nerve. The RLN contains adductor and abductor nerve fibers without special segregation of these nerve fibers within the RLN. Following the anastomosis, the nerve fibers regenerate in a mixed fashion.

omohyoid muscles. It is a motor nerve that is activated during phonation and respiration. The results of ARA are quite similar to those of DA of the RLN, with no recovery of vocal cord movement but recovery of phonation. Paradoxical movements of the vocal cords following ARA have never been observed. ARA requires only one anastomosis, which can be performed in an easy-to-access position of the neck near the larynx. Therefore, the time necessary for nerve regeneration and voice recovery following nerve reconstruction should also be shorter than that required for FNG. VRAs were performed in only two exceptional cases in which thyroid cancer invaded the RLN and ipsilateral vagus nerve, thus requiring resection of both nerves.

Dyspnea on inspiration can occur if bilateral RLNs are cut or injured. Depending on the degree of dyspnea, the airway may have to be opened *via* tracheostomy. Reconstruction of the RLN is not indicated for this disastrous condition because this procedure does not help restore the normal motion of the vocal cords; instead, the cords become fixated at the median position.

CONCLUSION

Of the patients with thyroid cancer who needed resection of the RLN, RLN reconstruction led to the recovery of phonatory function in nearly 90% of patients. Recovery was achieved in all patients regardless of patient characteristics, presence or absence of VCP preoperatively, reconstruction method, or surgical aid. Therefore, we suggest that all thyroid surgeons familiarize themselves with these reconstruction techniques and attempt reconstructing the RLN if necessary.

DATA AVAILABILITY STATEMENT

The original contributions presented in the study are included in the article/supplementary material. Further inquiries can be directed to the corresponding author.

AUTHOR CONTRIBUTIONS

HM and AM designed the study. HM reviewed clinical records, and prepared the article, tables, and figures. AM revised the article. All authors contributed to the article and approved the submitted version.

REFERENCES

1. Nishida T, Nakao K, Hamaji M, Kamiike W, Kurozumi K, Matsuda H. Preservation of Recurrent Laryngeal Nerve Invaded by Differentiated Thyroid Cancer. *Ann Surg* (1997) 226:85–91. doi: 10.1097/00000658-199707000-00012
2. Randolph GW, Dralle H, Abdullah H, Barczynski M, Bellantone R, Brauckhoff M, et al. Electrophysiologic Recurrent Laryngeal Nerve Monitoring During Thyroid and Parathyroid Surgery: International Standards Guideline Statement. *Laryngoscope* (2011) 121(Supplement 1): S1–16. doi: 10.1002/lary.21119
3. Wu CW, Dionigi G, Barczynski M, Chiang FY, Dralle H, Schneider R, et al. International Neuromonitoring Study Group Guidelines 2018: Part II: Optimal Recurrent Laryngeal Nerve Management for Invasive Thyroid Cancer-Incorporation of Surgical, Laryngeal, and Neural Electrophysiologic Data. *Laryngoscope* (2018) 128(Supplement 3):S18–27. doi: 10.1002/lary.27360
4. Miyauchi A, Ishikawa H, Matsusaka K, Maeda M, Matsuzuka F, Hirai K, et al. Treatment of Recurrent Laryngeal Nerve Paralysis by Several Types of Nerve Suture. *J Jap Surg Soc* (1993) 94:550–5.
5. Miyauchi A, Matsusaka K, Kihara M, Matsuzuka F, Hirai K, Yokozawa T, et al. The Role of Ansa-to-Recurrent-Laryngeal Nerve Anastomosis in Operations for Thyroid Cancer. *Eur J Surg* (1998) 164:927–33. doi: 10.1080/110241598750005093
6. Kihara M, Miyauchi A, Yabuta T, Higashiyama T, Fukushima M, Ito Y, et al. Outcome of Vocal Cord Function After Partial Layer Resection of the Recurrent Laryngeal Nerve in Patients With Invasive Papillary Thyroid Cancer. *Surgery* (2014) 155:184–9. doi: 10.1016/j.surg.2013.06.052
7. Miyauchi A, Inoue H, Tomoda C, Fukushima M, Kihara M, Higashiyama T, et al. Improvement in Phonation After Reconstruction of the Recurrent Laryngeal Nerve in Patients With Thyroid Cancer Invading the Nerve. *Surgery* (2009) 146:1056–62. doi: 10.1016/j.surg.2009.09.018
8. Miyauchi A, Yokozawa T, Kobayashi K, Hirai K, Matsuzuka F, Kuma K, et al. Opposite Ansa Cervicalis to Recurrent Laryngeal Nerve Anastomosis to Restore Phonation in Patients With Advanced Thyroid Cancer. *Eur J Surg* (2001) 167:540–1. doi: 10.1080/110241501316914939
9. Ezaki H, Ushio H, Harada Y, Takeichi N. Recurrent Laryngeal Nerve Anastomosis Following Thyroid Surgery. *World J Surg* (1982) 6:342–6. doi: 10.1007/BF01653553
10. Miyauchi A. *Surgical Techniques in Reconstruction of Injured RLN for Voice Rehabilitation*. Tokyo: Intermerc Co. (2001).
11. Miyauchi A, Masuoka H, Tomoda C, Takamura Y, Ito Y, Kobayashi K, et al. Laryngeal Approach to the Recurrent Laryngeal Nerve Involved by Thyroid Cancer at the Ligament of Berry. *Surgery* (2012) 152:57–60. doi: 10.1016/j.surg.2011.12.033
12. Crumley RL, Izdebski K. Vocal Quality Following Laryngeal Reinnervation by Ansa Hypoglossi Transfer. *Laryngoscope* (1986) 96:611–6. doi: 10.1288/00005537-198606000-00004

Conflict of Interest: The authors declare that the research was conducted in the absence of any commercial or financial relationships that could be construed as a potential conflict of interest.

frontiers | Frontiers in Endocrinology

ORIGINAL RESEARCH
published: 16 June 2022
doi: 10.3389/fendo.2022.856278

A Clinical Predictive Model of Central Lymph Node Metastases in Papillary Thyroid Carcinoma

Zipeng Wang[1†], Qungang Chang[1†], Hanyin Zhang[2], Gongbo Du[1], Shuo Li[1], Yihao Liu[1], Hanlin Sun[1] and Detao Yin[1,3,4]*

[1] Department of Thyroid Surgery, The First Affiliated Hospital of Zhengzhou University, Zhengzhou, China, [2] Department of Dermatology, First Affiliated Hospital of Zhengzhou University, Zhengzhou, China, [3] Engineering Research Center of Multidisciplinary Diagnosis and Treatment of Thyroid Cancer of Henan Province, Zhengzhou, China, [4] Key Medicine Laboratory of Thyroid Cancer of Henan Province, Zhengzhou, China

OPEN ACCESS

Edited by:
Terry Francis Davies, Icahn School of Medicine at Mount Sinai, United States

Reviewed by:
Carolina Ferraz, Santa Casa of Sao Paulo, Brazil
Dorina Ylli, MedStar Health Research Institute (MHRI), United States

***Correspondence:**
Detao Yin
detaoyin@zzu.edu.cn

[†]These authors have contributed equally to this work and share first authorship

Specialty section:
This article was submitted to Thyroid Endocrinology, a section of the journal Frontiers in Endocrinology

Received: *17 January 2022*
Accepted: *10 May 2022*
Published: *16 June 2022*

Citation:
Wang Z, Chang Q, Zhang H, Du G, Li S, Liu Y, Sun H and Yin D (2022) A Clinical Predictive Model of Central Lymph Node Metastases in Papillary Thyroid Carcinoma. Front. Endocrinol. 13:856278. doi: 10.3389/fendo.2022.856278

Background: Thyroid carcinoma is one of the most common endocrine tumors, and papillary thyroid carcinoma (PTC) is the most common pathological type. Current studies have reported that PTC has a strong propensity for central lymph node metastases (CLNMs). Whether to prophylactically dissect the central lymph nodes in PTC remains controversial. This study aimed to explore the risk factors and develop a predictive model of CLNM in PTC.

Methods: A total of 2,554 patients were enrolled in this study. The basic information, laboratory examination, characteristics of cervical ultrasound, genetic test, and pathological diagnosis were collected. The collected data were analyzed by univariate logistic analysis and multivariate logistic analysis. The risk factors were evaluated, and the predictive model was constructed of CLNM.

Results: The multivariate logistic analysis showed that Age ($p < 0.001$), Gender ($p < 0.001$), Multifocality ($p < 0.001$), *BRAF* ($p = 0.027$), and Tumor size ($p < 0.001$) were associated with CLNM. The receiver operating characteristic curve (ROC curve) showed high efficiency with an area under the ROC (AUC) of 0.781 in the training group. The calibration curve and the calibration of the model were evaluated. The decision curve analysis (DCA) for the nomogram showed that the nomogram can provide benefits in this study.

Conclusion: The predictive model of CLNM constructed and visualized based on the evaluated risk factors was confirmed to be a practical and convenient tool for clinicians to predict the CLNM in PTC.

Keywords: papillary thyroid carcinoma (PTC), predictive model, central lymph node metastasis (CLNM), nomogram, risk factors

INTRODUCTION

Thyroid carcinoma is one of the most popular endocrine tumors, and papillary thyroid carcinoma (PTC) is the most common pathological type (1, 2). The increased incidence of PTC is attributed to both the truly increased prevalence of thyroid diseases and the advances in imaging technology. Current studies have reported that PTC has a strong propensity for CLNM (3), and it is difficult to effectively detect central lymph node metastases (CLNMs) preoperatively (4–6). The most commonly involved central lymph nodes in thyroid carcinoma are the prelaryngeal (Delphian), pretracheal, and the right and left paratracheal nodes; the paratracheal nodes may be anterior as well as posterior to the recurrent laryngeal nerves (3). Whether to prophylactically dissect the central lymph nodes in PTC remains controversial (7). Dissection of the lymph nodes in the central region of the neck is considered necessary. Central lymph node dissection (CLND) is beneficial in eliminating macroscopic or microscopic metastatic sites. When CLNM is found in patients after surgery, a second operation is often necessary. Extra surgery not only is difficult but also increases the risk of complications (8). Prophylactic lymph node dissection of the central cervical facilitates accurate clinical staging (9). However, it has been argued that prophylactic dissection of the central lymph nodes is not necessary. Routine prophylactic CLND is considered uneconomical (10). Routine prophylactic central compartment dissection is particularly associated with temporary and permanent hypoparathyroidism and recurrent laryngeal nerve injury (4, 11, 12). Although numerous retrospective studies determined the benefits of prophylactic CLND by various investigators, the published results have been inconclusive. Due to the indolent nature of PTC, a very large sample size with extended follow-up for a randomized control trial examination is urgently needed. Therefore, preoperative access is of great clinical significance to accurately assess patients for CLNM. In this study, we analyzed the risk factors of CLNM and constructed a predictive model of CLNM to more accurately assess the risk of CLNM preoperatively and provide a practical and convenient tool for clinicians to predict the CLNM in PTC for clinical decision-making.

METHODS

Study Design

We screened all the patients who underwent thyroidectomy for PTC in Thyroid Surgery who were admitted to the First Affiliated Hospital of Zhengzhou University from January 2018 to October 2019. The inclusion criteria were as follows: 1) patients underwent thyroid surgery for the first time; 2) clinically and pathologically diagnosed as PTC. The exclusion criteria included the following: 1) other malignancies combined; 2) preoperative hyperthyroidism or hypothyroidism; 3) other diseases that cause swollen lymph nodes in the neck; 4) two or more thyroidectomies. A total of 2,554 patients including 982 patients with CLNMs (CLNM(+)), and 1,572 patients without CLNMs (CLNM(−)) were enrolled in this study. The enrollment flowchart of the participants is shown in **Figure 1**. The patients with CLNMs (CLNM(+)) and without CLNMs (CLNM(−)) were divided into the training group (n = 1,787) and the validation group (n = 767).

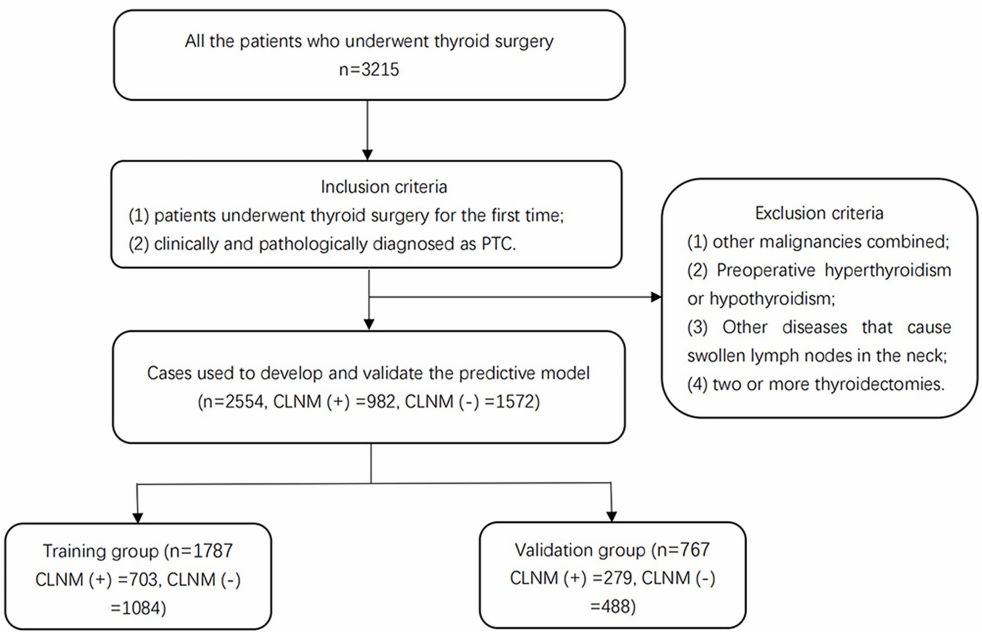

FIGURE 1 | Enrollment flowchart of participants used for model development and validation. PTC, papillary thyroid carcinoma; CLNM, central lymph node metastasis.

Data Collection

The basic information, laboratory examination, cervical ultrasound, genetic test, and pathological diagnosis were collected. The basic information included age and gender. The laboratory indices included free triiodothyronine (FT_3), free tetraiodothyronine (FT_4), thyroid-stimulating hormone (TSH), thyroid peroxidase antibodies (TPOAb), thyroglobulin antibodies (TgAb), and thyroglobulin (Tg). The characteristics of cervical ultrasound include multifocality and tumor size. Multifocality was defined as more than one lesion observed in cervical ultrasound and pathologically confirmed as PTC. Tumor size was the maximum diameter of the suspected nodule under ultrasound that was pathologically confirmed as PTC (8). All patients had a review of the cervical ultrasound with the same sonographer preoperatively. Genetic test results included *BRAF* and *TERT*. Pathological diagnosis included reports of the paraffin section of the primary lesion and central lymph node.

Statistical Analysis

Multivariate multiple imputations with chained equations were used to deal with a few missing data of several variables to decrease the bias (13). All the statistical analysis processes involved were completed by R software, version 4.1.1. p-Value <0.05 was considered statistically significant. The classification data were expressed as percentages, and means ± SD or medians (quartile 1, quartile 3) were described as continuous variables that satisfy or do not satisfy the normal distribution, respectively. The odds ratio (OR) values were calculated by univariate logistic regression of the variables. After the collinearity among variables was calculated and the colinear factors were eliminated, the potential variables with a p-value <0.05 were selected to perform the multivariate logistic regression. A clinical predictive model of CLNM in PTC was built based on the variables with statistical senses.

RESULTS

Baseline Characteristics of the Variables

The baseline characteristics of CLNM(+) and CLNM(−) are shown in **Table 1**. All the enrolled patients were randomly divided into the training group (n = 1,787) and the validation group (n = 767). There was no significant difference in the levels of these variables between the two groups (**Table 2**). Six potential predictors from 12 candidates were considered to have statistical significance ($p < 0.05$).

TABLE 1 | Baseline characteristics of enrolled patients.

Variables	CLNM (–) (n = 1,572)	CLNM (+) (n = 982)	p-Value
Age [years (IQR)]	47.000 (39.000, 54.000)	41.000 (32.000, 50.000)	<0.0001
Gender, n [male (%)]	269 (17.11)	285 (29.02)	<0.0001
FT_3 [pmol/L (IQR)]	4.910 (4.530, 5.320)	5.010 (4.630, 5.420)	<0.0001
FT_4 [pmol/L (IQR)]	11.185 (10.140, 12.322)	11.180 (10.162, 12.190)	0.6288
TSH [μIU/ml (IQR)]	2.530 (1.647, 3.720)	2.504 (1.640, 3.718)	0.3996
TPOAb [(+) (n (%)]	262 (16.67)	170 (17.31)	0.7123
TgAb [(+) (n (%)]	263 (16.73)	190 (19.35)	0.1027
Tg [ng/ml (SD)]	63.154 (404.596)	66.110 (290.648)	0.8422
BRAF [(+) (n (%)]	1,290 (82.06)	841 (85.64)	0.0207
TERT [(+) (n (%)]	4 (0.25)	1 (0.10)	0.6549
Multifocality [n (%)]	308 (19.59)	380 (38.70)	<0.0001
Tumor size (D ≥ 1 cm) (n, %)	382 (24.30)	600 (61.10)	<0.0001

CLNM, central lymph node metastasis; IQR, interquartile range; FT_3, free triiodothyronine; FT_4, free tetraiodothyronine; TSH, thyroid-stimulating hormone; TPOAb, thyroid peroxidase antibodies; TgAb, thyroglobulin antibodies; Tg, thyroglobulin.

TABLE 2 | Baseline characteristics showed there was no statistical difference between the training group and validation group.

Variables	Training group (n = 1,787)	Validation group (n = 767)	p-Value
Age [years (IQR)]	45.000 (36.000, 52.000)	45.000 (36.000, 52.000)	0.6943
Gender, n [male (%)]	392 (21.94)	162 (21.12)	0.685
FT_3 [pmol/L (IQR)]	4.950 (4.570, 5.350)	4.950 (4.580, 5.380)	0.8916
FT_4 [pmol/L (IQR)]	11.160 (10.090, 12.250)	11.260 (10.265, 12.295)	0.2107
TSH [μIU/ml (IQR)]	2.520 (1.660, 3.765)	2.508 (1.630, 3.620)	0.5867
TPOAb [(+) (n (%)]	318 (17.80)	114 (14.86)	0.0794
TgAb [(+) (n (%)]	322 (18.02)	131 (17.08)	0.6078
Tg [(ng/ml, (SD)]	16.100 (7.200, 33.690)	14.700 (6.380, 33.200)	0.2861
BRAF [(+) (n (%)]	1,503 (84.11)	628 (81.88)	0.183
TERT [(+) (n (%)]	4 (0.22)	1 (0.13)	1
Multifocality [n (%)]	482 (26.97)	206 (26.86)	0.991
Tumor size (D ≥ 1 cm) (n, %)	687 (38.44)	295 (38.46)	1

FT_3, free triiodothyronine; FT_4, free tetraiodothyronine; TSH, thyroid-stimulating hormone; TPOAb, thyroid peroxidase antibodies; TgAb, thyroglobulin antibodies; Tg, thyroglobulin.

Risk Factors and Predictive Model of Central Lymph Node Metastasis

Multivariate logistic analysis showed that Age (OR 0.947–0.966), Gender (OR 1.541–2.589), Multifocality (OR 2.348–3.815), *BRAF* (OR 1.044–1.926), and Tumor size (OR 4.127–6.416) were associated with CLNM (**Table 3**). The receiver operating characteristic curve (ROC curve) was drawn to evaluate the diagnostic effectiveness of the model (**Figure 2**). The ROC showed a high efficiency with an area under the ROC (AUC) of 0.781 (specificity 0.778, sensitivity 0.662, **Figure 2A**) in the training group. The effectiveness was verified in the validation group with an AUC of 0.736 (specificity 0.631, sensitivity 0.774), and the result is shown in **Figure 2B**. The model showed a great ability to distinguish the presence or absence of CLNM in the training group with a high value of AUC.

Then the model was evaluated by the calibration curve. The predicted values had good consistency in the training group (mean absolute error = 0.004) and the validation group (mean absolute error = 0.008) with the observed variables. The calibration curve showed that the model had a strong calibration ability (**Figure 3**).

To visualize the model, we plotted the nomogram of our predictive model based on the five variables: Age, Gender, Focal, *BRAF*, and Tumor size. Every variable was scored by drawing a straight line upward the "Points" line. The total points were the sum of the points obtained by the five variables. A straight line down to the axis named "CLNM risk" represents the risk of CLNM (**Figure 4**).

In the training group, we constructed a decision curve analysis (DCA) to identify the net benefit of the nomogram (**Figure 5**). The curve showed that when the threshold probability of patients is between 0.11 and 0.90, the nomogram can provide benefits.

DISCUSSION

PTC metastasis occurs most often in the central lymph nodes, with few distant metastases and low mortality, and the rate of

TABLE 3 | Potential risk factors identified by univariate and multivariate logistic regression analyses.

Variable	Univariable		Multivariable	
	OR (95% CI)	p	OR (95% CI)	p
Age (years)	0.960 (0.952–0.969)	<0.001	0.957 (0.947–0.966)	<0.001
Gender (male, %)	1.948 (1.554–2.445)	<0.001	1.996 (1.541–2.589)	<0.001
FT_3 (pmol/L)	1.364 (1.158–1.607)	<0.001		
FT_4 (pmol/L)	0.989 (0.935–1.045)	0.682		
TSH (μIU/ml)	0.990 (0.948–1.031)	0.633		
TPOAb(+) %	1.064 (0.830–1.361)	0.622		
TgAb(+) %	1.232 (0.964–1.572)	0.0935		
Tg (ng/ml)	1.000 (0.999–1.001)	0.349		
BRAF(+) %	1.327 (1.019–1.737)	0.0377	1.414 (1.044–1.926)	0.027
TERT(+) %	0.513 (0.025–4.018)	0.564		
Multifocality %	2.822 (2.278–3.500)	<0.001	2.989 (2.348–3.815)	<0.001
Tumor size (D ≥ 1 cm) %	5.299 (4.313–6.528)	<0.001	5.138 (4.127–6.416)	<0.001

FT_3, free triiodothyronine; FT_4, free tetraiodothyronine; TSH, thyroid-stimulating hormone; TPOAb, thyroid peroxidase antibodies; TgAb, thyroglobulin antibodies; Tg, thyroglobulin.

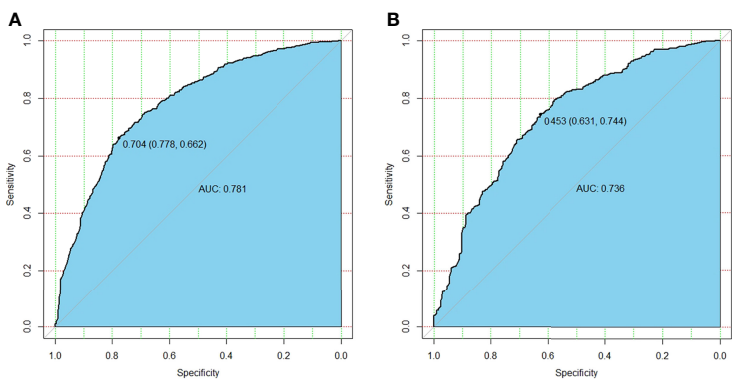

FIGURE 2 | The differential capability of the nomogram. **(A)** ROC curve based on the potential risk factors identified by multivariate logistic regression analysis showed great ability to distinguish the presence or absence of CLNM in the training group with a high value of AUC. **(B)** ROC curve based on the potential risk factors identified by multivariate logistic regression analysis showed great ability to distinguish the presence or absence of CLNM in the validation group. ROC, receiver operating characteristic; CLNM, central lymph node metastasis; AUC, area under the curve.

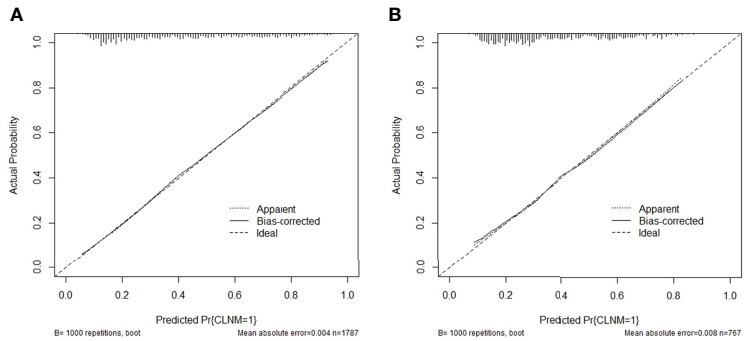

FIGURE 3 | Calibration curve of the predictive nomogram in the **(A)** training group or **(B)** validation group.

cervical lymph node metastasis detection by ultrasound is unsatisfactory, especially for CLNM (5, 14). Information gathered by prospective and randomized clinical studies is the key to determining whether prophylactic dissection of the central lymph nodes in PTC is necessary, but it is probably unavailable currently. Therefore, identification of patients with PTC preoperatively at greater risk of CLNM would be valuable. Prediction models and risk factors analysis based on clinical data have been developed increasingly in a wide variety of diseases in recent years.

To solve these problems, in this study, we collected and analyzed the risk factors and constructed a predictive model of CLNM. The model also showed a high calibration capacity. To the best of our knowledge, it is the first study aiming to construct and visualize a predictive model of CLNM. It is a predictive model that can help clinicians make appropriate treatments and help clinicians assess whether patients need CLND in PTC.

Some studies suggested that CLNM is significantly correlated with age (15, 16), which was similar to our study. Patients with younger age were more likely to be considered at a higher risk of CLNM.

Recent studies have shown that estrogen is a powerful stimulant for benign and malignant thyroid nodules. This explains why thyroid cancer is highly prevalent in women (17). However, in this study, there was a higher rate of CLNM in men. Some scholars confirmed that there were different subtypes of

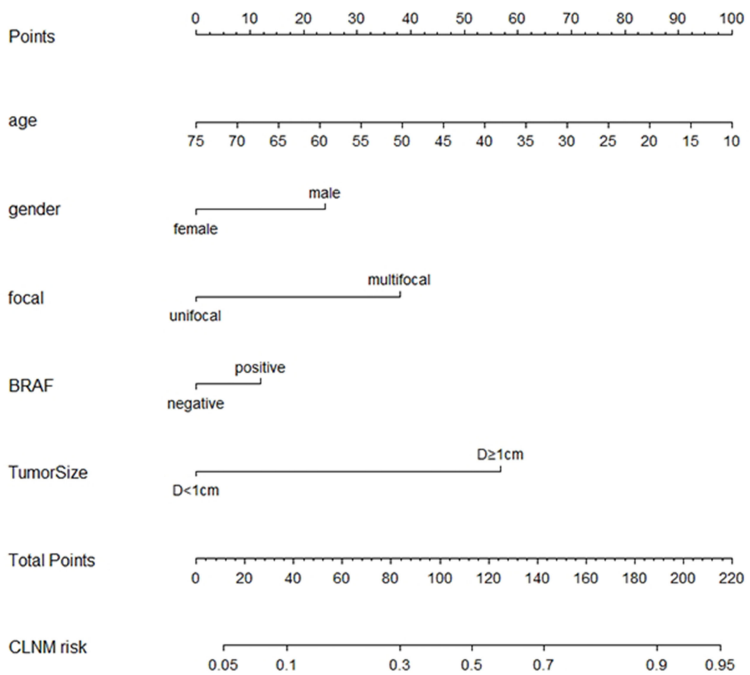

FIGURE 4 | Nomogram based on the five variables including Age, Gender, Focal, BRAF, and Tumor size.

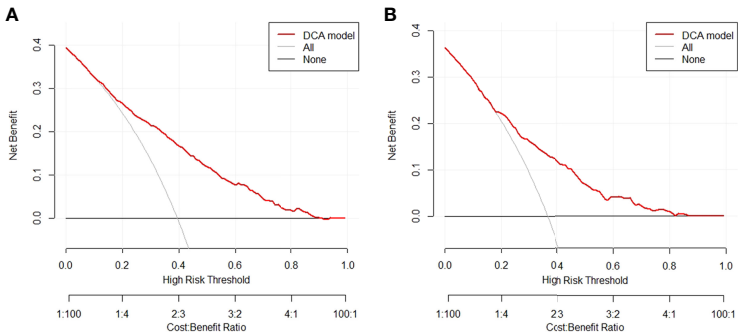

FIGURE 5 | Decision curve for the nomogram predicting CLNM in **(A)** training group or **(B)** validation group. CLNM, central lymph node metastasis.

estrogen receptors (ERs) that were considered a protective factor in PTC (17). This may be a potential cause of a higher rate of CLNM in male patients. The detailed knowledge of this regulation in thyroid cancer is still being debated.

Studies have shown that the risk of CLNM increases with the number of foci (11). The multifocal disease was defined as the presence of 2 or more foci of PTC, and each focus was recorded separately. In this study, CLNM rates were high in multifocal PTC with an OR of 2.989 (95% CI 2.348–3.815). With the application of high-resolution ultrasound, the preoperative diagnostic technology of PTC has made a huge breakthrough (18). Therefore, multifocality should be taken seriously during the preoperative ultrasound. When the cervical ultrasound showed that the suspicious lesions have significant multifocality, lobectomy and prophylactic CLNM should be considered.

BRAF genetic test was valuable for the diagnosis, prognosis, and therapy of PTC (19). In addition, some scholars revealed that *BRAF* mutations were associated with markers of clinical aggressiveness such as larger tumors, lymph node metastases, and poor clinical outcomes (20). In general, *BRAF* genetic test had strong practicability. Genetic testing in preoperative fine-needle aspiration biopsy (FNAB) was helpful to confirm the diagnosis, patients with a positive result for *BRAF* genetic test should be further evaluated, and there were stronger recommendations for prophylactic CLND.

Tumor size is an important risk factor for CLNM in PTC in the present study. This finding was similar to other studies that the risk of CLNM in PTC increases with tumor size (21, 22). In clinical practice, suspicious nodules larger than 10 mm should be managed with caution. Clinicians need to evaluate the patient's cervical lymph nodes to decide whether to perform prophylactic dissection of the lymph nodes. Our research, especially the nomogram, provides a good reference for clinicians.

In the univariate logistic regression model, the titer of FT_3 was statistically significant between the two groups. We searched the relevant literature and found that there is no clear relationship between thyroid hormone and CLNM of PTC. However, one scholar's research results caught our attention; this study showed a high correlation between PTC microcalcification and thyroid hormones (23). Microcalcification of thyroid nodules indicates that it was more likely to be malignant (24). Therefore, the titer of thyroid hormone may be related to the pathology of thyroid nodules, but it cannot be considered a risk factor for CLNM.

Some scholars have reached similar conclusions (25, 26); younger age, male sex, multifocality, and larger tumor size are the risk factors for cervical lymph node metastases in PTC. The predictive model was also constructed and visualized with a nomogram. However, our study aimed at risk factor analysis and predictive model construction for CLNM with a high AUC. In addition, not only the clinical baseline characteristics but also the genetic test result was included in this study. This was more instructive for patients with preoperative FNAB and *BRAF* genetic test.

The decision curve and nomogram in this study show the great utility of our model, and the 5 items in the nomogram are routine clinical variables that can easily be obtained by clinicians, indicating that it may be beneficial for clinicians to assess the need for prophylactic CLND. Our study has a large sample size of 2,554 patients and has excellent diagnostic effectiveness of CLNM with an AUC of 0.781 in the training group. The operation of the model is simple and fast, which can provide a reference for timely prophylactic CLND.

However, there are also several limitations in our study. First, all the enrolled patients came from the same hospital without external validation. Moreover, we still need to expand the sample size to reduce the heterogeneity. In addition, our predictive model is only suitable for PTC; there is still a lack of predictive ability of our model for other types of thyroid carcinoma.

DATA AVAILABILITY STATEMENT

The raw data supporting the conclusions of this article will be made available by the authors, without undue reservation.

ETHICS STATEMENT

The studies involving human participants were reviewed and approved by The First Affiliated Hospital of Zhengzhou

University Ethics Review Committee. Written informed consent for participation was not required for this study in accordance with the national legislation and the institutional requirements.

AUTHOR CONTRIBUTIONS

DY conceived of the idea and provided guidance. ZW wrote the manuscript and completed the figures. QC and HZ contributed to organizing the database. SL, YL, and HS carefully reviewed the manuscript. GD made critical revisions to the manuscript. All authors contributed to the article and approved the submitted version.

FUNDING

This study was also funded by the Key Medical Science and Technology Project of Henan Province (SBGJ202101014), which is also from the corresponding author DY, should be placed before funding Major Scientific Research Projects of Traditional Chinese Medicine in Henan Province (No. 20-21ZYZD14).

ACKNOWLEDGMENTS

We acknowledge Qungang Chang for the data collection.

REFERENCES

1. Xu S, Huang H, Qian J, Liu Y, Huang Y, Wang X, et al. Prevalence of Hashimoto Thyroiditis in Adults With Papillary Thyroid Cancer and Its Association With Cancer Recurrence and Outcomes. *JAMA Netw Open* (2021) 4(7):e2118526. doi: 10.1001/jamanetworkopen.2021.18526
2. Yasuhiro Ito MK, Takamura Y, Kobayashi K, Miya A, Miyauchi A. Prognosis and Prognostic Factors of Patients With Papillary Thyroid Carcinoma Requiring Resection of Recurrent Laryngeal Nerve Due to Carcinoma Extension. *Endocrine J* (2012) 59(3):247–52. doi: 10.1507/endocrj.ej11-0355
3. Carty SE, Doherty GM, Duh Q-Y, Kloos RT, Mandel SJ, Randolph GW, et al. Consensus Statement on the Terminology and Classification of Central Neck Dissection for Thyroid Cancer. *Thyroid* (2009) 11:2009. doi: 10.1089/thy.2009.0159
4. Sturgeon C, Yang A, Elaraj D. Surgical Management of Lymph Node Compartments in Papillary Thyroid Cancer. *Surg Oncol Clin N Am* (2016) 25(1):17–40. doi: 10.1016/j.soc.2015.08.013
5. Kim KE, Kim EK, Yoon JH, Han KH, Moon HJ, Kwak JY. Preoperative Prediction of Central Lymph Node Metastasis in Thyroid Papillary Microcarcinoma Using Clinicopathologic and Sonographic Features. *World J Surg* (2013) 37(2):385–91. doi: 10.1007/s00268-012-1826-3
6. Mazzaferri ELMD, Doherty GM, Steward DL. The Pros and Cons of Prophylactic Central Compartment Lymph Node Dissection for Papillary Thyroid Carcinoma. *Thyroid* (2009) 19(7) 2009. doi: 10.1089/thy.2009.1578
7. Fritze D, Doherty GM. Surgical Management of Cervical Lymph Nodes in Differentiated Thyroid Cancer. *Otolaryngol Clin North Am* (2010) 43(2):285–300. doi: 10.1016/j.otc.2010.01.005
8. Guang Y, He W, Zhang W, Zhang H, Zhang Y, Wan F. Clinical Study of Ultrasonographic Risk Factors for Central Lymph Node Metastasis of Papillary Thyroid Carcinoma. *Front Endocrinol (Lausanne)* (2021) 12:791970. doi: 10.3389/fendo.2021.791970
9. Hughes DT, White ML, Miller BS, Gauger PG, Burney RE, Doherty GM. Influence of Prophylactic Central Lymph Node Dissection on Postoperative Thyroglobulin Levels and Radioiodine Treatment in Papillary Thyroid Cancer. *Surgery* (2010) 148(6):1100–6; discussion 006-7. doi: 10.1016/j.surg.2010.09.019
10. Garcia A, Palmer BJ, Parks NA, Liu TH. Routine Prophylactic Central Neck Dissection for Low-Risk Papillary Thyroid Cancer Is Not Cost-Effective. *Clin Endocrinol (Oxf)* (2014) 81(5):754–61. doi: 10.1111/cen.12506
11. Al Afif A, Williams BA, Rigby MH, Bullock MJ, Taylor SM, Trites J, et al. Multifocal Papillary Thyroid Cancer Increases the Risk of Central Lymph Node Metastasis. *Thyroid* (2015) 25(9):1008–12. doi: 10.1089/thy.2015.0130
12. Sancho JJ, Lennard TW, Paunovic I, Triponez F, Sitges-Serra A. Prophylactic Central Neck Disection in Papillary Thyroid Cancer: A Consensus Report of the European Society of Endocrine Surgeons (ESES). *Langenbecks Arch Surg* (2014) 399(2):155–63. doi: 10.1007/s00423-013-1152-8
13. Buuren SG-O. Mice: Multivariate Imputation by Chained Equations in R. *J Stat Software* (2011) 45(3):1–67. doi: 10.18637/jss.v045.i03
14. Zhao W, He L, Zhu J, Su A. A Nomogram Model Based on the Preoperative Clinical Characteristics of Papillary Thyroid Carcinoma With Hashimoto's Thyroiditis to Predict Central Lymph Node Metastasis. *Clin Endocrinol (Oxf)* (2021) 94(2):310–21. doi: 10.1111/cen.14302
15. Ito Y, Miyauchi A, Kihara M, Higashiyama T, Kobayashi K, Miya A. Patient Age is Significantly Related to the Progression of Papillary Microcarcinoma of the Thyroid Under Observation. *Thyroid* (2014) 24(1):27–34. doi: 10.1089/thy.2013.0367
16. Zheng X, Peng C, Gao M, Zhi J, Hou X, Zhao J, et al. Risk Factors for Cervical Lymph Node Metastasis in Papillary Thyroid Microcarcinoma: A Study of 1,587 Patients. *Cancer Biol Med* (2019) 16(1):121–30. doi: 10.20892/j.issn.2095-3941.2018.0125
17. Derwahl M, Nicula D. Estrogen and Its Role in Thyroid Cancer. *Endocr Relat Cancer* (2014),21(15) T273–83. doi: 10.1530/ERC-14-0053
18. Khokhar MT, Day KM, Sangal RB, Ahmedli NN, Pisharodi LR, Beland MD, et al. Preoperative High-Resolution Ultrasound for the Assessment of Malignant Central Compartment Lymph Nodes in Papillary Thyroid Cancer. *Thyroid* (2015) 25(12):1351–4. doi: 10.1089/thy.2015.0176
19. Chen H, Song A, Wang Y, He Y, Tong J, Di J, et al. BRAF(V600E) Mutation Test on Fine-Needle Aspiration Specimens of Thyroid Nodules: Clinical Correlations for 4600 Patients. *Cancer Med* (2021) 11(1):40–9. doi: 10.1002/cam4.4419
20. Melo M, Gaspar da Rocha A, Batista R, Vinagre J, Martins MJ, Costa G, et al. TERT, BRAF, and NRAS in Primary Thyroid Cancer and Metastatic Disease. *J Clin Endocrinol Metab* (2017) 102(6):1898–907. doi: 10.1210/jc.2016-2785
21. Machens A, Holzhausen HJ, Dralle H. The Prognostic Value of Primary Tumor Size in Papillary and Follicular Thyroid Carcinoma. *Cancer* (2005) 103 (11):2269–73. doi: 10.1002/cncr.21055
22. Machens A, Hinze R, Thomusch O, Dralle H. Pattern of Nodal Metastasis for Primary and Reoperative Thyroid Cancer. *World J Surg* (2002) 26(1):22–8. doi: 10.1007/s00268-001-0176-3
23. Ha J, Lee J, Jo K, Han JS, Kim MH, Jung CK, et al. Calcification Patterns in Papillary Thyroid Carcinoma Are Associated With Changes in Thyroid Hormones and Coronary Artery Calcification. *J Clin Med* (2018) 7(8):183. doi: 10.3390/jcm7080183
24. Bu Kyung Kim YSC, Kwon HJ, Lee JS, Heo JJ, Han YJ, Park Y-H, et al. Relationship Between Patterns of Calcification in Thyroid Nodules and Histopathologic Findings. *Endocrine J* (2012) 60(2):150–60. doi: 10.1507/endocrj.ej12-0294
25. Feng Y, Min Y, Chen H, Xiang K, Wang X, Yin G. Construction and Validation of a Nomogram for Predicting Cervical Lymph Node Metastasis in Classic Papillary Thyroid Carcinoma. *J Endocrinol Invest* (2021) 44 (10):2203–11. doi: 10.1007/s40618-021-01524-5
26. Tian X, Song Q, Xie F, Ren L, Zhang Y, Tang J, et al. Papillary Thyroid Carcinoma: An Ultrasound-Based Nomogram Improves the Prediction of Lymph Node Metastases in the Central Compartment. *Eur Radiol* (2020) 30 (11):5881–93. doi: 10.1007/s00330-020-06906-6

Conflict of Interest: The authors declare that the research was conducted in the absence of any commercial or financial relationships that could be construed as a potential conflict of interest.

this article, or claim that may be made by its manufacturer, is not guaranteed or endorsed by the publisher.

frontiers | Frontiers in Endocrinology

ORIGINAL RESEARCH
published: 22 June 2022
doi: 10.3389/fendo.2022.924731

Safety Parameters of Quantum Molecular Resonance Devices During Thyroid Surgery: Porcine Model Using Continuous Neuromonitoring

Hsin-Yi Tseng[1], Tzu-Yen Huang[1], Yi-Chu Lin[1], Jia Joanna Wang[1,2], How-Yun Ko[1], Cheng-Hsun Chuang[1], I-Cheng Lu[3], Pi-Ying Chang[4], Gregory W. Randolph[5], Gianlorenzo Dionigi[6,7], Ning-Chia Chang[1,2] and Che-Wei Wu[1]*

[1] Department of Otorhinolaryngology-Head and Neck Surgery, International Thyroid Surgery Center, Kaohsiung Medical University Hospital, Kaohsiung Medical University, Kaohsiung, Taiwan, [2] Department of Otorhinolaryngology-Head and Neck Surgery, Kaohsiung Municipal Siaogang Hospital, Faculty of Medicine, College of Medicine, Kaohsiung Medical University, Kaohsiung, Taiwan, [3] Department of Anesthesiology, Kaohsiung Municipal Siaogang Hospital, Kaohsiung Medical University Hospital, Faculty of Medicine, College of Medicine, Kaohsiung Medical University, Kaohsiung, Taiwan, [4] Department of Anesthesiology, Kaohsiung Municipal Tatung Hospital, Kaohsiung Medical University Hospital, Faculty of Medicine, College of Medicine, Kaohsiung Medical University, Kaohsiung, Taiwan, [5] Division of Thyroid and Parathyroid Endocrine Surgery, Department of Otolaryngology—Head and Neck Surgery, Massachusetts Eye and Ear Infirmary, Harvard Medical School, Boston, MA, United States, [6] Division of General Surgery, Endocrine Surgery Section, Istituto Auxologico Italiano (IRCCS), Milan, Italy, [7] Department of Pathophysiology and Transplantation, Faculty of Medicine and Surgery, University of Milan, Milan, Italy

OPEN ACCESS

Edited by:
Terry Francis Davies, Icahn School of Medicine at Mount Sinai, United States

Reviewed by:
Pietro Giorgio Calo', University of Cagliari, Italy
Sung-Chan Shin, Pusan National University, South Korea

***Correspondence:**
Ning-Chia Chang
ncchang1972@gmail.com

Specialty section:
This article was submitted to Thyroid Endocrinology, a section of the journal Frontiers in Endocrinology

Received: *20 April 2022*
Accepted: *18 May 2022*
Published: *22 June 2022*

Citation:
Tseng H-Y, Huang T-Y, Lin Y-C, Wang JJ, Ko H-Y, Chuang C-H, Lu I-C, Chang P-Y, Randolph GW, Dionigi G, Chang N-C and Wu C-W (2022) Safety Parameters of Quantum Molecular Resonance Devices During Thyroid Surgery: Porcine Model Using Continuous Neuromonitoring. Front. Endocrinol. 13:924731. doi: 10.3389/fendo.2022.924731

Objectives: Quantum molecular resonance (QMR) devices have been applied as energy-based devices in many head and neck surgeries; however, research on their use in thyroid surgery is lacking. This study aimed to investigate the safety parameters of QMR devices during thyroidectomy when dissection was adjacent to the recurrent laryngeal nerve (RLN).

Methods: This study included eight piglets with 16 RLNs, and real-time electromyography (EMG) signals were obtained from continuous intraoperative neuromonitoring (C-IONM). QMR bipolar scissor (BS) and monopolar unit (MU) were tested for safety parameters. In the activation study, QMR devices were activated at varying distances from the RLN. In the cooling study, QMR devices were cooled for varying time intervals, with or without muscle touch maneuver (MTM) before contacting with the RLN.

Results: In the activation study, no adverse EMG change occurred when QMR BS and MU were activated at distances of 2 mm or longer from the RLNs. In the cooling study, no adverse EMG change occurred when QMR BS and MU were cooled in 2-second intervals or immediately after MTM.

Conclusion: QMR devices should be carefully used when performing RLN dissection during thyroid surgery. According to the activation and cooling safety parameters in this study, surgeons can avoid RLN injury by following standard procedures when using QMR devices.

Keywords: thyroid surgery, intraoperative neuromonitoring (IONM), recurrent laryngeal nerve (RLN), quantum molecular resonance (QMR) devices, porcine model safety parameters

INTRODUCTION

Hemostasis of the blood-rich thyroid gland is an important issue during thyroid surgery, and postoperative hematoma is a life-threatening complication that should be avoided as much as possible (1). As an equipment to assist hemostasis, many energy-based devices (EBDs) have been developed in the past 30 years and are widely used in thyroid surgery (2). High temperatures are unavoidable when using EBDs, and direct or indirect thermal energy can transfer to the recurrent laryngeal nerve (RLN) and result in thermal injury (3–5). RLN thermal injury causes more irreversible impairment of vocal cord movement than RLN mechanical injury, resulting in more voice disturbance (6, 7).

The quantum molecular resonance (QMR) device is an innovative EBD that has been safely and effectively applied in otolaryngology-head and neck surgeries such as phonomicrosurgery (8), tonsillectomy (9–11), oral surgery (12), and adenoidectomy (13). QMR devices are powered using electron energy quanta, which is generated by alternate current and high-frequency electron waves, and it is characterized by a well-defined dominant wave at 4 MHz, followed by waves at 8, 12 and 16 MHz with reduced amplitude (13, 14). As the electron energy quanta is delivered, cell molecular bonds in human tissue resonate, followed by subsequent bond breakage and a minimal temperature increase (13–16). The hemostasis of the QMR device is completed by triggering the denaturation of the protein fibrinogen to coagulate after breaking cell molecular bindings. The process also activates the physiological coagulation cascade without the need for necrotic plugs, which is contrary to methods that use other cauterization methods (13, 14). Vesalius Quantum (Telea Engineering, Vicenza, Italy) is a popular QMR system and was adopted in the current study. Two surgical instruments were most commonly used in head and neck surgery, including the QMR bipolar scissor (BS) and the QMR monopolar unit (MU). Details about Vesalius Quantum can be found at https://teleamedical.com/en/vesalius-quantum).

QMR devices have been applied as energy-based devices in many head and neck surgeries; however, research on their use in thyroid surgery and dissection adjacent to the recurrent laryngeal nerve (RLN) is lacking. The purpose of this study was to investigate real-time electromyographic (EMG) data for the RLN to define safety parameters for using a QMR device in thyroidectomy. For this purpose, we recorded the dynamic laryngeal EMG signals under continuous intraoperative neuromonitoring (C-IONM), when the QMR device was activated at various distances from the RLN in the activation study, and when the QMR device was cooled after activation for various durations with or without a muscle touch maneuver (MTM) in the cooling study.

MATERIALS AND METHODS

Animal Preparation and Anesthesia

This prospective porcine experimental study was performed by the IONM research team at Kaohsiung Medical University, Taiwan, which has a well-established C-IONM protocol for RLN research. The animal-use protocols comply with national/international regulations. Guidelines for animal experiments, including principles of replacement, reduction, and refinement, were strictly followed. This experimental study was also approved by the Institutional Animal Care and Use Committee of Kaohsiung Medical University, Taiwan (IACUC Approval No. 110129).

Anesthesia was initiated by intramuscular administration of 2 mg/kg tiletamine/zolazepam 30 minutes before the experiment. No muscle relaxants were used during anesthesia to avoid neuromuscular blockade, which could interfere with EMG signals during neuromonitoring. Endotracheal tube surface electrodes were used to record EMG signals. After the piglets were intubated, the tidal volume was set at 8–12 mL/kg, and the respiratory rate was set at 15 to 20 breaths per minute. General anesthesia was maintained with 1% to 2% sevoflurane.

IONM Equipment Setting and Operation

All piglets were placed in the supine position and intubated with a nerve integrity monitor size #6 EMG endotracheal tube (NIM Trivantage Tube, Medtronic, Jacksonville, Florida, USA). The EMG endotracheal tube as the recording electrode was applied to the piglets in the same conventional manner that it is applied to humans. The C-IONM monitoring system was performed by the Nerve Integrity Monitoring system (NIM 3.0, Medtronic, Jacksonville, Florida, USA) (**Figure 1A**). The automatic periodic stimulation (APS) as the stimulation electrode was placed on the vagus nerve (VN) (**Figure 1B**), and the nerve was stimulated continuously at 1 mA every second. The dynamic EMG signal changes during RLN injury were recorded efficiently and in real time.

The animal operation procedure began with a long transverse cervical incision, and the subcutaneous tissue and muscles were retracted away from the midline. The lateral border of the sternocleidomastoid (SCM) muscle was dissected and retracted medially. The thyroid gland, VNs, and RLNs were adequately exposed (**Figure 1B**). Next, RLNs were dissected and freed from

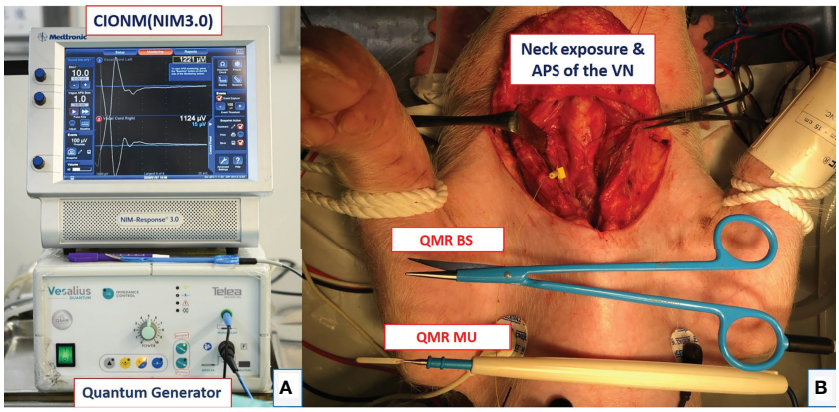

FIGURE 1 | Equipment setting and animal setting. **(A)** Setup of the continuous intraoperative neuromonitoring (C-IONM) system with the Nerve Integrity Monitor (NIM 3.0) system and Quantum generator system (MX 90, Telea Engineering, Vicenza, Italy). **(B)** Neck wound exposure with automated periodic stimulation (APS) placed on the vagus nerve (VN). The quantum molecular resonance (QMR) bipolar scissor (BS) and monopolar unit (MU) are shown.

fascia and kept dry for further experimental procedures. The APS was also set up at the fifth tracheal ring level with optimal stability. The amplitude and latency of the evoked response from VNs were calibrated to baseline values. Adverse EMG changes were defined as a 50% decrease in amplitude or a 10% increase in latency. Loss of signal (LOS) was defined as the amplitude of the RLN signal decreasing to less than 100 μV.

Study Design

There are two studies in this experiment. The activation study determined the distance from the RLN at which the QMR devices could be safely activated. The cooling study determined the time intervals and procedures required to cool the QMR devices before further use for hemostasis and dissection near the RLN. **Figure 1A** shows the QMR Generator system (MX 90, Telea Engineering, Vicenza, Italy), and the power was set at 5 in this study. The QMR BS and MU instruments are shown in **Figure 1B**.

Activation Study

Figures 2A, 2B, **3A, 3B** describe the designs of the QMR BS and QMR MU activation studies, respectively. Both devices were applied to soft tissue in a single activation for 3 seconds. The QMR device activations began with a distance of 5 mm from the RLN. If there was no adverse EMG event (e.g., significant adverse decrease in amplitude or increase in latency) after 3 repetitions,

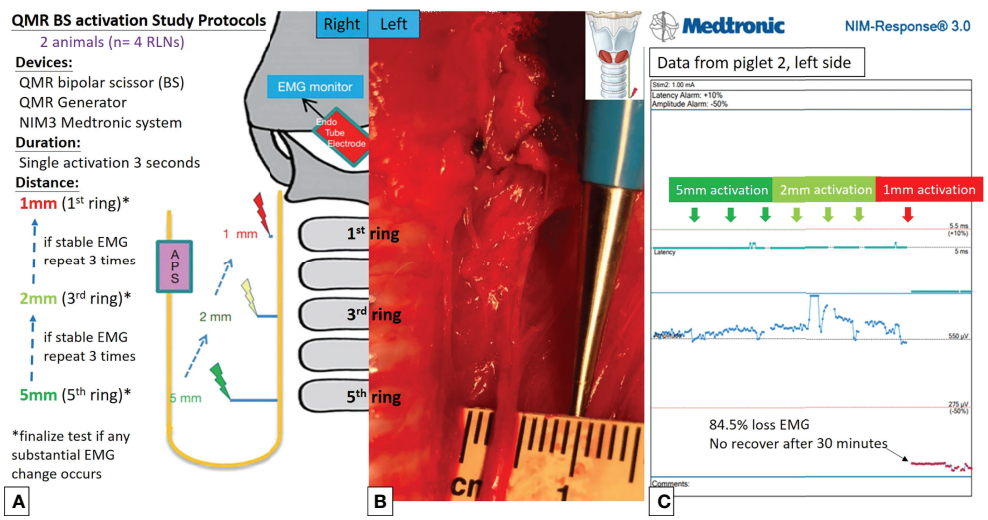

FIGURE 2 | QMR BS activation study protocols. **(A)** Flowcharts of the QMR BS activation study. **(B)** QMR BS was tested at a distance of 5 mm from the left RLN. **(C)** EMG recording of the left side RLN in Piglet 2 under C-IONM. The QMR BS was activated at distances of 5, 2, and 1 mm. After activation at 1 mm, the EMG showed sudden 84.5% EMG signal loss without recovery after 30 minutes of observation.

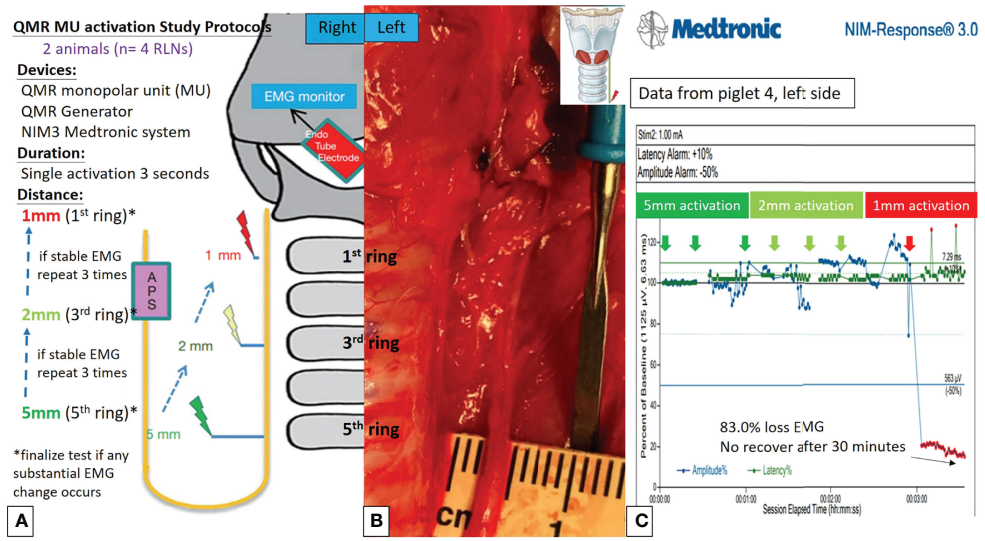

FIGURE 3 | QMR MU activation study protocols. **(A)** Flowcharts of the QMR MU activation study. **(B)** QMR MU was tested at a distance of 5 mm from the left RLN. **(C)** EMG recording of the left side RLN in Piglet 4 under C-IONM. The QMR MU was activated at distances of 5, 2, and 1 mm. After activation at 1 mm, the EMG showed a sudden 83.0% EMG signal loss without recovery after 30 minutes of observation.

the distance was progressively decreased to 2 mm (3 repetitions) and then to 1 mm (3 repetitions). Real-time EMG information under C-IONM was continuously recorded during each QMR device activation. If an adverse EMG event occurred, the RLN was interpreted as injured, and the procedure ended. Dynamic EMG changes were continuously recorded for at least 30 minutes to observe any recovery of the electrophysiological response.

Cooling Study

Figures 4A, 4B, **5A, 5B** describe the designs of the QMR BS and QMR MU cooling studies, respectively. The QMR device was applied to the SCM muscle in a single activation of 5 seconds followed by cooling for 5 seconds at room temperature. The blade of the QMR MU or the open blade of the QMR BS was then touched to the RLN for 3 seconds. If there was no

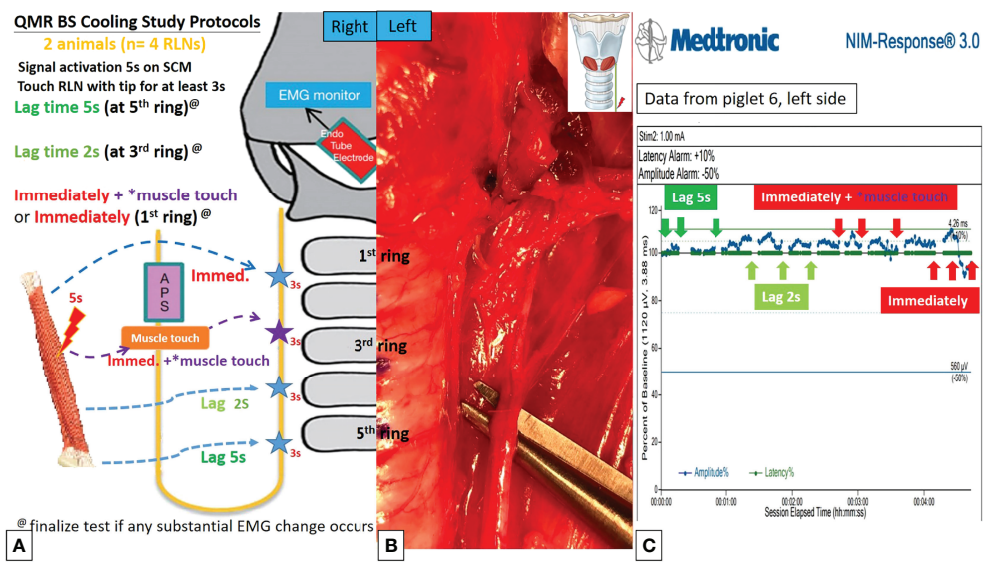

FIGURE 4 | QMR BS cooling study protocols. **(A)** Flowchart of the QMR BS cooling study. **(B)** The open blade of QMR BS touched the left RLN. **(C)** EMG recording of the left side RLN in Piglet 6 under C-IONM. After a single activation on sternocleidomastoid (SCM) muscle, the cooling study was performed with 5 seconds, 2 seconds, immediately without muscle touch maneuver (MTM), and immediately with MTM. The EMG results showed no adverse effects. The EMG signal remained stable in repeated tests.

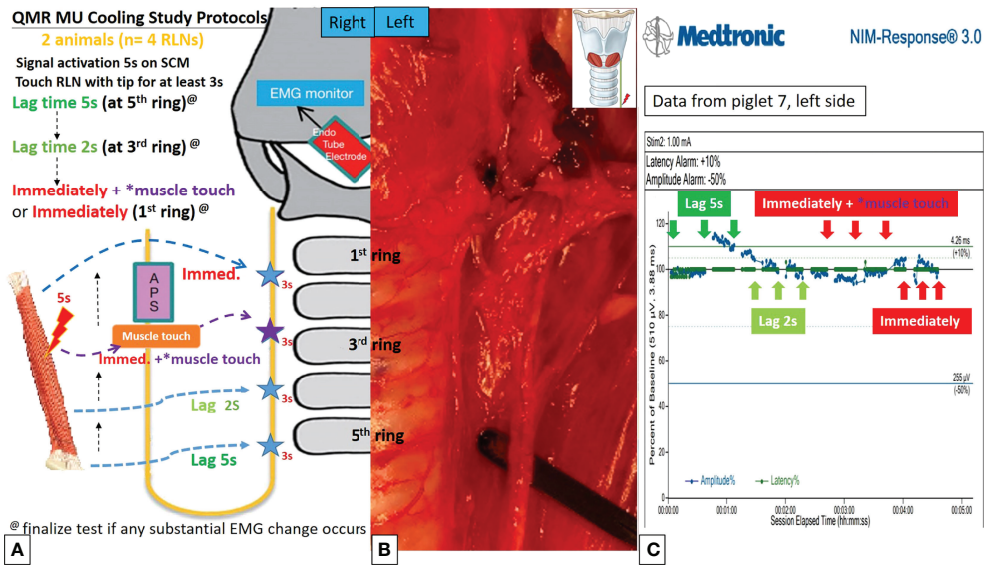

FIGURE 5 | QMR MU cooling study protocols. **(A)** Flowchart of the QMR MU cooling study. **(B)** The blade of the QMR MU touched the left RLN. **(C)** EMG recording of the left side RLN in Piglet 7 under C-IONM. After a single activation of the SCM muscle, the cooling study was performed for 5 seconds, 2 seconds, immediately without MTM, and immediately with MTM. The EMG results showed no adverse effects. The EMG signal remained stable in repeated tests.

adverse EMG event after 3 repetitions, the cooling time was decreased to 2 seconds, then immediately with "muscle touch maneuver (MTM)", and then immediately without MTM. MTM means that after a single activation of the SCM muscle and before contact with the RLN, the operator quickly contacts the QMR device (blade of QMR MU and open blade of QMR BS) with the ipsilateral strap muscle to achieve a contact cooling effect. Real-time EMG information under C-IONM was continuously recorded during the cooling procedure of each QMR device. If an adverse EMG event occurred, the RLN was interpreted as injured, and the procedure ended. Dynamic EMG changes were continuously recorded for at least 30 minutes to observe any recovery of the electrophysiological response.

RESULTS

The animal anesthesia, surgical approach, and C-IONM of the RLNs were successfully performed in all studies.

Activation Study

Activation study was performed in 8 RLNs of 4 piglets (animal No. 1-4). No adverse EMG events (amplitude decrease or latency increase) were observed when the QMR BS and QMR MU were activated at distances of 5 and 2 mm. With the QMR BS activated at a distance of 1 mm, all RLNs showed a signal decrease (63.0%, 60.0%, 84.5% loss and LOS) after a 30-minute observation (**Table 1**). The left RLN in piglet 2 showed 84.5% loss without recovery (**Figure 2C**). With the QMR MU activated at a distance of 1 mm, 3 of 4 RLNs showed a signal decrease (83.0% loss and 2 LOS) after a 30-minute observation (**Table 1**). The left RLN in piglet 4 showed 83.0% loss without recovery (**Figure 3C**).

Cooling Study

Cooling study was performed in 8 RLNs of 4 piglets (animal No. 5-8). In the QMR BS cooling study, no adverse EMG events were noted at any cooling time (5 seconds, 2 seconds, immediately with MTM, and immediately without MTM) (**Table 2**). The left RLN in piglet 6 showed a stable EMG signal without amplitude decrease or latency increase (**Figure 4C**).

TABLE 1 | Activation study: real-time EMG changes after QMR BS and QMR MU activation at varying distances to the RLN.

Animal No.	Side	5mm, amplitude [times]	2mm, amplitude [times]	1mm, amplitude [times]
1 (QMR BS)	Left	Stable [3]	Stable [3]	63.0% loss [1]
	Right	Stable [3]	Stable [3]	60.0% loss [1]
2 (QMR BS)	Left	Stable [3]	Stable [3]	84.5% loss [1]
	Right	Stable [3]	Stable [3]	LOS [1]
3 (QMR MU)	Left	Stable [3]	Stable [3]	Stable [3]
	Right	Stable [3]	Stable [3]	LOS [1]
4 (QMR MU)	Left	Stable [3]	Stable [3]	83.0% loss [1]
	Right	Stable [3]	Stable [3]	LOS [1]

EMG, electromyographic; QMR, Quantum molecular resonance; BS, bipolar scissor; MU, monopolar unit; RLN, recurrent laryngeal nerve; LOS, loss of signal.

TABLE 2 | Cooling study: real-time EMG changes after QMR BS and QMR MU activation and varying cooling time.

Animal No.	Side	5 seconds, amplitude [times]	2 seconds, amplitude [times]	Immediately with MTM, amplitude [times]	Immediately without MTM, amplitude [times]
5 (QMR BS)	Left	Stable [3]	Stable [3]	Stable [3]	Stable [3]
	Right	Stable [3]	Stable [3]	Stable [3]	Stable [3]
6 (QMR BS)	Left	Stable [3]	Stable [3]	Stable [3]	Stable [3]
	Right	Stable [3]	Stable [3]	Stable [3]	Stable [3]
7 (QMR MU)	Left	Stable [3]	Stable [3]	Stable [3]	Stable [3]
	Right	Stable [3]	Stable [3]	Stable [3]	LOS [1]
8 (QMR MU)	Left	Stable [3]	Stable [3]	Stable [3]	Stable [3]
	Right	Stable [3]	Stable [3]	Stable [3]	LOS [1]

EMG, electromyographic; QMR, Quantum molecular resonance; BS, bipolar scissor; MU, monopolar unit; LOS, loss of signal.

In the QMR MU cooling study, there were no adverse EMG events when the cooling time was more than 2 seconds or immediately with MTM. When the cooling time was immediately without MTM, 2 of 4 RLNs with LOS after 30 minutes of observation (**Table 2**). The left RLN in piglet 7 showed a stable EMG signal (**Figure 5C**).

DISCUSSION

The current study is the first to provide RLN safety parameters when using QMR devices in thyroid surgery. In the activation study, activation of the QMR BS and QMR MU at a distance longer than 2 mm from the RLN showed no adverse EMG events. In the cooling study, cooling of the QMR BS and QMR MU for 2 seconds or with MTM showed no adverse EMG events.

The application of EBDs during thyroid surgery has increased worldwide due to significantly reduced intraoperative blood loss, operating time, and postoperative hematoma rates (2, 17). In addition, the risk of thermal injury to nerves during thyroid surgery continues to increase (18). Sixty degree Celsius is a critical temperature, and exceeding this temperature will cause functional damage to the endoneurium (19, 20). Thermal injuries to nerves often occur suddenly and unexpectedly, and they are difficult to recognize visually and difficult to recover. Therefore, in addition to referring to the data provided by the manufacturer before using the new EBDs for thyroid surgery, a well-established C-IONM animal experimental model is helpful for safe application in clinical settings. Several animal studies have reported commonly used EBDs and their safety parameters during thyroidectomy. The safety parameters for devices such as the bipolar electrocautery, LigaSure, Harmonic scalpel, THUNDERBEAT, and FM devices were more than 2 mm to the nerve when activated, and a with 5 mm distance was best for monopolar electrocautery (21–27). All devices should be cooled by the MTM before contact with the RLN. The QMR MU and QMR BS are suggested to activate at 2 mm or longer from the RLN. Although the QMR BS showed a faster cooling time than QMR MU (less than the time the instrument required to move from the SCM muscle to the RLN), considering that the instruments are usually closed to the RLN during dissection, a MTM and an adequate cooling time (at least two seconds) are still essential cooling procedures that cannot be omitted.

The first experimental study of QMR energy involved performing a thoracotomy in rats and evaluating its effect histologically in 2007 (28). By resonating and breaking molecular boundaries, QMR devices are said to cut tissue while maintaining a low temperature around the tissue (29), and tissue dissection is not facilitated through thermal vaporization as it is with traditional electrocautery or lasers (13, 15). Some literature (13, 14) and the manufacturer's website report that the temperature can be lower than 50 degrees Celsius with minimal thermal spread depth. D'Eredità et al. reported a mean 43 ± 9 μm depth of injury with QMR, while the depth of injury was 126 ± 11 μm with coblation in the histopathological evaluation of tonsillectomy specimens (11). For hemostasis, unlike electro and radiosurgery devices that produce a relatively large-area of burnt vessel collapse, QMR devices deploy a special waveform (with a slight loss of resonance) that elevates the temperature to 45-65°C (12, 28). This waveform triggers the denaturation process of fibrinogen, which turns into fibrin and clots the blood without causing thermal damage to the blood vessels. The above contents fully illustrate the potential benefits of QMR devices used in thyroid surgery, such as low temperature, effective hemostasis, and a small range of lateral thermal spread. However, in the dry environment, the QMR device reached a maximum temperature of 72°C after a single activation (3 seconds), and need approximately 2 seconds to decrease the temperature below 60°C in our preliminary thermographic study. It must be emphasized that, according to the results of this study, thyroid surgeons must still maintain adequate activation distance and cooling time to ensure the safety of their clinical application.

For the application of QMR devices in thyroid surgery, the interchangeability between QMR BS and QMR MU is an advantage worth mentioning. Thyroid surgeons can choose appropriate instruments according to the requirements of the thyroid dissection. In some relatively dense structures, such as Berry's ligaments, the scissor structure of QMR BS can have advantages during dissection compared with the sealer structure of other EBDs. Hence, QMR instruments are more likely to be dissected when they are directly adjacent to the RLN, and knowledge of the neural safety parameters of QMR devices is even more necessary for thyroid surgeons.

Several limitations in the study need to be mentioned. First, this study only had a 30-minute observation period after an adverse EMG event, and nerves with incomplete signal loss may not predict postoperative neural function. However, because of the difficult-to-repair nature of thermal injury, the occurrence of

adverse EMG events is a well-established way to assess the neural safety parameters of a new EBD (21–27). Second, some aspects in this prospective porcine model study may not be applicable to human surgery. Several factors can affect heat transfer from the QMR devices to the RLNs, including the difference in body temperature between human and experimental animals and the temperature of the surrounding environment. However, animal studies still provide useful and reliable data for human surgery. Finally, to have stable contact between the QMR devices and RLNs to avoid motion-affected C-IONM recordings, the part of the QMR devices that make direct contact with RLNs is closed but not the exact same as that in clinical surgery, especially the QMR BS cooling study. Therefore, although this study showed that QMR requires a very short cooling time, it is still recommended that the MTM or a 2-second cooling time should be performed before neural dissection.

CONCLUSION

QMR devices should be carefully used when performing RLN dissection during thyroid surgery. Safety recommendations regarding the use of QMR MU and QMR BS are as follows: activation should be at least 2 mm from the RLN and cooling procedures should include the MTM or an adequate cooling time (at least two seconds). According to the activation and cooling safety parameters in this study, surgeons can avoid RLN injury by following standard procedures when using QMR devices.

DATA AVAILABILITY STATEMENT

The original contributions presented in the study are included in the article/supplementary material. Further inquiries can be directed to the corresponding author.

ETHICS STATEMENT

The animal study was reviewed and approved by Institutional Animal Care and Use Committee of Kaohsiung Medical University, Taiwan (IACUC Approval No. 110129).

AUTHOR CONTRIBUTIONS

Supervision – GR, GD, N-CC, and C-WW; Materials – H-YT, T-YH, Y-CL, JW, H-YK, C-HC, and C-WW; Data Collection and Processing – H-YT, T-YH, N-CC, and C-WW; Analysis and Interpretation- H-YT, T-YH, I-CL, and P-YC; Literature Search - H-YT, T-YH, Y-CL, JW, H-YK, and C-HC; Writing Manuscript – All authors. All authors have read and agreed to the published version of the manuscript. All authors contributed to the article and approved the submitted version.

FUNDING

This study was supported by grants from Kaohsiung Medical University Hospital, Kaohsiung Medical University (KMUH110-0R51), and Ministry of Science and Technology (MOST 110-2314-B-037-104-MY2, MOST 110-2314-B-037-120), Taiwan.

ACKNOWLEDGMENTS

The authors are grateful to Hui-Chun Chen (clinical nurse specialist, Department of Nursing, Kaohsiung Medical University Hospital [KMUH], Kaohsiung Medical University [KMU], Taiwan) and Hsiu-Ya Chen (nurse anesthetist, Department of Anesthesiology, KMUH, KMU, Taiwan) for their excellent technical assistance.

REFERENCES

1. Lang BH-H, Yih PC-L, Lo C-Y. A Review of Risk Factors and Timing for Postoperative Hematoma After Thyroidectomy: Is Outpatient Thyroidectomy Really Safe? *JWjos* (2012) 36(10):2497–502. doi: 10.1007/s00268-012-1682-1
2. Wang JJ, Huang T-Y, Wu C-W, Lin Y-C, Tseng H-Y, Liu C-H, et al. Improving Voice Outcomes After Thyroid Surgery–Review of Safety Parameters for Using Energy-Based Devices Near the Recurrent Laryngeal Nerve. *Front Endocrinol* (2021) 12. doi: 10.3389/fendo.2021.793431
3. Dionigi G, Boni L, Rausei S, Frattini F, Ferrari CC, Mangano A, et al. The Safety of Energy-Based Devices in Open Thyroidectomy: A Prospective, Randomised Study Comparing the LigaSure™(LF1212) and the Harmonic® FOCUS. *Langenbecks Arch Surg* (2012) 397(5):817–23. doi: 10.1007/s00423-011-0898-0
4. Dionigi G, Wu C-W, Kim HY, Rausei S, Boni L, Chiang F-Y. Severity of Recurrent Laryngeal Nerve Injuries in Thyroid Surgery. *World J Surg* (2016) 40(6):1373–81. doi: 10.1007/s00423-011-0898-0
5. Dionigi G, Alesina P, Barczynski M, Boni L, Chiang F, Kim H, et al. Recurrent Laryngeal Nerve Injury in Video-Assisted Thyroidectomy: Lessons Learned From Neuromonitoring. *Surg Endosc* (2012) 26(9):2601–8. doi: 10.1007/s00464-012-2239-y
6. Huang T-Y, Yu W-HV, Chiang F-Y, Wu C-W, Fu S-C, Tai A-S, et al. How the Severity and Mechanism of Recurrent Laryngeal Nerve Dysfunction During Monitored Thyroidectomy Impact on Postoperative Voice. *Cancers* (2021) 13 (21):5379. doi: 10.3390/cancers13215379
7. Huang T-Y, Yu W-HV, Chiang F-Y, Wu C-W, Fu S-C, Tai A-S, et al. Prognostic Indicators of Non-Transection Nerve Injury and Vocal Fold Motion Impairment After Thyroid Surgery–Correlation Between Intraoperative Neuromonitoring Findings and Perioperative Voice Parameters. *Front Endocrinol* (2021) 12. doi: 10.3389/fendo.2021.755231
8. Demirhan E, Çukurova İ, Arslan İB, Ozkan ET, Mengi E, Yigitbasi OG. Quantum Molecular Resonance–Assisted Phonomicrosurgery: Preliminary Experience. *Otolaryngology–Head Neck Surg* (2015) 152(1):189–92. doi: 10.1177/0194599814549729
9. Lorusso F, Gallina S, Modica D, Di Salvo N, Riggio F. Bipolar Quantum Molecular Resonance Versus Blunt Dissection Tonsillectomy. *B-ent* (2015) 11 (02):101–8.
10. Chang H, Hah JH. Comparison of Post-Tonsillectomy Pain With Two Different Types of Bipolar Forceps: Low Temperature Quantum Molecular Resonance Device Versus High Temperature Conventional Electrocautery. *Acta Oto-Laryngol* (2012) 132(sup1):S130–3. doi: 10.3109/00016489.2012.659752
11. D'Eredità R, Bozzola L. Molecular Resonance vs. Coblation Tonsillectomy in Children. *Laryngoscope* (2009) 119(10):1897–901. doi: 10.1002/lary.20210
12. Vescovi P, Manfredi M, Merigo E, Fornaini C, Rocca J-P, Nammour S, et al. Quantic Molecular Resonance Scalpel and its Potential Applications in Oral

Surgery. *Br J Oral Maxillofacial Surg* (2008) 46(5):355–7. doi: 10.1016/j.bjoms.2007.09.014
13. Tarantino V, D'Agostino R, Melagrana A, Porcu A, Stura M, Vallarino R, et al. Safety of Electronic Molecular Resonance Adenoidectomy. *Int J Pediatr Otorhinolaryngol* (2004) 68(12):1519–23. doi: 10.1016/j.ijporl.2004.07.013
14. Sebben JE. Electrosurgery Principles: Cutting Current and Cutaneous Surgery—Part I. *J Dermatol Surg Oncol* (1988) 14(1):29–31. doi: 10.1111/j.1524-4725.1988.tb03338.x
15. D'Agostino R, Tarantino V, Calevo MG. Blunt Dissection Versus Electronic Molecular Resonance Bipolar Dissection for Tonsillectomy: Operative Time and Intraoperative and Postoperative Bleeding and Pain. *Int J Pediatr Otorhinolaryngol* (2008) 72(7):1077–84. doi: 10.1016/j.ijporl.2008.03.018
16. Pozzato G, Vignato G. Teoria Della Risonanza Quantica Molecolare Nella Realizzazione Del Bisturi Elettronico "Vesalius". *Quintessence Int* (2003) 5 (6):153–5.
17. Dionigi G, Wu C-W, Kim H-Y, Liu X, Liu R, Randolph GW, et al. Safety of Energy Based Devices for Hemostasis in Thyroid Surgery. *Gland Surg* (2016) 5 (5):490. doi: 10.21037/gs.2016.09.01
18. Liu C-H, Wang C-C, Wu C-W, Lin Y-C, Lu I, Chang P-Y, et al. Comparison of Surgical Complications Rates Between LigaSure Small Jaw and Clamp-and-Tie Hemostatic Technique in 1,000 Neuro-Monitored Thyroidectomies. *Front Endocrinol* (2021) 12:313. doi: 10.3389/fendo.2021.638608
19. Wu C-W, Dionigi G, Sun H, Liu X, Kim HY, Hsiao P-J, et al. Intraoperative Neuromonitoring for the Early Detection and Prevention of RLN Traction Injury in Thyroid Surgery: A Porcine Model. *Surgery* (2014) 155(2):329–39. doi: 10.1016/j.surg.2013.08.015
20. Lin YC, Dionigi G, Randolph GW, Lu IC, Chang PY, Tsai SY, et al. Electrophysiologic Monitoring Correlates of Recurrent Laryngeal Nerve Heat Thermal Injury in a Porcine Model. *Laryngoscope* (2015) 125(8): E283–90. doi: 10.1002/lary.25362
21. Wu C-W, Huang T-Y, Chen H-C, Chen H-Y, Tsai T-Y, Chang P-Y, et al. Intra-Operative Neural Monitoring of Thyroid Surgery in a Porcine Model. *JoVE* (2019) (144):e57919. doi: 10.3791/57919
22. Wu CW, Chai YJ, Dionigi G, Chiang FY, Liu X, Sun H, et al. Recurrent Laryngeal Nerve Safety Parameters of the H Armonic F Ocus During Thyroid Surgery: Porcine Model Using Continuous Monitoring. *Laryngoscope* (2015) 125(12):2838–45. doi: 10.1002/lary.25412
23. Dionigi G, Chiang FY, Kim HY, Randolph GW, Mangano A, Chang PY, et al. Safety of LigaSure in Recurrent Laryngeal Nerve Dissection-Porcine Model Using Continuous Monitoring. *Laryngoscope* (2017) 127(7):1724–9. doi: 10.1002/lary.26271
24. Huang TY, Lin YC, Tseng HY, Dionigi G, Kim HY, Chai YJ, et al. Safety Parameters of Ferromagnetic Device During Thyroid Surgery: Porcine Model Using Continuous Neuromonitoring. *Head Neck* (2020) 42(10):2931–40. doi: 10.1002/hed.26334
25. Huang T-Y, Lin Y-C, Tseng H-Y, Dionigi G, Kim H-Y, Lu I-C, et al. Safety of Ligasure Exact Dissector in Thyroidectomy With Continuous Neuromonitoring: A Porcine Model. *Gland Surg* (2020) 9(3):702. doi: 10.21037/gs.2020.03.17
26. Kim HK, Chai YJ, Lee HY, Kim HY, Dionigi G. Comparing the Safety of Harmonic ACE and ACE+ Around the Recurrent Laryngeal Nerve in Swine Models. *JAoST Res* (2018) 94(6):285–90. doi: 10.4174/astr.2018.94.6.285
27. Kwak HY, Dionigi G, Kim D, Lee HY, Son GS, Lee JB, et al. Thermal Injury of the Recurrent Laryngeal Nerve by THUNDERBEAT During Thyroid Surgery: Findings From Continuous Intraoperative Neuromonitoring in a Porcine Model. *J Surg Res* (2016) 200(1):177–82. doi: 10.1016/j.jss.2015.06.066
28. Schiavon M, Calabrese F, Nicotra S, Marulli G, Pozzato G, Giacometti C, et al. Favorable Tissue Effects of Quantum Molecular Resonance Device (Vesalius®) Compared With Standard Electrocautery. *Eur Surg Res* (2007) 39(4):222–8. doi: 10.1159/000101745
29. Ricciardiello F, Pisani D, Viola P, Pellini R, Russo G, Longo G, et al. The Role of Quantic Molecular Resonance (QMR) in the Treatment of Inferior Turbinate Hypertrophy (ITH): Our Experience With Long-Term Follow-Up in Allergic and Nonallergic Rhinitis Refractory to Medical Therapy Preliminary Results. *Ear Nose Throat J* (2021) 01455613211001599. doi: 10.1177/01455613211001599

Conflict of Interest: The authors declare that the research was conducted in the absence of any commercial or financial relationships that could be construed as a potential conflict of interest.

Publisher's Note: All claims expressed in this article are solely those of the authors and do not necessarily represent those of their affiliated organizations, or those of the publisher, the editors and the reviewers. Any product that may be evaluated in this article, or claim that may be made by its manufacturer, is not guaranteed or endorsed by the publisher.

frontiers | Frontiers in Endocrinology

ORIGINAL RESEARCH
published: 30 June 2022
doi: 10.3389/fendo.2022.923804

Necessity of Routinely Testing the Proximal and Distal Ends of Exposed Recurrent Laryngeal Nerve During Monitored Thyroidectomy

Hsiao-Yu Huang[1], Ching-Feng Lien[1,2], Chih-Chun Wang[1,2], Chien-Chung Wang[1], Tzer-Zen Hwang[1,2], Yu-Chen Shih[3], Che-Wei Wu[4], Gianlorenzo Dionigi[5,6], Tzu-Yen Huang[4] and Feng-Yu Chiang[1,2]**

[1] Department of Otolaryngology-Head and Neck Surgery, E-Da Hospital, Kaohsiung, Taiwan, [2] School of Medicine, College of Medicine, I-Shou University, Kaohsiung, Taiwan, [3] Department of Otolaryngology, E-Da Cancer Hospital, Kaohsiung, Taiwan, [4] Department of Otorhinolaryngology-Head and Neck Surgery, International Thyroid Surgery Center, Kaohsiung Medical University Hospital, Faculty of Medicine, College of Medicine, Kaohsiung Medical University, Kaohsiung, Taiwan, [5] Division of General Surgery, Endocrine Surgery Section, Istituto Auxologico Italiano Istituto di Ricovero e Cura a Carattere Scientifico (IRCSS), Milan, Italy, [6] Department of Pathophysiology and Transplantation, University of Milan, Milan, Italy

OPEN ACCESS

Edited by:
Paolo Miccoli, University of Pisa, Italy

Reviewed by:
Erivelto Martinho Volpi, Centro de referencia no ensino do diagnóstico por imagem (CETRUS), Brazil
Ahmet Omer Ikiz, Dokuz Eylül University, Turkey

***Correspondence:**
Tzu-Yen Huang
tyhuang.ent@gmail.com
Feng-Yu Chiang
fychiang@kmu.edu.tw

Specialty section:
This article was submitted to Thyroid Endocrinology, a section of the journal Frontiers in Endocrinology

Received: *19 April 2022*
Accepted: *31 May 2022*
Published: *30 June 2022*

Citation:
Huang H-Y, Lien C-F, Wang C-C, Wang C-C, Hwang T-Z, Shih Y-C, Wu C-W, Dionigi G, Huang T-Y and Chiang F-Y (2022) Necessity of Routinely Testing the Proximal and Distal Ends of Exposed Recurrent Laryngeal Nerve During Monitored Thyroidectomy. Front. Endocrinol. 13:923804. doi: 10.3389/fendo.2022.923804

Objectives: Intraoperative neuromonitoring (IONM) is a useful tool to evaluate the function of recurrent laryngeal nerve (RLN) in thyroid surgery. This study aimed to determine the necessity and value of routinely testing the proximal and distal ends of RLN.

Methods: In total, 796 patients undergoing monitored thyroidectomies with standardized procedures were enrolled. All 1346 RLNs with visual integrity of anatomical continuity were routinely stimulated at the most proximal (R2p signal) and distal (R2d signal) ends after complete RLN dissection. The EMG amplitudes between R2p and R2d signals were compared. If the amplitude of R2p/R2d ratio reduction (RPDR) was over 10% or loss of signal (LOS) occurred, the exposed RLN was mapped to identify the injured point. Pre- and post-operative vocal cord (VC) mobility was routinely examined with video-laryngofiberscope.

Results: Nerve injuries were detected in 108 (8%) RLNs, including 94 nerves with incomplete LOS (RPDR between 13%-93%) and 14 nerves with complete LOS. The nerve injuries were caused by traction in 80 nerves, dissecting trauma in 23 nerves and lateral heat spread of energy-based devices in 5 nerves. Symmetric VC mobility was found in 72 nerves with RPDR ≤50%. The occurrence of abnormal VC mobility (weak or fixed) was 14%, 67%, 100%, and 100% among the different RPDR stratifications of 51%-60%, 61%-70%, 71%-80%, and 81-93%, respectively. Of the 14 nerves with complete LOS, all showed fixed VC mobility. Permanent VC palsy occurred in 2 nerves with thermal injury.

Conclusion: Routinely testing the proximal and distal ends of exposed RLN helps detect unrecognized partial nerve injury, elucidate the injury mechanism and determine injury severity. The procedure provides accurate information for evaluating RLN function after nerve dissection and should be included in the standard IONM procedure.

Keywords: recurrent laryngeal nerve (RLN), intraoperative neuromonitoring (IONM), thyroid surgery, electromyography (EMG), vocal cord (VC) mobility

INTRODUCTION

Intraoperative neuromonitoring (IONM) has been commonly applied in thyroid surgery to facilitate the identification of recurrent laryngeal nerve (RLN), evaluate nerve function after dissection, detect nerve injury and elucidate its mechanism, predict the outcome of vocal cord (VC) function and make the decision to perform staged thyroidectomy (1–6).

From the literature review, the era in the absence of standard IONM procedures revealed a high negative predictive value of 92%-100%, but a low and highly variable positive predictive value, ranging from 10% to 90% (7–13). The results suggested that patients with positive EMG signals after thyroid resection generally do not have VC palsy. Conversely, patients with loss of signal (LOS) have unpredictable VC functional outcomes, leading to unnecessary staged operation.

In recent years, through following the standard 4-step IONM procedures (V_1-R_1-R_2-V_2) and troubleshooting algorithms, the positive predictive value has greatly improved. When LOS occurs after RLN dissection, it always indicates nerve injury and the development of postoperative VC palsy (5, 6, 14–16). However, a positive EMG signal at the proximal end of RLN does not guarantee normal nerve function and normal postoperative VC function. In the absence of complete LOS, a partial nerve injury could be unrecognized and an unexpected VC palsy may occur (17, 18). In this study, we hypothesize that routinely testing the proximal and distal ends of exposed RLN may help detect unrecognized nerve injury, elucidating the injury mechanism, and determining injury severity.

MATERIALS AND METHODS

Patients

From January 2015 to October 2019, 796 patients (152 men and 644 women; ages ranging from 12 to 81 years; mean age, 50.4 years) underwent operations for various thyroid diseases by the same surgeon (F.-Y. C) were collected. There were 232 thyroid lobectomies and 564 total thyroidectomies (467 benign and 329 malignant thyroid diseases). Fourteen nerves were excluded from this study due to preoperative cord palsy (10 nerves) and intentional sacrifice due to cancer encasement (4 nerves). Thus, 1346 nerves at risk were enrolled in this study. The study was approved by the Institutional Review Board (IRB) of Kaohsiung Medical University Hospital, Taiwan: KMUHIRB-E (II)-20200348.

IONM Setup and Procedures

The standard procedures for equipment setup and anesthesia were performed by the IONM team of Kaohsiung Medical University Hospital. All patients were intubated with a regular oral endotracheal tube. After dissection of the thyroid pyramidal lobe, two paired subdermal needle electrodes (length 12.0 mm, Medtronic Xomed, Jacksonville, FL, USA) were obliquely inserted into the sub-perichondrium of the lateral thyroid cartilage on each side for EMG signal recording (19, 20).

During the operation, standardized IONM procedures were strictly followed. The VN (without dissecting the carotid sheath to expose the VN) was stimulated with a 5-10 mA stimulus current before and after RLN dissection, and V_1 and V_2 signals were obtained. The RLN was stimulated with 3-5 mA at the first identification, and the R_1 signal was obtained. After complete RLN dissection, the exposed RLN was stimulated at the most proximal end, and distal end near the laryngeal entry point, and R_{2p} and R_{2d} signals were obtained, respectively. The largest amplitudes of these five EMG signals (V_1-R_1-R_{2p}-R_{2d}-V_2) were registered in all cases. The amplitudes of the R_{2p} and R_{2d} signals were compared. If the amplitude of R_{2p}/R_{2d} ratio reduction (RPDR) was over 10% after repeated testing or LOS occurred, the whole exposed RLN was mapped to identify the weak or disrupted point of nerve conduction with 1 mA. The standardized IONM techniques in this study started with a preoperative examination of VC function (L_1), and an intraoperative 5-step procedure (V_1-R_1-R_{2p}-R_{2d}-V_2), and ended with a postoperative examination of VC function (L_2) for all patients (**Table 1**).

For the severity of nerve injury, complete LOS was defined as an absence of EMG signals (R_{2p} amplitude less than 100 μV) after nerve stimulation. Incomplete LOS was defined as when the R_{2p} amplitude was detectable (more than 100 μV), the RDPR was more than 10% and less than 100%. When nerve injury occurred, the mechanism of nerve injury (traction injury, dissecting trauma and thermal injury) and injury site (upper third, middle third and lower third portion of the exposed RLN) were registered. For the type of nerve injury, type 1 LOS was defined as a detectable injury site on the exposed RLN, and type 2 LOS was defined as no detectable injury site on the whole exposed RLN. For VC mobility, normal (symmetric) VC function was correlated with symmetric VC mobility during phonation, weak VC function was correlated with weak VC mobility (asymmetric and sluggish VC movement at the injury side), and VC palsy was correlated with fixed VC mobility. When VC palsy persisted for more than 6 months, it was regarded as permanent palsy.

The percentage and mean value were calculated using Microsoft Excel 2016 (Microsoft Corp., Redmond, WA, USA).

TABLE 1 | Standardized IONM procedures.

Procedures
L_1 Pre-operative examination of VC function with laryngofiberscope
V_1 Vagus nerve stimulation with 5-10 mA before thyroid dissection
R_1 RLN stimulation with 3-5 mA at first RLN identification
(R_{2p})* RLN stimulation with 3-5 mA at the most proximal end after RLN dissection
(R_{2d})* RLN stimulation with 3-5 mA at the distal end near the laryngeal entry point
V_2 Vagus nerve stimulation with 5-10 mA after resection of thyroid lobe
L_2 Post-operative examination of VC function with laryngofiberscope

**RLN mapping with 1 mA if the amplitude reduction of R_{2p}/R_{2d} signals over 10% or LOS*
IONM, intraoperative neuromonitoring; RLN, recurrent laryngeal nerve; VC, vocal cord.

RESULTS

Among 1346 RLNs with anatomical integrity in continuity after nerve dissection, nerve injury was detected in 108 (8%) nerves, including 94 nerves with incomplete LOS (RPDR ranging from 13% to 93%) and 14 nerves with complete LOS.

Of the 94 RLNs with incomplete LOS, the nerve injury site was detectable in all nerves. Seventy-three nerve injuries were caused by traction injury, 19 nerve injuries were caused by dissecting trauma, and 2 nerve injuries were caused by thermal injury. For injured nerves with RPDR ≤50%, the 72 corresponding patients had postoperative symmetric VC mobility; for injured nerves with RPDR between 51%-60%, weak VC mobility was found in 1 (14%) of 7 corresponding patients; for injured nerves with RPDR between 61%-70%, abnormal (2 weak and 2 fixed) VC mobility was found in 4 (67%) of 6 corresponding patients; for injured nerves with RPDR between 71%-80%, abnormal (1 weak and 2 fixed) VC mobility was found in 3 (100%) of 3 corresponding patients; for injured nerves with RPDR between 81%-93%, abnormal VC mobility was found in 6 (100%) of 6 corresponding patients, and all patients had fixed VC mobility (**Tables 2**, **3**).

Of the 14 RLNs with complete LOS, the nerve injury site was detectable on the exposed RLN in 11 nerves (type 1 LOS) and was not detectable on the exposed RLN in 3 nerves (type 2 LOS). Seven nerve injuries were caused by traction injury, 4 nerve injuries were caused by dissecting trauma, and 3 nerve injuries were caused by thermal injury. All 14 cases showed fixed VC mobility postoperatively. Temporary VC palsy occurred in 12 nerves, and permanent VC palsy occurred in 2 nerves with thermal injury (**Tables 2**, **4**).

Among 105 nerves with a detectable injury site, the weak or disrupted point of nerve conduction was localized at the region of Berry's ligament (within the upper portion of the exposed RLN) in 83 (79%) nerves (77 traction injuries, 3 dissecting traumas, and 3 thermal injuries), on the middle portion of the exposed RLN in 9 (9%) nerves (8 dissecting traumas and 1 thermal injury), and on the lower portion of the exposed RLN in 13 (12%) nerves (12 dissecting traumas and 1 thermal injury).

DISCUSSION

When applying IONM in thyroid surgery, the measurement of EMG amplitude from RLN stimulation may correlate with the number of motor units that contribute to polarization and reflect the neurophysiologic function of the nerve (21, 22). Theoretically, unchanged EMG amplitude after RLN dissection indicates normal nerve and VC functions postoperatively. Conversely, decreased EMG amplitude after nerve dissection indicates a nerve function deficit or a decreased number of motor units participating in polarization. Complete LOS after RLN dissection may indicate complete loss of nerve conduction and postoperative VC palsy. However, the correlation between the residual ratio of EMG amplitude after partial RLN injury and the sufficient muscle strength required for normal VC mobility is still unknown.

The intraoperative 4-step procedure (V_1-R_1-R_2-V_2) has been accepted as a standard IONM procedure by many studies (5, 6, 14–17). It was useful to evaluate nerve function by comparing the EMG signals between pre- and post-dissection of RLN. Unchanged or increased post-dissection EMG amplitudes (comparing R_2 and V_2 signals with R_1 and V_1 signals, respectively) indicated functional integrity of the RLN. Conversely, decreased R_2 and V_2 signals indicated RLN injury and the risk of postoperative VC palsy. However, when using an EMG endotracheal tube for signal recording, unstable EMG amplitudes often occur intraoperatively due to the change in contact quality between the EMG tube and vocal cords. Poor

TABLE 2 | The mechanism and severity of RLN injury and the outcome of VC mobility in 108 RLNs detected with injury.

Severity of nerve injury	Case number	Mechanism of nerve injury and injury site			VC mobility		
		Traction injury (U/M/L)	Dissecting trauma (U/M/L)	Thermal injury (U/M/L)	Sym	Weak	Fixed
Incomplete LOS (RPDR >10%, <100%)	94	73(73/0/0)	19(2/6/11)	2(0/1/1)	80	4	10
11%-20%	35	32	3	0	35	0	0
21%-30%	16	12	3	1	16	0	0
31%-40%	10	6	4	0	10	0	0
41%-50%	11	7	4	0	11	0	0
51%-60%	7	7	0	0	6	1	0
61%-70%	6	5	1	0	2	2	2
71%-80%	3	1	2	0	0	1	2
81%-90%	3	1	1	1	0	0	3
91%-93%	3	2	1	0	0	0	3
Complete LOS	14	7(4/0/0)[+]	4(1/2/1)	3(3/0/0)	0	0	14*
Total	108	80	23	5	80	4	24

[+]*type 1 complete LOS in 4 nerves with detectable injured point, type 2 complete LOS in 3 nerves without detectable injured point.*

**temporary palsy in 12 nerves, permanent palsy in 2 nerve with thermal injury.*

U/M/L, upper/middle/lower portion of the exposed RLN.

RLN, recurrent laryngeal nerve; VC, vocal cord; RPDR, R_{2p}/R_{2d} ratio reduction; LOS, loss of signal; sym, symmetric.

TABLE 3 | Intraoperative EMG signals and mechanism of nerve injury in the RLNs without complete LOS (detectable injury site and R_{2p}/R_{2d} reduction >50%).

No.	V_1 (μV)	R_1 (μV)	R_{2p} (μV)	R_{2d} (μV)	V_2 (μV)	R_{2p}/R_{2d} reduction	Injury site	Injury mechanism	VC mobility
1	949	1017	708	1431	655	51%	U(BL)	traction	sym
2	2051	2215	1188	2491	1037	52%	U(BL)	traction	sym
3	3598	3752	1337	2806	1068	52%	U(BL)	traction	sym
4	2728	2899	1393	3110	979	55%	U(BL)	traction	sym
5	1261	1358	512	1214	358	58%	U(BL)	traction	weak
6	1570	2237	989	2441	606	59%	U(BL)	traction	sym
7	1957	2354	954	2325	801	59%	U(BL)	traction	sym
8	2235	3695	1480	3855	1072	62%	U(BL)	traction	weak
9	1153	1278	364	1480	244	66%	U(BL)	traction	sym
10	921	843	396	1230	272	68%	U(BL)	traction	fixed^t
11	752	780	229	724	167	68%	L	trauma	fixed^t
12	2707	4570	1647	5254	903	69%	U(BL)	traction	sym
13	1175	1363	688	2264	462	70%	U(BL)	traction	weak
14	1728	3494	880	3422	543	74%	U(BL)	traction	weak
15	1889	2206	509	2144	577	76%	L	trauma	weak
16	1287	1658	346	1712	247	80%	M	trauma	fixed^t
17	1152	1289	145	755	138	81%	U(BL)	traction	fixed^t
18	1564	1735	351	1837	287	81%	L	thermal	fixed^t
19	1308	1521	188	1810	122	90%	L	trauma	fixed^t
20	2896	3015	250	3109	235	92%	U(BL)	traction	fixed^t
21	2779	3410	323	3822	190	92%	U(BL)	traction	fixed^t
22	2935	3773	232	3351	217	93%	U(BL)	trauma	fixed^t

EMG, electromyography; RLN, recurrent laryngeal nerve; LOS, complete loss of signal; VC, vocal cord; U(BL), upper portion of the exposed RLN (at the region of Berry's ligament); M, middle portion of the exposed RLN; L, lower portion of the exposed RLN; sym, symmetric; fixed ^{t}, temporary palsy.

contact quality caused by EMG tube displacement during the surgical maneuver on the trachea will lead to a significant decrease in EMG amplitudes or false LOS. Therefore, a decrease or loss of the post-dissection EMG amplitude would not necessarily be a nerve injury. Genther et al. reported that the risk of immediate postoperative VC palsy is approximately 72% when post-dissection EMG amplitudes are less than 200 μV (23). Pavier et al. reported that the risk of VC palsy is approximately 50% when post-dissection EMG amplitudes were under the value of 280 μV and suggested a staged thyroidectomy (24). The data of these 2 studies showed that the false-positive rate ranged from 28% to 50% and indicated that many patients might receive unnecessary second operations. Calò et al. reported that staged thyroidectomy was performed in 37 patients due to LOS, but 8 (22%) patients had normal VC function after their first operations (25). Melin et al. reported that the second operation was performed in 18 patients with LOS, but 8 (44%) patients were confirmed to have primarily intact vocal cord function (26).

In this study, we used the trans-thyroid cartilage EMG signal recording method (19, 27–29). The EMG amplitude will not be influenced by EMG tube displacement and the elicited signals remain high and stable during the entire course of operation that is important to monitor the actual status of RLN function. Furthermore, we routinely test the proximal and distal ends of the exposed RLN after complete nerve dissection. The procedure helps detect unrecognized partial nerve injury and determine its severity by comparing R_{2p} with R_{2d} signals. This series found that the outcomes of VC function were highly correlated with the severity of

TABLE 4 | Intraoperative EMG signals and mechanism of nerve injury in the RLNs with complete LOS.

No.	V_1 (μV)	R_1 (μV)	R_{2p} (μV)	R_{2d} (μV)	V_2 (μV)	R_{2p}/R_{2d} reduction	Injury site	Injurymechanism	VC mobility
1	2862	2993	LOS	3279	LOS	=100%	U(BL)	traction	fixed^t
2	1391	1581	LOS	1242	LOS	=100%	U(BL)	traction	fixed^t
3	2430	2882	LOS	2976	LOS	=100%	U(BL)	traction	fixed^t
4	3616	4600	LOS	5019	LOS	=100%	U(BL)	traction	fixed^t
5	1716	2585	LOS	LOS	LOS	=0%	nil	traction	fixed^t
6	2145	2521	LOS	LOS	LOS	=0%	nil	traction	fixed^t
7	1053	1384	LOS	LOS	LOS	=0%	nil	traction	fixed^t
8	2816	2756	LOS	3149	LOS	=100%	U(BL)	trauma	fixed^t
9	1532	3750	LOS	3818	LOS	=100%	L	trauma	fixed^t
10	729	1395	LOS	1289	LOS	=100%	M	trauma	fixed^t
11	1748	1784	1998	LOS	LOS	=100%	M	trauma	fixed^t
12	2154	3823	LOS	3750	LOS	=100%	U(BL)	thermal	fixed^t
13	1421	1600	LOS	1744	LOS	=100%	M	thermal	fixed^p
14	2860	3637	LOS	3171	LOS	=100%	U(BL)	thermal	fixed^p

EMG, electromyography; RLN, recurrent laryngeal nerve; LOS, complete loss of signal; VC, vocal cord; U(BL), upper portion of the exposed RLN (at the region of Berry's ligament); M, middle portion of the exposed RLN; L, lower portion of the exposed RLN; fixed ^{t}, temporary palsy; fixed ^{p}, permanent palsy.

nerve injury. In 14 nerves with post-dissection complete LOS, all cases showed fixed VC mobility postoperatively. In 94 nerves with RPDR over 10% (ranging from 13% to 93%), 72 nerves showed symmetric VC mobility where the RPDR was ≤50%. Abnormal VC mobility (weak or fixed VC movement) was only found in the nerves with RPDR >50%. The possibility of postoperative abnormal VC mobility was approximately 14%, 67%, 100%, and 100% among the different RPDR stratifications of 51%-60%, 61%-70%, 71%-80%, and 81-93%, respectively.

A weak or disrupted point of nerve conduction is important neurophysiological evidence of nerve injury. By mapping the exposed RLN, we can localize the injured point and clarify the possible mechanism of nerve injury. In this study, we found that the region of Berry's ligament is the most common site of nerve injury. Among 105 nerves with an injured point detected, 83 (79%) nerves were injured at this site, including 77 traction injuries, 3 dissecting traumas, and 3 thermal injuries. The injured point was localized at the middle portion of the exposed RLN in 10 (10%) nerves (9 dissecting trauma and 1 thermal injury) and at the lower portion in 12 (11%) nerves (11 dissecting trauma and 1 thermal injury).

This study also found that traction injury was the most common cause of RLN injury, of approximately 74% (80/108). The RLN can be injured at the region of Berry's ligament by stretching dense fibrous tissue or surrounding blood vessels during medial thyroid retraction. Of the 80 nerves with traction injuries, the injury points were located at Berry's ligament region in 73 nerves without LOS (**Figure 1**). In the other 7 nerves with LOS, 4 injury points were located at Berry's ligament region (type 1 LOS) (**Figures 2A, B**), and 3 injury points were not found (type 2 LOS), and the injury point may be located higher above the laryngeal entry point (**Figures 3A, B**). Dissecting trauma was the second most common cause of RLN injury, with a rate of approximately 21% (23/108). Of the 23 nerves injured by dissecting trauma, 3 nerve injuries occurred during dissection of the RLN from Berry's ligament, 8 nerve injuries occurred during dissection of the RLN from malignant tumors or recurrent benign tumors (**Figures 4A, B**), and 12 nerve injuries occurred during paratracheal node dissection. Thermal injury accounted for approximately 5% (5/108), and all 5 nerve injuries were caused by lateral heat spread of the energy-

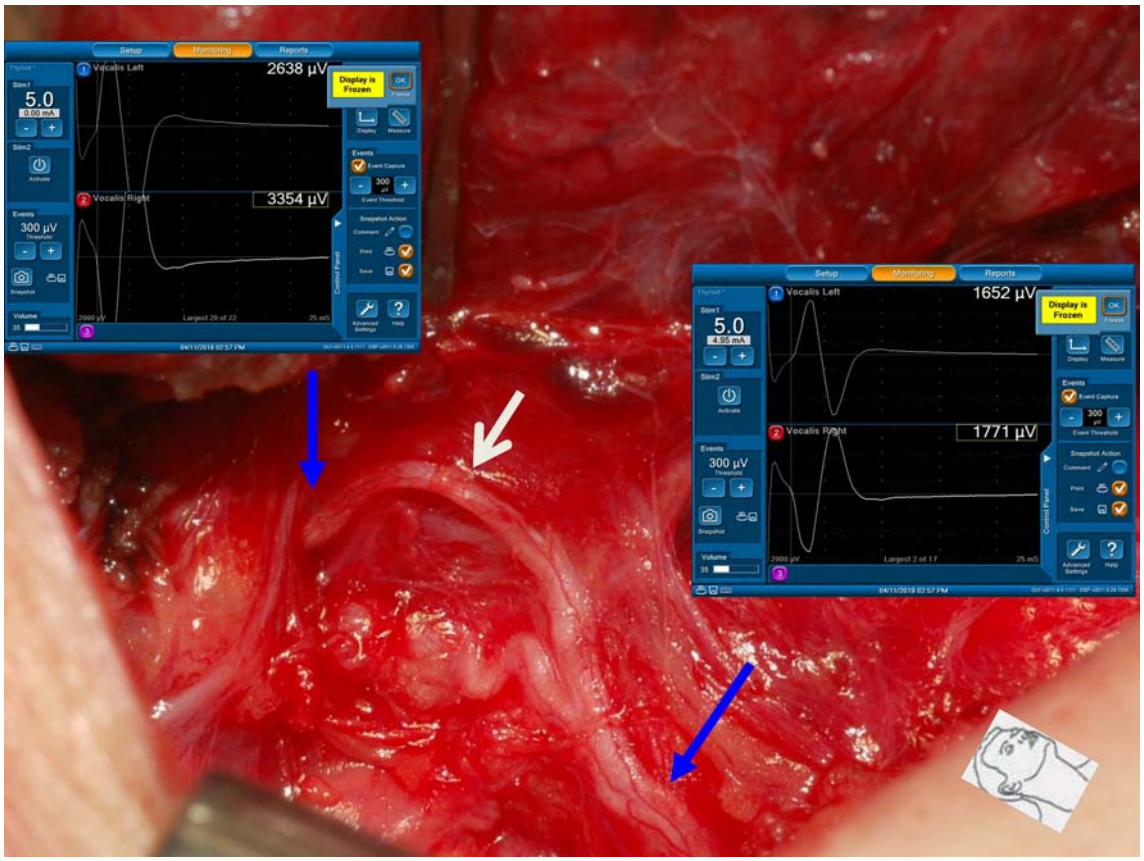

FIGURE 1 | A case of type 1 incomplete LOS. The anterior motor branch of the RLN was stretched upward during medial thyroid traction. After complete RLN dissection and comparing R_{2p} signal (1771 µV) with R_{2d} signal (3354 µV), it showed an amplitude reduction of approximately 47%, and a weak point of nerve conduction was mapped (white arrow).

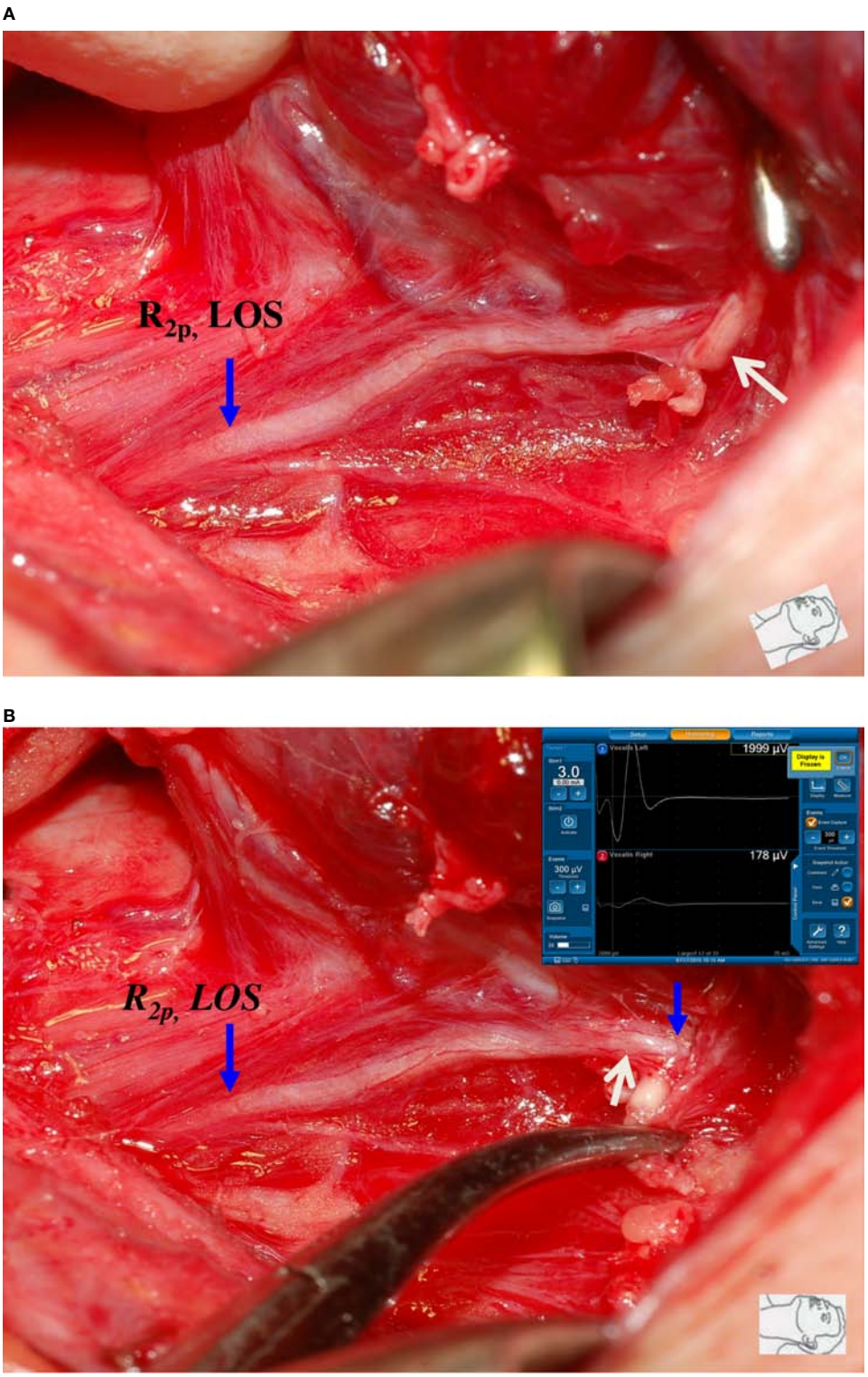

FIGURE 2 | A case of type 1 complete LOS. **(A)** The R_{2p} signal was lost, and a small artery (white arrow) was found to be intertwined with the RLN at the region of Berry's ligament. **(B)** After dissecting the intertwined vessel from the RLN, R_{2d} signal showed 1999 μV and R_{2p} signal showed complete LOS, a disrupted point of nerve conduction (white arrow) was detected. This was a type 1 LOS and the patient had temporary vocal cord palsy.

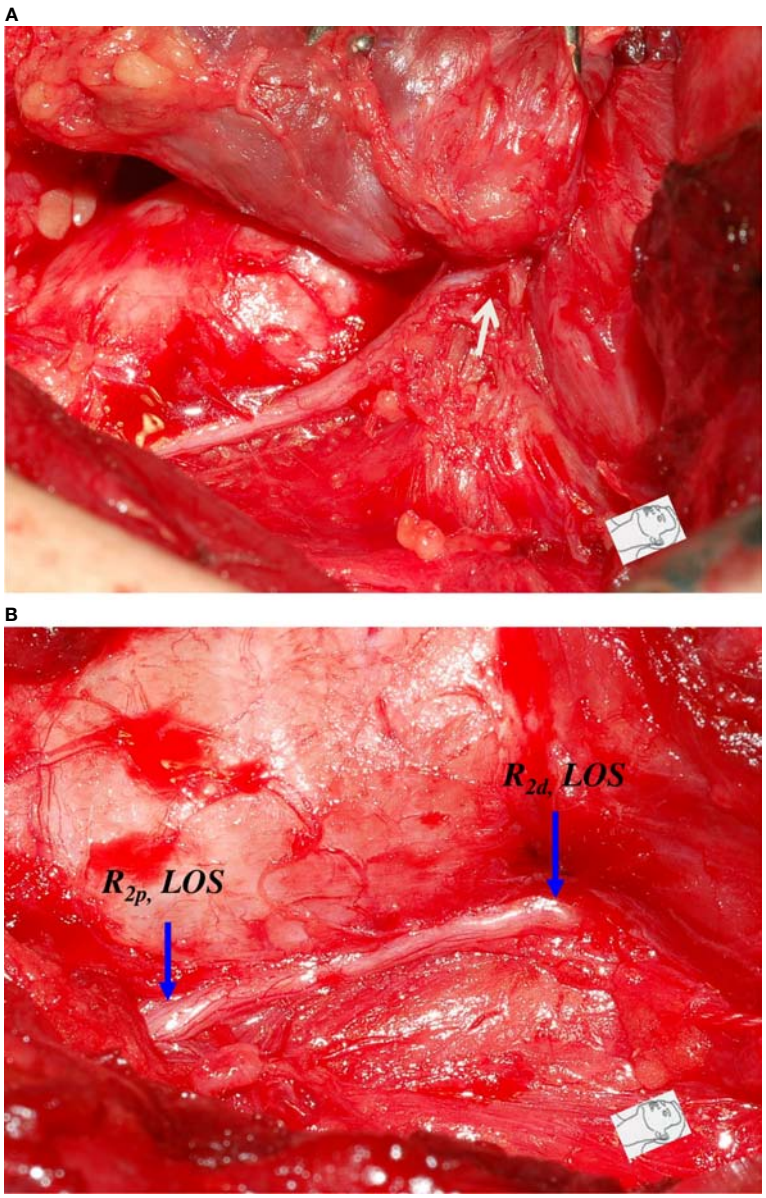

FIGURE 3 | A case of type 2 complete LOS. **(A)** The RLN was stretched upward (white arrow) at the region of Berry's ligament during medial thyroid traction. **(B)** After complete RLN dissection, both R_{2p} and R_{2d} signals showed complete LOS and no injured point was found on the exposed RLN. This was a type 2 LOS and it developed temporary vocal cord palsy.

based device (EBD) or electrocauterization (**Figures 5**, **6**). In 3 nerves with LOS, 2 nerves developed permanent VC palsy, and 1 developed temporary VC palsy. Another nerve with RPDR of 81% developed temporary VC palsy. The other nerve with RPDR of less than 50% showed symmetrical VC mobility after surgery.

From the results of this study, it can be found that permanent VC palsy rarely occurred in nerve injuries caused by traction or dissecting trauma, but there was a high rate of permanent VC palsy (40%, 2/5) in thermal injuries. The voice outcome and VC mobility prognosis are worse in patients with thermal RLN injuries than in those with mechanical RLN injuries (30, 31). Therefore, the use of EBDs or electrocauterization near the RLN should pay special attention to the safety distance. Several studies on animals have shown that activations of various EBDs at 2 mm are safe under electrophysiological evidence (32–34), but translating the data to clinical practice must be very careful. When EBD is activated, tissue contraction can reduce the safety distance and increase the risk of thermal injury. Additionally, hot tissue fluid contact with the RLN may also

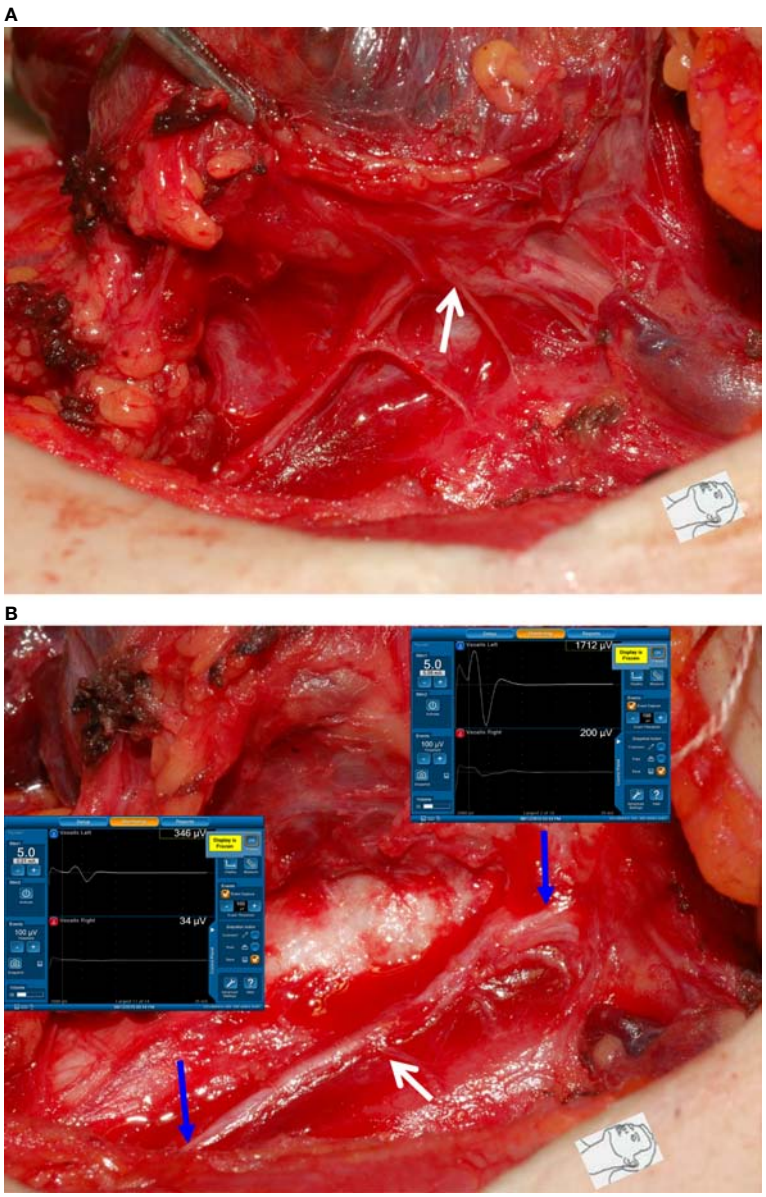

FIGURE 4 | Dissecting trauma of the RLN. **(A)** The RLN was adherent to thyroid cancer. **(B)** After complete RLN dissection and comparing R_{2p} signal (346 μV) with R_{2d} signal (1712 μV), it showed an approximately 80% amplitude reduction and an injured point caused by dissecting trauma was mapped (white arrow). The patient had temporary vocal cord palsy.

cause thermal injury (35). Lin et al. confirmed that complete LOS occurred when the RLN was in contact with hot water at 60°C (36). Therefore, we recommend that the RLN should be clearly visualized and that the safety distance from the nerve is best to have 5 mm (37). If the safe distance is less than 5 mm, particularly at the region of Berry's ligament, a small piece of wet gauze or forceps should be placed between the nerve and the EBD to prevent thermal injury caused by lateral heat spread or by hot tissue fluid. Based on the above, elucidating the mechanism (traction injury, dissecting trauma, and thermal injury) and type (detectable or undetectable injury site) of nerve injury while performing R_{2p} and R_{2d} steps enables thyroid surgeons to continuously improve surgical techniques and reduce surgical complications.

Several limitations should be mentioned in this study. First, this was an observational study without a control group. Second, the number of patients with complete LOS was relatively small; however, the characteristics of severe incomplete LOS and complete LOS can be clearly shown in this study. Last, the functional outcomes and prognosis of type 1 and type 2 LOS

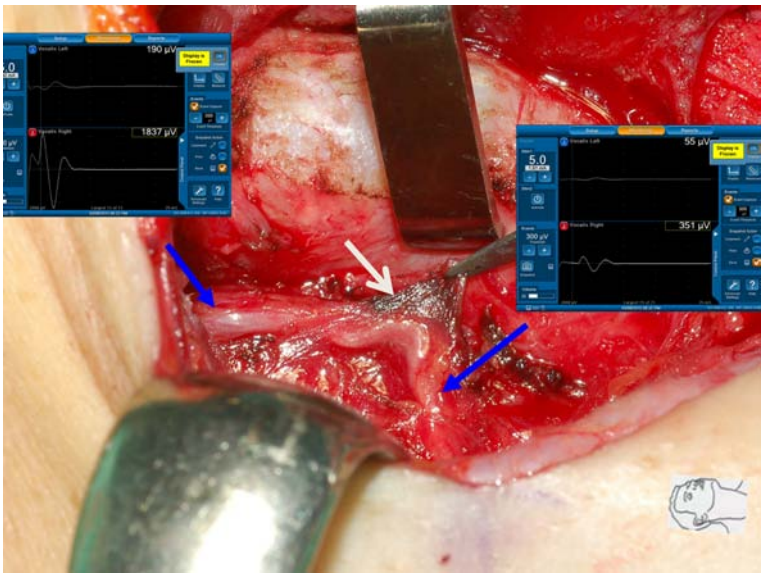

FIGURE 5 | Thermal injury of the RLN with incomplete LOS. The RLN was injured by lateral thermal spread of electrocauterization (white arrow). Comparing R_{2p} signal (351 μV) with R_{2d} signal (1837 μV) showed an approximately 81% amplitude reduction and the development of temporary vocal cord palsy.

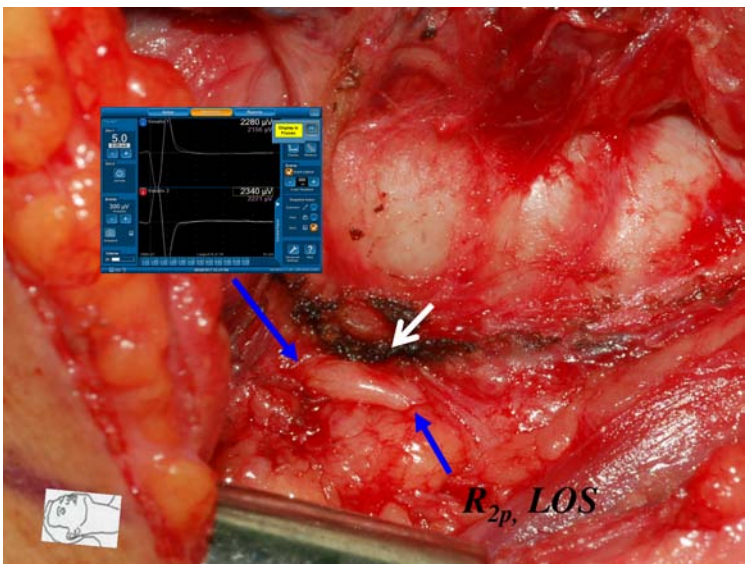

FIGURE 6 | Thermal injury of the RLN with complete LOS. The RLN was injured by lateral thermal spread of energy-based device (white arrow) at the region of Berry's ligament. Complete LOS occurred in R_{2p} signal, and the R_{2d} signal was 2340 μV. The patient had temporary vocal cord palsy.

warrant further study, and a well-designed study would help to highlight the advantages of R_{2p} and R_{2d} steps.

CONCLUSION

Routinely testing the proximal and distal ends of the exposed RLN is a simple and useful procedure to accurately evaluate RLN function after complete dissection. It helps detect unrecognized nerve injury and clarifies where and how the nerve was injured and determines the severity of nerve injury. The provided information will be useful to improve surgeons' surgical techniques and help make decisions regarding staged thyroidectomy. The additional step of testing the distal end of the exposed RLN should be included in the standard IONM procedure.

DATA AVAILABILITY STATEMENT

The original contributions presented in the study are included in the article/Supplementary Material. Further inquiries can be directed to the corresponding authors.

ETHICS STATEMENT

The studies involving human participants were reviewed and approved by Institutional Review Board (IRB) of Kaohsiung Medical University Hospital, Taiwan: KMUHIRB-E(II)-20200348. Written informed consent for participation was not required for this study in accordance with the national legislation and the institutional requirements.

AUTHOR CONTRIBUTIONS

Supervision – T-ZH, C-WW, GD, and F-YC; Materials – C-FL, T-ZH, Y-CS, T-YH, and F-YC; Data Collection and Processing – H-YH, Chih-CW, Chien-CW, Y-CS; Analysis and Interpretation – H-YH, C-FL, T-YH, and F-YC; Literature Search – H-YH, Chih-CW, Chien-CW, T-YH, and F-YC; Writing Manuscript – All authors. All authors have read and agreed to the published version of the manuscript.

FUNDING

This study was supported by grants from Kaohsiung Medical University Hospital, Kaohsiung Medical University (KMUH110-0R51), and Ministry of Science and Technology (MOST 110-2314-B-037-104-MY2, MOST 110-2314-B-037-120), Taiwan.

ACKNOWLEDGMENTS

The authors would like to thank all the patients included in this study.

REFERENCES

1. Wu C-W, Randolph G, Barczynski M, Schneider R, Chiang F-Y, Huang T-Y, et al. Training Courses in Laryngeal Nerve Monitoring in Thyroid and Parathyroid Surgery-The INMSG Consensus Statement. *Front Endocrinol* (2021) 12:708. doi: 10.3389/fendo.2021.795281
2. Liu N, Chen B, Li L, Zeng Q, Sheng L, Zhang B, et al. Mechanisms of Recurrent Laryngeal Nerve Injury Near the Nerve Entry Point During Thyroid Surgery: A Retrospective Cohort Study. *Int J Surg* (2020) 83:125–30. doi: 10.1016/j.ijsu.2020.08.058
3. Zhang D, Sun H, Tufano R, Caruso E, Dionigi G, Kim HY. Recurrent Laryngeal Nerve Management in Transoral Endoscopic Thyroidectomy. *Oral Oncol* (2020) 108:104755. doi: 10.1016/j.oraloncology.2020.104755
4. Hayward NJ, Grodski S, Yeung M, Johnson WR, Serpell J. Recurrent Laryngeal Nerve Injury in Thyroid Surgery: A Review. *ANZ J Surg* (2013) 83(1-2):15–21. doi: 10.1111/j.1445-2197.2012.06247.x
5. Chiang F-Y, Lu I-C, Kuo W-R, Lee K-W, Chang N-C, Wu C-W. The Mechanism of Recurrent Laryngeal Nerve Injury During Thyroid Surgery—the Application of Intraoperative Neuromonitoring. *Surgery* (2008) 143 (6):743–9. doi: 10.1016/j.surg.2008.02.006
6. Chiang F-Y, Lee K-W, Chen H-C, Chen H-Y, Lu I-C, Kuo W-R, et al. Standardization of Intraoperative Neuromonitoring of Recurrent Laryngeal Nerve in Thyroid Operation. *World J Surg* (2010) 34(2):223–9. doi: 10.1007/s00268-009-0316-8
7. Dralle H, Sekulla C, Lorenz K, Brauckhoff M, Machens A. Intraoperative Monitoring of the Recurrent Laryngeal Nerve in Thyroid Surgery. *World J Surg* (2008) 32(7):1358–66. doi: 10.1007/s00268-008-9483-2
8. Tomoda C, Hirokawa Y, Uruno T, Takamura Y, Ito Y, Miya A, et al. Sensitivity and Specificity of Intraoperative Recurrent Laryngeal Nerve Stimulation Test for Predicting Vocal Cord Palsy After Thyroid Surgery. *World J Surg* (2006) 30(7):1230–3. doi: 10.1007/s00268-005-0351-z
9. Hamelmann W, Meyer T, Timm S, Timmermann W. Kritische Beurteilung Und Fehlermöglichkeiten Des Intraoperativen Neuromonitoring (IONM) Bei Operationen an Der Schilddrüse. *Zentralbl Für Chirurgie* (2002) 127(05):409–13. doi: 10.1055/s-2002-31982
10. Hermann M, Hellebart C, Freissmuth M. Neuromonitoring in Thyroid Surgery: Prospective Evaluation of Intraoperative Electrophysiological Responses for the Prediction of Recurrent Laryngeal Nerve Injury. *Ann Surg* (2004) 240(1):9. doi: 10.1097/01.sla.0000132260.34503.02
11. Thomusch O, Sekulla C, Machens A, Neumann H-J, Timmermann W, Dralle H. Validity of Intra-Operative Neuromonitoring Signals in Thyroid Surgery. *Langenbeck's Arch Surg* (2004) 389(6):499–503. doi: 10.1007/s00423-003-0444-9
12. Beldi G, Kinsbergen T, Schlumpf R. Evaluation of Intraoperative Recurrent Nerve Monitoring in Thyroid Surgery. *World J Surg* (2004) 28(6):589–91. doi: 10.1007/s00268-004-7226-6
13. Chan W-F, Lo C-Y. Pitfalls of Intraoperative Neuromonitoring for Predicting Postoperative Recurrent Laryngeal Nerve Function During Thyroidectomy. *World J Surg* (2006) 30(5):806–12. doi: 10.1007/s00268-005-0355-8
14. Schneider R, Randolph GW, Dionigi G, Wu CW, Barczynski M, Chiang FY, et al. International Neural Monitoring Study Group Guideline 2018 Part I: Staging Bilateral Thyroid Surgery With Monitoring Loss of Signal. *Laryngoscope* (2018) 128:S1–S17. doi: 10.1002/lary.27359
15. Wu C-W, Wang M-H, Chen C-C, Chen H-C, Chen H-Y, Yu J-Y, et al. Loss of Signal in Recurrent Nerve Neuromonitoring: Causes and Management. *Gland Surg* (2015) 4(1):19. doi: 10.3978/j.issn.2227-684X.2014.12.03
16. Randolph GW, Dralle H, Group IIMS, Abdullah H, Barczynski M, Bellantone R, et al. Electrophysiologic Recurrent Laryngeal Nerve Monitoring During Thyroid and Parathyroid Surgery: International Standards Guideline Statement. *Laryngoscope* (2011) 121(S1):S1–S16. doi: 10.1002/lary.21119
17. Wu C-W, Hao M, Tian M, Dionigi G, Tufano RP, Kim HY, et al. Recurrent Laryngeal Nerve Injury With Incomplete Loss of Electromyography Signal During Monitored Thyroidectomy—Evaluation and Outcome. *Langenbeck's Arch Surg* (2017) 402(4):691–9. doi: 10.1007/s00423-016-1381-8
18. Wojtczak B, Sutkowski K, Kaliszewski K, Głód M, Barczyński M. Experience With Intraoperative Neuromonitoring of the Recurrent Laryngeal Nerve Improves Surgical Skills and Outcomes of non-Monitored Thyroidectomy. *Langenbeck's Arch Surg* (2017) 402(4):709–17. doi: 10.1007/s00423-016-1449-5
19. Chiang FY, Lu IC, Chang PY, Dionigi G, Randolph GW, Sun H, et al. Comparison of EMG Signals Recorded by Surface Electrodes on Endotracheal Tube and Thyroid Cartilage During Monitored Thyroidectomy. *Kaohsiung J Med Sci* (2017) 33(10):503–9. doi: 10.1016/j.kjms.2017.06.014
20. Chiang F-Y, Wu C-W, Chang P-Y, Wu S-H, Chen H-Y, Lin Y-C, et al. Trans-Thyroid Cartilage Recording for Neural Monitoring of the Recurrent Laryngeal Nerve in Thyroid Surgery. *Laryngoscope* (2020) 130(4):E280–E3. doi: 10.1002/lary.28049
21. Behm D, Whittle J, Button D, Power K. Intermuscle Differences in Activation. *Muscle Nerve* (2002) 25(2):236–43. doi: 10.1002/mus.10008
22. Roberts TJ, Gabaldón AM. Interpreting Muscle Function From EMG: Lessons Learned From Direct Measurements of Muscle Force. *Integr Comp Biol* (2008) 48(2):312–20. doi: 10.1093/icb/icn056

23. Genther DJ, Kandil EH, Noureldine SI, Tufano RP. Correlation of Final Evoked Potential Amplitudes on Intraoperative Electromyography of the Recurrent Laryngeal Nerve With Immediate Postoperative Vocal Fold Function After Thyroid and Parathyroid Surgery. *JAMA Otolaryngol Head Neck Surg* (2014) 140(2):124–8. doi: 10.1001/jamaoto.2013.6139
24. Pavier Y, Saroul N, Pereira B, Tauveron I, Gilain L, Mom T. Acute Prediction of Laryngeal Outcome During Thyroid Surgery by Electromyographic Laryngeal Monitoring. *Head Neck* (2015) 37(6):835–9. doi: 10.1002/hed.23676
25. Calò PG, Medas F, Conzo G, Podda F, Canu GL, Gambardella C, et al. Intraoperative Neuromonitoring in Thyroid Surgery: Is the Two-Staged Thyroidectomy Justified? *Int J Surg* (2017) 41:S13–20. doi: 10.1016/j.ijsu.2017.02.001
26. Melin M, Schwarz K, Lammers BJ, Goretzki PE. IONM-Guided Goiter Surgery Leading to Two-Stage Thyroidectomy—Indication and Results. *Langenbeck's Arch Surg* (2013) 398(3):411–8. doi: 10.1007/s00423-012-1032-7
27. Liu C-H, Huang T-Y, Wu C-W, Wang JJ, Wang L-F, Chan L-P, et al. New Developments in Anterior Laryngeal Recording Technique During Neuromonitored Thyroid and Parathyroid Surgery. *Front Endocrinol* (2021) 12. doi: 10.3389/fendo.2021.763170
28. Türk Y, Kıvratma G, Özdemir M, İçöz G, Makay Ö. The Use of Thyroid Cartilage Needle Electrodes in Intraoperative Neuromonitoring During Thyroidectomy: C Ase–Control Study. *Head Neck* (2021) 43(11):3287–93. doi: 10.1002/hed.26810
29. Wu C-W, Chiang F-Y, Randolph GW, Dionigi G, Kim HY, Lin Y-C, et al. Feasibility of Intraoperative Neuromonitoring During Thyroid Surgery Using Transcartilage Surface Recording Electrodes. *Thyroid* (2018) 28(11):1508–16. doi: 10.1089/thy.2017.0680
30. Huang T-Y, Yu W-HV, Chiang F-Y, Wu C-W, Fu S-C, Tai A-S, et al. How the Severity and Mechanism of Recurrent Laryngeal Nerve Dysfunction During Monitored Thyroidectomy Impact on Postoperative Voice. *Cancers* (2021) 13 (21):5379. doi: 10.3390/cancers13215379
31. Huang T-Y, Yu W-HV, Chiang F-Y, Wu C-W, Fu S-C, Tai A-S, et al. Prognostic Indicators of Non-Transection Nerve Injury and Vocal Fold Motion Impairment After Thyroid Surgery–Correlation Between Intraoperative Neuromonitoring Findings and Perioperative Voice Parameters. *Front Endocrinol* (2021) 12. doi: 10.3389/fendo.2021.755231
32. Wu CW, Chai YJ, Dionigi G, Chiang FY, Liu X, Sun H, et al. Recurrent Laryngeal Nerve Safety Parameters of the H Armonic F Ocus During Thyroid Surgery: Porcine Model Using Continuous Monitoring. *Laryngoscope* (2015) 125(12):2838–45. doi: 10.1002/lary.25412
33. Huang TY, Lin YC, Tseng HY, Dionigi G, Kim HY, Chai YJ, et al. Safety Parameters of Ferromagnetic Device During Thyroid Surgery: Porcine Model Using Continuous Neuromonitoring. *Head Neck* (2020) 42(10):2931–40. doi: 10.1002/hed.26334
34. Huang T-Y, Lin Y-C, Tseng H-Y, Dionigi G, Kim H-Y, Lu I-C, et al. Safety of Ligasure Exact Dissector in Thyroidectomy With Continuous Neuromonitoring: A Porcine Model. *Gland Surg* (2020) 9(3):702. doi: 10.21037/gs.2020.03.17
35. Yu X, Liu C, Yan M, Gong W, Wang Y. Hyperthermal Liquid, Spray, and Smog may be Potential Risk Factors for Recurrent Laryngeal Nerve Thermal Injury During Thyroid Surgeries. *Endocrine* (2021) 72(1):198–207. doi: 10.1007/s12020-020-02451-w
36. Lin YC, Dionigi G, Randolph GW, Lu IC, Chang PY, Tsai SY, et al. Electrophysiologic Monitoring Correlates of Recurrent Laryngeal Nerve Heat Thermal Injury in a Porcine Model. *Laryngoscope* (2015) 125(8): E283–E90. doi: 10.1002/lary.25362
37. Seehofer D, Mogl M, Boas-Knoop S, Unger J, Schirmeier A, Chopra S, et al. Safety and Efficacy of New Integrated Bipolar and Ultrasonic Scissors Compared to Conventional Laparoscopic 5-Mm Sealing and Cutting Instruments. *Surg Endosc* (2012) 26(9):2541–9. doi: 10.1007/s00464-012-2229-0

Conflict of Interest: The authors declare that the research was conducted in the absence of any commercial or financial relationships that could be construed as a potential conflict of interest.

frontiers | Frontiers in Endocrinology

ORIGINAL RESEARCH
published: 05 July 2022
doi: 10.3389/fendo.2022.916121

A Novel and Effective Model to Predict Skip Metastasis in Papillary Thyroid Carcinoma Based on a Support Vector Machine

Shuting Zhu[1†], Qingxuan Wang[2†], Danni Zheng[3†], Lei Zhu[4], Zheng Zhou[5], Shiying Xu[6], Binbin Shi[7], Cong Jin[3], Guowan Zheng[8,9] and Yefeng Cai[2,8,9*]*

[1] Department of Ultrasound, The First Medical Center of Chinese People's Liberation Army (PLA) General Hospital, Beijing, China, [2] Department of Thyroid Surgery, The First Affiliated Hospital of Wenzhou Medical University, Wenzhou, China, [3] Department of Breast Surgery, The First Affiliated Hospital of Wenzhou Medical University, Wenzhou, China, [4] Thyroid Surgery Department, The Fifth Hospital Affiliated to Wenzhou Medical University, Lishui Central Hospital, Lishui, China, [5] Department of Head and Neck Surgery, Bengbu Medical College Graduate School, Anhui, China, [6] Zhejiang Chinese Medical University, The Second Clinical Medical, Hangzhou, China, [7] Department of Medical Ultrasound,the First Affiliated Hospital of Wenzhou Medical University, Wenzhou, China, [8] Department of Head and Neck Surgery, Otolaryngology & Head and Neck Center, Cancer Center, Zhejiang Provincial People's Hospital (Affiliated People's Hospital, Hangzhou Medical College), Hangzhou, China, [9] Key Laboratory of Endocrine Gland Diseases of Zhejiang Province, Hangzhou, China

Introduction: Skip metastasis, referred to as lymph node metastases to the lateral neck compartment without involvement of the central compartment, is generally unpredictable in papillary thyroid carcinoma (PTC). This study aims to establish an effective predictive model for skip metastasis in PTC.

Meterials and Methods: Retrospective analysis was performed of clinical samples from 18192 patients diagnosed with thyroid cancer between 2016 to 2020. The First Affiliated Hospital of Wenzhou Medical University. The lateral lymph node metastasis was occureed in the training set (630 PTC patients) and validation set (189 PTC patients). The univariate and multivariate analyses were performed to detect the predictors of skip metastasis and the support vector machine (SVM) was used to establish a model to predict skip metastasis.

Results: The rate of skip metastasis was 13.3% (84/631). Tumor size (≤10 mm), upper location, Hashimoto's thyroiditis, extrathyroidal extension, absence of BRAFV600E mutation, and less number of central lymph node dissection were considered as independent predictors of skip metastasis in PTC. For the training set, these predictors performed with 91.7% accuracy, 86.4% sensitivity, 92.2% specificity, 45.2% positive predictive value (PPV), and 98.9% negative predictive value (NPV) in the model. Meanwhile, these predictors showed 91.5% accuracy,71.4% sensitivity, 93.1% specificity, 45.5% PPV, and 97.6% NPV in validation set.

OPEN ACCESS

Edited by:
Gianlorenzo Dionigi, University of Milan, Italy

Reviewed by:
Yin Detao, First Affiliated Hospital of Zhengzhou University, China
Ning Qu, Fudan University, China
Fei-lin Cao, Zhejiang Taizhou Hospital, China
Pu Cheng, Zhejiang University, China

***Correspondence:**
Guowan Zheng
0818331@163.com
Yefeng Cai
Cyfoncology@gmail.com

†These authors have contributed equally to this work

Specialty section:
This article was submitted to Thyroid Endocrinology, a section of the journal Frontiers in Endocrinology

Received: *08 April 2022*
Accepted: *01 June 2022*
Published: *05 July 2022*

Citation:
Zhu S, Wang Q, Zheng D, Zhu L, Zhou Z, Xu S, Shi B, Jin C, Zheng G and Cai Y (2022) A Novel and Effective Model to Predict Skip Metastasis in Papillary Thyroid Carcinoma Based on a Support Vector Machine. Front. Endocrinol. 13:916121. doi: 10.3389/fendo.2022.916121

Conclusion: This study screened the predictors of the skip lateral lymph node metastasis and to establish an effective and economic predictive model for skip metastasis in PTC. The model can accurately distinguish the skip metastasis in PTC using a simple and affordable method, which may have potential for daily clinical application in the future.

Keywords: predict model, skip lymph node metastasis, papillary thyroid carcinoma, support vector, BRAF mutation

INTRODUCTION

The incidence of thyroid cancer has remarkably increased in the last 40 years worldwide primarily because of the increase in the incidence of papillary thyroid carcinoma (PTC) (1). Papillary thyroid carcinoma, a common endocrine malignancy, accounts for 90% of thyroid cancer (2, 3). The dissemination of PTC cells follows a predictable stepwise pattern, metastasizing from the central lymph node (CLN) compartment to the lateral lymph node (LLN) compartment (4, 5). Thus, CLN is considered as the first step of lymphatic drainage of PTC in most previous studies (6, 7). However, lateral lymph node metastasis (LLNM) of PTC without central lymph node metastasis (CLNM) is also found (8). This unpredictable pattern of LNM is known as skip metastasis of PTC.

Skip metastasis is not unique to PTC. This metastatic form without stepwise spread also exists in gastric, colorectal, lung, and breast carcinoma (9–12). Giving inadequate attention to any tumor may adversely affect treatment outcomes and cause poor prognosis. In addition, skip metastasis is not a rare phenomenon. For example, skip metastasis of gastrointestinal cancer is frequent because the location of the lymphatic drainage tract is complicated (13). Skip metastasis is also common in PTC, and its incidence ranges from 5% to 25% (the data are obtained from different samples) (14).

Some studies have suggested that regional lymph node metastasis (LNM) is a vital factor in poor prognosis of patients with PTC (15). In addition, LLNM has shown stronger connection with locoregional recurrence and unfavorable prognosis than CLNM in patients with PTC (16). However, whether skip LNM is associated with a relatively poor prognosis remains unclear (14). Some studies show that LNM can increase the risk of lymph node recurrence, and the reoperation of recurrence can increase operative complications and medical costs to some degree (17–19). Therefore, skip metastasis in clinical diagnosis and treatment must be given importance to avoid risks as much as possible.

Preoperative ultrasonographic evaluation and biopsy results of cervical lymph nodes primarily determined the operative mode of PTC. Suspicious and/or biopsy-proven nodal metastases should be treated with a formal compartmental resection (20). Therefore, the neglect of skip metastasis may lead to incomplete surgical resection. However, few effective methods to predict skip metastasis in PTC were identified. Therefore, our study investigated the frequency and risk factors for skip metastasis and established a model to predict skip metastasis, make a reasonable surgical project or follow-up plan, and achieve treatment effectiveness.

Abbreviations: PTC, papillary thyroid carcinoma; SVM, support vector machine; CLN, central lymph node; LLN, lateral lymph node; CLNM, central lymph node metastasis; LLNM, lateral lymph node metastasis; CLND, central lymph node dissection; LLND, lateral lymph node dissection; CI, confidence interval; OR, odds ratio; PPV, positive predictive value; NPV, negative predictive value.

MATERIALS AND METHODS

Patients

Two sets of patients were included in the training set and validation set. Patients in the training set were used to investigate the predictors of skip metastasis and to establish predictive models, whereas patients in the validation set were used to examine the efficacy of the predictive models. A total 631 patients with PTC who received initial thyroidectomy with central lymph node dissection (CLND) plus lateral lymph node dissection (LLND) at the First Affiliated Hospital of Wenzhou Medical University during January 2016 to September 2019 were included in the training set. Meanwhile, 189 external patients who received the same surgical procedure during October 2019 to June 2020 were included in the validation set (**Figure 1**). All of the patients were identified as PTC with LLNM by postoperative pathological report. Each set was further divided into the skip metastasis group and non-skip metastasis group.

The exclusion criteria were as follows: insufficient data or unknown clinicopathologic profile, undetermined histology, history of neck surgery or irradiation, negative lateral lymph node metastases, and other types of thyroid cancer (follicular thyroid cancer, medullary thyroid cancer, anaplastic thyroid cancer, etc.). The study obtained approval from the Ethics Committee of the First Affiliated Hospital of Wenzhou Medical University.

Operational Approach

The operation was performed by the same experienced surgical team and the same standard procedure. The scope of CLND was up to the thyroid cartilage notch, down to the carotid sheath, posterior to the prevertebral fascia, and final to the innominate vein. In this study, the lateral lymph node compartment included levels II, III, IV, and V. The area was drawn up to the posterior belly of the digastric muscle, down to the subclavian vein, and next to the anterior border of the trapezius muscle.

Parameter Analysis

Our study collected information through electronic clinical records, pathological records, and preoperative ultrasonographic images. Patient's baseline information (gender and age) and

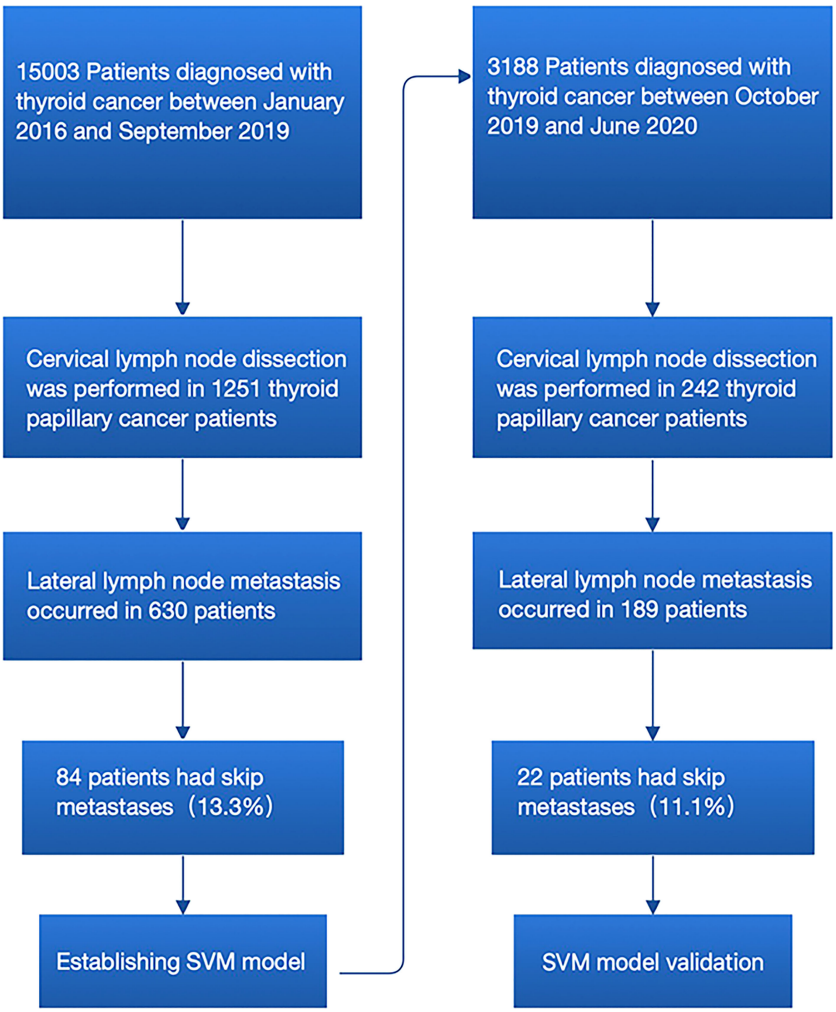

FIGURE 1 | Flowchart for the process of establishment and validation of skip metastasis prediction model of PTC.

clinical data (hashimoto's thyroiditis, body mass index [BMI], metabolic syndrome, hypertension, and diabetes) were analyzed. In addition, the thyroid nodule sonographic features were evaluated and analyzed, by three experienced sonographers, on the basis of the size of tumor, location, margin, taller-than-wide shape, calcification, vascularization, multifocality, extrathyroidal extension, and the information about cervical lymph node. The information about $BRAF^{V600E}$ mutation was collected as well.

We analyzed the largest tumor or the most suspicious dominant nodule of the thyroid, when multiple nodules were found. Standard preoperative sonography of PTC tumor boundaries was performed to determine the size, and taller-than-wide shape. Moreover, the thyroid gland was trisected vertically, dividing it into three locations (upper, middle, and lower) to determine the location of tumors. Calcification was defined as the hyperechoic spots with or without acoustic shadows or as simple fine acoustic shadows in ultrasound (21). The multifocality of a tumor was confirmed when more than one mass was found based on the preoperative ultrasound examination or the intraoperative pathological diagnose (22). Extrathyroidal extension was defined as the tumor perimeter in contact with >25% of the thyroid capsule in a malignant lesion or the loss of the capsule line (23). The diagnosis of hashimoto's thyroiditis relies on the demonstration of circulating antibodies to thyroid antigens (mainly anti-thyroglobulin >30U/ml (normal range is 0-4U/ml); anti-thyroperoxidase (anti-TPO) >30U/ml) (normal range is 0-9U/ml) and reduced echogenicity and prominent heterogeneous thyroid parenchyma on thyroid sonogram in a patient with proper clinical features (24). The information of cervical lymph node was obtained from the final pathological reports.

Model Development

A support vector machine (SVM) was used for establishing skip metastasis prediction models. The prediction models were established by Libsvm 3.20 with the modeling platform of MATLAB 2019a. The C-SVC, RBF kernel functions and grid search method were used to debug the model. The grid c bound,

grid c step, grid g bound, and grid g step were −8 to 8, 0.5, −8 to 8, and 0.5, respectively. The fold number of cross-validation was 5. As we divided patients into two groups, the positive value indicated skip metastasis, and the negative value indicated non-skip metastasis.

$$P(label) = \mathbf{sgn}(\sum_{n=1}^{\infty} ni = (0\mathbf{wi}\ \ \mathbf{exp}(-\mathbf{ganma}|\mathbf{xi} - \mathbf{x}|2 + \mathbf{b})))$$

Statistics

The data showed a normal distribution through an independent two-sample Student's t-test. Statistical analysis was performed using SPSS version 26.0 (SPSS, Chicago, IL, USA). Categorical variables were compared with the results of Chi-square test or Fisher's exact test. The difference between two sides was statistically significant, when P value ≤ 0.05. All factors with significant associations based on univariate analysis were included for multivariate analysis using forward stepwise selection.

RESULTS

The Baseline Information in the Training and Validation Set

1. Gender: The female percent is 67.6% (426/630) in the training set and 61.9% (117/189) in the validation set.
2. Age: The average age of training set is 45.28 ± 12.48 years (range, 17–84 years), and that of the validation set is 46.69 ± 12.11 years (range, 21–74 years).
3. The size of a primary tumor: the mean size is 14.25 ± 8.88 mm (range, 1–67mm) and 12.25 ± 7.74 mm (range, 1–40mm) in the training set and validation set, respectively.
4. The mean number of total harvested CLN is 7.57 ± 5.71 (range, 1–28) in the training set and 6.95 ± 5.18 (range, 1–35) in the validation set.
5. The rate of skip metastasis is 13.3% (84/630) in the training test and 11.6% (22/189) in the validation set.
6. The rate of $BRAF^{V600E}$ mutation is 75.1% (473/630) in the training test and 82.0% (155/189) in the validation set (**Table S1**).

Predictors of Skip Metastasis of PTC in the Training Set

Data from the training set were used to investigate the predictors of skip metastasis in PTC. The first step of analysis was comparing the clinicopathological factors between the skip metastasis group and non-skip metastasis by univariate analysis. The following characteristics of patients were more likely observed in the skip metastasis group (**Table 1**): age>45 (P=0.008), tumor size ≤ 10 mm (P=0.001), Hashimoto's thyroiditis (P=0.009), upper tumor location (P<0.001), well-defined margin (P=0.05), extrathyroidal extension (P=0.002), absence of $BRAF^{V600E}$ mutations (P=0.006), BMI≥25 (P=0.024), and less number of CLND (the mean number of the skip metastasis was 5.17 ± 3.81, P=0.001).

Further multivariate analysis showed that tumor size (≤10 mm; OR 2.331; P=0.003; 95% CI 1.342–4.049), upper location (OR 2.595; P<0.001; CI 1.535–4.388), Hashimoto's thyroiditis (OR 3.968; P<0.001; CI 2.178–7.229), extrathyroidal extension (OR 3.506; P<0.001; CI 1.962–6.265), absence of $BRAF^{V600E}$ mutation (OR 0.373; P<0.001; CI 0.212–0.658), and less number of CLND (OR 1.304; P<0.001; CI 1.193–1.423) were independent predictors of skip metastasis in PTC (**Table 2**). As mentioned previously, a difference in BMI values and well-defined margin was found between the skip metastasis group and non-skip metastasis group in univariate analysis. No further evidence indicated that such characteristics were independent predictors of skip metastasis in PTC.

Information about LLN Between the Skip Metastasis Group and Non-skip Metastasis Group

In addition, the information about LLN between the skip metastasis group and non-skip metastasis group was compared (**Table 3**). We found that the number of LLNM of skip metastasis was less than that of non-skip metastasis (mean 2.04 ± 1.71 and 3.30 ± 2.59, respectively; P<0.001). No contralateral LLNM was found in 84 patients with skip metastasis, whereas 26 patients in the non-skip metastasis group showed contralateral LLNM. Therefore, the difference in contralateral LLNM was found between the two groups (P=0.037). By contrast, no difference was found in the number of LLND between the two groups (P=0.509).

Training Set: Establishing a Model to Predict Skip Metastasis

The predictive panel was built using SVM, which combined the six independent predictors (tumor size, location, Hashimoto's thyroiditis, extrathyroidal extension, $BRAF^{V600E}$ mutation, and number of CLND). In addition, skip metastasis in the training set was predicted by this panel (**Table 4**). These predictors performed with high 91.7% accuracy in the panel (sensibility: 86.4%, specificity: 92.2%, positive predictive value [PPV]: 45.2%, negative predictive value [NPV]: 98.9%), albeit the accuracy of each individual factor was low (**Table 5**). Parameters c, g, and b were 16, 0.0884, and −0.5531, respectively, which were used to make the 3D view (**Figure 2**).

Validation Set: Validating the Model in External Independent Samples

The 189 (22 skip metastasis and 167 non-skip metastasis) external independent samples were used to validate panel performance. The panel also achieved high accuracy in the validation set, with 91.5% accuracy (173/189 samples correctly classified, **Table 4**). Moreover, the specificity and NPV maintained a highly level, 93.1% and 97.6, respectively, in the validation set. On the contrary, the sensitivity and PPV were slightly decreased (71.4% and 45.5%, respectively). The AUC (Area under the curve) of SVM model in ROC Curve is 0.721 (**Figure 3**).

TABLE 1 | Comparison of clinicopathological factors between skip metastasis and non-skip metastasis with PTC. .

Characteristics	Skip metastasis		F	P value
	Present (n=84)	Absent (n=546)		
Sex			2.412	0.12
Male (n, %)	21 (25.0%)	183 (33.5%)		
Female (n, %)	63 (75.0%)	363 (66.5%)		
Age at diagnosis (years)	49.55 ± 11.73	44.62 ± 12.48	6.995	0.008*
≤45 (n, %)	33 (39.3%)	299 (54.8%)		
>45 (n, %)	51 (60.7%)	247 (45.2%)		
Tumor size (mm)	12.83 ± 8.85	14.47 ± 8.87	10.859	0.001*
≤10 (n, %)	50 (59.5%)	217 (39.9%)		
>10 (n, %)	34 (40.5%)	329 (60.1%)		
Multifocality (n,%)			3.249	0.071
Yes (n, %)	21 (25%)	191 (35.0%)		
No (n, %)	63 (75%)	355 (65.0%)		
Hashimoto's thyroiditis			6.784	0.009*
Yes (n, %)	29 (34.5%)	118 (21.6%)		
No (n, %)	55 (65.5%)	428 (78.4%)		
Tumor location			15.066	<0.001*
Upper (n, %)	41 (48.8%)	152 (27.8%)		
Lower/middle/isthmus (n, %)	43 (51.2%)	394 (72.2%)		
Taller than wide			0.74	0.39
Yes (n, %)	17 (20.2%)	134 (24.5%)		
No (n, %)	67 (79.7%)	412 (73.4%)		
Calcification			0.873	0.35
Calcification (n, %)	68 (81.0%)	462 (84.6%)		
Absence (n, %)	16 (19.0%)	84 (15.4%)		
Margin			3.369	0.05*
Well-defined (n, %)	63 (73.8%)	333 (61.0%)		
Without well-defined margin (n, %)	21 (26.2%)	213 (38.5%)		
Shape			1.365	0.243
Regular (n, %)	20 (23.8%)	164 (30.0%)		
Irregular (n, %)	64 (76.2%)	382 (70.0%)		
Extrathyroidal extension			10.077	0.002*
Yes (n, %)	35 (41.7%)	137 (25.1%)		
No (n, %)	49 (58.3%)	409 (74.9%)		
Vascularization			1.715	0.19
Present (n, %)	13 (15.5%)	58 (10.6%)		
Absence (n, %)	71 (84.5%)	488 (89.4%)		
$BRAF^{V600E}$			7.44	0.006*
Mutation (n, %)	53 (63.1%)	420 (76.9%)		
No mutation (n, %)	31 (26.7%)	126 (23.1%)		
BMI			5.065	0.024*
<25 (n, %)	50 (59.5%)	391 (71.6%)		
≥25 (n, %)	34 (40.5%)	155 (28.4%)		
hypertension			0.963	0.326
Yes (n, %)	19 (22.6%)	99 (18.3%)		
No (n, %)	65 (77.3%)	447 (81.9%)		
diabetes			0.856	0.355
Yes (n, %)	6 (7.1%)	26 (4.8%)		
No (n, %)	78 (92.9%)	520 (95.2%)		
Metabolic syndrome			2.097	0.148
Yes (n, %)	18 (21.4%)	83 (15.2%)		
No (n, %)	66 (78.6%)	463 (84.8%)		
Cervical lymphadenopathy			0.826	0.363
Yes (n, %)	54 (64.3%)	378 (69.2%)		
No (n, %)	30 (35.7%)	168 (30.8%)		
Central lymph nodes dissected number	5.17 ± 3.81	6.73 ± 3.79	3.269	0.001*

**P value ≤ 0.05.*

DISCUSSION

To date, PTC in 30%–80% of patients was accompanied by other forms of LNM (6). PTC with LNM was linked to local recurrence and cancer-specific mortality in certain patients (5, 25). The complications from re-operation of PTC, for example, hemorrhage, hypothyroidism, laryngeal nerve injury, and lymphatic leakage, were increased compared with the initial operation. Therefore, predicting LNM is important for surgeons to precisely determine neck dissections.

TABLE 2 | Multivariate analysis between the clinicopathologic factors and skip metastasis.

Characteristic	OR	95% CI	P value
Tumor size (≤10 mm)	2.331	1.342-4.049	0.003*
Extrathyroidal extension	3.506	1.962-6.265	<0.001*
Hashimoto's thyroiditis	3.968	2.178-7.229	<0.001*
BRAFV600E mutation	0.373	0.212-0.658	0.001*
locating in the upper pole	2.595	1.535-4.388	<0.001*
Less CLND number	1.304	1.193-1.423	<0.001*

**P value ≤ 0.05.*

TABLE 3 | Comparison of LLN between skip metastasis and non-skip metastasis with PTC.

	Skip metastasis		F/t value	P Value
	Present (n = 84)	Absent (n = 546)		
The number of LLND (Mean ± SD)	10.79 ± 7.34	11.43 ± 8.49	-0.611	0.509
The number of LLNM (Mean ± SD)	2.04 ± 1.71	3.30 ± 2.59	-5.816	<0.001*
Contralateral LLNM			Fish Test	0.037*
Yes	0	26		
No	84	526		

**P value ≤ 0.05.*

TABLE 4 | The predictive model and pathological diagnosis for skip metastasis in both training and validation set.

		Predicting Model		
		Positive	Negative	Total
Pathological diagnosis in Train set	positive	38	46	84
	negative	6	540	546
	total	44	586	630
Pathological diagnosis in Test set	positive	10	12	22
	negative	4	163	167
	total	14	175	189

TABLE 5 | The predictive value for the model and independent predictors.

Independent predictors	sensitivity	Specificity	PPV*	NPV*	accuracy
Size	13.8%	87.0%	41.7%	60.1%	57.6%
Location	21.2%	90.2%	48.8%	72.2%	69.0%
Number of central lymph node	20.1%	94.3%	79.8%	51.3%	55.1%
Extrathyroidal extension	20.3%	89.3%	41.7%	74.9%	70.5%
$BRAF^{V600E}$ mutation	19.7%	88.8%	36.9%	76.9%	71.6%
Hashimoto's thyroiditis	19.7%	88.6%	34.5%	78.4%	72.5%
The model	86.4%	92.2%	45.2%	98.9%	91.7%

**PPV, positive predictive value; NPV, negative predictive value.*

The underestimation of skip metastasis of PTC will result in incomplete lymph node dissection during the operation and ultimately lead to a poor prognosis in patients with PTC. However, when the CLN is negative, no further LLND will be performed unless lateral cervical lymphadenopathy is proven by preoperative biopsy and imaging modalities (26). However, a high false negative rate of LLNM by preoperative examination is found (27, 28). For example, about 30% of metastatic lymph nodes in level 3 could not be detected by preoperative examination in previous studies (27). Therefore, accurate assessment of the characteristics and mechanisms of the occurrence of skip metastasis to provide clinical guidance, such as close follow-up or more aggressive surgery, will improve the prognosis of thyroid cancer. In this research, the incidence and detailed characteristics associated with skip metastasis were evaluated by our group.

The reported rate of skip metastasis varies considerably, ranging from 5% to 25% (14). The difference in the frequency

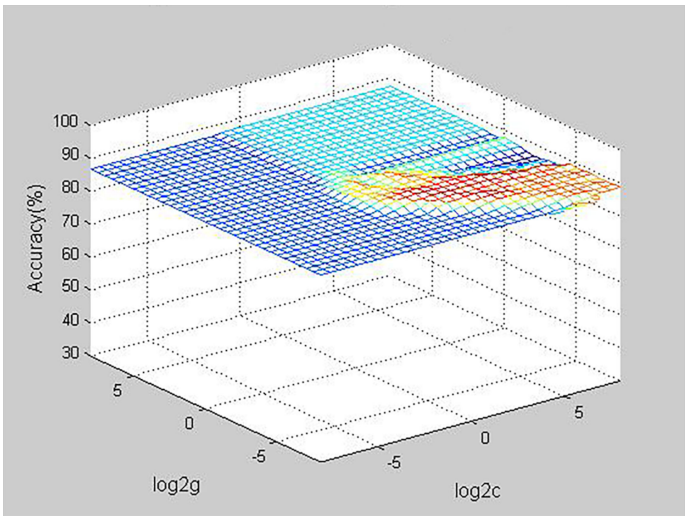

FIGURE 2 | D view of the predictive value for the model (the best parameter c is 16, the parameter g is 0.0884, the parameter b is -0.5531).

of skip metastasis might be due to the different regions and sample sizes. Given the small sample data in most previous studies, the accuracy of data is limited. In our study, we found that the frequency of skip metastasis was 13.3% (84/630), which was the largest sample analysis in skip metastasis. The high rate of skip metastasis indicates that we do not ignore the presence of skip metastasis in the clinical work, although the prognostic relationship between skip metastasis and PTC remains unknown. This form of metastatic spread to regional lymph nodes is also found in other cancer. The non-small-cell lung cancer and colorectal cancer were reported as a prognostic benefit (29, 30). On the contrary, the presence of metastases confers a poor prognosis when synchronous skip metastases are present in osteosarcoma (31). In previous studies, no significant difference in PTC-tumor-free survival was observed between the skip metastasis and non-skip metastasis groups (32). However, these results remain to be verified.

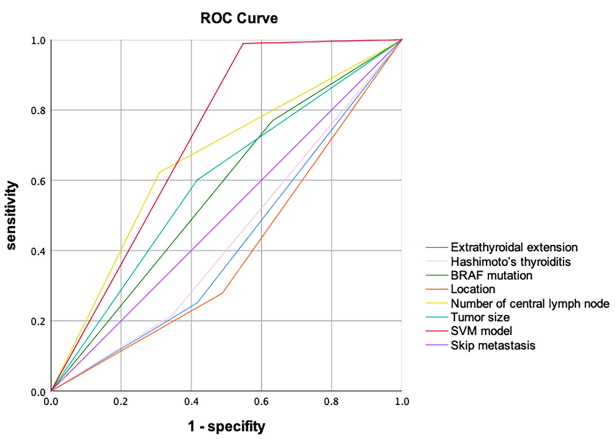

FIGURE 3 | The ROC Curve of the SVM model (The AUC is 0.721).

Machine learning (ML) is type of classifier learning from past date to predict future data. SVM is one of many ML methods (33). Compared to the other ML methods, SVM has very powerful ability to recognize subtle patterns in complex datasets (34). Moreover, Golub et al. had demonstrated the superior performance of SVM in classifying high-dimensional and low sample size data (35). Since 2000, the SVM has been used in many complex classification of cancer study, such as the cancer subtypes, the outcome prognosis, drug benefit prediction, tumorigenesis drivers, or a tumor-specific biological process (36–40). Therefore, in this study, the artificial intelligence of SVM was used to recognize many important factors in a variety of risk characteristics and establish a model to predict skip metastasis in PTC.

In this study, we found six independent predictors (tumor size ≤10 mm, located in the upper pole, Hashimoto's thyroiditis, no $BRAF^{V600E}$ mutation, extrathyroidal extension, and less number of CLND) for skip metastasis in PTC. Some of these clinicopathological or sonographic features were considered as risk factors for skip metastasis in previous studies, but the results were disputed. For example, the positive correlation between upper location and skip metastasis has been shown in many earlier studies (14, 32, 41). This connection may be interpreted by the anatomical structure, which could migrate along the superior thyroid artery to LLN and leap over CLN. Some studies have reported that the skip area in level II or/and III is a predictor of skip metastasis (41, 42). In addition, tumor size ≤ 10 mm, well-defined margin and

extrathyroidal extension were recognized as predictors of skip metastasis (28, 41–43). Furthermore, we observed that skip metastasis could easily occur in PTC patients with Hashimoto's thyroiditis and without $BRAF^{V600E}$ mutation. What's more, the less number of CLND as a predictor was found in both this study and previous studies (44).

To date, the leading causes of skip metastasis are not completely clarified yet. Skip metastasis may be due to the following reasons: first, nodal metastasis bypasses, without normal anatomical lymphatic channels, were observed (14, 45). Thus, less aggressive nodules (tumor size <10 mm) are more easily characterized by skip metastasis as they passes through the metastasis bypasses before invading the central lymph node compartment. Previous reports have suggested that the absence of $BRAF^{V600E}$ mutation and Hashimoto's thyroiditis-positive PTC were associated with a less aggressive disease (43). Second, extrathyroidal extension or neck treatment alters the normal lymphatic channels and induces skip metastasis; In addition, inadequate CLND sampling may cause false negative findings. For example, metastatic lymph node missed during LND could cause a negative finding. Therefore, a less number of CLND is a risk factor of skip metastasis.

A predictive model for skip metastasis was first established in this research. This model has a good performance and high accuracy, indicating its strong clinical feasibility. In addition, the model has high specificity and NPV, which indicates that the model has a high ability to exclude patients with non-skip metastasis. If the model predicts a non-skip metastasis, then the probability that this result is correct is 98.9%. Therefore, patients with non-skip metastasis can be basically excluded when they are predicted negative by this model. Furthermore, although the sensitivity decreased in the validation set (71.4%) compared with the training set (86.4%). The predictive sensitivity of model was significantly higher than that of each single factor. However, the disadvantage of the model's PPV (45.2%) is not obvious. Since there were few guidelines to support perform prophylactic LLND in the cN0 thyroid cancer with high risk of skip metastasis, this model focused on identifying the non-skip metastasis patients and ensure the higher specificity and NPV. Therefore, if the model predicts a high risk of skip metastasis, close follow-up or more aggressive surgery could be considered according to the status of disease.

The current study has several limitations. First, this study is a single-center retrospective study; hence, the results may have some differences from other studies. For further research, we are undertaking a multicenter prospective study. Second, although the model can be more convenient and accurate to guide the operation, whether the model has survival benefits remains unknown. Therefore, more follow-up studies will be conducted in the future.

In conclusion, we found that the rate of skip metastasis was 13.3% (84/631), which was the largest sample analysis so far. We screened six predictors of the skip lateral lymph node metastasis: tumor ≤10 mm, locating in the upper pole, Hashimoto's thyroiditis, extrathyroidal extension, less number of CLND and without $BRAF^{V600E}$ mutation. This study is the first to explore the association of Hashimoto's thyroiditis and $BRAF^{V600E}$ mutation with skip metastasis. Moreover, we established an effective predictive model for skip metastasis in PTC. This model can accurately distinguish the skip metastasis in PTC using a simple and affordable method, which may have the potential for daily clinical application in the future.

DATA AVAILABILITY STATEMENT

The raw data supporting the conclusions of this article will be made available by the authors, without undue reservation.

ETHICS STATEMENT

The studies involving human participants were reviewed and approved by The Ethics Committee of the First Affiliated Hospital of Wenzhou Medical University. The patients/participants provided their written informed consent to participate in this study.

AUTHOR CONTRIBUTIONS

GZ and YC contributed to the conception and design of the research. BS and CJ contributed to collected the clinical information. SZ, QW and DZ contributed to performed the statistical analysis and make the charts. YC, ZZ and SX contributed to establish the model. All authors contributed to manuscript revision, and all authors read and approved the submitted version.

FUNDING

This work was kindly supported by the grant from Major Science and Technology Projects of Zhejiang Province (NO.2015C03052); National Natural Science Foundation of China-Zhejiang Joint Fund (No. U20A20382); National Natural Science Foundation of China (No. 81703575, 82103199, 81827170 and 81802673); Key Research and Development Program of Zhejiang Province (No. 2021C03081).

SUPPLEMENTARY MATERIAL

The Supplementary Material for this article can be found online at: https://www.frontiersin.org/articles/10.3389/fendo.2022.916121/full#supplementary-material

Supplementary Table 1 | The baseline data of training set and validation set.

REFERENCES

1. Bray F, Ferlay J, Soerjomataram I, Siegel RL, Torre LA, Jemal A. Global Cancer Statistics 2018: Globocan Estimates of Incidence and Mortality Worldwide for 36 Cancers in 185 Countries. *CA Cancer J Clin* (2018) 68 (6):394–424. doi: 10.3322/caac.21492
2. Seib CD, Sosa JA. Evolving Understanding of the Epidemiology of Thyroid Cancer. *Endocrinol Metab Clin North Am* (2019) 48(1):23–35. doi: 10.1016/j.ecl.2018.10.002
3. Pellegriti G, Frasca F, Regalbuto C, Squatrito S, Vigneri R. Worldwide Increasing Incidence of Thyroid Cancer: Update on Epidemiology and Risk Factors. *J Cancer Epidemiol* (2013) 2013:965212. doi: 10.1155/2013/965212
4. Machens A, Hinze R, Thomusch O, Dralle H. Pattern of Nodal Metastasis for Primary and Reoperative Thyroid Cancer. *World J Surg* (2002) 26(1):22–8. doi: 10.1007/s00268-001-0176-3
5. Machens A, Holzhausen HJ, Dralle H. Skip Metastases in Thyroid Cancer Leaping the Central Lymph Node Compartment. *Arch Surg* (2004) 139(1):43–5. doi: 10.1001/archsurg.139.1.43
6. Lee YM, Sung TY, Kim WB, Chung KW, Yoon JH, Hong SJ. Risk Factors for Recurrence in Patients With Papillary Thyroid Carcinoma Undergoing Modified Radical Neck Dissection. *Br J Surg* (2016) 103(8):1020–5. doi: 10.1002/bjs.10144
7. Noguchi S, Noguchi A, Murakami N. Papillary Carcinoma of the Thyroid. I. Developing Pattern of Metastasis. *Cancer* (1970) 26(5):1053–60. doi: 10.1002/1097-0142(197011)26:5<1053::aid-cncr2820260513>3.0.co;2-x
8. Gimm O, Rath FW, Dralle H. Pattern of Lymph Node Metastases in Papillary Thyroid Carcinoma. *Br J Surg* (1998) 85(2):252–4. doi: 10.1046/j.1365-2168.1998.00510.x
9. Ilic N, Petricevic A, Arar D, Kotarac S, Banovic J, Ilic NF, et al. Skip Mediastinal Nodal Metastases in the Iiia/N2 Non-Small Cell Lung Cancer. *J Thorac Oncol* (2007) 2(11):1018–21. doi: 10.1097/JTO.0b013e318158d471
10. Zhang C, Zhang L, Xu T, Xue R, Yu L, Zhu Y, et al. Mapping the Spreading Routes of Lymphatic Metastases in Human Colorectal Cancer. *Nat Commun* (2020) 11(1):1993. doi: 10.1038/s41467-020-15886-6
11. Maruyama K, Gunven P, Okabayashi K, Sasako M, Kinoshita T. Lymph Node Metastases of Gastric Cancer. General Pattern in 1931 Patients. *Ann Surg* (1989) 210(5):596–602. doi: 10.1097/00000658-198911000-00005
12. Rosen PP, Lesser ML, Kinne DW, Beattie EJ. Discontinuous or "Skip" Metastases in Breast Carcinoma. Analysis of 1228 Axillary Dissections. *Ann Surg* (1983) 197(3):276–83. doi: 10.1097/00000658-198303000-00006
13. Tangoku A, Seike J, Nakano K, Nagao T, Honda J, Yoshida T, et al. Current Status of Sentinel Lymph Node Navigation Surgery in Breast and Gastrointestinal Tract. *J Med Invest* (2007) 54(1-2):1–18. doi: 10.2152/jmi.54.1
14. Qiu Y, Fei Y, Liu J, Liu C, He X, Zhu N, et al. Prevalence, Risk Factors and Location of Skip Metastasis in Papillary Thyroid Carcinoma: A Systematic Review and Meta-Analysis. *Cancer Manag Res* (2019) 11:8721–30. doi: 10.2147/CMAR.S200628
15. Chow SM, Law SC, Chan JK, Au SK, Yau S, Lau WH. Papillary Microcarcinoma of the Thyroid-Prognostic Significance of Lymph Node Metastasis and Multifocality. *Cancer* (2003) 98(1):31–40. doi: 10.1002/cncr.11442
16. Sywak M, Cornford L, Roach P, Stalberg P, Sidhu S, Delbridge L. Routine Ipsilateral Level Vi Lymphadenectomy Reduces Postoperative Thyroglobulin Levels in Papillary Thyroid Cancer. *Surgery* (2006) 140(6):1000–5; discussion 5-7. doi: 10.1016/j.surg.2006.08.001
17. Wada N, Duh QY, Sugino K, Iwasaki H, Kameyama K, Mimura T, et al. Lymph Node Metastasis From 259 Papillary Thyroid Microcarcinomas: Frequency, Pattern of Occurrence and Recurrence, and Optimal Strategy for Neck Dissection. *Ann Surg* (2003) 237(3):399–407. doi: 10.1097/01.SLA.0000055273.58908.19
18. Nixon IJ, Wang LY, Ganly I, Patel SG, Morris LG, Migliacci JC, et al. Outcomes for Patients With Papillary Thyroid Cancer Who Do Not Undergo Prophylactic Central Neck Dissection. *Br J Surg* (2016) 103 (3):218–25. doi: 10.1002/bjs.10036
19. Shaha AR. Complications of Neck Dissection for Thyroid Cancer. *Ann Surg Oncol* (2008) 15(2):397–9. doi: 10.1245/s10434-007-9724-x
20. Niu XH. [Interpretation of 2020 Nccn Clinical Practice Guidelines in Oncology-Bone Cancer]. *Zhonghua Wai Ke Za Zhi* (2020) 58(6):430–4. doi: 10.3760/cma.j.cn112139-20200204-00061
21. Solbiati L, Cioffi V, Ballarati E. Ultrasonography of the Neck. *Radiol Clin North Am* (1992) 30(5):941–54.
22. Al Afif A, Williams BA, Rigby MH, Bullock MJ, Taylor SM, Trites J, et al. Multifocal Papillary Thyroid Cancer Increases the Risk of Central Lymph Node Metastasis. *Thyroid* (2015) 25(9):1008–12. doi: 10.1089/thy.2015.0130
23. Moon HJ, Kim EK, Yoon JH, Kwak JY. Differences in the Diagnostic Performances of Staging Us for Thyroid Malignancy According to Experience. *Ultrasound Med Biol* (2012) 38(4):568–73. doi: 10.1016/j.ultrasmedbio.2012.01.002
24. Caturegli P, De Remigis A, Rose NR. Hashimoto Thyroiditis: Clinical and Diagnostic Criteria. *Autoimmun Rev* (2014) 13(4-5):391–7. doi: 10.1016/j.autrev.2014.01.007
25. Zhang L, Wei WJ, Ji QH, Zhu YX, Wang ZY, Wang Y, et al. Risk Factors for Neck Nodal Metastasis in Papillary Thyroid Microcarcinoma: A Study of 1066 Patients. *J Clin Endocrinol Metab* (2012) 97(4):1250–7. doi: 10.1210/jc.2011-1546
26. Haugen BR. 2015 American Thyroid Association Management Guidelines for Adult Patients With Thyroid Nodules and Differentiated Thyroid Cancer: What Is New and What Has Changed? *Cancer* (2017) 123(3):372–81. doi: 10.1002/cncr.30360
27. Fraser S, Zaidi N, Norlen O, Glover A, Kruijff S, Sywak M, et al. Incidence and Risk Factors for Occult Level 3 Lymph Node Metastases in Papillary Thyroid Cancer. *Ann Surg Oncol* (2016) 23(11):3587–92. doi: 10.1245/s10434-016-5254-8
28. Lim YS, Lee JC, Lee YS, Lee BJ, Wang SG, Son SM, et al. Lateral Cervical Lymph Node Metastases From Papillary Thyroid Carcinoma: Predictive Factors of Nodal Metastasis. *Surgery* (2011) 150(1):116–21. doi: 10.1016/j.surg.2011.02.003
29. Li X, Li X, Fu X, Liu L, Liu Y, Zhao H, et al. Survival Benefit of Skip Metastases in Surgically Resected N2 Non-Small Cell Lung Cancer: A Multicenter Observational Study of a Large Cohort of the Chinese Patients. *Eur J Surg Oncol* (2020) 46(10 Pt A):1874–81. doi: 10.1016/j.ejso.2019.12.015
30. Shiozawa M, Akaike M, Yamada R, Godai T, Yamamoto N, Saito H, et al. Clinicopathological Features of Skip Metastasis in Colorectal Cancer. *Hepatogastroenterology* (2007) 54(73):81–4.
31. Yang P, Gilg M, Evans S, Totti F, Stevenson J, Jeys L, et al. Survival of Osteosarcoma Patients Following Diagnosis of Synchronous Skip Metastases. *J Orthop* (2020) 18:121–5. doi: 10.1016/j.jor.2019.10.003
32. Feng JW, Qin AC, Ye J, Pan H, Jiang Y, Qu Z. Predictive Factors for Lateral Lymph Node Metastasis and Skip Metastasis in Papillary Thyroid Carcinoma. *Endocr Pathol* (2020) 31(1):67–76. doi: 10.1007/s12022-019-09599-w
33. Cruz JA, Wishart DS. Applications of Machine Learning in Cancer Prediction and Prognosis. *Cancer Inform* (2007) 2:59–77. doi: 10.1177/117693510600200030
34. Huang S, Cai N, Pacheco PP, Narrandes S, Wang Y, Xu W. Applications of Support Vector Machine (Svm) Learning in Cancer Genomics. *Cancer Genomics Proteomics* (2018) 15(1):41–51. doi: 10.21873/cgp.20063
35. Golub TR, Slonim DK, Tamayo P, Huard C, Gaasenbeek M, Mesirov JP, et al. Molecular Classification of Cancer: Class Discovery and Class Prediction by Gene Expression Monitoring. *Science* (1999) 286(5439):531–7. doi: 10.1126/science.286.5439.531
36. Alexander EK, Kennedy GC, Baloch ZW, Cibas ES, Chudova D, Diggans J, et al. Preoperative Diagnosis of Benign Thyroid Nodules With Indeterminate Cytology. *N Engl J Med* (2012) 367(8):705–15. doi: 10.1056/NEJMoa1203208
37. Furey TS, Cristianini N, Duffy N, Bednarski DW, Schummer M, Haussler D. Support Vector Machine Classification and Validation of Cancer Tissue Samples Using Microarray Expression Data. *Bioinformatics* (2000) 16 (10):906–14. doi: 10.1093/bioinformatics/16.10.906
38. Moler EJ, Chow ML, Mian IS. Analysis of Molecular Profile Data Using Generative and Discriminative Methods. *Physiol Genomics* (2000) 4(2):109–26. doi: 10.1152/physiolgenomics.2000.4.2.109
39. Segal NH, Pavlidis P, Antonescu CR, Maki RG, Noble WS, DeSantis D, et al. Classification and Subtype Prediction of Adult Soft Tissue Sarcoma by Functional Genomics. *Am J Pathol* (2003) 163(2):691–700. doi: 10.1016/S0002-9440(10)63696-6
40. Shen Y, Lai Y, Xu D, Xu L, Song L, Zhou J, et al. Diagnosis of Thyroid Neoplasm Using Support Vector Machine Algorithms Based on Platelet Rna-Seq. *Endocrine* (2021) 72(3):758–83. doi: 10.1007/s12020-020-02523-x
41. Zhao H, Huang T, Li H. Risk Factors for Skip Metastasis and Lateral Lymph Node Metastasis of Papillary Thyroid Cancer. *Surgery* (2019) 166(1):55–60. doi: 10.1016/j.surg.2019.01.025
42. Nie X, Tan Z, Ge M. Skip Metastasis in Papillary Thyroid Carcinoma Is Difficult to Predict in Clinical Practice. *BMC Cancer* (2017) 17(1):702. doi: 10.1186/s12885-017-3698-2

43. Lei J, Zhong J, Jiang K, Li Z, Gong R, Zhu J. Skip Lateral Lymph Node Metastasis Leaping Over the Central Neck Compartment in Papillary Thyroid Carcinoma. *Oncotarget* (2017) 8(16):27022–33. doi: 10.18632/oncotarget.15388
44. Jin WX, Jin YX, Ye DR, Zheng ZC, Sun YH, Zhou XF, et al. Predictive Factors of Skip Metastasis in Papillary Thyroid Cancer. *Med Sci Monit* (2018) 24:2744–9. doi: 10.12659/MSM.907357
45. Lim YC, Koo BS. Predictive Factors of Skip Metastases to Lateral Neck Compartment Leaping Central Neck Compartment in Papillary Thyroid Carcinoma. *Oral Oncol* (2012) 48(3):262–5. doi: 10.1016/j.oraloncology.2011.10.006

Conflict of Interest: The authors declare that the research was conducted in the absence of any commercial or financial relationships that could be construed as a potential conflict of interest.

frontiers | Frontiers in Endocrinology

TYPE Original Research
PUBLISHED 22 July 2022
DOI 10.3389/fendo.2022.918741

OPEN ACCESS

EDITED BY
Gianlorenzo Dionigi,
University of Milan, Italy

REVIEWED BY
Nada Santrac,
Institute of Oncology and Radiology of Serbia, Serbia
Che-Wei Wu,
Kaohsiung Medical University, Taiwan
Zhuoying Wang,
Shanghai Jiao Tong University, China
Yu-Long Wang,
Fudan University, China

*CORRESPONDENCE
Jugao Fang
fangjugao@163.com

†These authors have contributed equally to this work

SPECIALTY SECTION
This article was submitted to Thyroid Endocrinology, a section of the journal Frontiers in Endocrinology

RECEIVED 12 April 2022
ACCEPTED 30 June 2022
PUBLISHED 22 July 2022

CITATION
Shi Q, Xu J, Fang J, Zhong Q, Chen X, Hou L, Ma H, Feng L, He S, Lian M and Wang R (2022) Clinical advantages and neuroprotective effects of monitor guided fang's capillary fascia preservation right RLN dissection technique. *Front. Endocrinol.* 13:918741. doi: 10.3389/fendo.2022.918741

Clinical advantages and neuroprotective effects of monitor guided fang's capillary fascia preservation right RLN dissection technique

Qian Shi†, Jiaqi Xu†, Jugao Fang*, Qi Zhong, Xiao Chen, Lizhen Hou, Hongzhi Ma, Lin Feng, Shizhi He, Meng Lian and Ru Wang

Department of Otorhinolaryngology Head and Neck Surgery, Beijing Tongren Hospital, Capital Medical University, Beijing, China

Objective: To investigate the feasibility and advantages of Fang's capillary fascia preservation right recurrent laryngeal nerve (RLN) dissection technique (F-R-RLN dissection) with preservation of the capillary network and fascia between the RLN and common carotid artery for greater neuroprotective efficiency compared with traditional techniques.

Methods: We retrospectively analyzed 102 patients with papillary thyroid carcinoma undergoing right level VI lymph node dissection in our department from March 2021 to January 2022. Sixty patients underwent F-R-RLN dissection (the experimental group) and 42 patients underwent standard dissection (the control group). The intraoperative electrical signal amplitude ratios of the RLN, the number of dissected lymph nodes, and the preservation rates of the parathyroid glands were recorded and compared between the two groups.

Results: The electrical signal amplitude ratio of the lower neck part point of the RLN to the upper laryngeal inlet point in the experimental group was significantly lower than the ratio in the control group (p = 0.006, Z-score = -2.726). One patient suffered transient RLN paralysis in both groups, but this resolved within 1 month after operation. There were no significant differences between the two groups in terms of the number of level VIa or level VIb lymph nodes dissected, nor in the rate of preservation of the parathyroid glands.

Conclusions: F-R-RLN dissection is a thorough dissection technique that is effective at preventing an electrical signal amplitude decrease in the RLN, and at preventing RLN paralysis by preserving its blood supply.

KEYWORDS

thyroid cancer, recurrent laryngeal nerve, neuroprotective, lymph node dissection, parathyroid preservation

Introduction

Papillary thyroid carcinoma accounts for more than 90% of malignant thyroid tumors, and its incidence has been increasing over recent decades (1). In spite of its indolent characteristics, it has a propensity to spread to the lymph nodes, particularly those in the level VI compartment (2). Due to the potential injury to the right recurrent laryngeal nerve (RLN) (3), the best approach to level VI lymph node dissection remains a debated issue. In traditional lymph node dissection, the middle and lower parts of the right cervical RLN are separated from surrounding tissues to achieve adequate dissection of the lymph nodes posterior to the nerve, which may cause interruption or even devascularization of the RLN. Since March 2021, Monitor Guided Fang's Capillary Fascia Preservation Right RLN Dissection Technique (F-R-RLN dissection) has been adopted by our department. In this technique, the RLN is slightly spared laterally to facilitate both exposure of the dissection area and preservation of the capillary network adjacent to the RLN. This study aimed to investigate the feasibility and advantages of F-R-RLN dissection compared with the traditional level VI dissection method, which involves dissecting the nerve circumferentially.

Materials and methods

Patients

A total of 102 patients with papillary thyroid carcinoma requiring right level VI lymph node dissection from March 2021 to January 2022 at the Department of Otolaryngology Head and Neck Surgery in Beijing Tongren Hospital were retrospectively included. The inclusion criteria were: (1) The invoked potential signal ratio R1/R2d (distal R2: the R2 in the upper laryngeal inlet part) was between 90 to 110%, which suggested the intubation was correct, (2) the nerve monitoring circuit was integral, and (3) they were not disturbed by muscle relaxants. The exclusion criteria were: (1) confirmed invasion (established preoperatively or intraoperatively) to the RLN or tracheoesophagus from the primary tumor or the lymph nodes; (2) history of vocal cord dysfunction; or (3) cases of papillary thyroid carcinoma relapse. The study was approved by the ethics review board of the Beijing Tongren Hospital, Capital Medical University, and all patients signed informed consent.

Sixty patients underwent F-R-RLN dissection and 42 patients underwent traditional lymph node dissection. All patients were treated by the same group of healthcare practitioners, which included anesthetists, surgeons, and laryngoscopy operators. Intraoperative neuromonitoring (IONM) was conducted using the Medtronic Xomed NIM-Response 3.0, with the electric current set to 2.0 mA. Surgery was performed under general endotracheal anesthesia. An injection of 0.2 mg/kg of Mivacron (muscle relaxant with effective maintenance time of about 20 minutes) was used for induction of anesthesia and no additional muscle relaxant and antagonist were administrated during surgery. We began to measure R1 30-40 minutes after the induction of anesthesia to reduce the disturbance of muscle relaxant. In all patients, electrical signals from the vagus nerve and RLN were routinely measured using the standard four-step (V1-R1-R2-V2) IONM procedure (4, 5).

Surgical technique

Level VIb is primarily located in the area delineated by the RLN and trachea. It has a triangular shape due to the anatomical characteristics of the right RLN as it bends around the subclavian artery, and the caudal side is adjacent to the common carotid artery (Figure 1). Based on these anatomical features, F-R-RLN dissection highlights that an adequate exposure and dissection of the level VIb lymph nodes can be achieved by slightly dislocating the RLN laterally to the surface of the common carotid artery and dislocating the laryngeal body to the left and upper side.

F-R-RLN dissection for the experimental group

All surgeries commenced with routine incision of the skin and subcutaneous tissue and freeing of the strap muscles to expose the right lobe of the thyroid and right level VI lymphatic connective tissue. Next, the central lymphatic fatty tissue superior to the RLN was dissected *en bloc*; this included the perithyroid, pretracheal, and tracheoesophageal groove lymph nodes. The right level VIa dissection began from the level of the hyoid bone and continued down to the level of the suprasternal notch or the upper edge of the innominate artery. The area extended laterally to the right common carotid artery and medially to the paratracheal lymph nodes and was limited to the level of the RLN. The right lymphatic fatty tissue inferior to the RLN was identified and excised in an ipsilateral level VIb dissection. In VIb dissection, the medial border was the trachea and the lateral border was the inner edge of the common carotid artery. The upper border was the entry site of the RLN into the larynx and the lower border was the intersection of the innominate artery and tracheoesophageal groove. The level VIb dissection was posteriorly limited at the level of the esophageal wall and superficially limited at the level of the RLN.

Electrical signals from the vagus nerve were recorded as V1. The vagus nerve was inspected and exposed, the middle thyroid vein was severed, and the ipsilateral thyroid lobe was raised to the medial side. The inferior parathyroid gland and its vascular supply were identified. The thyrothymic ligament was raised in a fan shape, such that the vertex was formed by the inferior parathyroid gland, while preserving the vascular pedicle of the parathyroid gland. Next, the inferior parathyroid gland and its

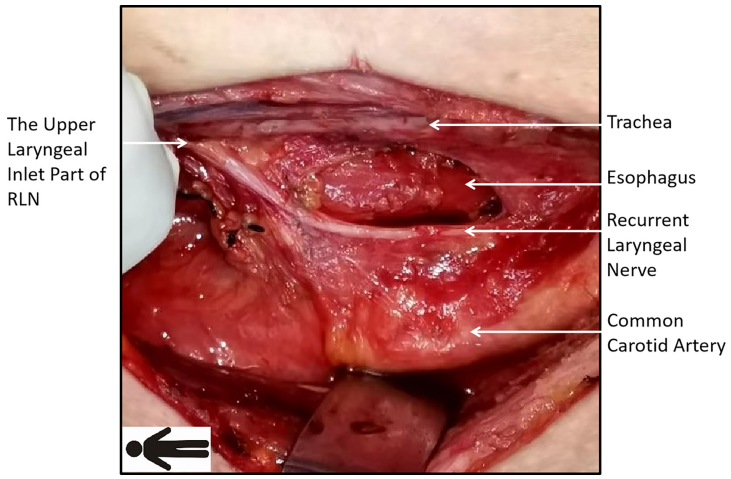

FIGURE 1
Course of the right recurrent laryngeal nerve (RLN): the right RLN runs obliquely with its inferior side closer to the common carotid artery. Level VIb, limited by the nerve and trachea, is shaped as a triangle with its top on the upper side.

vascular supply were freed to the lateral inferior side. A probe was inserted at the RLN in the tracheoesophageal groove at the level of the inferior thyroid pole and R1 was recorded (Figure 2A). The lymphatic connective tissue superficial to the RLN was briefly inspected, after which the lateral border of the level VIa area was incised and the area from the entrance of the inferior thyroid artery into the thyroid to the caudal site of the common carotid artery was dissected. At the caudal pole of the common carotid artery, the RLN was commonly adherent to the artery with less anatomical variation, which formed a suitable starting point for RLN dissection. The RLN was gently dislocated to the medial edge of the common carotid artery while dislocating the larynx to the upper left for adequate exposure of the right level VIb compartment. A meticulous level VIb dissection was performed along the esophagus after removing lymphatic fatty tissue. These tissue samples were preserved (Figure 2B). Branches of the RLN were severed by surgical scissors, which minimized potential electrical injury to the stem by electric scalpels. A layer of thin fascia encasing the capillaries of the RLN was then exposed between the RLN and common carotid artery. The medial border of the level VIa lymphatic connective tissue was separated along the tracheal midline after dissection from the lateral wall of the trachea to its midline (Figure 2C). The inferior limit was cut off at the level of the suprasternal fossa. The prelaryngeal lymph nodes were then meticulously dissected. The RLN was dissected upwards to its entrance into the larynx, after which the thyroid lobe was completely excised. The evoked potential R2 in the lower neck part was defined as proximal R2 (R2p), and the evoked potential R2 in the upper laryngeal inlet part was defined as distal R2 (R2d) (Figure 2C). Additional tissue was excised based on the tumor location and size (Table 1).

Conventional level VI dissection technique for the control group

In the control group, the middle and lower two-thirds of the right cervical RLN were separated from the surrounding tissue circumferentially and moved upwards for adequate dissection of the lymph nodes. Apart from the technique used for exposure of the level VI compartment, the remaining surgical steps were similar to those in the experimental group.

Data recorded

Evoked potentials V1, R1, R2p, R2d, and V2 were recorded for all patients. R2p and R2d were recorded after level VI dissection. The regression of neural electromyography (EMG) signals after exposing the entire RLN was quantified by the ratio of R2p to R2d. Postoperative vocal cord movement was also evaluated by stroboscopy. The number of dissected lymph nodes *en bloc* in levels VIa and VIb, the number of metastasized lymph nodes according to pathological reports, the preservation rate of the parathyroid glands *in situ*, and the changes in serum calcium and parathyroid hormone before and after surgery were recorded. In our study, hypoparathyroidism was defined as serum intact parathyroid hormone (iPTH) < 15 ng/L (normal range: 15–65 ng/L) or postoperative clinical symptoms of hypocalcemia (neuromuscular irritability including paresthesia, muscle cramps, tetany, or seizures) with or without a serum calcium level of less

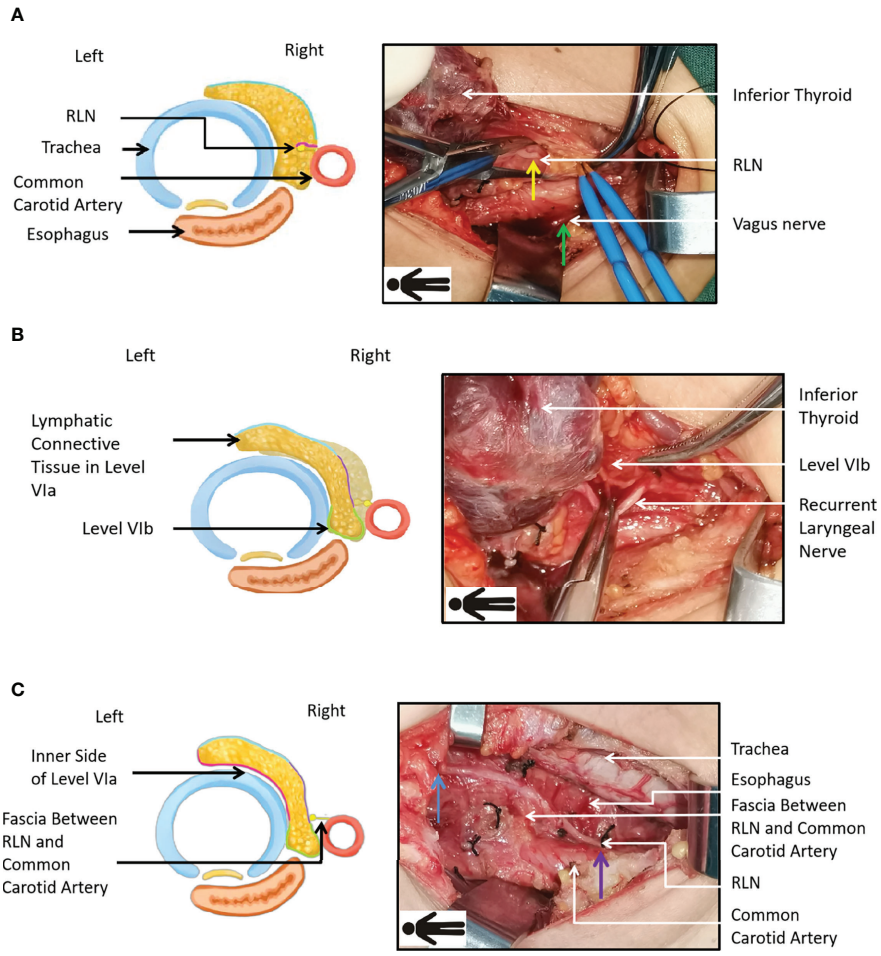

FIGURE 2
Technique of Fang's capillary fascia preservation right recurrent laryngeal nerve (F-R-RLN) dissection. **(A)** Dissecting superficial lymph connective tissue of RLN and cutting the lateral border of level VIa (the purple line in the figure). The green arrow points to the V1 electrical signal monitor point from the vagus nerve and the yellow arrow points to the R1 electric signal monitor point from the RLN. **(B)** Sparing RLN laterally to the superior and inner side of the common carotid artery and dissecting level VIb lymph connective tissue (the green line in the figure). **(C)** Preserving the capillary network encased by the fascia between the RLN and the common carotid artery and dissecting level VI lymph connective tissue (the red line in the figure). The blue arrow points to the R2d in the upper laryngeal inlet part. The purple arrow points to the R2p in the lower neck part. *Laryngeal body is dislocated to the left and upper side in order to expose level VIb and therefore the esophagus is shifted to the right side of the trachea.*.

than 2.0 mmol/L (8.0 mg/dL). Transient hypoparathyroidism was defined as postoperative hypoparathyroidism lasting less than 6 months. Permanent hypoparathyroidism was defined as postoperative hypoparathyroidism lasting more than 6 months (6).

Statistical analysis

SPSS 20.0 (Chicago, Illinois, USA) was used for statistical analysis. Data on the number of dissected lymph nodes were presented as medians (quartiles) because of their non-normal distribution. Two independent sample t-tests or Mann-Whitney U tests were conducted to compare numeric variables. The differences in categorical variables were analyzed with the Pearson Chi-square test or Fisher's exact test. P-values < 0.05 were labeled statistically significant.

Results

In the F-R-RLN dissection, the RLN is mildly dislocated and only the medial branches are severed. The capillary network encased by fascia between the RLN and the common carotid artery is preserved. Figure 3 shows the operative field after operation.

TABLE 1 The procedure during Fang's capillary fascia preservation right recurrent laryngeal nerve (F-R-RLN) dissection technique.

Steps	Operation
Step 1	Initial vagal nerve stimulation (V1)
Step 2	RLN stimulation at the level of the inferior thyroid pole (R1)
Step 3	Incision of the lateral border of the level VIa area
Step 4	**Dislocation of the RLN to the medial edge of the common carotid artery**
Step 5	Dislocation of the larynx to the upper left for complete exposition of the VIb level
Step 6	Dissection of the VIb level along the esophagus
Step 7	**Preservation of the thin fascia encasing the capillaries of the RLN between the RLN and common carotid artery**
Step 8	Separation of the medial and inferior border of the level VIa along the trachea
Step 9	Dissection of the prelaryngeal lymph nodes
Step 10	Dissection of the RLN to its entrance into the larynx and excision of the thyroid lobe
Step 11	Stimulation of the RLN in the lower neck part (R2p) and the upper laryngeal inlet part (R2d), as well as stimulation of the vagal nerve (V2)

The bold words show the key steps in the procedure.

Patients and disease characteristics

The baseline demographic and clinical characteristics of patients are shown in Table 2. There were no significant differences between the experimental and control groups in gender, the number of primary lesions, the size of primary lesions, T stage, N stage, invasion of strap muscles, concomitant or not with Hashimoto's thyroiditis, and preferences for partial versus total thyroidectomy.

Variations in EMG signal amplitude

The R2p/R2d ratio was categorized into three levels (>90%, 50% ~90%, <50%), and patients in both the control and experimental groups were divided into these 3 subcategories. The cases of each subcategory, their percentages in the total cases, and the prevalence of vocal cord dysfunction in each subgroup were recorded (Table 3). There were significant differences between the control and experimental groups in terms of EMG amplitude changes (the non-parametric Mann-Whitney test, $p = 0.006$, Z-score = -2.726). In one patient in the experimental group, R2p and V2 were lost during surgery in spite of a complete RLN stem. The patient experienced hoarseness on the first postoperative day, and subsequent laryngoscopy showed that his right vocal cord was fixed at the paramedian position. His vocal cord movement and phonation recovered 1 month after surgery. The rate of transient RLN paralysis in the experimental group was 1.7%. In the control group, one patient also experienced signal loss of R2p and V2 in spite of an apparently intact RLN trunk. Similar to the patient in the

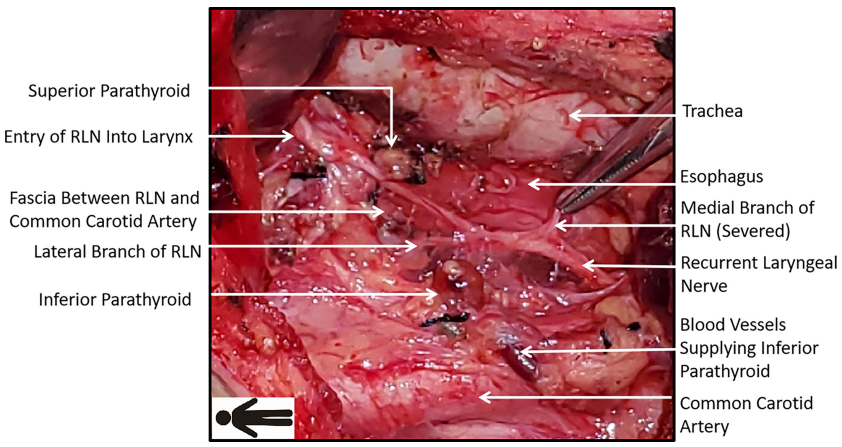

FIGURE 3
Operative field after Fang's capillary fascia preservation right recurrent laryngeal nerve (F-R-RLN) dissection technique: the capillary network encased by fascia between the RLN and the common carotid artery and the branches of RLN running laterally are preserved.

10.3389/fendo.2022.918741

TABLE 2 Patients and disease characteristics between two groups.

	Experimental Group (n=60)	Control Group (n=42)	P-Value
Gender			0.670
Male	19	15	
Female	41	27	
Number of lesions			0.111
Single	32	29	
Multifocal	28	13	
The size of primary lesions*			0.254
<1cm	27	20	
1-2cm	21	8	
2-4cm	7	9	
>4cm	5	5	
N stage			0.650
N0	27	17	
N1*	33	25	
< 0.5cm	25	20	
0.5-1.0cm	5	3	
>1.0cm	3	2	
Hashimoto's Thyroiditis			0.283
Yes	17	8	
No	43	34	
Invasion of strap muscles			1.000
Yes	3	2	
No	57	40	
Surgical Procedure			0.924
Right lobe and isthmus + right level VI dissection	28	20	
Total thyroidectomy + bilateral level VI dissection	32	22	

*The size of primary lesions was the greatest diameter of a primary lesion diagnosed by pathology (the greatest diameter if multifocal). The patients with N1 were stratified according to the maximum diameter of the invaded lymph nodes in the right level VI.

experimental group, hoarseness and vocal cord fixation was observed on the first postoperative day, which resolved 1 month after surgery.

Number of dissected lymph nodes and metastasis rate

There were no significant differences between the experimental and control groups in the number of dissected lymph nodes and the metastasis rate. In the experimental group, the overall number of dissected level VI lymph nodes was significantly larger compared with the number in the level VIa area, which indicated that enough VIb lymph nodes were dissected in the experimental group and F-R-RLN dissection technique might help to dissect the level VI lymph nodes thoroughly (Tables 4, 5).

Preservation of the right inferior parathyroid gland

In F-R-RLN dissection, the protection of the parathyroid gland is initiated prior to the dissection. The inferior parathyroid

TABLE 3 Variation of recurrent laryngeal nerve (RLN) signal amplitude and vocal cord movement after level VI lymph node dissection.

	R2p/R2d	Experimental group			Control group		
		Case of RLN	Ratio (%)	Vocal cord dysfunction	Case of RLN	Ratio (%)	Vocal cord dysfunction
Group 1	>90%	38	63.3 (38/60)	0	15	35.7 (15/42)	0
Group 2	50%~90%	20	33.3 (20/60)	0	24	57.1 (24/42)	0
Group 3	<50%	2	3.3 (2/60)	1	3	7.1 (3/42)	1

R2p, proximal R2, RLN signal amplitude in the lower neck part after dissection; R2d, distal R2, RLN signal amplitude in the upper laryngeal inlet part after dissection.

TABLE 4 Dissected lymph nodes in level VI.

	Experimental group			Control group			P-value of Medians
	Q1	Median (Min-max)	Q3	Q1	Median (Min-max)	Q3	
lymph nodes in level VIa	4	6 (1-22)	8	3	4.5 (1-13)	6	0.513
lymph nodes in level VIb	1	2.5 (0-8)	4	1	3 (0-8)	3	0.699

Lymph nodes in level VIa and VIb were represented by their respective medians. Q1: the first quartile; Q3: the third quartile. Min: the minimal number of lymph nodes dissected in the level VIa and VIb groups; Max: the maximal number of lymph nodes dissected in the level VIa and VIb groups.

TABLE 5 Level VI lymph node metastasis ratio.

	Experimental group	Control group
level VIa metastasis	55.0% (33/60)	40.5% (17/42)
level VIb metastasis	15% (9/60)	11.9% (5/42)

Level VIa and VIb metastasis rates were calculated by the ratio of patients for whom lymph node metastasis occurred to the total number of patients in each group.

glands are initially inspected after raising the right thyroid lobe. If the parathyroids are clearly exposed and the blood supply can be identified, the sternothyroid ligament is moved outwards and downwards, creating a fan-like shape, in which the vertex is formed by the parathyroid glands and the pedicle is formed by the parathyroid blood vessels (Figure 4).

No significant differences were demonstrated between the two groups in terms of the *in-situ* preservation rates, implantation rates, or total detection rates of the right inferior parathyroid gland: these were 76.6% (46/60), 16.6% (10/60), and 93.3% (56/60), respectively, for the experimental group and 78.6% (33/42), 11.9% (5/42), and 90.6% (38/42), respectively, for the control group. For patients undergoing total thyroidectomy, postoperative transient hypoparathyroidism occurred in nine cases in the experimental group (28.1% or 9/32) and in five cases in the control group (22.7% or 5/22). There were no significant differences between the two groups. Permanent hypoparathyroidism was not reported in either group.

Discussion

Papillary thyroid carcinoma has a predilection to metastasize to the cervical lymph nodes. One of the most common compartments of cervical lymph node metastasis is level VI (7), where the prevalence of metastasis can reach 47.6%, even in thyroid microcarcinoma (8). Additionally, occult metastasis to

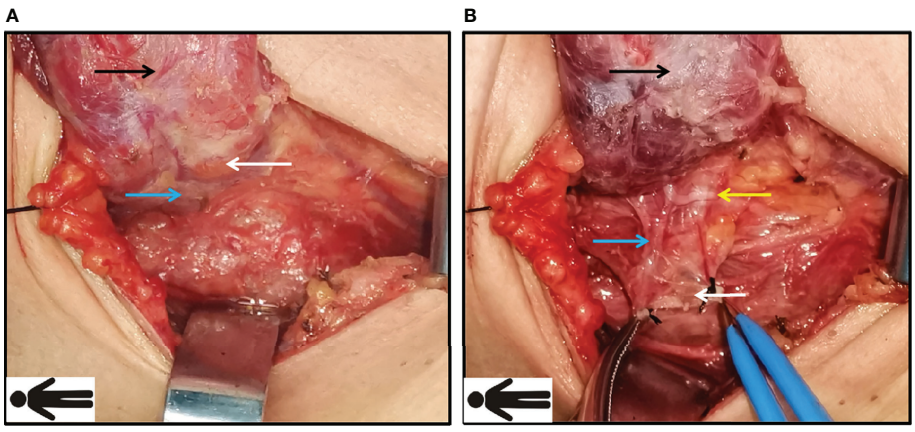

FIGURE 4
Preservation of inferior parathyroid gland during Fang's capillary fascia preservation right recurrent laryngeal nerve (F-R-RLN) dissection technique. **(A)** Inspect the inferior parathyroid glands (the white arrow) and its blood supply (blue arrow) after raising the lobe. **(B)** Protect and raise sternothyroid ligament outwards and downwards, creating a fan-like shape, in which the vertex is formed by the parathyroid and the parathyroid blood vessels; the sternothyroid ligament is intact. *Black arrow: the right lobe of thyroid; white arrow: the inferior right parathyroid gland; blue arrow: the blood supply of parathyroid gland; yellow arrow: the recurrent laryngeal nerve (RLN).*

level VI lymph nodes can be detected by pathology in 50% of patients who have no radiological evidence of lymph node metastasis before surgery (9). It has been suggested that cervical central lymph node metastasis is closely associated with both local recurrence and with the occurrence of lymph node metastasis after initial cancer surgery (10). Postoperative recurrence and level VI lymph node metastases increase the likelihood of impacting the adjacent nerves and parathyroid glands during re-operation because of adhesion, indistinct anatomic structure, and scarring from the initial operation. Given the high prevalence and detrimental effect of level VI lymph node invasion, an adequate dissection of the level VI lymph nodes is of great importance.

The indications for prophylactic central neck dissection (pCND) remain controversial. The guidelines in Europe and America recommend that pCND should be performed primarily in patients with stage T3, T4, and cN1b carcinoma (11). In China and Japan, pCND is performed routinely, based on the rationale that 50% of occult cervical lymph node metastases are missed during preoperative examination but detected postoperatively, which in turn impacts staging and postoperative management (12). In particular, the guidelines in China emphasize parathyroid and RLN preservation, and concomitant ipsilateral pCND, to reduce the risk of postoperative complications and to improve quality of life (13).

Since the cervical esophagus is mainly located on the left, there is minimal lymphatic and connective tissue posterior to the left RLN. Conversely, on the corresponding area on the right, posterior to the RLN, anterior to the prevertebral fascia, and superficial to the esophagus, lymphatic and fatty tissue of the level VIb can be found. The morbidity of level VIb lymph node metastasis in patients with recurrence is reportedly significantly higher than the morbidity of patients who are undergoing surgery for the first time (12). In our study, patients with level VIb lymph node metastasis accounted for 13.7% of the total cohort (14/102) (14), which is consistent with the range reported in the literature (7.0% to 27.03%) (15). However, level VIb lymph node dissection is complex and may induce several complications. An inadequate dissection will enhance operative difficulties, increase the risk of injury to the RLN and parathyroid glands during surgery, and delay the opportunity for radical excision (16). It is therefore crucial to develop an efficient and thorough technique for level VIb lymph node dissection.

In conventional level VI dissection, especially dissection in the level VIb area, the middle and lower two-thirds of the right RLN are routinely mobilized circumferentially (17), and the medial and lateral lymphatic connective tissue around the RLN are dissected (18). Excessive mobilization of the RLN may increase the risk of injury to it, by way of physical injury from repeated traction (19), *via* electrical injury by electric currents during the severing of the tracheoesophageal branches (20), or by neural degeneration and necrosis by devascularization (5).

As for the number of dissected lymph nodes, our study compared the F-R-RLN dissection with the conventional dissection technique and found that there were no significant differences between the experimental and control groups in terms of the number of dissected lymph nodes in the level VIa and VIb compartments, or in the relative incidence of metastasis. In the experimental group, the median number of dissected level VIa lymph nodes was 6 and the median number of dissected level VIb lymph nodes was 2.5, which is in accordance with the literature (17). The number of level VI lymph nodes dissected *en bloc* in the experimental group was significantly greater than the number of lymph nodes obtained from simple level VIa dissection (Z-score = -3.080, $p = 0.002$), which implies that F-R-RLN dissection can achieve thorough level VIb dissection.

Apart from the complete dissection of lymphatic connective tissue, some other benefits might be associated with F-R-RLN dissection, as well. Firstly, injury to the RLN caused by repeated traction is avoided by slightly sparing the RLN laterally. Secondly, the RLN branches are preserved as much as possible, with only the medial tracheoesophageal branch sacrificed. Thirdly, the blood supply is preserved by maintaining a thin layer of connective tissue between the RLN and common carotid artery, which encases the vasculature (Figure 3). The incidence of transient vocal cord dysfunction after level VIb lymph node dissection was 7.4% according to the literature (6). The incidence in the experimental group in our study was 1.7% (1/60), and it was completely resolved 1 month after surgery. A possible explanation is that an esophageal branch of the RLN was accidentally severed by the bipolar electric scalpel 3 mm away from the RLN trunk during level VIb dissection. The degree of signal amplitude loss as quantified by R2p/R2d in the experimental group was significantly lower compared to the degree of signal amplitude loss in the control group. The ratio exceeded 90% in 63.3% of patients in the experimental group, which represented a significant improvement compared with the results from patients undergoing the traditional dissection technique (35.7%). According to the literature data (21), there is a close correlation between an intraoperative decrease in the RLN electrical signal amplitude and postoperative RLN paralysis (22). The results of our study show that F-R-RLN dissection helps to protect the RLN and mitigate the risk of nerve signal interruptions. However, there was no significant difference between the two groups in the incidence of transient vocal cord dysfunction. There was just one case of vocal cord dysfunction in each group. It is difficult to interpret this finding due to the low sample size and the fact that our surgeons were highly skilled. A larger sample size may be needed to substantiate our findings.

Regarding the protection offered to the parathyroid gland, this was initiated prior to the dissection. If the parathyroids were in their usual site, the parathyroid glands and the pedicle of the blood

vessels were preserved *in situ* (Figure 4). However, if the parathyroid glands could not be clearly exposed, the sternothyroid ligament was still raised because there were no lymph nodes evident in the ligament, representing vestigial tissue from embryogenesis (23). In some cases, the parathyroid glands could be detected after elevating the ligament. The glands were preserved in the same way as described above. It has been reported that the incidence of transient and permanent hypoparathyroidism ranges from 14 to 60% and 4 to 11%, respectively (24). The incidence of unintentional parathyroidectomy ranges from 3.7% to 29.0% in the literature (25). In our study, the preservation rate of the parathyroid glands was 76.6% (46/60), and the incidence of unintentional parathyroidectomy was 6.7%, which is in line with previous reports. For patients undergoing total thyroidectomy in the experimental group, the incidence of postoperative transient hypoparathyroidism was 28.1% (9/32), and no permanent hypoparathyroidism occurred. There were no significant differences between the experimental and control groups in the rates of *in situ* preservation, transplantation, detection, or hypoparathyroidism, which suggests that F-R-RLN dissection is an effective method for parathyroid preservation.

The chylous leakage usually occurs after left level IV dissection and seldom happens after left or right level VI dissection. In our research, all patients underwent right level VI dissection and there were no cases of chylous leakage. Chylous leakage should be noted as a possible complication after level VI lymph node dissection due to aberrant drainage.

Conclusion

Monitor Guided Fang's Capillary Fascia Preservation Right RLN Dissection Technique offers some advantages over conventional techniques, including more thorough exposure and dissection of the level VI lymph nodes while preserving the RLN. This novel method can avoid excessive dissection of the RLN, reduce the probability of thermal injuries, and protect the blood supply to the RLN, which might decrease the incidence of postoperative complications and might improve surgical safety outcomes.

Data availability statement

The original contributions presented in the study are included in the article/**Supplementary Material**. Further inquiries can be directed to the corresponding author.

Ethics statement

The studies involving human participants were reviewed and approved by The ethics review board of the Beijing Tongren Hospital, Capital Medical University. The patients/participants provided their written informed consent to participate in this study.

Author contributions

QS, JQX, and JGF contributed to the conception and design of the study. QS designed the experiment and organized the database. JQX wrote the first draft of the manuscript. QZ, XC, LZH, HZM, LF, HSZ, ML and RW contributed to the statistical analysis. All authors contributed to manuscript revision and have read and approved the final submitted version.

Funding

This study was financially supported by the Beijing Natural Science Foundation Program and the Scientific Research Key Program of the Beijing Municipal Commission of Education (no. KZ201910025034), the Beijing Municipal Administration of Hospitals' Ascent Plan (no. DFL20180202), the Capital Health Development Research Project (no. Shoufa-2018-2-2054), the National Key Research and Development Plan (2020YFB1312805), and the China Health Promotion Foundation and Thyroid Research Project for Young and Middle-Aged Doctors.

Conflict of interest

The authors declare that the research was conducted in the absence of any commercial or financial relationships that could be construed as a potential conflict of interest.

Publisher's note

Supplementary material

The Supplementary Material for this article can be found online at: https://www.frontiersin.org/articles/10.3389/fendo.2022.918741/full#supplementary-material.

References

1. Jazdzewski K, Murray E, Franssila K, Jarzab B, Schoenberg D, de la Chapelle A. Common SNP in pre-miR-146a decreases mature miR expression and predisposes to papillary thyroid carcinoma. *Proc Natl Acad Sci USA* (2008) 105 (20):7269–74. doi: 10.1073/pnas.0802682105

2. Lombardi D, Accorona R, Paderno A, Cappelli C, Nicolai P. Morbidity of central neck dissection for papillary thyroid cancer. *Gland Surgery* (2017) 6(5):492–500. doi: 10.21037/gs.2017.05.07

3. Hughes DT, Rosen JE, Evans DB, Grubbs E, Wang TS, Solorzano CC. Prophylactic central compartment neck dissection in papillary thyroid cancer and effect on locoregional recurrence. *Ann Surg Oncol* (2018) 25(9):2526–34. doi: 10.1245/s10434-018-6528-0

4. Ji YB, Ko SH, Song CM, Sung ES, Tae K. Feasibility and efficacy of intraoperative neural monitoring in remote access robotic and endoscopic thyroidectomy. *Oral Oncol* (2020) 103:104617. doi: 10.1016/j.oraloncology.2020.104617

5. Chiang FY, Lu IC, Kuo WR, Lee KW, Wu CW. The mechanism of recurrent laryngeal nerve injury during thyroid surgery - the application of intraoperative neuromonitoring. *Surgery* (2008) 143(6):743–9. doi: 10.1016/j.surg.2008.02.006

6. Kaderli R, Riss P, Geroldinger A, Selberherr A, Scheuba C, Niederle B. Primary hyperparathyroidism: Dynamic postoperative metabolic changes. *Clin Endocrinol* (2018) 88(1):129–38. doi: 10.1111/cen.13476

7. Hou D, Xu H, Yuan B, Liu J, Lu Y, Liu M, et al. Effects of active localization and vascular preservation of inferior parathyroid glands in central neck dissection for papillary thyroid carcinoma. *World J Surg Oncol* (2020) 18(1):95. doi: 10.1186/s12957-020-01867-y

8. Simó R, Nixon I, Rovira A, Vander Poorten V, Sanabria A, Zafereo M, et al. Immediate intraoperative repair of the recurrent laryngeal nerve in thyroid surgery. *Laryngoscope* (2021) 131(6):1429–35. doi: 10.1002/lary.29204

9. Joliat GR, Guarnero V, Demartines N, Schweizer V, Matter M. Recurrent laryngeal nerve injury after thyroid and parathyroid surgery incidence and postoperative evolution assessment. *Medicine* (2017) 96(17):e6674. doi: 10.1097/MD.0000000000006674

10. Cirocchi R, Arezzo A, D'Andrea V, Abraha I, Popivanov GI, Avenia N, et al. Intraoperative neuromonitoring versus visual nerve identification for prevention of recurrent laryngeal nerve injury in adults undergoing thyroid surgery. *Cochrane Database Systematic Rev* (2019) 1:Cd012483. doi: 10.1002/14651858.CD012483.pub2

11. Liu ZM, Wang LQ, Yi PF, Wang CY, Huang T. Risk factors for central lymph node metastasis of patients with papillary thyroid microcarcinoma: a meta-analysis. *Int J Clin Exp Pathol* (2014) 7(3):932–7.

12. Grodski S, Cornford L, Sywak M, Sidhu S, Delbridge L. Routine level VI lymph node dissection for papillary thyroid cancer: surgical technique. *ANZ J Surgery* (2007) 77(4):203–8. doi: 10.1111/j.1445-2197.2007.04019.x

13. Canu GL, Medas F, Conso G, Boi F, Calò PG. Is prophylactic central neck dissection justified in patients with cN0 differentiated thyroid carcinoma? an overview of the most recent literature and latest guidelines. *Annali Italiani di Chirurgia* (2020) 91(5):451–7.

14. Haugen BR. 2015 American Thyroid association management guidelines for adult patients with thyroid nodules and differentiated thyroid cancer: What is new and what has changed? *Cancer* (2017) 123(3):372–81. doi: 10.1002/cncr.30360

15. Lallemant B, Reynaud C, Alovisetti C, Debrigode C, Ovtchinnikoff S, Chapuis H, et al. Updated definition of level VI lymph node classification in the neck. *Acta Oto-Laryngologica* (2007) 127(3):318–22. doi: 10.1080/00016480600806299

16. Ito Y, Miyauchi A, Oda H, Masuoka H, Higashiyama T, Kihara M, et al. Appropriateness of the revised Japanese guidelines' risk classification for the prognosis of papillary thyroid carcinoma: A retrospective analysis of 5,845 papilla y thyroid carcinoma patients. *Endocrine J* (2019) 66(2):127–34. doi: 10.1507/endocrj.EJ17-0061

17. Luo DC, Xu XC, Ding JW, Zhang Y, Zhang W. Clinical value and indication for the dissection of lymph nodes posterior to the right recurrent laryngeal nerve in papillary thyroid carcinoma. *Oncotarget* (2017) 8(45):79897–905. doi: 10.18632/oncotarget.20275

18. Roman BR, Randolph GW, Kamani D. Conventional thyroidectomy in the treatment of primary thyroid cancer. *Endocrinol Metab Clinics North America* (2019) 48(1):125–41. doi: 10.1016/j.ecl.2018.11.003

19. More Y, Shnayder Y, Girod DA, Sykes KJ, Carlisle MP, Chalmers B, et al. Factors influencing morbidity after surgical management of malignant thyroid disease. *Ann Otology Rhinol Laryngol* (2013) 122(6):398–403. doi: 10.1177/000348941312200609

20. Das AT, Prakash SB, Priyadarshini V. Outcomes of capsular dissection technique with use of bipolar electrocautery in total thyroidectomy: a rural tertiary center experience. *J Clin Diagn Res JCDR.* (2016) 10(12) Mc01–03. doi: 10.7860/JCDR/2016/24201.8975

21. Schneider R, Randolph GW, Sekulla C, Phelan E, Thanh PN, Bucher M, et al. Continuous intraoperative vagus nerve stimulation for identification of imminent recurrent laryngeal nerve injury. *Head Neck-Journal Sci Specialties Head Neck* (2013) 35(11):1591–8. doi: 10.1002/hed.23187

22. Phelan E, Schneider R, Lorenz K, Dralle H, Kamani D, Potenza A, et al. Continuous vagal IONM prevents recurrent laryngeal nerve paralysis by revealing initial EMG changes of impending neuropraxic injury: A prospective, multicenter study. *Laryngoscope.* (2014) 124(6):1498–505. doi: 10.1002/lary.24550

23. Chang H, Na YR, Seok-Mo K, Bup-Woo K, Sang LY, Chul LS, et al. The clinical significance of the right para-oesophageal lymph nodes in papillary thyroid cancer. *Yonsei Med J* (2015) 56(6):1632–7. doi: 10.3349/ymj.2015.56.6.1632

24. Marcinkowska M, Sniecikowska B, Zygmunt A, Brzezinski J, Dedecjus M, Lewinski A. Postoperative hypoparathyroidism in patients after total thyroidectomy - retrospective analysis. *Neuroendocrinol Letters* (2017) 38 (7):488–94.

25. Manouras A, Markogiannakis H, Lagoudianakis E, Antonakis P, Genetzakis M, Papadima A, et al. Unintentional parathyroidectomy during total thyroidectomy. *Head Neck-Journal Sci Specialties Head Neck* (2008) 30(4):497–502. doi: 10.1002/hed.20728

frontiers | Frontiers in Endocrinology

TYPE Original Research
PUBLISHED 25 July 2022
DOI 10.3389/fendo.2022.937870

OPEN ACCESS

EDITED BY
Gianlorenzo Dionigi,
University of Milan, Italy

REVIEWED BY
Naveen Prasad Gopalakrishnan Ravikumar,
Oregon Health and Science University, United States
Pu Cheng,
Zhejiang University, China
Kuailu Lin,
University Hospital Carl Gustav Carus, Germany

*CORRESPONDENCE
Bo-jian Xie
drxiebojian@163.com
Fei-lin Cao
oncologyyxq@outlook.com

†These authors have contributed equally to this work and share first authorship

SPECIALTY SECTION
This article was submitted to Thyroid Endocrinology, a section of the journal Frontiers in Endocrinology

RECEIVED 06 May 2022
ACCEPTED 01 July 2022
PUBLISHED 25 July 2022

CITATION
Yan X-q, Ma Z-s, Zhang Z-z, Xu D, Cai Y-j, Wu Z-g, Zheng Z-q, Xie B-j and Cao F-l (2022) The utility of sentinel Lymph node biopsy in the lateral neck in papillary thyroid carcinoma.
Front. Endocrinol. 13:937870.
doi: 10.3389/fendo.2022.937870

The utility of sentinel Lymph node biopsy in the lateral neck in papillary thyroid carcinoma

Xing-qiang Yan[1†], Zhao-sheng Ma[1†], Zhen-zhen Zhang[2†], Dong Xu[1], Yang-jun Cai[1], Zeng-gui Wu[1], Zhong-qiu Zheng[1], Bo-jian Xie[1*] and Fei-lin Cao[1*]

[1]Department of Surgical Oncology, Taizhou Hospital of Zhejiang Province, Wenzhou Medical University, Linhai, China, [2]Department of plastic surgery, Enze Hospital of Taizhou Enze Medical Center (Group), Luqiao, China

Background: Regional lymph node metastases (LNMs) are very common in papillary thyroid carcinoma (PTC) and associate with locoregional recurrence. The appropriate management of cervical lymph nodes is very important. Therefore, this study evaluated the application of sentinel lymph node biopsy (SLNB) in the lateral neck in PTC patients.

Methods: This prospective study was conducted from 1 November 2015 to 31 December 2017 and recruited 78 PTC patients treated with SLNB in the lateral neck and prophylactic lateral neck dissection (compartments II–IV) followed by thyroidectomy or lobectomy and central neck dissection.

Results: There were 78 PTC patients enrolled and sentinel lymph nodes (SLNs) were detected among 77 patients. A total of 30 patients were diagnosed with SLN metastases (SLNMs). The remaining 47 patients were pathologically negative of SLN, whereas 4 patients were found with metastases in the non-SLN samples. The detection rate, sensitivity, specificity, and accuracy rate of SLNB in the lateral neck were 98.7%, 87.1%, 98.7%, and 93.6%, respectively. However, the values varied greatly in each specific compartment of the lateral neck, and all of them were no more than 80%. These 34 PTC patients diagnosed with lateral compartment LNM (LLNM) were more likely to be younger (41.38 vs. 48.95 years old, $p = 0.002$) and exhibit extrathyroidal extension (56.8% vs. 31.7%, $p = 0.026$) and central compartment LNM (66.7% vs. 12.1%, $p < 0.001$). Tumors located in the upper third of the thyroid lobe also had a significantly higher probability of LLNM compared with those in middle or inferior location (66.7% vs. 35.3% vs. 34.8%, $p = 0.044$). At last, age (OR=0.912, $p = 0.026$), tumor location (upper vs inferior, OR=17.478, $p = 0.011$), and central compartment LNM (OR=25.364, $p < 0.001$) were independently predictive of LLNM.

Conclusions: SLNB can help surgeons to identify some PTC patients who may benefit from therapeutic lateral neck dissection and protect some patients

from prophylactic lateral neck dissection. However, it cannot accurately indicate specific lateral compartment-oriented neck dissection. Meanwhile, LLNM is more likely to occur in PTC patients with younger age or upper pole tumors or central compartment LNM.

KEYWORDS

sentinel lymph node biopsy (SLNB), papillary thyroid carcinoma (PTC), lymph node metastases (LNMs), lateral neck dissection, lateral compartment-oriented neck dissection

Introduction

Thyroid cancer is the most common malignant tumor in the endocrine system and head and neck tumors, causing 586,000 cases worldwide and ranking 9th in incidence in 2020 (1). Papillary thyroid carcinoma (PTC) accounts for the vast majority of thyroid cancers. Regional lymph node metastases (LNMs) are very common in patients with PTC, about up to 80% in the central compartment and up to 60% in the lateral compartment of the neck (2–4). Although the incidence of regional LNM is greatly high in PTC, the impact of regional LNM on the prognosis remains unclear. Meanwhile, regional LNM has been reported in association with a higher rate of locoregional recurrence (2, 5, 6). Surgical resection of clinically nodal-positive disease in PTC is considered to improve the results of both recurrence and survival. Therefore, it is generally believed that therapeutic cervical lymph node dissection is indicated in PTC patients with clinically evident cervical LNM. The 2015 American Thyroid Association guidelines recommend that therapeutic lateral neck dissection should be performed for patients with biopsy-proven metastatic lateral cervical lymphadenopathy (7). By contrast, routine prophylactic modified radical neck dissection is not advised and has not been proved with benefit. Therefore, the appropriate management of cervical lymph nodes is very important to PTC patients, which is helpful to improve survival, decrease regional recurrence, and avoid overtreatment.

Sentinel lymph node biopsy (SLNB) is used to assess the status of regional draining lymph nodes, and it has become a standard method for treating several types of human malignant tumors, especially for melanoma and breast cancer (8, 9). However, the application of SLNB in the treatment of PTC has not been thoroughly studied. SLNB in thyroid carcinoma was first reported in 1998 (10). In the last two decades, many studies have evaluated the feasibility and utility of SLNB in PTC patients, and most of these studies focused on the application of SLNB to replace the prophylactic central neck dissection. However, there are few studies that investigated the application of SLNB in lateral compartment lymph nodes in PTC patients. In a previous study, we investigated the utility of SLNB in central compartment lymph nodes and found that this technique was feasible, safe, and useful (11). Therefore, we investigated the application of SLNB in lateral compartment lymph nodes in this study and hypothesized that this technique could identify and remove cervical nodal disease in the primary surgery and eventually avoid a second surgery.

Patients and methods

Ethics statement

This study was approved by the Ethics Committee of Taizhou Hospital of Zhejiang Province, and written informed consent was obtained from all the PTC patients prior to enrollment. The collection and analysis of all data were anonymous.

Patients

This prospective study was conducted on 78 patients with PTC. All patients underwent surgical treatment by SLNB in the lateral compartment lymph nodes and prophylactic lateral neck dissection (compartments II–IV) at our hospital from 1 November 2015 to 31 December 2017. All of the enrolled patients were diagnosed with PTC preoperatively based on fine-needle aspiration biopsy (FNAB) and imaging evaluation of cervical lymph nodes by ultrasound with or without computed tomography before operation. Patients with clinically occult lymph nodes or suspicion of LNM but without confirmation by FNAB were included in this study, while patients diagnosed preoperatively with lateral compartment LNM (LLNM) based on FNAB were excluded. Patients with previous neck surgery were also excluded from this study.

Surgical procedure

All the surgery operations were performed by experienced surgeons who had performed more than two hundred thyroid surgeries per year within the past decade and had experience with handling thyroid SLN procedures. A transverse low-collar skin incision was followed by separation of the skin flap and a longitudinal incision in the linea alba cervicalis. Then, the thyroid pseudocapsule was carefully opened to completely expose the thyroid gland without injury to the capsule. The primary tumor location was confirmed intraoperatively according to the preoperative ultrasonography, then approximately 0.5 ml of carbon nanoparticle suspension or 1% methylene blue dye was injected into the parenchyma surrounding the primary tumor using a 27-gauge needle. Within minutes, the lateral neck region along the jugular vein was exposed and explored, searching for the stained lymph nodes. The black- or blue-stained lymph nodes were identified *via* tracing the dyeing lymphatic vessels. These stained lymph nodes, defined as sentinel lymph nodes (SLNs), were carefully removed and sent to the pathology department for frozen biopsy and routine pathology. Subsequently, prophylactic lateral neck dissection (compartments II–IV) was performed, followed by total thyroidectomy or lobectomy and central neck dissection. The remaining nonstained lymph nodes in the lateral compartment of neck, defined as non-SLNs, were sent for routine pathology. All the diagnoses were made by two experienced pathologists, and all the final diagnoses were based on routine pathology findings.

Data analysis

Descriptive statistics were used to analyze the characteristics of the patients and tumors. Univariate analysis and multivariate logistic regression analysis were applied to analyze the association between the LNM and clinicopathological factors. The t-test and chi-square test were used for the measurements and count data, respectively. SPSS version 19 (SPSS Inc., Chicago, IL, USA) was used in all of the statistical analyses, and statistical significance was defined as a p-value less than 0.05.

Results

The characteristics of all patients and tumors are shown in Table 1. In total, 78 patients with low to intermediate risk PTC were recruited in this study. There were 63 (80.8%) women and 15 (19.2%) men with a mean age of 45.65 years old (ranging from 21 to 71 years old). A total of 42 (53.8%) patients were diagnosed with PTC, while 36 (46.2%) patients were diagnosed

TABLE 1 Patient demographics and tumor characteristics (n = 78).

Characteristic	Value
Sex	
Male	15 (19.2%)
Female	63 (80.8%)
Age (years old)	
Mean ± SD (range)	45.65 ± 11.09 (21-71)
Tumor location	
Left	31 (39.7%)
Right	47 (60.3%)
Upper	21 (26.9%)
Middle	34 (43.6%)
Inferior	23 (29.5%)
Cervical adenopathy	
Present	18 (23.1%)
Absent	60 (76.9%)
Tumor type	
PTMC	36 (46.2%)
PTC	42 (53.8%)
Multifocality	
Multifocal	31 (39.7%)
Unifocal	47 (60.3%)
Extrathyroidal extension	
Present	37 (47.4%)
Absent	41 (52.6%)
Thyroiditis	
Present	26 (33.3%)
Absent	52 (66.7%)
BRAF mutation	
Present	66 (84.6%)
Absent	12 (15.4%)
Hypoparathyroidism	
Present	35 (44.9%)
Absent	45 (55.1%)
RAI therapy	
Present	27 (34.6%)
Absent	51 (65.4%)
LNM in total	49 (62.8%)
Central compartment	45 (57.7%)
Lateral compartment	34 (43.6%)
Compartment II	19 (24.4%)
Compartment III	26 (33.3%)
Compartment IV	20 (25.6%)
SLN in lateral compartment	77 (98.7%)
Compartment II	58 (74.4%)
Compartment III	62 (79.5%)
Compartment IV	58 (74.4%)
Number of nodes	
SLN (mean)	473 (6.1)
Non-SLN (mean)	881 (11.3)
Total-LN (mean)	2019 (25.9)
Follow-up time (range) (month)	62.4 (47-71)

PTMC, papillary thyroid microcarcinoma; PTC, papillary thyroid carcinoma; LNM, lymph node metastases; SLN, sentinel lymph node; Total-LN, total lymph nodes.

with papillary thyroid microcarcinoma (PTMC). A total of 18 (23.1%) patients showed cervical adenopathy by the preoperative imaging evaluation. Nearly half of the patients presented extrathyroidal extension (37, 47.4%), and one-third of the patients were diagnosed with multifocality (31, 39.7%) and thyroiditis (26, 33.3%). Majority of the patients presented BRAF mutations (84.6%). About two-fifths of the patients (35, 44.9%) had transient hypoparathyroidism in post-operation, but all of them recovered to normal in six months. Nearly one-third of the patients (27, 34.6%) received adjuvant radioactive iodine therapy after surgery. In the final pathology findings, 49 (62.8%) patients were diagnosed with LNM, of whom 45 (57.7%) patients had central compartment LNM and 34 (43.6%) patients had LLNM. The stained lymph nodes were identified among 77 patients, and the remaining one patient without dyeing lymph node was pathologically negative of lymph nodes in the study. A total of 2,019 lymph nodes were removed, of which 473 SLN and 881 non-SLN were removed from the lateral compartment of the neck. All the patients were followed up every 6 months for the first two years and then annually thereafter. The mean follow-up time was 62 months, ranging from 47 to 71 months. No one relapsed during the follow-up.

The results of SLNB are shown in Table 2. A total of 77 patients succeeded in SLNB in the lateral compartment of the neck. There were 30 patients who were diagnosed with SLN metastases (SLNM), of whom 20 were detected with further metastases in the non-SLN samples. The remaining 47 patients were pathologically negative of SLN, whereas 4 patients exhibited metastases in the non-SLN samples. The detection rate, sensitivity, specificity, and accuracy rate of SLNB in the lateral compartment of the neck were 98.7%, 87.1%, 98.7%, and 93.6%, respectively. However, the values varied greatly in the different areas of the lateral compartment of the neck. There were 58 patients who were detected to have SLN in compartment II, of whom 11 patients were SLN positive and 47 patients were SLN negative. However, 3 patients exhibited metastases in the non-SLN samples in the group of SLN negative. The detection rate, sensitivity, specificity, and accuracy rate were 74.4%, 58.4%, 74.4%, and 70.5%, respectively. A total of 62 patients showed SLN in compartment III, of whom 19 patients were positive in SLN and 3 patients were positive in non-SLN among the remaining patients. The detection rate, sensitivity, specificity, and accuracy rate of compartment III were 79.5%, 68.6%, 79.5%, and 75.6%, respectively. In compartment IV, SLN was found among 58 patients, of whom 10 patients were SLN positive. Meanwhile, 4 patients were pathologically positive in non-SLN among the patients with SLN negative. The detection rate, sensitivity, specificity, and accuracy rate of compartment IV were 74.4%, 53.1%, 74.4%, and 69.2%, respectively.

The association between LLNM and clinical factors was also analyzed. PTC patients with LLNM were significantly younger than those without LLNM (41.38 vs. 48.95 years old, $p = 0.002$). Tumors located in the upper third of the thyroid lobe had a significantly higher probability of LLNM compared with those in the middle or inferior location (66.7% vs. 35.3% vs. 34.8%, $p = 0.044$). Patients with extrathyroidal extension were more likely to have LLNM than those without extrathyroidal extension (56.8% vs. 31.7%, $p = 0.026$). What is more, PTC patients with central compartment LNM indicated a significantly higher incidence of LLNM (66.7% vs. 12.1%, $p < 0.001$). However, other factors such as sex, cervical adenopathy, thyroiditis, multifocality, tumor size, and BRAF mutations did not show statistical significance for LLNM (Table 3). A multivariate logistic regression analysis was performed to determine whether these factors were independently correlated with LLNM. At last, age (OR=0.912, $p = 0.026$), tumor location (upper vs inferior, OR=17.478, $p = 0.011$), and central compartment LNM (OR=25.364, $p < 0.001$) were independently predictive of LLNM (Table 4).

Discussion

Nowadays, the management of cervical lymph node dissection in the treatment of PTC is still one of the most controversial issues. As everyone knows, LLNM in PTC patients is very common, and most of these LNMs may be occult diseases (4). Traditionally, regional LNM has been thought to be

TABLE 2 Results of SLNB in the lateral compartment (n = 78).

	Lateral compartment	Compartment II	Compartment III	Compartment IV
SLN detection	77	58	62	58
SLN positive	30	11	19	10
SLN negative	47	47	43	48
Misdiagnosis	4	3	3	4
Missed diagnosis	1	20	16	20
Detection rate	98.7%	74.4%	79.5%	74.4%
Sensitivity	87.1%	58.4%	68.6%	53.1%
Specificity	98.7%	74.4%	79.5%	74.4%
Accuracy rate	93.6%	70.5%	75.6%	69.2%

SLNB, sentinel lymph node biopsy; SLN, sentinel lymph node.

TABLE 3 Comparison of patients with and without LNM in the lateral compartment (n = 78).

	Metastases (n=34)	Non-metastases (n=44)	P-value
Sex			
Female/Male	27/7	36/8	0.789
Age (mean ± SD) (years old)	41.38 ± 11.00	48.95 ± 10.08	0.002*
Tumor location			
Left/Right	14/20	17/27	0.820
Upper/Middle/Inferior	14/12/8	7/22/15	0.044*
Cervical adenopathy			
Present/Absent	9/25	9/35	0.532
Tumor type			
PTC/PTMC	20/14	22/22	0.438
Multifocality			
Multifocal/Unifocal	16/18	15/29	0.246
Extrathyroidal extension			
Present/Absent	21/13	16/28	0.026*
Thyroiditis			
Present/Absent	12/22	14/30	0.747
BRAF mutation			
Present/Absent	28/6	38/6	0.626
Central compartment LNM			
Present/Absent	30/4	15/29	0.000*

PTMC, papillary thyroid microcarcinoma; PTC, papillary thyroid carcinoma; LNM, lymph node metastases; * p<0.05.

associated with a higher rate of locoregional recurrence and decreased survival (2, 5, 6, 12–14). Therapeutic neck dissection, which is advocated for PTC patients with positive nodes by the FNAB, can decrease the recurrence and improve the survival. Although micro-metastases do not carry the same clinical significance as those of macro-metastases, PTC patients with these LNMs will also take a high risk of recurrence and secondary surgery (2). Moreover, there is still a lack of sufficient evidence regarding the confirmation of the efficacy and benefit of prophylactic neck dissection for PTC patients. Due to the efficacy of SLNB for the melanoma and breast cancer, the role of SLNB for PTC patients has been studied. Our previous study investigated SLNB in the central compartment of the neck and suggested that this technique was helpful in the decision-making in central neck dissection for some patients (11). Therefore, we further investigated the role of SLNB in the lateral compartment of the neck and hypothesized that SLNB could identify LNM and could be used as an indicator for selective lateral neck dissection.

SLN serves as the first station in the lymphatic drainage basin, receiving lymph flow from the primary tumor and reflecting the status of the remaining lymph nodes. A

TABLE 4 Multivariate analysis of the clinicopathological factors for patients with lateral compartment LNM (n = 78).

Factors	Odds Ratio	95% CI	P-value
Sex (Female vs. Male)	1.387	0.211 – 9.127	0.734
Age	0.912	0.841 - 0.989	0.026*
Tumor location (Left vs. Right)	1.038	0.254 – 4.248	0.959
Tumor location (Upper vs. Inferior)	17.478	1.924 - 158.785	0.011*
Tumor location (Middle vs. Inferior)	1.930	0.313 - 11.908	0.479
Cervical adenopathy (Present vs. Absent)	0.432	0.060 – 3.108	0.405
Tumor type (PTC vs. PTMC)	2.086	0.519 – 8.383	0.300
Multifocality (Multifocal vs. Unifocal)	3.331	0.639 – 17.371	0.153
Extrathyroidal extension (Present vs. Absent)	0.319	0.082 – 1.244	0.100
Thyroiditis (Present vs. Absent)	0.492	0.089 – 2.721	0.416
BRAF mutation (Present vs. Absent)	0.158	0.018 – 1.368	0.094
Central compartment LNMs (Present vs. Absent)	25.364	4.486 – 143.416	0.000*

PTMC, papillary thyroid microcarcinoma; PTC, papillary thyroid carcinoma; LNM, lymph node metastases; CI, confidence interval; * p<0.05.

successful SLNB requires accurately identifying and localizing the SLN. Generally, SLNB is performed by the use of vital dye, lymphoscintigraphy, or the combined technique. Recently, a review and a meta-analysis both found that the radioisotope technique had a slightly higher SLN detection rate than that of the dye method and the combined technique in PTC patients. However, the sensitivity, specificity, accuracy, and false negative were similar among these three techniques (15, 16). Although the radioisotope technique has advantages in the detection rate, it is very difficult to implement in small hospitals because of the strict management system on radioactive substances. In addition, radiocontamination may occur by accident. The dye method seems to be simple and easy to implement, but a relatively steep learning curve is needed for the surgeons (17). The surgeons need to know the dosage and flow rate of the tracer and protect the lymphatic vessels from destruction during the operation. The combined technique is more complex and difficult to implement, and the outcome is not better than that of other methods. Thus, the vital dye method is by far the most widely used in SLNB worldwide. But the sample size of PTC patients with the radioisotope technique is also increasing (16). In the present study, the dye method was used due to the previous extensive experience of SLNB in the central compartment of the neck.

As we all know, because of the considerable heterogeneity of the SLNB detection rate and its high false-negative rate, the accuracy of this procedure in PTC still remains questionable. There are three studies designed for evaluating the utility of SLNB in the lateral compartment lymph nodes (18–20). The detection rate ranges from 91.8% to 100%, and the accuracy rate ranges from 91.8% to 96.5% in these two studies that used the dye method (18, 20). Another study used the radioisotope technique and showed that the detection rate is 63.8%. The accuracy rate is not provided because the routine lateral neck dissection is not performed (19). In the present study, the detection rate(98.7%) and the accuracy rate(96.3%) of SLNB in the lateral compartment were similar to these previous studies. These results suggested that SLNB might be useful for a decision to perform selective lateral neck dissection in PTC patients. In another word, if any one of the SLNs was positive, the lateral neck dissection should be performed. On the contrary, when all of the SLNs were negative, the lateral neck dissection could be abandoned. In this way, SLN-positive patients may benefit from therapeutic lateral neck dissection, and SLN-negative patients will spare the prophylactic procedure. Meanwhile, the detection rate, sensitivity, specificity, and accuracy rate of each specific lateral compartment of the neck were analyzed in this study. Among these compartments, the detection rate ranged from 74.4% to 79.5%, the sensitivity ranged from 53.1% to 68.6%, the specificity ranged from 74.4% to 79.5%, and the accuracy rate ranged from 69.2% to 70.5%. Due to the relatively low detection rate and accuracy rate in every specific lateral compartment of the neck, lateral compartment-oriented neck dissection could not be performed based on the SLN status in this study. Therefore, SLNB can identify some patients who may benefit from therapeutical lateral neck dissection and protect some patients from prophylactic lateral neck dissection, but SLNB should be abandoned as an index of compartment-oriented neck dissection.

There is a generally accepted assumption that cervical LNM in PTC follows the gradual progression from the central to lateral compartment of the neck. Moreover, lymph nodes that skip metastases to the lateral compartment of the neck are present only in a small number of PTC patients (21, 22). In the present study, we found 45 (57.7%) patients who had central compartment LNM, of whom 30 were accompanied with LLNM simultaneously, and just only 4 (5.1%) patients had skip metastases. Both univariate analysis and multivariate regression analysis showed that LNM in the lateral compartment of the neck was significantly correlated with that in the central compartment of the neck. The details of the relationship between central compartment LNM and LLNM are shown in the supplementary table (Table S1). Meanwhile, LLNM was more likely to occur in younger patients in the present study, and a comprehensive analysis in two national databases reported that the outcome of survival was associated with cervical LNM among patients younger than 45 years old (14). Extrathyroidal extension was significantly associated with LLNM in univariate analysis but not in multivariate regression analysis. In the previous study, we found that extrathyroidal extension was independently predictive of LNM in the central compartment of the neck (11). Central compartment LNM might cover the impact of the extrathyroidal extension in multivariate regression analysis in this study. Both univariate analysis and multivariate regression analysis showed that upper pole PTC had a significantly higher probability of LLNM, so that the first station of LNM may be in compartment II rather than the central compartment of the neck among these patients (4). Therefore, factors such as younger age, upper pole tumors, and central compartment LNM may be very important for the decision-making in lateral neck dissection.

However, the present study has several limitations. Firstly, we did not evaluate the role of SLNB in compartment V, which may impact the detection rate and the accuracy rate in this study, even though the LNM in compartment V is relatively rare compared to that in other lateral compartments of the neck, and the vast majority of such metastases are observed only in the context of multicompartment metastases (4, 18, 23). Secondly, the number of patients enrolled in this study is not enough, which might affect the accurate evaluation of the SLNB utility. Thirdly, the mean time of follow-up is about 5 years, which may be not enough for an indolent carcinoma. Since PTC may relapse in 5 years or later after initial surgery, long-term follow-up is necessary to show the reality of recurrence. Fourthly, lateral neck dissection may not be an appropriate method for patients with negative SLN, which may cause unnecessary complications. Active surveillance and long-term follow-up for these patients may be more appropriate.

Conclusion

In conclusion, SLNB can help surgeons to identify some PTC patients who may benefit from therapeutic lateral neck dissection and protect some patients from prophylactic lateral neck dissection. However, because of the relatively low detection rate and accuracy rate in every specific lateral compartment of the neck, SLNB cannot accurately indicate specific lateral compartment-oriented neck dissection. Meanwhile, LLNM is more likely in PTC patients with younger age or upper pole tumors or central compartment LNM.

Data availability statement

The raw data supporting the conclusions of this article will be made available by the authors, without undue reservation.

Ethics statement

The studies involving human participants were reviewed and approved by the Ethics Committee of Taizhou Hospital of Zhejiang Province. The patients/participants provided their written informed consent to participate in this study.

Author contributions

Study conception and design: F-LC and X-QY. Acquisition of data: X-QY, Z-SM, Z-ZZ, Z-GW, Z-QZ and Y-JC. Analysis and interpretation of data: B-JX, F-LC, DX and X-QY. Drafting of manuscript: X-QY, Z-SM and Z-ZZ. Critical revision of manuscript: B-JX, F-LC and DX. X-QY, Z-SM and Z-ZZ have contributed equally to this work and share first authorship. B-JX and F-LC have contributed equally to this work and share corresponding authorship. All authors contributed to the article and approved the submitted version.

Funding

This work was kindly supported by the grant from Science and Technology Plan Projects of Taizhou (NO.20ywb33).

Acknowledgments

The authors would like to thank Prof. Mei-xian Zhang for her valuable suggestion that has helped improve the quality of the manuscript.

Conflict of interest

The authors declare that the research was conducted in the absence of any commercial or financial relationships that could be construed as a potential conflict of interest.

Publisher's note

Supplementary material

The Supplementary Material for this article can be found online at: https://www.frontiersin.org/articles/10.3389/fendo.2022.937870/full#supplementary-material

SUPPLEMENTARY TABLE 1
The relationship of between CLNM and LLNM.

References

1. Sung H, Ferlay J, Siegel RL, Laversanne M, Soerjomataram I, Jemal A, et al. Global cancer statistics 2020: GLOBOCAN estimates of incidence and mortality worldwide for 36 cancers in 185 countries. *CA: Cancer J Clin* (2021) 71(3):209–49. doi: 10.3322/caac.21660

2. Randolph GW, Duh QY, Heller KS, LiVolsi VA, Mandel SJ, Steward DL, et al. The prognostic significance of nodal metastases from papillary thyroid carcinoma can be stratified based on the size and number of metastatic lymph nodes, as well as the presence of extranodal extension. *Thyroid* (2012) 22(11):1144–52. doi: 10.1089/thy.2012.0043

3. Thompson AM, Turner RM, Hayen A, Aniss A, Jalaty S, Learoyd DL, et al. A preoperative nomogram for the prediction of ipsilateral central compartment lymph node metastases in papillary thyroid cancer. *Thyroid* (2014) 24(4):675–82. doi: 10.1089/thy.2013.0224

4. Cracchiolo JR, Wong RJ. Management of the lateral neck in well differentiated thyroid cancer. *Eur J Surg Oncol J Eur Soc Surg Oncol Br Assoc Surg Oncol* (2018) 44(3):332–7. doi: 10.1016/j.ejso.2017.06.004

5. Pereira JA, Jimeno J, Miquel J, Iglesias M, Munné A, Sancho JJ, et al. Nodal yield, morbidity, and recurrence after central neck dissection for papillary thyroid carcinoma. *Surgery* (2005) 138(6):1095–100. doi: 10.1016/j.surg.2005.09.013

6. Leboulleux S, Rubino C, Baudin E, Caillou B, Hartl DM, Bidart JM, et al. Prognostic factors for persistent or recurrent disease of papillary thyroid carcinoma with neck lymph node metastases and/or tumor extension beyond the thyroid capsule at initial diagnosis. *J Clin Endocrinol Metab* (2005) 90(10):5723–9. doi: 10.1210/jc.2005-0285

7. Haugen BR, Alexander EK, Bible KC, Doherty GM, Mandel SJ, Nikiforov YE, et al. 2015 American Thyroid association management guidelines for adult patients with thyroid nodules and differentiated thyroid cancer: The American thyroid association guidelines task force on thyroid nodules and differentiated thyroid cancer. *Thyroid* (2016) 26(1):1–133. doi: 10.1089/thy.2015.0020

8. Balch CM, Soong SJ, Atkins MB, Buzaid AC, Cascinelli N, Coit DG, et al. An evidence-based staging system for cutaneous melanoma. *CA: Cancer J Clin* (2004) 54(3):131–49. doi: 10.3322/canjclin.54.3.131

9. Lyman GH, Giuliano AE, Somerfield MR, Benson AB3rd, Bodurka DC, Burstein HJ, et al. American Society of clinical oncology guideline recommendations for sentinel lymph node biopsy in early-stage breast cancer. *J Clin Oncol Off J Am Soc Clin Oncol* (2005) 23(30):7703–20. doi: 10.1200/jco.2005.08.001

10. Kelemen PR, Van Herle AJ, Giuliano AE. Sentinel lymphadenectomy in thyroid malignant neoplasms. *Arch Surg (Chicago Ill 1960)* (1998) 133(3):288–92. doi: 10.1001/archsurg.133.3.288

11. Yan X, Zeng R, Ma Z, Chen C, Chen E, Zhang X, et al. The utility of sentinel lymph node biopsy in papillary thyroid carcinoma with occult lymph nodes. *PLoS One* (2015) 10(6):e0129304. doi: 10.1371/journal.pone.0129304

12. Zaydfudim V, Feurer ID, Griffin MR, Phay JE. The impact of lymph node involvement on survival in patients with papillary and follicular thyroid carcinoma. *Surgery* (2008) 144(6):1070–7. doi: 10.1016/j.surg.2008.08.034

13. Podnos YD, Smith D, Wagman LD, Ellenhorn JD. The implication of lymph node metastasis on survival in patients with well-differentiated thyroid cancer. *Am Surgeon* (2005) 71(9):731–4. doi: 10.1177/000313480507100907

14. Adam MA, Pura J, Goffredo P, Dinan MA, Reed SD, Scheri RP, et al. Presence and number of lymph node metastases are associated with compromised survival for patients younger than age 45 years with papillary thyroid cancer. *J Clin Oncol Off J Am Soc Clin Oncol* (2015) 33(21):2370–5. doi: 10.1200/jco.2014.59.8391

15. Garau LM, Rubello D, Morganti R, Boni G, Volterrani D, Colletti PM, et al. Sentinel lymph node biopsy in small papillary thyroid cancer: A meta-analysis. *Clin Nucl Med* (2019) 44(2):107–18. doi: 10.1097/rlu.0000000000002378

16. Garau LM, Rubello D, Muccioli S, Boni G, Volterrani D, Manca G. The sentinel lymph node biopsy technique in papillary thyroid carcinoma: The issue of false-negative findings. *Eur J Surg Oncol J Eur Soc Surg Oncol Br Assoc Surg Oncol* (2020) 46(6):967–75. doi: 10.1016/j.ejso.2020.02.007

17. Garau LM, Rubello D, Ferretti A, Boni G, Volterrani D, Manca G. Sentinel lymph node biopsy in small papillary thyroid cancer. A review on novel surgical techniques. *Endocrine* (2018) 62(2):340–50. doi: 10.1007/s12020-018-1658-5

18. Huang N, Ma B, Guan Q, Wang Y, Zhou L, Wei W, et al. Lateral cervical lymph node mapping in papillary thyroid carcinoma: A prospective cohort study. *Chin J Clin Oncol* (2018) 45(20):1053–6. doi: 10.3969/j.issn.1000-8179.2018.20.675

19. Lee SK, Kim SH, Hur SM, Choe JH, Kim JH, Kim JS. The efficacy of lateral neck sentinel lymph node biopsy in papillary thyroid carcinoma. *World J surg* (2011) 35(12):2675–82. doi: 10.1007/s00268-011-1254-9

20. Markovic I, Goran M, Buta M, Stojiljkovic D, Zegarac M, Milovanovic Z, et al. Sentinel lymph node biopsy in clinically node negative patients with papillary thyroid carcinoma. *J BUON* (2020) 25(1):376–82.

21. Lee YS, Shin SC, Lim YS, Lee JC, Wang SG, Son SM, et al. Tumor location-dependent skip lateral cervical lymph node metastasis in papillary thyroid cancer. *Head Neck* (2014) 36(6):887–91. doi: 10.1002/hed.23391

22. Roh JL, Park JY, Rha KS, Park CI. Is central neck dissection necessary for the treatment of lateral cervical nodal recurrence of papillary thyroid carcinoma? *Head Neck* (2007) 29(10):901–6. doi: 10.1002/hed.20606

23. Cabrera RN, Chone CT, Zantut-Wittmann D, Matos P, Ferreira DM, Pereira PSG, et al. Value of sentinel lymph node biopsy in papillary thyroid cancer: initial results of a prospective trial. *Eur Arch Oto-Rhino-Laryngology* (2015) 272(4):971–9. doi: 10.1007/s00405-014-3018-2

Advantages of publishing in Frontiers

OPEN ACCESS
Articles are free to read for greatest visibility and readership

FAST PUBLICATION
Around 90 days from submission to decision

HIGH QUALITY PEER-REVIEW
Rigorous, collaborative, and constructive peer-review

TRANSPARENT PEER-REVIEW
Editors and reviewers acknowledged by name on published articles

Frontiers
Avenue du Tribunal-Fédéral 34
1005 Lausanne | Switzerland

Visit us: www.frontiersin.org
Contact us: frontiersin.org/about/contact

REPRODUCIBILITY OF RESEARCH
Support open data and methods to enhance research reproducibility

DIGITAL PUBLISHING
Articles designed for optimal readership across devices

FOLLOW US
@frontiersin

IMPACT METRICS
Advanced article metrics track visibility across digital media

EXTENSIVE PROMOTION
Marketing and promotion of impactful research

LOOP RESEARCH NETWORK
Our network increases your article's readership